

Therapeutic application of Argonaute-2 to enhance neurovascular repair and inflammatory restitution in stroke

Marta Sofia Machado Pereira

Tese para obtenção do Grau de Doutor em
Biomedicina
(3^o ciclo de estudos)

Orientador: Doutora Raquel Margarida da Silva Ferreira
Co-orientador: Doutora Ana Clara Braz Cristóvão

Júri:
Prof. Doutor José Ignácio Verde Lusquinus
Prof. Doutor Cláudio Areias Franco
Prof^a. Doutora Ana Paula Pereira da Silva Martins
Prof^a. Doutora Vera Luísa Santos Neves

27 de novembro de 2023

Declaração de Integridade

Eu, Marta Sofia Machado Pereira, que abaixo assino, estudante com o número de inscrição D2420 do 3º Ciclo de estudos em Biomedicina da Faculdade de Ciências da Saúde, declaro ter desenvolvido o presente trabalho e elaborado o presente texto em total consonância com o **Código de Integridades da Universidade da Beira Interior**.

Mais concretamente afirmo não ter incorrido em qualquer das variedades de Fraude Académica, e que aqui declaro conhecer, que em particular atendi à exigida referenciação de frases, extratos, imagens e outras formas de trabalho intelectual, e assumindo assim na íntegra as responsabilidades da autoria.

Universidade da Beira Interior, Covilhã 04/12/2023

Marta Sofia Machado Pereira

Dedicatory

A todas as pessoas que de alguma forma me ajudaram e foram os meus pilares, em especial, aos meus pais e ao meu avô *Buzinho*.

Acknowledgments

O caminho não foi fácil. Nem sempre as coisas decorreram como planeado. Houveram muitos tropeços e também muita aprendizagem. Rodeada das pessoas certas chego à meta final. Um especial agradecimento,

À minha Orientadora científica, Raquel, pela partilha de conhecimento, conselhos, paciência, ajuda e orientação durante este percurso;

À minha Co-Orientadora científica, Ana Clara, pela grande disponibilidade em ajudar e pela partilha de conhecimento, motivação e boa-disposição;

Ao meu grupo de investigação no Centro de Investigação em Ciências da Saúde da Universidade da Beira Interior, em especial à Catarina, à Marta e à Professora Liliana e, a duas importantes bússolas deste percurso;

To the research group that kindly hosted me in Barcelona, specially to Professor Anna, Alba, and Miguel;

Às entidades financiadoras que permitiram a concretização deste projeto, em especial à Fundação para a Ciência e a Tecnologia;

Aos meus amigos do laboratório, da faculdade e de treinos por estarem sempre ao meu lado e me darem sempre o melhor de vocês;

Ao Jorge, por tudo o que jamais irei conseguir agradecer, por seres o meu confidente e por teres feito tudo isto possível;

Aos meus pais, os meus melhores amigos, os meus maiores ouvintes, por todo o amor incondicional, encorajamento e porque sem vocês, também nada teria sido possível;

À Covilhã, e tudo o que ela me deu, ensinou e encerrou.

A todos os que estão no meu coração, muito obrigada,

Marta

Resumo

O acidente vascular cerebral (AVC) é a principal causa de morte e incapacidade em adultos em Portugal e a segunda causa de morte em todo o mundo. Nos próximos anos, estima-se um agravamento desta condição de saúde como resultado do aumento da esperança média de vida e com o aumento de indivíduos que apresentam fatores de risco para o AVC. Atualmente, a trombólise intravenosa (através da administração de alteplase ou da trombectomia endovascular) é o tratamento preconizado para os doentes com AVC, apesar de apresentar eficácia limitada devido à estreita janela terapêutica onde pode ser usada sem causar transformações hemorrágicas, limitando o benefício a muitos doentes e destacando a necessidade de se desenvolverem terapias alternativas e mais seguras. O desenvolvimento de estratégias destinadas a potenciar os mecanismos neuroprotetores endógenos surgiu como uma alternativa segura à trombólise, no entanto, estas abordagens têm subestimado a importância da vasculatura cerebral na recuperação após um AVC. Anteriormente, foi demonstrado que a remodelação vascular cerebral está correlacionada com maiores taxas de sobrevivência e melhoria da função neurológica a longo prazo em pacientes que sofreram um AVC. Assim, neste trabalho de investigação, foi proposta a modulação de um mecanismo endógeno, a Argonauta (Ago)-2, para recuperar a função vascular cerebral comprometida após isquémia cerebral e, consequentemente, contribuir para uma recuperação do parênquima cerebral após um AVC. Para além de coordenar o tráfego e a atividade dos microRNA, a proteína Ago2 é essencial para assegurar a sobrevivência celular e a formação de túbulos capilares em células endoteliais periféricas. No entanto, estes mecanismos e o papel da Ago2 no endotélio cerebral isquémico ainda permanecem desconhecidos. Neste sentido, foi aferido, em primeiro lugar, o potencial desta proteína no processo inflamatório, considerado um dos eventos patológicos mais importantes que ocorre após o AVC e que pode levar à mortalidade a curto prazo ou promover a incapacidade a longo prazo do paciente. Os dados *in vitro* (em culturas primárias de células endoteliais e gliais do cérebro de murganho estimuladas com lipopolissacarídeo) e *in vivo* (em murganhos adultos injetados intraperitonealmente com lipopolissacarídeo) revelaram que a aplicação exógena da Ago2, sub-expressa pela vasculatura cerebral neste contexto patológico, normalizou marcadores endoteliais associados ao dano induzido pelo processo inflamatório e que, por sua vez, restabeleceu a função glial e neuronal previamente comprometidas. Em seguida, e tendo aferido o potencial da Ago2 para os estudos em contexto de isquémia cerebral, foi definida uma estratégia que promovesse o aumento dos níveis intracelulares desta proteína (também sub-expressa em contexto

isquêmico) e a sobrevivência endotelial. A entrega controlada de ácido retinóico (uma molécula sinalizadora com propriedades anti-inflamatórias e pró-angiogênicas) através de nanopartículas poliméricas (RA-NP) foi a estratégia definida. Os dados *in vitro* (em culturas primárias de células endoteliais do cérebro de murganho privadas de oxigênio e glucose) revelaram o potencial protetor das RA-NP em condições isquêmicas, apenas observado pela reposição dos níveis basais da proteína Ago2 (um efeito mediado pela via do óxido nítrico), comprovando, uma vez mais, a importância desta proteína na função vascular. Adicionalmente, os dados *in vivo* (murganhos adultos sujeitos à oclusão transitória da artéria cerebral média) mostraram que a administração sistêmica das RA-NP promoveu a sobrevivência do tecido lesado, normalizou a resposta inflamatória e promoveu a reparação neurovascular (com um efeito pró-angiogênico robusto) na região de penumbra durante a isquemia cerebral. No entanto, mais estudos são necessários para estabelecer uma correlação entre o resultado observado *in vivo* e a proteína Ago2 e para se desvendar as interações desta proteína com o ácido retinóico. Em suma, o trabalho experimental desenvolvido ao longo desta tese forneceu evidências de que a modulação do mecanismo endógeno Ago2 pode ser considerada uma abordagem neuroprotetora, com grande potencial terapêutico na recuperação após o AVC. Para além disso, revelou uma ferramenta nanotecnológica capaz de modular este sistema e, com potencial para ser usada, em conjunto com terapias já existentes, a nível sistêmico de forma segura.

Palavras-chave

Acidente vascular cerebral;isquemia cerebral;vasculatura cerebral;argonata-2;ácido retinóico;sistemas de entrega;administração sistêmica;neuroinflamação;angiogênese

Resumo alargado

O acidente vascular cerebral (AVC) é, atualmente, a principal causa de morte em Portugal e a segunda causa de morte em todo o mundo, de acordo com os últimos dados epidemiológicos. Adicionalmente, o AVC está associado a uma elevada taxa de morbidade em adultos e as projeções atuais indicam que esta condição de saúde irá agravar-se com o aumento da esperança média de vida e com o aumento do número de indivíduos com fatores de risco para a ocorrência de um AVC, destacando-se a obesidade, a diabetes, a hipertensão arterial, o sedentarismo e o consumo de tabaco e álcool. O AVC ocorre em consequência da interrupção abrupta no fornecimento de sangue ao cérebro causado pelo bloqueio de uma artéria (AVC isquémico; corresponde a 87% de todos os casos de AVC) ou pelo rompimento de um vaso sanguíneo (AVC hemorrágico). Após a ocorrência de um AVC, o maior fator que influencia a extensão da lesão e condiciona o sucesso e elegibilidade dos tratamentos é o intervalo temporal entre a manifestação dos sintomas e a intervenção médica (designado por janela terapêutica), sendo que neste contexto ‘tempo é cérebro’. Em 2006, a implementação de protocolos de emergência nas fases pré- e intra-hospitalares, nomeadamente o Programa Via Verde do AVC, permitiu reduzir consideravelmente este intervalo temporal, aumentando o número de pacientes elegíveis à aplicação das terapias existentes, com impacto positivo nos índices de mortalidade e morbidade. No entanto, apesar destas melhorias progressivas, este intervalo temporal ainda se encontra fora da janela de tempo preconizada (entre 1 a 1.5 horas). A terapia existente, que tem por base a rápida dissolução química ou mecânica do trombo obstrutivo, é a trombólise intravenosa, através da administração de alteplase (durante as 4.5 horas após o início dos sintomas) ou trombectomia endovascular (durante as 24 horas após o início dos sintomas). Se os tratamentos forem aplicados aos pacientes depois das janelas terapêuticas estabelecidas, os riscos de transformações hemorrágicas severas são elevados. Assim, são necessárias alternativas terapêuticas que contornem esta limitação temporal e assegurem a redução da incapacidade neurológica e motora dos pacientes. O desenvolvimento de estratégias destinadas a potenciar os mecanismos neuroprotetores endógenos surgiu como uma alternativa segura à trombólise intravenosa, no entanto, estas abordagens têm subestimado a importância da vasculatura cerebral neste contexto. Anteriormente, foi demonstrado que a remodelação vascular na zona de penumbra isquémica (zona adjacente ao foco isquémico) está correlacionada com maiores taxas de sobrevivência e melhoria da função neurológica a longo prazo em modelos animais e em pacientes que sofreram um AVC. Assim, estratégias neuroprotetoras centradas na manipulação da vasculatura cerebral podem

constituir uma abordagem promissora para mitigar os efeitos do AVC, quebrando o padrão da maioria das abordagens centradas na função neuronal. Neste sentido, foi proposta a modulação de um mecanismo endógeno, a Argonauta-2 (Ago2), para promover a função vascular cerebral comprometida após isquemia e, conseqüentemente, contribuir para uma recuperação do parênquima cerebral após um AVC. Como a proteína Ago2 é preferencialmente internalizada pelas células endoteliais cerebrais, a nossa proposta contorna os desafios da passagem de fármacos e moléculas pela barreira hematoencefálica, constituindo uma nova abordagem para futuras terapias. Relativamente à proteína Ago2, sabe-se que é o principal componente do complexo de indução do silenciamento de RNA responsável por coordenar o tráfego e atividade dos microRNA responsáveis pela regulação da expressão genética pós-transcricional. Adicionalmente, a Ago2 é essencial para assegurar a sobrevivência celular e a formação de túbulos capilares em células endoteliais periféricas, sugerindo um possível papel na angiogênese. No entanto, em condições de hipóxia, os seus níveis de expressão surgem aumentados, possivelmente para assegurar a entrega de microRNA e garantir a função vascular. Em concordância, outros estudos realizados numa linha celular derivada de rim humano embrionário e numa linha celular de adenocarcinoma de cólon humano mostraram que, para além dos níveis de expressão, a atividade da Ago2 é afetada pela hipóxia, ocorrendo a sua hidroxilação. Nessas condições, a hidroxilação da Ago2 aumentou o processamento de microRNA, numa linha de células musculares lisas da artéria pulmonar humana. Adicionalmente, o silenciamento desta proteína está correlacionado com a diminuição da expressão e sinalização do fator de crescimento endotelial vascular, um potente indutor angiogénico, em células de carcinoma hepatocelular. Tomadas em conjunto, estas evidências sugerem um forte envolvimento desta proteína na função vascular, no entanto, o papel da Ago2 e estes mecanismos no endotélio cerebral isquémico ainda permanecem desconhecidos.

Tendo isto em consideração, o primeiro objetivo desta tese foi aferir o potencial protetor da Ago2 num dos eventos patológicos mais importantes que ocorre após o AVC e que pode levar à mortalidade a curto prazo ou promover a incapacidade a longo prazo do paciente, nomeadamente o processo inflamatório. Para isso, foram realizadas culturas primárias de células endoteliais e gliais (astrócitos e microglia) do cérebro de murganho (7 dias de vida), com estimulação com lipopolissacarídeo (LPS), uma endotoxina que induz uma forte resposta pró-inflamatória. Os dados *in vitro* mostraram que a estimulação com LPS perturbou a integridade das junções endoteliais aderentes e regulou negativamente os níveis de Ago2 em culturas primárias de células endoteliais cerebrais. Neste tipo celular, o tratamento exógeno com a Ago2 recuperou os níveis

intracelulares desta proteína, restaurou a expressão basal da caderina-endotelial vascular, e regulou negativamente a liberação de óxido nítrico induzida por LPS. O óxido nítrico é um potente vasodilatador que em concentrações excessivas pode aumentar a permeabilidade vascular, potenciando a disfunção endotelial. Em contraste, nos astrócitos não foram observadas alterações significativas nos níveis de Ago2 em resposta ao processo inflamatório, nem respostas relevantes após a modulação do mecanismo endógeno Ago2 (a Ago2 endógena apenas se mostrou crítica na manutenção dos níveis basais do fator de necrose tumoral- α). Por outro lado, e nas mesmas condições, a microglia sobre-expressou a proteína Ago2; o silenciamento desta proteína, conteve a resposta inflamatória, impedindo a liberação de óxido nítrico e de interleucina-6, uma potente citocina pró-inflamatória. Em seguida, a microglia foi exposta a meio condicionado de células endoteliais para aferir o potencial da Ago2 na interação entre o endotélio cerebral e a resposta inflamatória. Esta abordagem não foi igualmente considerada para os astrócitos uma vez que estes não responderam à modulação do mecanismo endógeno Ago2. Os resultados mostraram que o secretoma de células endoteliais cerebrais, tratadas com Ago2, teve um efeito protetor sobre a ativação da microglia e sobre a liberação de moléculas pró-inflamatórias. Posteriormente, os resultados anteriores foram aferidos num modelo *in vivo* de inflamação. Em particular, o papel da Ago2 em marcadores de disrupção da integridade endotelial foi avaliado, assim como a reatividade glial e função neuronal em murganhos adultos injetados intraperitonealmente com LPS (que induz uma resposta inflamatória sistêmica), seguido por uma injeção diária de Ago2 durante três dias consecutivos. Em primeiro lugar, foi confirmado no modelo *in vivo* que a injeção intraperitoneal de LPS comprometeu a integridade da barreira hematoencefálica, observada pela disrupção do complexo caderina-endotelial vascular que, por sua vez, afetou a função neuronal e desencadeou um processo pro-inflamatório mediado pelas células da glia (resultados comprovados através de marcadores de ativação glial). Neste contexto, a administração de Ago2 restaurou a integridade da barreira, sendo este um dos focos de muitas terapias cerebrais e, que por vezes, se demonstra difícil de alcançar, e normalizou a ativação glial no córtex e no hipocampo. Por sua vez, foi observado um efeito neuroprotetor robusto no hipocampo, nomeadamente um aumento da expressão de mediadores implicados na sobrevivência neuronal, na transmissão sináptica e na formação de memória e aprendizagem. Este resultado resultou possivelmente da ação direta da Ago2 sobre o endotélio cerebral, que restabeleceu a função glial e neuronal. Em suma, foi demonstrado que a modulação do mecanismo Ago2 pode ser considerada uma abordagem promissora para a recuperação da unidade neurovascular comprometida pela inflamação e apresenta potencial para estudos num modelo de isquémia cerebral.

Em seguida, os níveis de expressão da Ago2 foram avaliados em culturas primárias de células endoteliais cerebrais de murganho (7 dias de vida) expostas a condições isquêmicas, mimetizadas pela privação de oxigênio e glicose seguido de um período de recuperação. Os resultados *in vitro* demonstraram que, em condições isquêmicas, ocorre uma diminuição significativa dos níveis intracelulares de Ago2 através da sua degradação por autofagia, semelhante às evidências obtidas em condições inflamatórias. Como a inibição da autofagia, um mecanismo basal importante para a sobrevivência celular e manutenção da homeostasia cerebral, não recuperou a viabilidade endotelial comprometida em condições isquêmicas (apenas reverteu a perda intracelular de Ago2), foi definida uma estratégia com potencial para aumentar os níveis intracelulares de Ago2 e, em simultâneo, promover a sobrevivência endotelial. Assim, e considerando os efeitos protetores já descritos em modelos *in vitro* e *ex vivo* em contexto isquêmico, a entrega controlada de ácido retinóico (RA) através de nanopartículas poliméricas (RA-NP) foi a abordagem farmacológica proposta. O RA é uma molécula sinalizadora com propriedades anti-inflamatórias e pró-angiogénicas. Para potenciar estas propriedades protetoras e eliminar as propriedades indesejadas, como a rápida degradação em condições fisiológicas e após exposição à luz, baixa solubilidade na fase aquosa e uma janela de concentrações ótima para exercer os seus efeitos protetores, o nosso grupo de investigação desenvolveu um sistema de entrega controlada desta molécula (RA-NP). Esta tese explora, pela primeira vez, o potencial deste sistema num modelo *in vivo* de isquémica cerebral e na modulação do mecanismo endógeno Ago2. Apesar do RA e da Ago2 apresentarem um perfil protetor da vasculatura cerebral, a sua interação nunca foi estudada anteriormente. Em condições isquêmicas, os resultados *in vitro* mostraram que o tratamento com as RA-NP impediu a perda da viabilidade endotelial e recuperou os níveis intracelulares de Ago2. Adicionalmente, através da inibição da expressão (com siAgo2) e da atividade (com o inibidor BCI-137) da Ago2, os dados mostraram que as RA-NP apenas induzem efeitos protetores na vasculatura cerebral na presença desta proteína, um efeito que ocorreu através da via de sinalização Akt/eNOS/NO. Em seguida, estes efeitos foram explorados num modelo *in vivo* de AVC (murganhos adultos submetidos à oclusão da artéria cerebral média, seguido de uma injeção intravenosa com as RA-NP), numa fase aguda (3 dias após o início do AVC) e subaguda (7 dias após o início do AVC). Os resultados *in vivo* mostraram que a injeção intravenosa única das RA-NP aumentou a sobrevivência do tecido e normalizou a resposta inflamatória, na fase aguda. Na fase subaguda, as RA-NP promoveram a proteção neuronal e a reparação neurovascular, na região de penumbra isquémica. É importante realçar que, na fase subaguda, as RA-NP exibiram um efeito pró-angiogénico robusto na zona de penumbra isquémica, sendo este um mecanismo crucial para promover a restauração do fluxo

sanguíneo cerebral e, conseqüentemente, para recuperar a função neurológica perdida. No entanto, os dados *in vivo* não revelaram uma recuperação funcional do animal após o AVC, apesar da tendência muito positiva na fase subaguda. Em relação aos efeitos observados nas fases aguda e subaguda com a Ago2 e, de igual modo, à interação desta proteína com o RA, mais estudos são necessários para estabelecer estas correlações.

Em suma, e apesar de serem necessários mais estudos futuros, a investigação experimental desenvolvida ao longo desta tese forneceu evidências de que a modulação do mecanismo endógeno Ago2 pode ser considerada uma abordagem neuroprotetora com grande potencial terapêutico na recuperação após um AVC. Para além disso, foi revelada uma ferramenta nanotecnológica capaz de modular este mecanismo e com aplicabilidade para ser usada a nível sistémico de forma segura. No futuro, a combinação desta abordagem com as terapias já existentes pode levar a menores taxas de morbidade, com um recurso mínimo aos prestadores de cuidados de saúde, e com uma redução de custos para o sistema de saúde em todo o mundo.

Abstract

Stroke is the leading cause of death and adult disability in Portugal and the second cause of death worldwide. In the coming years, this health condition will worsen due to the increase in average life expectancy and the increase in the number of individuals with risk factors for stroke. Currently, the recommended treatment for stroke patients is the intravenous thrombolysis therapy (with alteplase or endovascular thrombectomy), although it has limited efficacy due to the narrow therapeutic window where it can be applied without causing hemorrhagic transformations, limiting the benefit to many patients and highlighting the need to develop alternative and safer therapies. The development of strategies aiming to potentiate endogenous neuroprotective mechanisms has emerged as a safe alternative to thrombolysis, however, these approaches have undervalued the importance of the cerebral vasculature in the post-stroke recovery. Previously, it was demonstrated that cerebral vascular remodeling is correlated with higher survival rates and improved long-term neurological function in stroke patients. Accordingly, in this research work, it was proposed the modulation of the Argonaute (Ago)-2 endogenous mechanism to enhance the brain vascular function compromised by cerebral ischemia and, consequently, contributing to full parenchymal recovery after a stroke. Besides being the major coordinator of microRNA traffic and activity, Ago2 protein is pivotal for cell survival and tube network formation in peripheral endothelial cells. However, these mechanisms and the role of Ago2 in the ischemic brain vasculature remain unknown. In this sense, the potential of this protein in the inflammatory process was first assessed. This pathological process is one of the most important post-stroke pathological events that can lead to short-term mortality or promote long-term disability. Accordingly, *in vitro* (mouse primary brain cultures of endothelial and glial cells stimulated with lipopolysaccharide) and *in vivo* (adult mice intraperitoneally injected with lipopolysaccharide) data revealed that exogenous Ago2 application (downregulated in brain vasculature in these conditions) normalized endothelial markers associated with inflammatory-induced damage which, in turn, reestablished previously compromised glial and neuronal function. Then, after confirming the potential of Ago2 for cerebral ischemia studies, a strategy to enhance the Ago2 intracellular levels (also downregulated in the ischemic context) and to promote endothelial cell survival was defined. The controlled release of retinoic acid (a signaling molecule with defined anti-inflammatory and pro-angiogenic properties) via polymeric nanoparticles arose as a promising approach. *In vitro* data (mouse primary brain cultures of endothelial cells subjected to oxygen and glucose deprivation) revealed the

protective potential of RA-NP in ischemic conditions, only observed by restoring basal levels of Ago2 protein (an effect mediated by the nitric oxide signaling), highlighting the importance of Ago2 in vascular function. Additionally, *in vivo* data (adult mice subjected to transient occlusion of the middle cerebral artery) showed that the systemic administration of this formulation promoted tissue survival, normalized inflammatory response, and promoted neurovascular repair (with a robust pro-angiogenic effect) in the peri-infarct region after stroke. However, further studies are needed to establish a correlation between the observed *in vivo* outcome and the Ago2 protein, and of RA-NP treatment and to decipher interactions between this protein and retinoic acid. Altogether, the experimental research developed throughout this Thesis provided evidence that the modulation of the Ago2 endogenous mechanism can be envisioned as a neuroprotective approach in post-stroke recovery. Furthermore, it revealed a safe nanotechnological tool able to modulate this system, suitable for intravenous administration, and compatible with pre-existing therapies.

Keywords

Stroke;brain ischemia;cerebral vasculature;argonaute-2;retinoic acid;delivery systems;systemic administration;neuroinflammation;angiogenesis

Funding

The work developed in this Thesis was supported by national funds through the POCI - COMPETE 2020 - Operational Programme Competitiveness and Internationalisation in Axis I (POCI-01-0145-FEDER-007491), the Fundação para a Ciência e Tecnologia (FCT), the Technology/MCTES attributed to Health Sciences Research Centre, Faculty of Health Sciences, University of Beira Interior (CICS-UBI) (UID/Multi/00709/2013, UIDB/00709/2020, and UIDP/00709/2020), the infrastructure PPBI - Portuguese Platform of BioImaging (POCI-01-0145-FEDER-022122), the funding attributed to author Marta Pereira by FCT (SFRH/BD/137440/2018), the funding attributed to supervisor Doctor Raquel Ferreira by FCT (IF/00178/2015/CP1300/CT0001), and L'Oréal - UNESCO Portugal for Women in Science, the funding attributed to collaborator Doctor Alba Grayston (ISCIH, FI17/00073), the funding attributed to collaborator Doctor Lino Ferreira (PTDC/BTM-SAL/5174/2020, EXPL/BTMORG/1348/2021; grants from the INTERREG Atlantic Area (EAPA_791/2018_NEUROATLANTIC Project), INTER-REG V A España Portugal (POCTEP) (0624_2IQBIONEURO_6_E), and the European Regional Development Fund (ERDF)), the funding attributed to Miguel García-Gabilondo (PERIS SLT017/20/000197 from Generalitat de Catalunya), and the funding attributed to Doctor Anna Rosell (RICORS-Stroke Network from ISCIH (RD21/0006/0007)).



Scientific publications and communications

Scientific articles related to this Thesis:

- Machado-Pereira M, Grayston A, Garcia-Gabilondo M, Francisco V, Cristóvão AC, Marto JP, Vieira H, Viana-Baptista M, Ferreira L, Bernardino L, Rosell A, Ferreira R. Retinoic Acid-Loaded Nanoparticles Promote Neurovascular Protection in Stroke. *Stroke*. 2023 Apr;54(4):e149-e151. doi: 10.1161/STROKEAHA.122.041839.

- Machado-Pereira M, Saraiva C, Bernardino L, Cristóvão AC, Ferreira R. Argonaute-2 protects the neurovascular unit from damage caused by systemic inflammation. *J Neuroinflammation*. 2022 Jan 6;19(1):11. doi: 10.1186/s12974-021-02324-7.

Other scientific articles developed throughout the PhD:

- Esteves M, Cristóvão AC, Machado-Pereira M, Ferreira R, Bernardino L. MicroRNA-124-3p modulates alpha-synuclein expression levels in a paraquat-induced in vivo model for Parkinson's Disease. *Neurotoxicity Research*. 2023 (*submitted on 15 April 2023*).

Oral communications related to this Thesis:

- Machado-Pereira M, Cristóvão AC, Ferreira L, Bernardino L, Ferreira R. Retinoic acid-loaded nanoparticles protect cerebral vascular dysregulation under ischemia. 2022. I International Meeting on the Brain Vasculature| Lisbon, Portugal.

- Machado-Pereira M, Pais, JP, Bernardino L, Cristóvão AC, Ferreira R. Role of argonaute-2 in neurovascular repair after ischemic stroke. 2020. XV Annual Health Sciences Research Centre - University of Beira Interior (CICS-UBI) Symposium| Covilhã, Portugal.

- Machado-Pereira M, Pais JP, Bernardino L, Cristóvão AC, Ferreira R. Papel da Argonauta-2 na recuperação vascular em isquémia. 2019. 20º Congresso do Núcleo de Estudos da Doença Vascular Cerebral da Sociedade Portuguesa de Medicina Interna| Porto, Portugal.

Poster communications related to this Thesis:

- Machado-Pereira M, Grayston A, Garcia-Gabilondo M, Cristóvão AC, Ferreira L, Bernardino L, Rosell A, Ferreira R. Retinoic acid-loaded nanoparticles promote neurovascular repair in stroke. 2022. XVII International CICS-UBI Symposium| Covilhã, Portugal (*best poster award*).

- Machado-Pereira M, Pais JP, Bernardino L, Cristóvão AC, Ferreira R. Therapeutic role of Argonaute-2 in stroke. 2019. III International Congress in Health Sciences Research: Towards Innovation and Entrepreneurship - Trends in Aging and Cancer| Covilhã, Portugal (*best poster award*).

Thesis Overview

The research conducted in this Thesis was mostly developed in the Health Sciences Research Centre of the University of Beira Interior (Covilhã, Portugal) and the Neurovascular Research Laboratory, Vall d'Hebron Institut de Recerca of the Universitat Autònoma de Barcelona (Barcelona, Spain). It presented results from the expertise and combined synergy of multidisciplinary teams from national (Health Sciences Research Centre and NeuroSoV, UBImedical, University of Beira Interior (Covilhã, Portugal); Center for Neuroscience and Cell Biology Medicine of the University of Coimbra and the Faculty of Medicine of the University of Coimbra (Coimbra, Portugal); NMS Research, Nova Medical School, Faculdade de Ciências Médicas of the Universidade Nova de Lisboa and Applied Molecular Biosciences Unit, Department of Chemistry, NOVA School of Science and Technology, Universidade NOVA de Lisboa and Associate Laboratory i4HB – Institute for Health and Bioeconomy, NOVA School of Science and Technology, Universidade Nova de Lisboa (Lisboa, Portugal)) and international (Neurovascular Research Laboratory) units and one hospital center (Department of Neurology, Hospital Egas Moniz, Centro Hospitalar de Lisboa Ocidental (Lisboa, Portugal)).

In this Thesis, it was proposed a novel strategy for post-stroke recovery, based on the modulation of the Argonaute (Ago)-2 endogenous mechanism, which works from the first line of damage (cerebral vasculature) to full parenchymal recovery after a stroke. Accordingly, it is composed of seven chapters and its organization is as follows. **Chapter 1** introduces stroke, the pathophysiological mechanisms, the pre-existing acute therapies, and the importance of strengthening the cerebral vasculature following brain ischemia. Additionally, it contextualizes the relevance of Ago2, presents the functions of retinoic acid (RA), as the therapeutic agent proposed to modulate the Ago2 system, and provided the specific aims outlined for the work plan. **Chapter 2** encloses the methodology section, providing detailed information regarding the data collection and analysis. **Chapter 3** illustrates the role of Ago2 in the neurovascular unit under systemic inflammatory challenge, a mechanism that impairs the outcome in stroke. **Chapter 4** presents the potential of using a RA delivery system in the modulation of the Ago2 endogenous mechanism and in the neurovascular response after a stroke. **Chapter 5** discusses the research obtained in this Thesis and presents suggestions for future research. **Chapter 6** encloses a summary of the findings obtained throughout this research. Finally, **Chapter 7** contains a list of references for the entire Thesis.

Index

Chapter 1 – Introduction	1
1.1 Ischemic stroke	1
1.1.1 Epidemiology, definition, and diagnosis	1
1.1.2 Pathophysiology and ischemic cascade	3
1.1.3 Experimental models	6
1.1.4 Prevention strategies and acute therapeutic approaches	10
1.2 NVU: a focus on cerebral vasculature	13
1.2.1 NVU concept and cellular composition	13
1.2.2 Physiological function of cerebral vasculature	16
1.2.3 Cerebral endothelial dysfunction: implications for CNS	17
1.2.4 Targeting the cerebral vasculature for brain repair in pathological conditions	18
1.3 Argonaute proteins	20
1.3.1 Structural and functional insights of the Ago protein family	20
1.3.2 Ago post-translational modifications and signaling pathways	24
1.3.3 Ago2 functions in angiogenesis and inflammation	26
1.4 Retinoic Acid signaling molecule	27
1.4.1 RA metabolism and signaling pathways	27
1.4.2 Effects of RA in brain angiogenesis and neuroinflammation	30
1.4.3 RA delivery systems for brain repair	32
1.5 Aims	33
Chapter 2 – Materials and Methods	35
2.1 Primary brain cultures	35
2.1.1 Primary brain endothelial cell cultures	35
2.1.2 Primary brain glial cell cultures	36
2.2 <i>In vitro</i> models	37
2.2.1 <i>In vitro</i> model of inflammation	37
2.2.2 <i>In vivo</i> model of ischemia	37
2.3 Animal studies	37
2.3.1 Animal model of inflammation	37
2.3.2 Animal model of ischemia	38
2.4 Cell viability assays	39
2.5 Cell membrane damage assays	40

2.6 Autophagy assays	40
2.7 Griess assays	40
2.8 Ago2 treatments and injections	40
2.9 RA-NP synthesis	41
2.10 RA-NP treatments and injections	41
2.11 Immunostaining analysis	42
2.11.1 Immunocytochemistry analysis	42
2.11.2 Immunohistochemistry analysis	42
2.12 Vessel density analysis	44
2.13 WB analysis	44
2.14 Neurological scores and sensorimotor tests	46
2.15 Infarct volume analysis	46
2.16 Hemorrhage transformation analysis	47
2.17 Biodistribution studies	47
2.18 Biochemical analysis/toxicity studies	47
2.19 ELISA	48
2.20 Data analysis	48
Chapter 3 – Argonaute-2 protects the neurovascular unit from damage caused by systemic inflammation	49
3.1 Abstract	49
3.2 Introduction	50
3.3 Results	51
3.3.1 LPS induces Ago2 downregulation and endothelial activation	51
3.3.2 Microglial, but not astrocytic Ago2, is necessary for LPS-induced cell activation	53
3.3.3 Ago2-restored endothelium reduces microglia activation	55
3.3.4 Systemic administration of Ago2 normalizes endothelial and glial activation in the mouse cortex	57
3.3.5 Systemic administration of Ago2 normalizes inflammatory response and induces neuroprotection in the mouse hippocampus	59
3.4 Discussion	61
3.5 Conclusions	66
Chapter 4 – Retinoic acid-loaded nanoparticles promote neurovascular protection in stroke	69
4.1 Abstract	69
4.2 Introduction	70
4.3 Results	71

4.3.1 OGD compromises endothelial viability and induces autophagic Ago2 degradation	71
4.3.2 RA-NP require Ago2 to recover vascular function compromised by ischemia	74
4.3.3 Treatment with intravenous RA-NP protects from brain injury but does not restore functional outcome after ischemia	78
4.3.4 Treatment with intravenous RA-NP promotes neuronal survival	82
4.3.5 Treatment with intravenous RA-NP normalizes the inflammatory response acutely after cerebral ischemia	85
4.3.6 Treatment with intravenous RA-NP stimulates angiogenesis in the subacute phase	86
4.4 Discussion	88
4.5 Conclusions	94
Chapter 5 – General discussion	97
Chapter 6 – Conclusions	103
Chapter 7 – References	105

List of Figures

Chapter 1 – Introduction

- Figure 1.1 – Schematic illustration representing the temporal profile of the main pathophysiological mechanisms occurring after stroke onset. 3
- Figure 1.2 – Schematic representation of NVU structure. 14
- Figure 1.3 – Schematic domain arrangement of Ago protein. 22
- Figure 1.4 – RA metabolism and signaling pathway. 29

Chapter 2 – Materials and Methods

- Figure 2.1 – Characterization of primary brain endothelial cell cultures. 35
- Figure 2.2 – Characterization of primary brain glial cell cultures. 36
- Figure 2.3 – Schematic representation of the experimental setup used in the animal model of inflammation. 38
- Figure 2.4 – Schematic representation of the experimental setup used in the animal model of ischemia. 39

Chapter 3 – Argonaute-2 protects the neurovascular unit from damage caused by systemic inflammation

- Figure 3.1 – LPS-induced Ago2 downregulation correlates with loss of endothelial function. 52
- Figure 3.2 – Ago2 is not involved in LPS-induced astrocyte activation. 54
- Figure 3.3 – Ago2 silencing reduces microglial inflammatory responses. 55
- Figure 3.4 – Ago2-restored endothelium normalizes microglia response. 56
- Figure 3.5 – Systemic administration of Ago2 restores endothelial barrier function and normalizes glial activation in the cortex. 57
- Figure 3.6 – Systemic administration of Ago2 normalizes inflammatory activation and induces neuroprotection in the hippocampus. 59
- Figure 3.7 – Representative confocal images of GFAP, CD11b (green) and Ago2 (red) obtained in cortex and hippocampal slices from mice injected with saline (CTR) and 2 mg/kg LPS. 60
- Figure 3.8 – Proposed model for Ago2 regulation of the endothelial and glial crosstalk. 67

Chapter 4 – Retinoic acid-loaded nanoparticles promote neurovascular protection in stroke

Figure 4.1 – Ischemia compromised BEC viability and downregulated Ago2.	72
Figure 4.2 – Ischemia following a recovery period compromised BEC viability and induced autophagic Ago2 degradation.	73
Figure 4.3 – Basal BEC viability, eNOS, NO, and Ago2 expression levels after RA-NP treatment.	74
Figure 4.4 – RA-NP required Ago2 to recover vascular function compromised by ischemia.	76
Figure 4.5 – Real-time imaging of BEC after treatments.	77
Figure 4.6 – Schematic representation of the experimental setup used herein and biodistribution analysis.	78
Figure 4.7 – Intravenous injection of RA-NP enhanced tissue survival in MCAO-subjected animals.	79
Figure 4.8 – Intravenous injection of RA-NP did not complete functional outcome in MCAO-subjected animals.	80
Figure 4.9 – RA-NP increased neuronal survival after brain ischemia.	83
Figure 4.10 – RA-NP normalized the acute inflammatory response after cerebral ischemia.	85
Figure 4.11 – RA-NP ameliorated vascular function in the subacute phase.	87
Figure 4.12 – Proposed model for RA-NP regulation of the brain vascular function, via Ago2, under ischemia.	95

List of Tables

Chapter 1 – Introduction

Table 1.1 – Overview of characteristics, advantages, and limitations of focal ischemic stroke animal models	8
Table 1.2 – Post-translational Ago modifications.	24

Chapter 2 – Materials and Methods

Table 2.1 – List of primary and secondary antibodies, and dilutions used for immunocytochemistry.	42
Table 2.2 – List of primary and secondary antibodies, and dilutions used for immunohistochemistry.	43
Table 2.3 – List of primary, secondary, and housekeeping antibodies used for WB analysis.	45

Chapter 4 – Retinoic acid-loaded nanoparticles promote neurovascular protection in stroke

Table 4.1 – Serum levels of ALT, AST, CK, urea, sodium, lipase, and α -amylase measured three and seven days post-MCAO.	81
--	----

List of Abbreviations

ADH	Alcohol dehydrogenase
Ago	Argonaute
ALT	Alanine aminotransferase
AST	Aspartate aminotransferase
ATP	Adenosine triphosphate
BafA1	Bafilomycin A1
BBB	Blood-brain barrier
BCA	Bicinchoninic acid
BDNF	Brain-derived neurotrophic factor
BEC	Brain endothelial cells
BSA	Bovine serum albumin
CBF	Cerebral blood flow
CCK-8	Cell counting kit-8
CD	Cluster of differentiation
CK	Creatine kinase
CM	Conditioned media
CNS	Central nervous system
CRABP	Cellular retinoic acid binding protein
CREB	Cyclic adenosine monophosphate response element-binding protein
CMP	Chromatin modifying proteins
CO ₂	Carbon dioxide
CT	Computed tomography
CTR	Control
CYP26	Cytochrome P450 family 26 enzymes
Cy5	Cyanine5 N-hydroxysuccinimide ester
C-P4H	Collagen prolyl-4-hydroxylase
D	Day
DIC	Differential interference contrast
DMEM-HG	Dulbecco's Modified Eagle's Medium-high glucose
DMSO	Dimethyl sulfoxide
DNA	Deoxyribonucleic acid
DS	Dextran sulfate
dsRNA	Double-stranded ribonucleic acid
EC	Endothelial cell
EC-CM	Endothelial cell-conditioned media
ECA	External carotid artery
EDTA	Ethylenediamine tetraacetic acid
EGF	Epidermal growth factor
ELISA	Enzyme-linked immunosorbent assay
eNOS	Endothelial nitric oxide synthase
ET	Endothelin
E.g.	For example
FABP5	Fatty acid-binding protein type 5
FITC	Fluorescein isothiocyanate

GAPDH	Glyceraldehyde 3-phosphate dehydrogenase
GDNF	Glial cell line-derived neurotrophic factor
GFAP	Anti-glial fibrillary acidic protein
GLUT1	Glucose transporter isoform 1/Slc2a1
Gw182	Glycine-tryptophan (W)-repeat-containing protein of 182 kilodalton
HEPES	4-(2-hydroxyethyl)-1-piperazineethanesulfonic acid
HK	Housekeeping
HUVEC	Human umbilical vein endothelial cells
Iba-1	Anti-ionized calcium binding adaptor molecule-1
ICA	Internal carotid artery
IL	Interleukin
iNOS	Inducible nitric oxide synthase
i.e.	In other words
kDa	Kilodalton
LDH	lactate dehydrogenase
LPS	Lipopolysaccharide
MAP2	Microtubule-associated protein 2
MCA	Middle cerebral artery
MCAO	Middle cerebral artery occlusion
miR	Micro ribonucleic acid
MMP	Matrix metalloproteinase
MRI	Magnetic resonance imaging
mRNA	Messenger ribonucleic acid
N	N-terminal
NaCl	Sodium chloride
NADPH	Nicotinamide adenine dinucleotide phosphate
NeuN	Neuronal nuclear protein
NO	Nitric oxide
NOS	Nitric oxide synthase
NOX	Nicotinamide-adenine dinucleotide phosphate oxidase
NP	Nanoparticles
NRP	Neuropilin
NVU	Neurovascular unit
N ₂	Nitrogen
OGD	Oxygen and glucose deprivation
OGD/R	Oxygen and glucose deprivation followed by a recovery period
O ₂	Oxygen
pAkt	Phosphorylated- serine/threonine-protein kinase
PAZ	PIWI/Argonaute/Zwille
PBS	Phosphate-buffered saline
PEG	Poly(ethylene glycol)
PEI	Polyethylenimine
PFA	Paraformaldehyde
PIWI	P-element-induced Wimpy tested
PI3K	Phosphoinositide 3-kinase
PLGA	Poly(lactic-co-glycolic acid)
PPAR	Peroxisome proliferator activated protein
Pp38	Phosphorylated p38 mitogen-activated protein kinase
PSD-95	Postsynaptic density protein 95

PTEN	Phosphatase and tensin homolog
p47phox	Nicotinamide adenine dinucleotide phosphate oxidase cytosolic protein p47phox
p62	Ubiquitin-binding autophagy substrate receptor
P-bodies	Processing bodies
RA	Retinoic acid
RAGE	Receptor for advanced glycation end products
RALDH	Retinaldehyde dehydrogenase
RA-NP	Retinoic acid-loaded nanoparticles
RAR	Retinoic acid receptors
RARE	Retinoic acid-response element
RBP	Retinol binding protein
RDH	Retinol dehydrogenases
RISC	Ribonucleic acid-induced silencing complex
RNA	Ribonucleic acid
ROS	Reactive oxygen species
rt-PA	Recombinant tissue plasminogen activator
RXR	Retinoid X receptors
TGF- β	Transforming growth factor-beta
TLR4	Toll-like receptor 4
TNF- α	Tumor necrosis factor-alpha
TTC	2,3,5-triphenyltetrazolium chloride
TRAF6	Tumor necrosis factor-alpha receptor-associated factor 6
TRE	Total radiant efficiency
RA	Retinoic acid
RISC	RNA-induced silencing complex
ROI	Regions of interest
ROS	Reactive oxygen species
SEM	Standard error of the mean
siR	Short (or small) interfering ribonucleic acid
ssRNA	Single-stranded ribonucleic acid
STAIR	Stroke treatment academic industry roundtable
STRA6	Retinoic acid 6 receptor
S100B	S100 calcium-binding protein B
VE	Vascular endothelial
VEGF	Vascular endothelial growth factor
VEGFR2	Vascular endothelial growth factor receptor 2
WB	Western blot
ZO	Zonula occludens
β -III tubulin	Beta-III tubulin

Chapter 1

Introduction

1.1 Ischemic stroke

Stroke is a leading cause of mortality and disability worldwide with enormous socioeconomic implications for the economy and healthcare systems (Feigin *et al.* 2022) and available projections estimate that this health condition will rise in the coming years (World Stroke Organization Annual Report 2021). The most common subtype of stroke is ischemic stroke, accounting for 87% of all strokes (Roger *et al.* 2011). Despite considerable advances, there is still a lack of effective treatments that reverse the symptoms and disability for all patients due to the narrow therapeutic window of existing therapies where benefits overlap risks, highlighting the need for developing novel and safer therapies. To better understand this serious medical condition, the following subchapter will briefly introduce stroke, its pathophysiologic mechanisms, and the experimental models used for research, as well as the existent strategies for prevention and treatment.

1.1.1 Epidemiology, definition, and diagnosis

According to the global health estimates from the World Health Organization, in 2019, stroke was the second leading cause of death (after ischemic heart diseases) and the third leading cause of adult disability (just beyond neonatal disorders and ischemic heart diseases) (Global Health Estimates 2019; Feigin *et al.* 2022). In 2019, approximately 100 million people worldwide suffered and live with the effects of stroke (World Stroke Organization Annual Report 2021), a burden that increased substantially from 1990 to 2019 (Feigin *et al.* 2019). In the same period, stroke was the leading cause of death in Portugal (Statistics Portugal 2021). To aggravate this situation, there was a significant increase in stroke mortality and incidence rates in people younger than 70 years; in particular, the risk of stroke in people over 25 years has increased from 1 in 6 to 1 in 4, implying that globally, every fourth person aged over 25 years will have a stroke in their lifetime (World Stroke Organization Annual Report 2021). Worryingly, this scenario will continue to rise in the coming years due to population growth, increasing life expectancy (World Stroke Organization Annual Report 2021), and people with risk factors for the occurrence of a stroke (e.g., obesity, diabetes mellitus, arterial hypertension, sedentary lifestyle, and consumption of tobacco and alcohol) (Feigin *et al.* 2019). Additionally, the impact of stroke goes beyond patient mortality and disability, since it leaves an enormous burden on informal caregivers (person, family member or not, who guarantees care and daily support to stroke patients without economic remuneration) (Achilike *et al.* 2020). After receiving treatment in medical facilities, patients

return home, where informal caregivers provide long-term support (Garnett *et al.* 2022). This long-term situation negatively impacts caregiver health and wellness since may promote depression, anxiety, impaired cognitive function, decreased quality of life, and, ultimately, mortality (Rigby *et al.* 2009). Although efforts have been done to create health and social services to assist caregivers, there is still a lack of support improving their quality of life (Garnett *et al.* 2022). Thus, post-stroke management is undoubtedly a medical and social emergency.

Despite its global impact, the concept of stroke is not consistently defined in clinical practice and research; nonetheless, the traditional definition of stroke is a neurological deficit that occurs when the blood supply to an area of the brain is suddenly interrupted or when a blood vessel in the brain bursts (Sacco *et al.* 2013). Blood carries oxygen (O₂) and essential nutrients needed to maintain the metabolic demand of the brain. There are three primary types of strokes: (i) transient ischemic attack (also called a mini-stroke, characterized by a blood clot that typically reverses on its own) (Panuganti *et al.* 2022), (ii) hemorrhagic stroke (characterized by bleeding from a burst or leaking blood vessel in the brain and further subdivided into intracerebral or subarachnoid hemorrhage) (Unnithan *et al.* 2022), or (iii) ischemic stroke (characterized by an inadequate blood supply to an area of the brain due to a blockage of an artery – focal ischemia). From those, ischemic stroke is the most common subtype, accounting for 87% of all strokes (Roger *et al.* 2011), and can be instigated by a thrombotic or embolic obstruction of a cerebral artery. In the case of thrombosis, inadequate cerebral blood flow (CBF, defined as the blood volume that flows per unit mass or volume of brain tissue per time unit) occurred due to a plaque build-up constricting inside of brain arteries, causing a thrombotic stroke. In the case of embolic stroke, a blood clot formed outside of the brain breaks loose and migrates to the brain, causing a sudden decrease in CBF and, ultimately, cell death (Musuka *et al.* 2015).

Depending on the affected area, patients can display different symptoms and impairments; typically, the most common include headache, loss of vision, speech deficits, deficits in sensation, limb paresis, and semi-paralysis (Rathore *et al.* 2002). Atypical symptoms include binocular blindness, dysphagia, dysarthria, foreign accent, confusion, amnesia, altered consciousness, and isolated vertigo (Hankey 2017). Strokes are usually diagnosed and identified by doing physical tests in patients (namely the FAST (Facial drooping, Arm weakness, Speech difficulties, and Time) test (Hankey and Blacker 2015)) and analyzing brain scan images (obtained by non-contrast brain computerized tomography (CT) scan and diffusion-weighted brain magnetic resonance imaging (MRI) (Hankey 2017)). The primary aim of neuroimaging is to identify the presence of other types of brain diseases and to differentiate between ischemic and hemorrhagic stroke. CT scans are sensitive for detecting cerebral mass lesions and acute hemorrhages; however, these scans may not be sensitive enough to detect an ischemic stroke (especially if it has a small infarct size or is located in the posterior fossa). On the other hand, the diffusion-weighted MRI has higher resolution and sensitivity than CT to detect an acute ischemic stroke. Nevertheless, MRI scanners are less available and more expensive than CT scanners and cannot be performed on patients with certain types of implanted devices (e.g., pacemakers). For these reasons, guidelines from the American Heart Association/American Stroke Association Stroke Council recommend that an

MRI scan should only be prescribed if it can be obtained as quickly as a CT scan; if not, the CT scan is the recommended test (Yew and Cheng 2009). In this context, 'time is brain' (Gomez 1993) and the available acute stroke treatments cannot wait for more detailed imaging reports when the historic and physical analysis are consistent for a stroke. In the future, less expensive and more accessible diagnostic tools to quickly detect ischemic stroke should be developed, as portable devices and/or diagnostic biomarker panels that may have widespread usage if they were considered useful in clinical decision-making) (Patil *et al.* 2022).

Considering that ischemic stroke is the most common subtype, the focus of this Thesis was the ischemic stroke, and the following discussions are related to this subtype.

1.1.2 Pathophysiology and ischemic cascade

The pathophysiology of ischemic stroke is complex and has been extensively investigated in the last years. A plethora of signaling pathways (e.g., bioenergetic failure, ionic imbalance, excitotoxicity, oxidative stress, inflammation, blood-brain barrier (BBB) dysfunction, and cell death) closely interconnected is already uncovered (Figure 1.1). Therefore, targeting any of the events of this ischemic cascade may constitute a potential therapeutic approach for stroke (Brouns and De Deyn 2009; Qin *et al.* 2022).

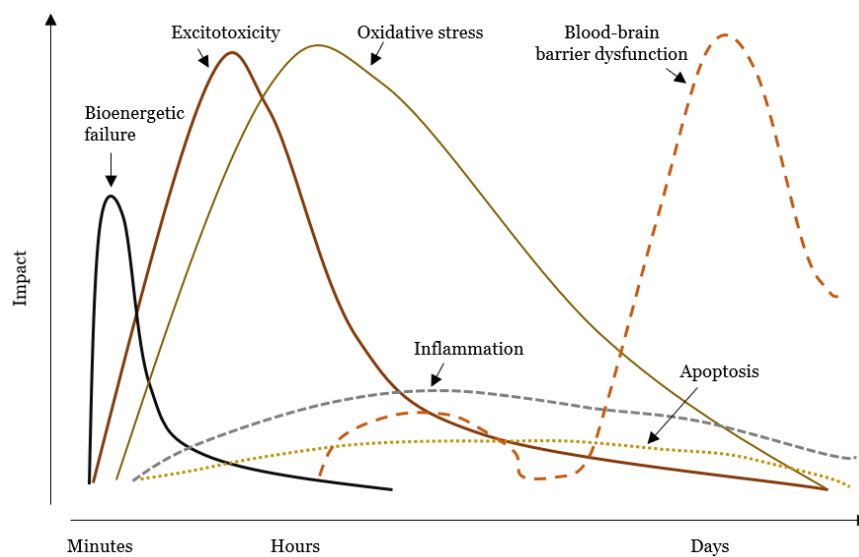


Figure 1.1 – Schematic illustration representing the temporal profile of the main pathophysiological mechanisms occurring after stroke onset. A cascade of damaging events occurs, demising the brain tissue. The x-axis of the graphic represents the event evolution over time (from minutes to days of focal onset) and the y-axis represents the impact on cerebral damage (Adapted from Brouns and De Deyn 2009).

As previously mentioned, ischemic stroke occurs due to insufficient delivery of O₂ and nutrients to the brain (hypoperfusion) caused by an embolic or thrombotic occlusion to a major cerebral artery (Musuka *et al.* 2015). Moreover, it is characterized by the development of two main regions,

namely an irreversibly damaged ischemic core and a salvageable peri-infarct region. The ischemic core is an electrically and functionally inactive cerebral region characterized by irreversible and necrotic cell death, while the peri-infarct region (or penumbra) is a heterogenous and electrically impaired region with the potential to be salvage (Liu *et al.* 2010). In this sense, clinical therapies for acute stroke usually target the peri-infarct region, and its salvage by prompt reperfusion will ensure a better clinical outcome following a stroke (Liu *et al.* 2012).

After hypoperfusion, the oxidative glycolysis (the main energy source for increased brain activity) becomes a less effective anaerobic pathway and induces bioenergetic failure by decreasing adenosine triphosphate (ATP) production in the mitochondria (Hertz 2008). Lower production of ATP within minutes of ischemic insult results in the dysfunction of all energy-dependent metabolic processes and changes in ion pumps located in cell membranes, altering the intracellular ion concentrations (by decreasing potassium levels and increasing calcium and sodium levels). The ionic imbalance across the plasma membrane also promotes the inflow of water and consequently, cytotoxic edema due to a rapid swelling of neurons and glial cells (Yao *et al.* 2021). Additionally, intracellular calcium levels become too high and trigger an uncontrolled and detrimental release of glutamate (the major excitatory neurotransmitter in the brain) that mediates excitotoxic synaptic transmission (Belov Kirdajova *et al.* 2020). At the same time, nuclear and cytosolic proteases are activated (e.g., endonucleases cleave deoxyribonucleic acid (DNA) sequences to cause apoptosis and calpains hydrolyze cytoskeletal proteins), leading to an amplification of the initial ischemic insult (excitotoxicity). If the energy supply was not re-established in time, these changes may induce rapid necrotic cell death (Khanna *et al.* 2014). Additionally, O₂ and nitrogen-derived radicals are generated, and oxidative stress is triggered due to an imbalance between the overexpression of reactive oxygen species (ROS) and the decreased ability of the cellular antioxidant defense system to neutralize these substances (Chan 2001). Previously, it was hypothesized that oxidative stress has a major role in neuronal damage following ischemic stroke. Accordingly, antioxidant approaches to scavenge ROS were evaluated in clinical trials. However, these approaches failed to reveal a robust amelioration in a phase III trial in stroke patients (Shuaib *et al.* 2007). Although this hypothesis has not been proven so far, the involvement of ROS in ischemia injury was not rejected and novel approaches focusing on more relevant sources of oxidative stress have been investigated (Radermacher *et al.* 2013). For example, nicotinamide adenine dinucleotide phosphate (NADPH) oxidase (NOX) is another relevant source of oxidative stress, which in turn induces the expression of additional free radicals and triggers cell death (He *et al.* 2021). In mice, genetic deletion of NOX2 (Kahles *et al.* 2007) or pharmacological inhibition of NOX4 (Kleinschnitz *et al.* 2010), the main NOX isoforms expressed in the CNS, significantly reduced infarct size and improved neurological outcome following experimental stroke. Although the inhibition of NOX activity represents a promising strategy for stroke therapy, the lack of specificity and toxicity of existing inhibitors (e.g., diphenyleneiodonium, apocynin, plumbagin, VAS2870) still need to be optimized before being translated to clinical practice (Kim *et al.* 2017). The oxidative stress following ischemic stroke also triggers the development of inflammatory responses, initially to help the clearance of damaged

tissues and then contribute to aggravating tissue damage. After cerebral ischemia, glial cells (microglia and astrocytes) are activated within minutes, driving acute inflammation as the defense and repair mechanisms to maintain brain homeostasis; in particular, reactive microglia (the resident immune cells of the central nervous system (CNS)) can polarize into classic pro-inflammatory phenotype and alternative protective phenotype. The classic microglia phenotype (identified by CD11b, CD16, CD32, and CD86 markers) aggravates damage by producing pro-inflammatory mediators (e.g., interferon-gamma, interleukin (IL)-1 β , IL-6, tumor necrosis factor (TNF)- α , ROS, nitric oxide (NO), matrix metalloproteinase (MMP)-9 and -3, and chemokine interferon- γ inducible protein) (Lian *et al.* 2021). In this context, pro-inflammatory mediators initiate pro-death signaling pathways and induce the expression of adhesion molecules (e.g., intercellular adhesion molecule-1, vascular adhesion molecule-1), selectins (e.g., E- and P-selectins), and integrins on endothelial cells. These adhesion molecules contribute to leukocyte rolling, adhesion to the endothelium, and infiltration into the brain (Profaci *et al.* 2020). The infiltration of leukocytes occurs within hours after stroke onset (with neutrophils being the first immune infiltrating cells, followed by monocytes, macrophages, and T cells (Wu *et al.* 2022)) and promotes the release of cytotoxic agents that damage the extracellular matrix, increase BBB permeability, and exacerbate brain edema. Considering these evidence, therapeutic strategies aimed to inhibit neurotoxic microglial activation may be promising pathways/paves for stroke treatment. In fact, the inhibition of microglial activation (via toll-like receptor 4 signaling pathway) in transient focal cerebral ischemia rats was correlated with decreased neurological deficits, reduced infarct volume, and attenuated apoptosis in the peri-infarct region (Sun *et al.* 2015). Additionally, approaches for promoting alternative polarization of microglia constitute another relevant topic. The alternative microglia phenotype (identified by Ym1 and CD206 markers (Perego *et al.* 2011)) suppresses inflammation and promotes tissue recovery by producing anti-inflammatory cytokines (e.g., IL-10, IL-4, IL-13, transforming growth factor-beta (TGF- β), and insulin-like growth factor 1). Due to the impact of microglial activation and polarization on neuroinflammation, targeting microglial expression patterns is a promising therapeutic strategy for ischemic stroke (Lian *et al.* 2021) and has shown protection and neurological recovery in experimental stroke models (Zhang *et al.* 2019; Hu *et al.* 2022). Modulation of microglial polarization can be achieved with transcription factors and receptors, ion channels, genes, and drugs (Jiang *et al.* 2020). Besides the microglia, astrocytes mediate inflammatory response and BBB function. In the acute phase, astrocytes display a neurotoxic phenotype (e.g., identified by C3d marker), inducing the release of IL-1 β to disrupt tight junctions and BBB; in contrast, in the subacute phase, they may display a neuroprotective phenotype (e.g., identified by S100A10 marker), releasing VEGF-A to promote angiogenesis and BBB repair. Nonetheless, these mechanisms and the time window in which astrocytes exert their functions following ischemic stroke need to be further explored (Li *et al.* 2022).

Lastly, the ischemic cascade activates other signaling pathways (e.g., MAPK family, p53, p38, c-jun, and cyclin dependent kinase-5) that culminate in cell death, namely necrosis in the ischemic core and apoptosis in the penumbra region (Rami and Kögel 2008). Taken together, multiple

efforts have been conducted to elucidate these pathophysiological mechanisms in order to screen potential therapeutic targets for stroke. Accordingly, experimental models of focal cerebral ischemia (including *in vitro* and animal models) are indispensable tools in stroke research.

1.1.3 Experimental models

The complex pathophysiology of ischemic stroke cannot be only investigated in *in vitro* models with single cells or brain tissue samples with the absence of blood vessels, blood flow, and leukocyte infiltration. However, these models allow the study of specific mechanisms under energy-deficient conditions similar to cerebral ischemia (e.g., mechanisms of cell death and autophagy) (Holloway and Gavins 2016). Ischemic conditions can be modeled *in vitro* by the removal of O₂ and glucose and by chemical or enzymatic inhibition of cellular metabolism. The most widely used *in vitro* model of ischemic stroke is oxygen and glucose deprivation (OGD), where glucose is removed from the medium, and the normal O₂/carbon dioxide equilibrated medium is replaced by nitrogen/carbon dioxide equilibrated medium in a hypoxic chamber (Sommer 2017). Additionally, it is also possible to mimic glutamatergic excitotoxicity (an event of the ischemic cascade mentioned in subsection 1.1.2) by exposing the culture to glutamate or N-Methyl-D-aspartate (NMDA; a glutamate receptor agonist) (Holloway and Gavins 2016). For studying brain cell-specific responses to OGD, primary cell cultures have shown invaluable benefits (Sommer 2017) since they have high transendothelial electrical resistance, a measurement of electrical resistance across a cellular monolayer, and a strong indicator of the integrity and permeability of the cellular barriers, in comparison with cells lines (Holloway and Gavins 2016). For these reasons and for the purpose of this Thesis, primary cell cultures were performed and exposed to OGD to mimic ischemia. Unfortunately, and besides the paucity of cellular interactions, primary cell cultures use neonatal rodent cells, which may have questionable relevance to adult humans. Therefore, it is crucial to combine them with animal studies to get a similar cellular environment and anatomic conditions of human stroke (Fluri *et al.* 2015).

Animal models of focal cerebral ischemia are highly predictable, have similar cerebrovascular anatomy to humans, and allow direct access to brain tissue and the possibility to study vasculature and perfusion (Kuriakose and Xiao 2020). The majority of stroke experiments have been conducted in small animals (e.g., mice and rats) due to their lower obtaining and maintenance cost (when compared to larger animals), greater ethical acceptability (Fluri *et al.* 2015), and because they are genetically modifiable (Herson and Traystman 2015). Since in humans 70% of all ischemic strokes result from the occlusion of the middle cerebral artery (MCA) (Bogousslavsky *et al.* 1988), the MCA occlusion (MCAO) model is one of the standard models of stroke. The MCA supplies blood to the primary sensory and motor cortices of the brain, mainly associated with control of the upper limbs and face; thus, its occlusion results in sensory and motor impairments, which are common disabilities following a stroke. Accordingly, the intraluminal MCAO is the most common method of focal ischemic stroke used in more than 40% of stroke research for neuroprotection experiments in rat and mouse models (Howells *et al.* 2010). It was first described

by Koizumi and colleagues (Koizumi *et al.* 1986) and later modified by Longa and colleagues, who reported a different technique to insert the monofilament and occlude the origin of the MCA (Longa *et al.* 1989). In the method developed by Koizumi and colleagues, a monofilament is introduced through an incision in the common carotid artery (CCA), into the internal carotid artery (ICA) until the entrance of the MCA. In the method developed by Longa and colleagues, a monofilament is introduced from the external carotid artery (ECA) into the ICA to block the origin of the MCA (McCabe *et al.* 2018; Li Y *et al.* 2021). This minimally invasive procedure can be used to induce transient or permanent focal cerebral ischemia, exhibiting tremendous differences in various pathophysiological mechanisms (e.g., neuronal apoptosis, neuroinflammation, and oxidative stress) (Li and Zhang 2021). While transient MCAO results in smaller infarct volumes and larger penumbra region, permanent MCAO origins severe and irreversible injury which may contribute to the failure of many neuroprotective agents. Thus, considering all these facts, researchers tend to prefer the former model (transient MCAO) (Xu *et al.* 2013). Despite the infarct size and distribution can considerably differ among laboratories, due to selected strains or filaments, the diameter of the suture tip, or the insertion distance of the suture, this model is widely chosen by the researchers due to lack of craniotomy, ease of manipulation, accurate control of the ischemic duration, and the presence of a significant and salvageable penumbra (McCabe *et al.* 2018; Li Y *et al.* 2021). In mice, C57BL/6 and SV/129 are the most commonly used strains due to their susceptibility to ischemic injury and, consequently, for the production of sizable infarct volumes (Kuriakose and Xiao 2020). In addition, others reported that the MCAO model is appropriate to reproduce neuronal cell death mechanisms, cerebral inflammation, and BBB damage (mechanisms in focus in this research work) (Fluri *et al.* 2015). For these reasons, in the present Thesis, the intraluminal filament model of transient MCAO was reproduced in C57BL/6 mice. Importantly, despite its benefits and advantages, it is important to point out that the intraluminal filament MCAO model does not mimic the mechanism of occlusion observed in humans, which is thromboembolism. To mimic this mechanism, embolic MCAO models (e.g., microsphere- or macrosphere-induced stroke model and thromboembolic clot model) were already developed. However, these models have some drawbacks, including the lack of experimental control regarding the exact duration of ischemia (Herson and Traystman 2014). Thus, the intraluminal filament MCAO model remains the preferred model for stroke research since it produces more reproducible results.

Other animal models are available for experimental research, although they are highly invasive (craniotomy model), do not completely mimic the human pathophysiology mechanisms (photothrombosis model), and do not control the duration of ischemia (endothelin (ET)-1 model) (Kuriakose and Xiao 2020). The characteristics, advantages, and limitations of available focal ischemic stroke animal models are summarized in Table 1.1.

Table 1.1 – Overview of characteristics, advantages, and limitations of focal ischemic stroke animal models. Abbreviations: ECA, external carotid artery; ET, endothelin; ICA, internal carotid artery; MCA, middle cerebral artery; MCAO, middle cerebral artery occlusion. (Adapted from Fluri *et al.* 2015; Kuriakose and Xiao 2020; Li and Zhang 2021).

Focal ischemic stroke model (commonly used animals)	Approaches	Insult regions	Advantages	Limitations
ET-1 model (Rats, mice)	ET-1 exogenous application (a potent and long-acting vasoconstrictive peptide) close to the origin of the MCA. The artery constriction is controlled through the dose of ET-1 injected.	Caudate nucleus and cortex.	-Transient and permanent occlusion possible; -Less invasive; -Low mortality.	-Duration of ischemia not controllable; - ET-1 may induce astrocytosis and facilitates axonal sprouting (interfering with the interpretation of neural repair experiments).
Photothrombosis model (Rats, mice)	Systemic injection of a photosensitive dye (Rose-Bengal) followed by focal irradiation of the cortex through the intact skull with a certain range of wavelength laser beams.	Ipsilateral cortex.	-Enables well-defined localization of an ischemic lesion; -Highly reproducible; -Less invasive; -Low mortality; -Suitable for poststroke epileptogenesis studies.	-Minimal peri-infarct cortex; -Causes early vasogenic edema; -Not suitable for investigating neuroprotective agents.

(table continues on the next page)

Intraluminal filament MCAO model (Rats, mice)	Introduction of a monofilament from the ECA into the ICA and advancing it to block the origin of the MCA.	Anterior neocortex and the lateral part of the caudate putamen supplied by the MCA (transient occlusion); Caudoputamen and cortex (permanent occlusion).	-Transient and permanent occlusion possible; -Allows the study of ischemia-reperfusion injury; -Exhibits ischemic penumbra; -Highly reproducible.	-Reproducibility depends on surgical skill; -Spontaneous hyperthermia; -Risk of hemorrhage; -Not suitable for studying thrombolysis.
Embolitic stroke model				
Microsphere- or macrosphere-induced stroke model (Rats)	Insertion of artificial spheres into the MCA or ICA via the ECA using a microcatheter, which passively enters the cerebral circulation through the blood flow.	Parietotemporal cortex, hippocampus, thalamic striatum, and a small region of the contralateral hemisphere.	-Microspheres induce graded infarcts; -Preserves the blood supply to the hypothalamus (avoiding hypothalamic infarctions and subsequent hyperthermia).	-Heterogeneous ischemic infarcts; -Not suitable for transient occlusion and thrombolysis.
Thromboembolic clot model (Rats)	Application of clots or thrombin-induced clots from autologous blood.		-Closely mimics a large proportion of human strokes and therefore, is suitable to study thrombolytic agents alone or combined with neuroprotective drugs.	- Variability of the rate and timing of reperfusion; -Lack of experimental control regarding the exact duration of ischemia; -Heterogeneous ischemic infarcts.

Despite the benefits of animal models and the vast amount of promising obtained data, the clinical translation has been disappointing, mostly due to differences between animal models and humans. Accordingly, two main reasons could justify these hurdles: (i) the strict control that has been done to the animals in the laboratory does not reflect the human condition (where the perception of symptoms and/or the immediate medical assistance still contribute to the diversity of mechanisms and, consequently, the clinical results), and (ii) the majority of animals used in the research studies are healthy, young, of a similar age, and of the same gender, which do not mimic the human condition (where the majority of strokes occurs in elderly patients with

associated comorbidities) (Jickling *et al.* 2015). Recently, Pound and Ram categorized additional clinical translational problems, highlighting: (i) poor external validity of animal studies (the inability of animal models to mimic human disease progression, difficulty recapitulating human risk factors, comorbidities, and the use of clinically irrelevant outcome measures); (ii) poor internal validity of animal studies (failure to control bias, lack of pre-trial sample size calculations, inappropriate analyses, and poor physiological monitoring), and (iii) problems relating to clinical trials (insufficient selectivity in targeting patients and late administration of experimental drugs). Other explanations include weak preclinical evidence and publication bias (Pound and Ram 2020). To overcome these problems and improve scientific rigor, Stroke Treatment Academic Industry Roundtable (STAIR) guidelines were developed and later updated, including (i) the study of a dose-response, namely the minimum effective and maximum tolerated dose; (ii) the recognition of the therapeutic window for neuroprotection; (iii) the study of multiple endpoints and the development of behavioral studies at least 2 to 3 weeks after stroke; (iii) the monitoring of physiological parameters; (iv) the study in multiple species, and (v) the recognition of other reproducibility parameters, including good scientific practice, studies in aged animals with comorbidities and from different genders, and interaction studies with medications prescribed for stroke patients. (Lyden *et al.* 2021). Thus, future stroke research should focus on these recommendations to adjust the proposals as much as possible to the human condition.

1.1.4 Prevention and acute treatment strategies

The growing burden of stroke suggests that primary prevention of the first stroke and secondary prevention of subsequent or recurrent stroke have been ineffective. Considering that up to 90% of all ischemic strokes worldwide could be prevented with the primary prevention of recognized vascular risk factors (including lifestyle modification, hypertension, hyperglycemia, lipid disorders, antithrombotic therapy, asymptomatic carotid stenosis) (Diener and Hankey 2020; Mosconi and Paciaroni 2022), primary prevention is a public health priority. Primary prevention includes the establishment of healthy dietary and lifestyle habits (e.g., reduction of smoke consumption and alcohol intake, keeping a healthy body weight, and getting regular checkups) (Kleindorfer *et al.* 2021). Population education and synergy strategies between healthcare providers, government agencies, R&D institutions, and the population are examples of promising strategies to effectively implement primary prevention (Owolabi *et al.* 2022). Additionally, after the first stroke, the risk of recurrent stroke without treatment increases over time; in particular, it increases by 10% after 1 week, 15% after 1 month (Coull *et al.* 2004), 25% after 5 years, and 40% after 10 years (Mohan *et al.* 2011), suggesting that secondary prevention is another health concern that can reduce the risk of recurrent stroke up to 80-90% (Rothwell *et al.* 2007). Secondary prevention includes additional carotid endarterectomy or stenting (surgical procedures to remove a build-up of fatty deposits in carotid arteries), closure of patent foramen ovale (a small opening in the wall between the right and left upper chambers of the heart) after cryptogenic stroke (a stroke of unknown cause), treatment of insulin resistance, and best medical treatment of

intracranial stenosis (a severe narrowing of an artery within the skull) (Diener and Hankey 2020; Kleindorfer *et al.* 2021). Globally, the implementation of primary and secondary prevention strategies will not only significantly reduce the burden of stroke but also substantially decrease the burden of other major diseases (including heart and renal disease, type 2 diabetes, dementia, and some types of cancer, since the risk factors are common), reducing the economic burden (Owolabi *et al.* 2022).

Additionally, considerable efforts have been made to improve outcome after a stroke. To date, the only approved therapeutic approach for selected ischemic stroke patients is the reperfusion therapy using intravenous thrombolysis therapy, with recombinant tissue plasminogen activator (within 4.5 hours of stroke onset) or endovascular mechanical thrombectomy (within 24 hours of stroke onset). The primary goal of both approaches is to remove the occlusive blood clot for revascularization; blood clotting is a physiological response to vessel injury and involves the development of a loose platelet plug, followed by the activation of a coagulation cascade, resulting in a fibrin mesh that strengthens the clot (Bhaskar *et al.* 2018). Intravenous thrombolytic with recombinant tissue plasminogen activator (rt-PA or alteplase, the only Food and Drug Administration-approved drug) is the gold effective treatment for ischemic stroke (NINDS t-PA Stroke Study Group 1997; Green and Shuaib 2006). Other tissue plasminogen activators, namely reteplase or r-PA (NCT05295173) and tenecteplase or TNK t-PA (NCT03785678, NCT05281549), are being investigated in patients with acute ischemic stroke. These activators are a class of proteolytic enzymes that attaches to the fibrin in the blood clots and catalyzes the conversion of plasminogen to plasmin, inducing clot dissolution (Rouf *et al.* 1996); however, excessive plasmin-mediated fibrinolysis may induce bleeding, which ultimately result in patient death (Zhao T *et al.* 2019). In fact, hemorrhagic transformations constitute one main drawback of thrombolytic therapy. Additionally, it has limited efficacy due to its narrow therapeutic window where it can be applied (within 4.5 hours after the onset of symptoms), making only 12% of ischemic stroke patients eligible for this treatment (Vanacker *et al.* 2016). Extending the therapeutic window beyond 4.5 hours, i.e., delayed rt-PA treatment has already been tested, however, it induced severe hemorrhagic transformations and ultimately led to patient death (National Institute of Neurological Disorders and Stroke rt-PA Stroke Study Group 1997; Knecht *et al.* 2017). Other perfusion/blood thinners approaches were considered, namely the use of anticoagulants to slow down the development of clots (e.g., aspirin) and antiplatelets to prevent platelets from clumping together to form a clot (e.g., heparin). However, these approaches were associated with an increased risk of intracranial hemorrhage without providing a benefit in functional outcomes (van der Steen *et al.* 2022). Another established treatment for acute ischemic stroke is mechanical endovascular thrombectomy (Goyal *et al.* 2016; Tawil and Muir 2017), a minimally invasive procedure to mechanically fragment a blood clot or thrombus from an artery via coil retriever, aspiration, stent-retriever, or mechanical disruption using laser or ultrasound (Bhaskar *et al.* 2018). It improves clinical outcome and reduces disability in stroke patients, especially who are receiving oral anticoagulants (patients not selected for pharmacological thrombolysis) (Chen *et al.* 2022). However, this procedure is time-consuming, expensive, and still has some procedural

complications (Nogueira *et al.* 2018). Endovascular mechanical thrombectomy can be combined with intravenous thrombolytic with rt-PA (called bridge therapy), taking advantage of the best of both approaches (Bhaskar *et al.* 2018). Beyond the reperfusion therapy using thrombolysis, the modulation of endogenous mechanisms (e.g., excitotoxicity, cellular apoptosis, inflammation, oxidative stress, and BBB dysfunction) through neuroprotective approaches can be used as an effective strategy for stroke treatment; recently, the combination of both strategies (reperfusion and neuroprotection) has been investigated. Accordingly, Vos and colleagues reviewed the ongoing clinical trials investigating the effects of neuroprotective agents in combination with reperfusion therapies. Among all neuroprotective agents tested, only five reported positive clinical outcomes (Vos *et al.* 2022) and none was focused on supporting cerebral vascular function in the peri-infarct region (highlighting the relevance and innovation of the proposal under study in this Thesis). For similar purposes, cell-based approaches have been emerging with promising preclinical results (Seyedaghamiri *et al.* 2022), despite being still prone to improvements. These approaches are based on the systemic application or infusion into the infarcted area of neural stem/progenitor cells or bone-marrow-derived stem cells (due to their ability to undergo both self-renewal and differentiation may promote the release of pro-angiogenic and neurogenic molecules) (Rust 2020). Nonetheless, besides having a low capacity to cross the BBB, some reports demonstrated that their injection could increase the possibility of an intravascular clot and/or induce tumorigenicity *in situ* (George *et al.* 2018; Lukomska *et al.* 2019). Taken together, it is remarkable that the paradigm in stroke treatment has been shifting over time. Early research prioritized the discovery of novel thrombolytic drugs with better reperfusion efficacy than rt-PA, while recent investigations are concentrated on improving this treatment through the combination with antiplatelet or neuroprotective drugs, for example, (i) NCT04890366 is testing the combination of rt-PA with the immune modulator dimethyl fumarate, an Nrf2 activator that regulates the expression of several antioxidant and/or defense proteins (Farina *et al.* 2021); (ii) NCT05188417 is investigating the effect of rt-PA with tirofiban, an antagonist of fibrinogen binding to the glycoprotein IIb/IIIa receptor that inhibits platelet aggregation (Tao *et al.* 2021); (iii) NCT03284463 is combining the rt-PA with the neuroprotective drug glibenclamide that reduces infarct volume, inhibits neuronal cell death, promotes neurogenesis and angiogenesis, and improved sensorimotor and cognitive function by blocker the Sur1-Trpm4 channel in transient and permanent stroke models (Simard *et al.* 2014). Additionally, previous approaches exclusively focused on the recovery of neuronal function, while this neurocentric view has been replaced by the concept of the neurovascular unit (NVU), which encompasses the neuronal, glial, and vascular components and their interaction (Tiedt *et al.* 2022). Current stroke treatments are focused on targeting this unit using pleiotropic agents that act in multiple mechanisms of the ischemic cascade (Lyden *et al.* 2021). Thus, recognizing the relevance of this unit will lead to a higher probability of success in the context of stroke, leading us to explore in the following subchapter the roles of the NVU, focusing on cerebral vasculature, as a key and undervalued NVU component.

1.2 NVU: a focus on cerebral vasculature

The NVU constitutes a highly structured and dynamic multicellular system that maintains brain homeostasis. However, under cerebral ischemia, dysfunctions of the NVU occur and contribute to the progression of stroke pathophysiological mechanisms (Wang *et al.* 2021). Within the NVU, cerebral vasculature plays an active role in several processes, including the control of BBB permeability and CBF. Thus, the maintenance of proper cerebrovascular function after cerebral ischemia may offer considerable benefits in post-stroke recovery. Accordingly, there are evidence that vascular remodeling is positively correlated with longer patient survival (Krupinski *et al.* 1994) and active brain angiogenesis reduces loss of cognitive and motor function in stroke (Hayashi *et al.* 2003; Buga *et al.* 2014; Eldahshan *et al.* 2021). Considering that there is a lack of effective strategies targeting cerebral vasculature in stroke, possibly due to constraints in identifying neuroprotective approaches directed to brain blood vessels without inducing hemorrhagic transformations, the focus of this Thesis was to investigate a protective approach directed to this NVU component. Thus, the following subchapter will discuss the cellular composition and role of NVU, with a focus on cerebral vasculature function, and the importance of its targeting for brain repair in pathological conditions.

1.2.1 NVU concept and cellular composition

The NVU concept emerged from the first Stroke Progress Review Group meeting, where it was postulated that a successful stroke therapy must restore and maintain the normal function of the NVU by reestablishing the CBF in the microvascular bed, preserving vascular integrity, and minimizing neuronal death (Stroke Progress Review Group 2001). Later, besides stroke, this concept was gradually applied to other CNS disorders to identify more effective therapies, including Alzheimer's disease (Lee and Pienaar 2014), Parkinson's disease (Kortekaas *et al.* 2005), dementia (Beishon and Panerai 2021), Huntington's disease (Drouin-Ouellet *et al.* 2015), and amyotrophic lateral sclerosis (Garbuzova-Davis *et al.* 2008).

The NVU is a dynamic and interdependent structure composed of neurons, glial cells (astrocytes, microglia, and oligodendrocytes), vascular cells (endothelial cells, pericytes, and vascular smooth muscle cells), and the basement membrane (Sato *et al.* 2022) (Figure 1.2). On the inner surface of the brain blood vessels are found the brain endothelial cells (BEC), which control the selective and hemodynamic movement of molecules due to their unique properties (detailed in subsection 1.2.2). These cells are a central component of BBB and the first line of defense against the entrance of external pathogens and immune cells (Li J *et al.* 2021), highlighting the importance of protecting this cellular component and improving its activity under pathological conditions. Additionally, BEC are surrounded by a thin supporting basement membrane composed of collagen IV, laminin, fibronectin, heparan sulfate proteoglycans, and nidogens (Xu *et al.* 2018), in close interaction with a non-complete layer of pericytes with contractile properties. Pericytes covering microvessels, along with smooth muscle cells covering large-diameter vessels like

arteries and veins, are mural cells responsible for the regulation of blood pressure and the structural integrity of the vascular wall and, consequently, supporting brain angiogenesis (Sweeney *et al.* 2016; Brown *et al.* 2019). In the outer part of the basement membrane, astrocytes mediate the BBB permeability via the upregulation of tight junction proteins in BEC, regulate pericyte-mediated vascular changes (Abbott 2002), and promote brain networks by predominantly inducing excitatory synaptogenesis through the secretion of thrombospondin (Christopherson *et al.* 2005), glypican 4 and 6 (Allen *et al.* 2012), EphrinA3 (Carmona *et al.* 2009), cholesterol/ApoE (Mauch *et al.* 2001), and brain-derived neurotrophic factor (BDNF) (Gómez-Casati *et al.* 2010). Additionally, microglial cells are widely distributed in the CNS and can interact with neurons to regulate synapse pruning by removing synapses from less active neurons (Paolicelli *et al.* 2011) or with cerebral vasculature to modulate the BBB permeability (Dudvarski Stankovic *et al.* 2016). Lastly, oligodendrocytes provide metabolic support to neurons (Philips and Rothstein 2017), mediate neural transmission and plasticity through BDNF signaling (Jang *et al.* 2019), and modulate BBB permeability by upregulating tight junction proteins in BEC via TGF- β signaling (Seo *et al.* 2014).

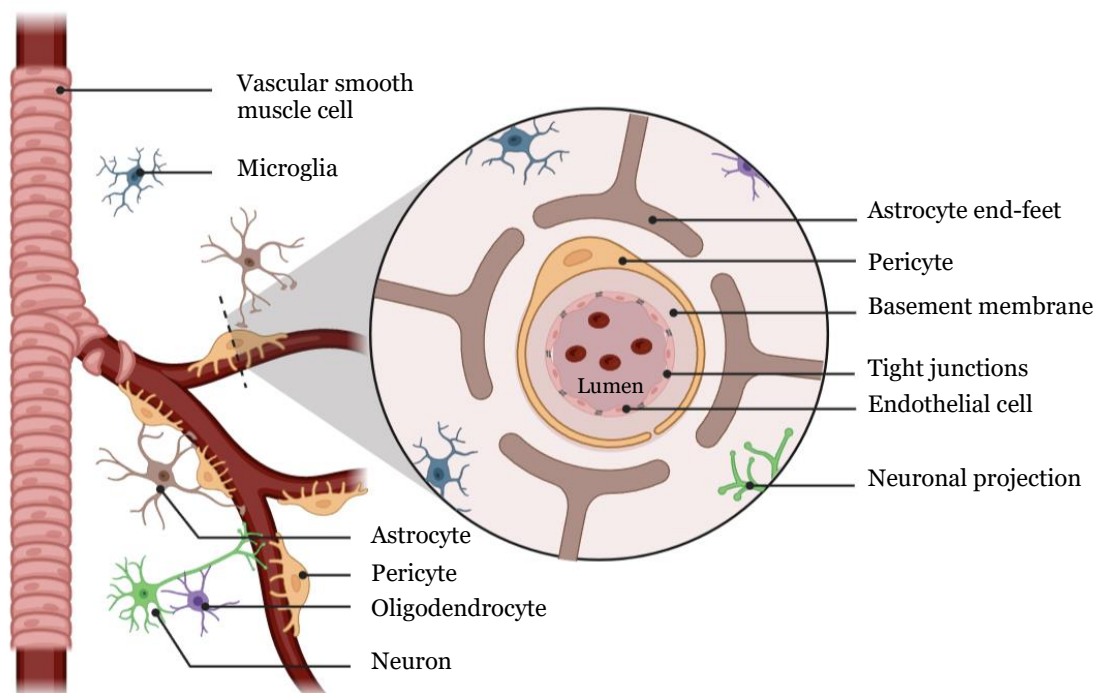


Figure 1.2 – Schematic representation of NVU structure. The NVU is composed of neurons, glial cells (microglia, astrocytes, and oligodendrocytes), and vascular cells (endothelial cells, pericytes, and vascular smooth muscle cells), which together regulate CBF and BBB function (Adapted from Tenreiro *et al.* 2016).

Collectively, in response to changes in neuronal activity, the dynamic interactions between NVU cells regulate local perfusion through alterations in vascular intraluminal diameter, a mechanism termed neurovascular coupling or functional hyperemia (Carmignoto and Gomez-Gonzalo 2010). This process initiates when glutamate produced by activated neurons stimulates astrocytes and pericytes to release vasoconstrictive and vasodilatory mediators, which may control the tone of

the surrounding vasculature and, consequently, regulate local CBF (Girouard and Iadecola 2006). Additionally, the interaction between NVU cells results in a highly efficient and selective BBB (Wang *et al.* 2021), restricting the passage of most molecules from the systemic circulation into the CNS. In particular, large molecules are unable to cross the BBB and only 2% of small molecules that are lipid soluble and have a molecular weight less than 400 Da can cross it (also, O₂ and carbon dioxide passively diffuse across the BBB) (Pardridge *et al.* 2003). Although the special anatomical properties of the BBB allow CNS protection, this barrier constitutes the major roadblock to the development of effective brain drug delivery systems. In particular, 95% of molecules did not progress toward drug development because of BBB physiological characteristics (Dong 2018). To circumvent the restrictive BBB properties and increase the drug concentration in the brain, physiochemical modifications of the therapeutic drugs have been considered, namely their lipidization (i.e., the addition of lipid analogs to the polar groups of the therapeutic molecules to increase its permeability and passive diffusion through the BBB). Although these approaches have considerable potential (Patel *et al.* 2009), they may modify drug molecule structure, therapeutic effectiveness, and increase the penetration through the biological membranes *in vivo*, thereby promoting a rapid removal from the blood (Pardridge 2005). Alternatively, nanotechnology-based drug delivery systems (e.g., polymeric and solid lipid nanoparticles (NP), nanogels, nanoemulsions, and nanoliposomes) have great potential for brain drug delivery (Patel *et al.* 2009). They are extremely versatile, and their physiochemical properties can be modified in countless ways (e.g., changing the composition, size, surface coating, solubility, cellular transport mechanisms, and delivery route) to enhance the stability in blood circulation and to promote efficient drug delivery in the brain (Saraiva *et al.* 2016; Ferreira and Bernardino 2020). In the preclinical stroke research, different nanosystems have been used for treatment and diagnosis (Nozohouri *et al.* 2020; Correa-Paz *et al.* 2021) and their combination with pre-existing therapies (namely with rt-PA) improve neurological outcome and decrease lesion progression in rodent stroke models (Tiebosch *et al.* 2012; Fukuta *et al.* 2017). Nevertheless, these nanostructures still face some brain and systemic toxicity problems. For example, metallic (iron or gold) NP accumulation in the brain over a long period of time can trigger neuronal apoptosis, mitochondrial dysfunction, and neuroinflammation (Cheng *et al.* 2021; Liao *et al.* 2022). Lastly, strategies to temporarily disrupt the BBB, with osmotic agents or ultrasound mechanisms, are used to enhance CNS chemotherapy (Patel *et al.* 2009; Rapoport 2001). However, as BBB permeability increases following almost CNS diseases, including ischemic stroke (Liu *et al.* 2015), the brain therapy paradigm should shift and it would be highly interesting to take advantage of this BBB opening to achieve more effective drug delivery, rather than considering it just a simple anatomical disruption. Collectively, for effective brain targeting and therapy, nanotechnology-based drug delivery systems or other strategies (e.g., brain permeability enhancers, viral vectors, exosomes, delivery through active transporters) need to recognize and consider the properties of the cerebral vasculature, detailed in the following subsection.

1.2.2 Physiological function of cerebral vasculature

The cerebral vasculature is composed of a thick-walled layer of BEC (named endothelium) that lines the inner of blood vessels and defines the interface between the vascular system and the brain parenchyma. In comparison with peripheral endothelial cells, BEC display unique properties to maintain brain function, including increased expression of mitochondria, low expression of leukocyte adhesion molecules, reduced wall thickness, lack of fenestrations, and specialized junction proteins. Increased expression of mitochondria is crucial to produce the ATP needed to sustain the metabolic work capability of the BBB and supply the ion gradient necessary for some of the transport functions (Sanchez-Covarrubias *et al.* 2014). Additionally, BEC express a very low amount of leukocyte adhesion molecules (including E- and P-selectins) needed for leukocyte entrance into the CNS, thus restricting the movement of immune cells into the brain. This is also regulated by endothelial junctions between BEC that limit the extravasation of leukocytes, metastatic cells, and solutes across the vessel wall, contributing to maintain BBB integrity and permeability (Stamatovic *et al.* 2008). These junctions orchestrate molecular and physical signals that induce a proper angiogenic process and, consequently, vascular remodeling (Szymborska and Gerhardt 2018). They are composed of multiple adhesion proteins, namely adherens and tight proteins. Adherens proteins include cadherins, catenins, and nectins that provide stability of inter-endothelial cell communication and control the permeability for plasma molecules with large molecular weight (McConnell *et al.* 2017). Among them, vascular endothelial (VE)-cadherin (also known as cadherin 5 or CD144) is the most important molecule for the maintenance of the vascular structure (Sauteur *et al.* 2014) by inducing the Rho/GTPase activation (Giannotta *et al.* 2013). VE-cadherin is essential during initial vessel assembly processes since its inactivation or truncation in embryos is lethal due to a defect in the signaling of vascular endothelial growth factor (VEGF) and its receptor (VEGFR) (Carmeliet *et al.* 1999). Additionally, tight proteins include claudins, occludins, junctional adhesion molecules, and endothelial cell-selective adhesion molecules that control the permeability for plasma molecules with smaller molecular weights (Duong and Vestweber 2020) and maintain BEC polarity, contributing to the maintenance of the BBB integrity. BEC polarity represents the asymmetric distribution of proteins, namely transporters and efflux pumps, allowing specific functions in different regions within the same cell (Worzfeld and Schwaninger 2016). Although both junctional complexes are composed by different proteins, both are physically connected with the actin cytoskeleton to maintain their stability and functionality, besides having similar roles in signaling pathways, including the regulation of gene transcription (Hartsock and Nelson 2008). Besides adhesion molecules, tyrosine-protein kinase receptor Tie-2 (Braun *et al.* 2019), the sphingosine 1-phosphate receptor (Wang and Dudek 2009), and integrins stabilize endothelial junctions (Hynes 2009). Altogether the adhesion molecules, receptors, and integrins not only maintain the barrier integrity but also act as signaling molecules to assist endothelial response to inflammatory molecules or growth factors. For example, BEC β 5 integrin is essential to recruit the focal adhesion kinase to the adhesion sites (Avraham *et al.* 2003) and, consequently, to induce BEC tube formation (Haskell *et al.* 2003). Nonetheless, pathological events (like as cerebral

ischemia) may disrupt the characteristics and function of these tight junctions, which, in turn, compromise vascular function and promotes BBB breakdown. In ischemic stroke, BBB breakdown is one of the earliest pathophysiological events, occurring within the first 6 hours after its onset in animals (Strbian *et al.* 2008) and human studies (Merali *et al.* 2017). Fortunately, this deleterious event is reversible and provides a therapeutic target for CNS therapies. Accordingly, the main mechanisms underlying BBB dysfunction are summarized in the following subsection.

1.2.3 Cerebral endothelial dysfunction: implications for CNS

CNS disorders are often related to BBB dysfunction due to a pro-thrombogenic and pro-inflammatory BEC phenotype that intensifies neuroinflammation (Archie *et al.* 2021; Sato *et al.* 2022) and, ultimately, may cause intracerebral hemorrhage (Bernardo-Castro *et al.* 2020). Thus, understanding the mechanisms that compromise cerebral endothelial function, usually associated with BBB dysfunction, may provide insights to develop effective treatments for stroke and other CNS diseases. It has been reported that cerebral endothelial dysfunction predominantly occurs due to an impairment in endothelium-derived NO bioactivity, disruption of endothelial junctions, and increased ROS levels. NO is the most important endothelium-derived vasodilation mediator produced from the conversion of L-arginine to L-citrulline through the tightly regulated activity of the endothelial nitric oxide synthase (eNOS or NOS₃) (Vanhoutte *et al.* 2016). After its production within the cytosol of BEC, NO diffuses into adjacent vascular smooth muscle cells, then activating soluble guanylyl cyclase and increasing the synthesis of 3,5-cyclic guanosine monophosphate, which, ultimately, mediate vascular tone (Jin and Loscalzo 2010). Although the production of NO within the brain vasculature is also dependent on the activity of the inducible isoform (iNOS) (Hemmerich *et al.* 1985), eNOS is the most predominant isoform expressed in the vasculature (Förstermann *et al.* 1994). Under physiological conditions, the eNOS-derived NO controls vascular tone, regulates CBF (Atochin and Huang 2010), and acts as a messenger during long-term potentiation (a form of synaptic plasticity in the hippocampus implicated in spatial learning) (Hawkins *et al.* 1998). Under pathological conditions, such as traumatic brain injury (Robertson *et al.* 2011), Alzheimer's disease (Austin *et al.* 2013), and stroke (Sawada and Liao 2009), a dysregulation in the eNOS activity is observed, impacting endogenous NO levels and, consequently, affecting CBF. Additionally, the overproduction of NO was correlated with increased infarct size and intensified cerebral vascular injury in the striatum of a rat model of MCAO, through the reduction of claudin-5 and ZO-1 expression levels (Mohammadi 2016), while the inactivation of the enzyme responsible for NO production decreased cerebral edema (Mohammadi *et al.* 2011). Considering that vascular remodeling is rapidly initiated via eNOS following ischemic stroke (Liu *et al.* 2014; Lapi and Colantuoni 2015) and increases patient survival (Krupinski *et al.* 1994), the modulation of eNOS/NO signaling pathway can be recognized as a potential therapeutic approach for the post-stroke recovery. Thus, it was assessed in the experimental research of this Thesis. Another hallmark of endothelial dysfunction is the impaired activity and expression of endothelial junction proteins, which increase paracellular permeability

and, consequently, damage the neuronal microenvironment (Li *et al.* 2021). It occurs due to an increase in cytosolic calcium levels (initially observed after cerebral ischemia), which activates myosin light chain kinase, increasing its phosphorylation and subsequently promoting actin contraction. In turn, occurs a redistribution of actin-bound endothelial junction proteins (namely the occludin, VE-cadherin, and ZO-1), leading to the loss of their primary sealing function and BBB breakdown (Wang *et al.* 2018). Accordingly, in a rat model of MCAO, increased BBB permeability within 3 days after onset was correlated with decreased levels of claudin-5, occludin, and ZO-1 proteins (Jiao *et al.* 2011). Lastly, the increased calcium levels, neutrophil recruitment, and mitochondrial dysfunction trigger the overproduction of ROS (Pun *et al.* 2009), which constitutes another feature of endothelial junction dysfunction and breakdown of the extracellular matrix via activation of MMP, subsequently resulting in BBB leakage (Gasche *et al.* 2001; Gu *et al.* 2011). In a rat model of MCAO, claudin 5 and occludin were susceptible to ROS (Zhang S *et al.* 2018) and, in another model of intracerebral hemorrhage, MMP-2 and MMP-9 activated by ROS downregulated the levels of ZO-1 (Zeng Z *et al.* 2020). It is reported that ROS may induce cytoskeleton rearrangements and redistribution, thereby disrupting the stability of the endothelial junctions. In particular, ROS produced from xanthine/xanthine oxidase system induced redistribution and degradation of occludin and claudin-5 in BEC through the activation of Ras homolog family member A (RhoA), phosphoinositide 3-kinase (PI3K), and serine/threonine-protein kinase (Akt; also known as PKB) signaling pathways (Schreibelt *et al.* 2007). Collectively, the discovery of agents aiming to control the mechanisms that induce cerebral endothelial dysfunction may lead to the development of promising therapeutic strategies for manipulating BBB disruption and subsequent neurological dysfunction in the treatment of stroke and in other CNS diseases. In the following section, the current approaches targeting cerebral vasculature were reviewed.

1.2.4 Targeting the cerebral vasculature for brain repair in pathological conditions

Despite numerous efforts, to date, there is a lack of effective treatments for brain repair in pathological conditions, not because there is a lack of promising candidates, but mainly due to the difficulty in targeting cerebral vasculature and delivering neuroprotective agents in therapeutic concentrations to the brain in a safe manner (Pardridge 2005). Nonetheless, several strategies have been proposed to bypass the barrier features of cerebral vasculature and take advantage of endogenous transport mechanisms. So far, the most promising strategies include gene-based therapies (including viral and non-viral vectors) and drug delivery nanocarriers (e.g., metallic, polymeric, lipid, and targeted nanoparticles, whereas the latter can be conjugated to a variety of targeting moieties including peptides, monoclonal antibodies, and plasma proteins) (Hersh *et al.* 2016). In the setting of stroke, intracerebral administration of adenoviral vectors expressing fibroblast growth factor 2 (a potent angiogenic factor) reduced the infarct area and promote a neurologic improvement in a rat model of transient MCAO (Watanabe *et al.* 2004). In

addition, epigenetic approaches using miR have been proposed: for example, lentiviral-mediated overexpression of miR-210 promoted brain angiogenesis by upregulating brain-derived neurotrophic factors in an ischemic mouse model (Zeng *et al.* 2016). Also, endothelium-targeted deletion of miR-15a/16-1 cluster *in vitro* by lentivirus and *in vivo* using knockout mice promoted post-stroke brain angiogenesis and enhanced cognitive recovery (Sun *et al.* 2020). In another CNS disorder, namely in the context of Alzheimer's disease, lentivirus-mediated overexpression of miR-124 promoted vascular integrity in the hippocampus and cerebral cortex in a transgenic amyloid precursor protein/presenilin-1 mouse model (Li *et al.* 2019). Despite viral vectors being a good option for efficient gene delivery to CNS, they present some disadvantages, including small packaging capacity, elevated costs, immunogenicity, mutagenicity, and risk of oncogenesis. Thus, non-viral vector-based gene therapies are emerging due to their safety profile, low cost, and high-scale production (Gallego *et al.* 2022). For example, miR-124-loaded RVG29-poly(ethylene glycol) (PEG)-poly(lactic-co-glycolic acid) (PLGA) NP prevented ischemic brain injury and contributed to the recovery of neurologic function (Hao *et al.* 2020). The RVG29 peptide is used to enhance the brain-specific function of a range of systemically delivered agents, particularly nucleic acids (Cook *et al.* 2015). Also, drug delivery nanocarriers decorated with specific ligands for the vasculature provide a promising opportunity for brain delivery and repair. For example, chitosan nanospheres loaded with a caspase-3 inhibitor and decorated with anti-mouse transferrin receptor monoclonal antibody, which recognizes the transferrin type 1 expressed on the cerebral vasculature, were designed. Accordingly, besides efficiently crossing the BBB, this formulation improves neurological repair by decreasing infarct volume, and neurological deficit in a mouse model of MCAO (Karatas *et al.* 2009). In addition, the intracerebral implantation of human neural stem cells attached on the surface of VEGF-releasing PLGA microparticles allowed the development of a vascular network, by attracting host endothelial cells into this neuroscaffolding in a rat model of transient MCAO (Bible *et al.* 2012). A more complex combined system using hyaluronic acid-based biodegradable hydrogel scaffold, mixed with PLGA microspheres containing VEGF and angiopoietin-1 (crucial mediator for vessel maturation) enhanced brain angiogenesis *in situ* in a MCAO mice model (Ju *et al.* 2014). Importantly, a number of osmotic agents have been used to enhance the delivery of nanoparticles (Muldoon *et al.* 1995; Maia *et al.* 2011; Machado-Pereira *et al.* 2018), recombinant proteins stem cells (Jiao *et al.* 1996), and viral vectors (Foley *et al.* 2014) by modifying vascular permeability in the brain and increase paracellular diffusion, including mannitol (Gonzales-Portillo *et al.* 2014) and arabinose (Fredericks and Rapoport 1988), leading to osmotic retraction of the endothelium, thereby opening tight junctions. Ultimately, the administration route is also an important criterion for the success of any of the previously proposed approaches. The local administration (e.g., intracerebral injection) definitively improves the effectiveness of the treatment, however, it is too invasive and may promote local inflammation. Alternatively, systemic administration is the most popular choice for animal and clinical studies and retroorbital sinus administration has emerged as a safe alternative and low distress systemic route, compared with lateral tail vein injection (Yardeni *et al.* 2011; Wang *et al.* 2015). Recently, the nose-to-brain administration route represents another promising and less invasive strategy able to precisely reach the brain (Gallego *et al.* 2022),

however, it still presents some disadvantages (e.g., requires a small volume to administer, agents are rapidly eliminated due to mucociliary clearance, and the frequent use of this route may lead to mucosal damage). In addition, it can be challenging for clinical practice since it requires patient cooperation, which may not be feasible after a stroke and during an epileptic seizure, for example (Lochhead and Thorne 2012; Musumeci *et al.* 2019). Ultimately, all of the aforementioned approaches and delivery routes have advantages and limitations, and the development of safe strategies to achieve therapeutic concentrations of agents in the brain remains a challenge in a pathological context. The second part of the work presented in this thesis explores the use of PEI-based nanoparticles that allow the controlled release of a neuroprotective agent (with mannitol in their constitution) for improving vascular brain function by potentiating the Ago2 endogenous mechanism, an approach that may be promising in stroke. For a better understanding of this endogenous mechanism, the following subchapter details the function of the Ago family, with a special focus on the function of Ago2.

1.3 Ago proteins

Ago proteins represent a highly conserved family found in almost all eukaryotes and are key players in gene-silencing pathways (RNAi) guided by small non-coding RNA components (including miR, short interfering RNA (siR), and PIWI-associated RNA). In particular, these proteins bind to siR or miR to guide post-transcriptional gene silencing either by destabilization of the messenger RNA (mRNA) or by translational repression (Hutvagner and Simard 2008). Ago proteins are key for embryonic development, cell differentiation, and stem cell maintenance (Peters and Meister 2007). In humans, among the four Ago-like proteins, Ago2 has been widely studied due to its unique slicer catalytic activity essential for miR processing (Fagerberg *et al.* 2013; Koester and Dougherty 2022). Besides being essential for early embryonic development (Cheloufi *et al.* 2010), Ago2 is required for cell survival, tube network formation (Asai *et al.* 2008), and VEGF signaling (Ye ZL *et al.* 2015) in peripheral endothelial cells, suggesting a possible involvement of this protein in the vascular function. Nonetheless, the role of Ago2 and the mechanisms mentioned above remain unknown in ischemic cerebral endothelium, despite its potential. Thus, the Ago protein family and the mechanisms underlying their biological functions will be addressed in the following subchapter, with a particular emphasis on Ago2 roles.

1.3.1 Structural and functional insights of the Ago protein family

Ago protein family was first discovered in a plant mutagenesis screen to identify new genes involved in *Arabidopsis thaliana* development. In this study, the phenotypic consequence of losing Ago1, observed by the absence of the lateral expansion of the leaf blade, during the *Arabidopsis* development highlighted the importance of the Ago family (Bohmert *et al.* 1998). Later, the members of this highly conserved family were identified in almost all eukaryotes,

bacteria, and archaea (Tolia *et al.* 2007). According to the domain architecture, the eukaryotic Ago family is categorized into four clades: (i) Ago-like proteins, termed by *Arabidopsis* Ago1, (ii) PIWI-like proteins, named by *Drosophila melanogaster* Piwi, maintain germline stem cell function, (iii) WAGO proteins (also called group III Ago), typified by worm *Caenorhabditis elegans*-specific Ago, act as secondary Ago proteins, and (iv) Trypanosoma Ago family, termed by *Trypanosoma brucei*, inhibits transposon activity (Bollmann *et al.* 2018).

In this research work, the focus was the Ago-like subfamily since it comprises most Ago proteins involved in cytoplasmatic posttranscriptional gene silencing and nuclear transcriptional regulation and can be found in all tissues ubiquitously (e.g., brain, heart, kidney, liver, lung, spleen, adipose, thymus, testis, placenta) (Carmell *et al.* 2002; Sasaki *et al.* 2003; Valdmanis *et al.* 2012). In humans, four Ago-like proteins are expressed (Ago1–4), containing a molecular weight of about 100 kDa. Although containing few non-conserved amino acids in their functional domains (Nakanishi 2022), they display four distinct conserved domains, including (i) the amino-terminal (N) domain, (ii) the PIWI-Argonaute-Zwille (PAZ) domain, (iii) the Middle (MID) domain, and (iv) the P-element-induced whimpy tested (PIWI) domain. These domains are connected by two less characterized regions named Linker 1 (L1) and Linker 2 (L2) (Giorgi *et al.* 2012). In particular, the N-terminal domain contains a variable N-terminal region that facilitates the separation of the small RNA:target duplex after slicing through interrupting the duplex structure (Kwak and Tomari 2012). The PAZ domain (also present in Dicer, a ribonuclease required for miR biogenesis) confers an RNA binding pocket that binds Ago protein into the 3' end overhang of small RNA (Ma *et al.* 2004). The MID domain functionally coordinates with the PAZ domain and provides an RNA binding platform that binds the 5' phosphate of small RNA through a highly conserved tyrosine in the nucleotide-binding pocket (Ma *et al.* 2004; Frank *et al.* 2012). Finally, the PIWI domain contains the catalytic triad DDH required for endonucleolytic cleavage of target RNA, promoting its degradation and post-transcriptional silencing (Parker *et al.* 2004) (Figure 1.3). Although it was initially thought that only Ago2 possessed catalytic and slicing activity, later it was demonstrated that Ago3 also has the catalytic tetrad within the PIWI domain (Park *et al.* 2017). However, the Ago3 slicer activity is a controversial question since it depends on other unidentified Ago3-accessory proteins (Park *et al.* 2017; Park *et al.* 2020), highlighting the relevance of Ago2. It has been suggested that the different chromosome location might be the reason only Ago2 displays the complete slicer activity. In humans, Ago2 gene is located on chromosome 8q24.36, while Ago1, Ago3, and Ago4 genes are clustered together and located on chromosome 1p34.3 (Höck and Meister 2008). In accordance, a similar pattern is observed in mice: Ago2 gene is located on chromosome 15qD3, while Ago1, Ago3, and Ago4 genes are located on chromosome 4qD2.2 (Valdmanis *et al.* 2012).

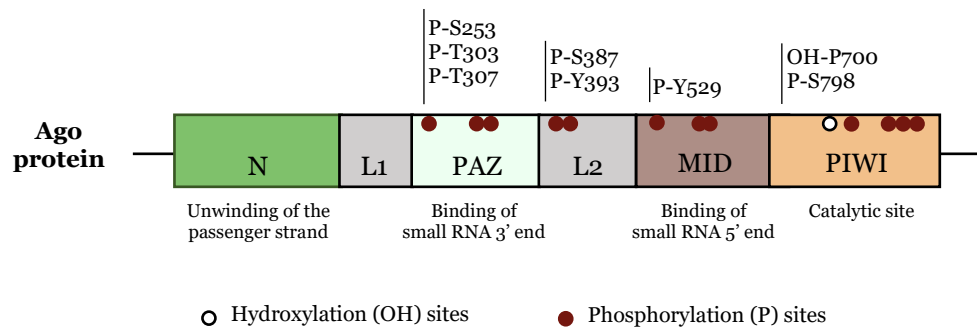


Figure 1.3 – Schematic domain arrangement of Ago protein and post-translational modifications. The functions of PAZ, PIWI-Argonaute-Zwille MID, and PIWI domains and the hydroxylation and phosphorylation sites are indicated. Abbreviations: L1, Linker1; L2, Linker2; MID, Middle domain; N, amino-terminal domain; P, proline; PAZ, PIWI-Argonaute-Zwille domain; PIWI, P-element-induced whimpy tested domain; S, serine; T, threonine; Y, Tyrosine. (Adapted from Schirle *et al.* 2012; Müller *et al.* 2020).

At the cellular level, Ago-like proteins are diffusely distributed in the cytoplasm, and a small fraction is observed in cytoplasmic processing bodies (P-bodies) and in stress granules (Leung *et al.* 2006; Leung and Sharp 2013). In the cytoplasm, Ago proteins are the major component of the RNA-induced silencing complex (RISC; which also includes DICER, TRBP, and PACT) responsible for small RNA silencing. The RISC complex incorporates one strand of miR or siR and then both annealing to a complementary mRNA sequence to regulate gene expression. siR triggers the degradation of mRNA, whereas miR can induce either mRNA degradation or suppression of protein synthesis (depending on the complementarity sequence to the target gene transcript) (Hutvagner and Simard 2008; Bodak *et al.* 2017a; Bodak *et al.* 2017b). Within the cytoplasm, Ago proteins can migrate to P-bodies due to two post-translational modifications: phosphorylation or hydroxylation (Horman *et al.* 2013) (detailed in subsection 1.3.2). In P-bodies, Ago proteins associate with multiple proteins like GW182 (Jakymiw *et al.* 2005; Liu *et al.* 2005b), Dcp1/2 Liu *et al.* 2005a), and rck/p54 (Chu and Rana 2006) and possibly target mRNA degradation or translational repression (Kulkarni *et al.* 2007). However, this idea has been challenged since in *Drosophila*, Ago proteins repress target mRNA without P-bodies (Eulalio *et al.* 2007). Moreover, Ago2 has been associated with other cytoplasmic structures. Upon cellular stress conditions (e.g., oxidative stress, heat shock, viral infection, and ischemia) or when translation initiation is inhibited, Ago proteins (along with miR) migrate from the cytoplasm to the stress granules (Leung and Sharp 2013) and associate with HuR (Bhattacharyya *et al.* 2006) and rck/p54 (Chu and Rana 2006). Remarkably, the targeting of Ago proteins to stress granules only occurs in the presence of miR, and the same is not observed for P-bodies (Leung *et al.* 2006). Nevertheless, it remains unclear which of these structures are essential for Ago function. Although mainly found in the cytoplasm, Ago proteins are also found in the nucleus, where they can perform multiple functions. In particular, cytoplasmic Ago proteins can enter the nucleus by nuclear import pathways (e.g., importin 8) in complexes with double-stranded RNA (dsRNA), miR, single-stranded RNA (ssRNA) or as a free form and exert multi-functional roles: (i) RNA activation: recruitment of chromatin modifying proteins (CMP) by complexes with Ago-dsRNA

or miR increases active chromatin marks (e.g., methylation of the H3K4me3, a major active histone mark in eukaryotes), promoting transcription at the targeted promoter; (ii) Transcriptional gene silencing: recruitment of CMP by complexes with Ago-dsRNA or miR increases repressive chromatin marks (e.g., H3K9/K27 methylation), inhibiting transcription at the targeted promoter; (iii) Alternative splicing: complexes with exogenous dsRNA-Ago forces exon exclusion or inclusion by targeting intronic or exonic sequences involved in splicing. Additionally, Ago proteins (possibly guided by ssRNA) are recruited to chromatin and interact with other chromatin components (e.g., HP1 γ or SR proteins), promoting H3K9me3 mark deposition. Consequently, RNA polymerase II elongation rate is slowed, which in turn facilitates spliceosome recruitment and allows alternative splicing of the variant exons (Huang and Li 2014); and (iv) DNA damage repair process: Ago proteins (that enter into the nucleus as a free form) incorporate the double-strand-break-induced small RNA generated from double-strand breaks and facilitate DNA damage repair by directly interacting with repair proteins or by affecting local chromatin structures via CMP (Wei *et al.* 2012). Nonetheless, despite these described signaling pathways, the nuclear functions of Ago proteins remain unclear in mammalian cells.

Additionally, the expression of the four Ago proteins differs among them during early development. The Ago2 is the most abundant Ago-like protein during early preimplantation development in embryonic and primitive endoderm lineages, in humans and mice. Interestingly, in the Ago expression profile illustrated by Muller and colleagues, it is possible to note that in humans (and not in mice), at the late blastocyst stage, a decrease in Ago2 simultaneously with an increase in Ago1 is observed, which may suggest an important Ago1 function just before implantation and highlights their differential functions (Müller *et al.* 2020). During early development at postimplantation stages, Ago2 knockout in mice is lethal (embryos grow retarded and developmentally delayed, displaying severe phenotypic defects, such as cardiac failure and impaired neuronal tube closure) (Liu *et al.* 2004; Alisch *et al.* 2007; Morita *et al.* 2007; Cheloufi *et al.* 2010), while Ago1, Ago3, and Ago4 knockout mice are viable (Modzelewski *et al.* 2012; Van Stry *et al.* 2012). In addition, mice lacking the Ago2 slicer activity die shortly after birth with anemia. These findings suggest the essential roles of Ago2 and its slicer activity-dependent RNA silencing. During the evolutionary journey of the Ago family during embryonic and extra-embryonic development, discrete post-translational modifications have been identified (although not all fully defined), positively or negatively impacting RISC activity and Ago stability. These modifications have been linked to disease phenotypes and have been further investigated in cancer models. In terms of biological implications, Ago proteins have been implicated in cancer (Taubert *et al.* 2007), systemic autoimmune diseases (Jakymiw *et al.* 2006), and Fragile X syndrome (Jin *et al.* 2004). In cancer, increased levels of Ago proteins were reported in epithelial skin cancer (Sand *et al.* 2012), colon cancer (Li *et al.* 2010), breast cancer (Adams *et al.* 2009), and serous ovarian carcinoma (Vaksman *et al.* 2012). In systemic autoimmune diseases, the autoimmune response is initiated to components of the RNAi pathway, where Ago proteins play key roles (Jakymiw *et al.* 2006; Filková *et al.* 2012). In fragile X syndrome (one of the most common forms of hereditary intellectual disability caused by a loss of expression of the fragile X

mental retardation protein), the fragile X mental retardation protein has been found in biochemically purified Ago complexes and is involved in miR biogenesis (Jin *et al.* 2004). Since Ago proteins are involved in several diseases (and in others yet to be revealed in the future), it is important to identify the specific functions of Ago in pathological conditions, which are largely controlled by post-translational modifications. Ultimately, modulating Ago protein activities may be a promising point of therapeutic intervention for several diseases.

1.3.2 Ago post-translational modifications and signaling pathways

The importance of Ago post-translational modifications has been mainly described in cancer. Nonetheless, since these modifications regulate a variety of signaling events within the cell, critical for development timing (Seet *et al.* 2006), it is possible to speculate that may also interfere with other diseases. In particular, Ago proteins are commonly phosphorylated and hydroxylated (to enhance their silencing activity, stability, and binding to small RNA), and ubiquitinated (when they are dysfunctional and need to be degraded) (Wu *et al.* 2020), in response to cellular modifications (not yet fully elucidated). In the table below, Ago post-translational modifications and their biological consequences are summarized (Table 1.2). Likewise, Figure 1.3 details the location where these modifications occur in the Ago protein (although there are some discrepancies in this location among the reported studies) (Schirle *et al.* 2012; Müller *et al.* 2020).

Table 1.2 – Post-translational Ago2 modifications. Abbreviations: Ago, Argonaute; Akt, protein kinase B; EGFR, Epidermal growth factor receptor; HEK, human embryonic kidney cells; MAPK, mitogen-activated protein kinase; MEF, mouse embryonic fibroblasts; miR, microRNA; P, proline; S, serine. (Adapted from Lai *et al.* 2014; Müller *et al.* 2020).

Post-translational Ago modification	Conserved human Ago1-4	Molecular implications	Cellular system identified	References
Phosphorylation				
S387 (depends on p38 MAPK or Akt3)	Not conserved in Ago3 (others Ago-like proteins yes)	-Increases translational repression; -Decreases cleavage activity; -Reduces secretion into exosomes and increases association with P-bodies.	HeLa, HEK-293T, HEK-293, DLD1 colon cancer lines, MEF, U2OS, H1299	Zeng <i>et al.</i> 2008; Rudel <i>et al.</i> 2011; Horman <i>et al.</i> 2013; Lopez-Orozco <i>et al.</i> 2015; Quévillon Huberdeau <i>et al.</i> 2017; McKenzie <i>et al.</i> 2016; Bidge <i>et al.</i> 2017

(table continues on the next page)

Y393 (depends on EGFR)	Not conserved in Ago3 (others Ago-like proteins yes)	-Decreases maturation of Ago2-mediated miR under hypoxia; -Inhibits miR maturation and loading.	HEK-293, HEK-293T, HeLa, MDA-MB-231, IMR90	Rüdel <i>et al.</i> 2011; Shen <i>et al.</i> 2013; Yang <i>et al.</i> 2014
Y529	Yes	-Impair miR binding.	HEK-293, HeLa, LPS-activated RAW 246.7 primary macrophages	Rüdel <i>et al.</i> 2011; Mazumder <i>et al.</i> 2013; Lopez-Orozco <i>et al.</i> 2015
S798	Only investigated in Ago2	-Lost Ago association with P-bodies and stress granules.	HeLa	Lopez-Orozco <i>et al.</i> 2015
Hydroxylation				
P700	Yes	-Increases Ago2 stability; -Increases miR levels/activity (during hypoxia).	HEK-293T, HeLa S3, U2OS, MEF and PASMCMC	Qi <i>et al.</i> 2008; Wu <i>et al.</i> 2011
Ubiquitination				
Sites unknown	Only investigated in Ago2	-Induces Ago2 turnover and represses miR activity.	HEK-293T, A549, lung cancer tissue arrays, mouse xenografted tumor model	Adams <i>et al.</i> 2009; Rybak <i>et al.</i> 2009; Bronevetsky <i>et al.</i> 2013; Smibert <i>et al.</i> 2013

Although further studies are needed to map these post-translational modifications in other pathological contexts, it is becoming clearer that ubiquitination is linked to loss of Ago protein stability, while hydroxylation stabilizes the protein. Moreover, Ago2 and Ago4 proteins seem to be more susceptible to hydroxylation by collagen prolyl-4-hydroxylase (C-P4H; which catalyzes proline hydroxylation) than Ago3 protein *in vitro* (Qi *et al.* 2008). These findings may have clinical relevance for pharmacological approaches aiming to increase or disturb the stability of Ago2 and Ago4 proteins. By contrast, the association between the phosphorylated Ago and its stability is more contradictory; so far, it is only clear that the phosphorylation of Ago proteins directly affects their localization and functions (Wu *et al.* 2020). Despite the rapid advances established over the past decades, further studies to map these post-translational modifications are needed since, besides representing a relevant advance in understanding Ago2 activity, they may provide new avenues to modulate global activity and miR levels, important in countless CNS disorders.

1.3.3 Ago2 functions in angiogenesis and inflammation

Among the four Ago proteins, only Ago2 (also known as eukaryotic translation initiation factor 2C2) has the capability to silence target mRNA through its complete slicer activity (Meister et al. 2004; Liu et al. 2014), leaving it in a special position for investigation. In addition, Ago2 proteins are robustly expressed during human and mouse early development (Valdanis *et al.* 2012; Hauptmann *et al.* 2015), suggesting the essential roles of Ago2. So far, the functions of Ago2 in the cerebral angiogenic response remain unexplored. Thus, this subchapter provides a brief review of the functional significance of Ago2 in peripheral angiogenesis (although this is still an underexplored point), mainly in the context of cancer, where deregulation of Ago2 levels has been reported and associated with a pro-angiogenic activity. Ago2 overexpression has been more reported in most cancers, including breast (Conger *et al.* 2016; Casey *et al.* 2019), colon (Papachristou *et al.* 2011; Li *et al.* 2010), ovarian (Vaksman *et al.* 2012), gastric (Zhang *et al.* 2013), and glioma (Feng *et al.* 2014). However, others also reported a strong reduction, namely in melanoma (Völler *et al.* 2016), childhood acute lymphoblastic leukemia (Piroozian *et al.* 2019), and clear cell renal cell cancer (Lee *et al.* 2019). This inconsistency in Ago2 expression levels could be due to the differences in cancer types and miR expression patterns. Ago2 upregulation is associated with a global increase expression of miR (Winter and Diederichs 2011; Martinez and Gregory 2013). In the context of cancer, Ago2 may promote angiogenesis via the phosphatase and tensin homolog (PTEN)/VEGF signaling pathway (human hepatocellular cell lines HepG2, Hep3B, Huh7) (Ye ZL *et al.* 2015). In particular, Ago2 regulates human hepatocellular cell growth by enhancing the capacity of the oncogenic miR-21a to repress their target tumor suppressor genes (e.g., PTEN) (Zhang *et al.* 2014; Ye Z *et al.* 2015). In addition, the pro-angiogenic activity of Ago2 was also reported in multiple myeloma, *in vitro* and *in vivo*, by upregulating the expression of the pro-angiogenic let-7 family and the miR-17/92 cluster and downregulating the anti-angiogenic miR-145 to stimulate the formation of new blood vessels (Wu *et al.* 2014). Moreover, others reported the regulatory effect of Ago2 on tumor angiogenesis via p63 isoforms; in particular, p63 physically interacted with Ago2, promoting its activation (Wang et al 2022). Interestingly, upon hypoxia, Ago2 can be hydroxylated which promotes its stabilization, as well as promotes the release of pro-angiogenic miR-210 (Qi *et al.* 2008; Hale *et al.* 2014; Bavelloni *et al.* 2017). Collectively, these evidence suggest that Ago2 is a potential target for cancer treatment and a promising biomarker in this context. In addition, the crucial role of Ago2 in stimulating angiogenesis was also demonstrated in a non-pathological vascular context. In particular, Ago2 knockdown induced apoptosis and disabled vessel formation in human peripheral endothelial cell line (Asai *et al.* 2008).

Despite the lack of knowledge regarding the role of Ago2 in brain angiogenesis, much less is known about its role in inflammation-induced brain damage. A study conducted in murine macrophage-like cell line RAW 264.7 (peripheral macrophages, which share functional similarities with microglia) evaluated the effect of LPS treatment on Ago2. The researchers concluded that the early response to LPS induced Ago2 phosphorylation and miR dissociation

(shutting down miR-mediated repression) and enhanced the synthesis of proinflammatory cytokines. Conversely, longer exposure to LPS reverted these processes. These results suggest that Ago2 may be involved in the classical microglia response (pro-inflammatory phenotype). In the same study, variations in Ago2 levels and cell location were not reported (Mazumder *et al.* 2013). Another study demonstrated that chronic inflammation is triggered by Ago2 and Dicer downregulation, impairing the miR generation (peripheral blood mononuclear cells from post-traumatic stress disorder patients) (Bam *et al.* 2017). Additionally, certain Ago2-miR complexes (including miR-139-5p, miR-142-3p, miR-142-5p, and miR-223) can also regulate the inflammatory process (neutrophils isolated from skin wounds) (de Kerckhove *et al.* 2018). Moreover, miR-132-mediated Ago2 suppression in human dermal lymphatic endothelial cells affected the levels of miR-221 and miR146a, which are involved in angiogenesis and inflammation, respectively (Poliseno *et al.* 2006; Taganov *et al.* 2006; Li *et al.* 2009; Leonov *et al.* 2015). Ultimately, it is evident that Ago2 may be involved in numerous biological processes by modulating miR activity and expression levels. Thus, the manipulation of its activity may provide a clinically applicable approach to normalize the inflammatory response and modulate angiogenesis in CNS disorders.

1.4 Retinoic acid signaling molecule

Retinoic acid (RA) is the main biologically active metabolite of vitamin A (retinol) and regulates a variety of biological processes from the embryo to adulthood, by interacting with nuclear receptors that control gene expression (Maden 2007). To overcome the limitations (e.g., cytotoxicity, broad side effects, photosensitivity) and potentiate the benefits of this pleiotropic molecule, RA-containing nanoparticles (RA-NP) were developed by our group (Maia *et al.* 2011). Taking advantage of their protective properties in cell survival, angiogenesis, and inflammation (Ferreira *et al.* 2016; Machado-Pereira *et al.* 2017; Machado-Pereira *et al.* 2018), RA-NP were proposed in this Thesis as a pharmacological approach to modulate the Ago2 endogenous mechanism and induce BEC protection following cerebral ischemia. Consequently, the interaction between RA and Ago2 was assessed for the first time in the present research work. Accordingly, the biology of this signaling molecule, the mechanisms underlying RA function in brain angiogenesis and neuroinflammation, and the available RA delivery formulations for brain therapy will be addressed in the following subchapter.

1.4.1 RA metabolism and signaling pathways

RA is a small metabolic product of retinol (vitamin A) (Maden 2007) and its designation derives from its involvement in retinal biology, a membrane of the eye responsible to convert light energy into neural activity. In the retina, the binding of 11-*cis*-retinal (another derivate of retinol) to opsins constitutes the chemical basis of vision (Wald 1968; Kusakabe *et al.* 2009). Retinol and its

metabolic products (retinoids) are composed of three chemical groups, namely a cyclic ring, a polyunsaturated chain, and a terminal group. Within the polyunsaturated chain, the alternated sequences of double C=C bounds are responsible for retinoid color (yellow, orange, or red) and constitute the molecular region easily destabilized after the light exposition (an undesired RA property that may promote its degradation). Additionally, the differences in attachment mechanisms of the terminal group at the end of the polyunsaturated chain give rise to the different retinol derivatives (Di Masi *et al.* 2015). Among them, all-*trans* RA is the active and most common form found *in vivo* (Paik J *et al.* 2000; Blomhoff R and Blomhoff HK 2006). Thus, the abbreviation RA in this Thesis refers to all-*trans* RA. Prior to the RA generation, retinol is extracted from plant (provitamin A carotenoids) or animal (retinyl esters) dietary sources since humans are unable to produce this vitamin themselves (Maden *et al.* 2002; Vilhais-Neto and Pourquié 2008). The dietary retinol uptake is mediated by small intestinal epithelial cells from where it is brought to the liver for long-term storage as retinyl esters (Harrison 2012). The liver contains enzymes responsible to mediate retinoid effects and those needed for RA synthesis, catabolism, and excretion (Shirakami *et al.* 2012). When RA is needed by the organism, retinol is secreted from the liver, as retinol binding protein (RBP)-bound complexes, to the bloodstream for peripheral circulation. At the target cells, the RBP-bound complexes are taken into the cytosol via surface RBP receptors, namely the RA 6 receptor (STRA6), and are metabolized into RA in a two-step oxidative process (Kawaguchi *et al.* 2007). The first step consists of retinol oxidation to retinaldehyde, a slow and reversible reaction mediated by the alcohol dehydrogenase (ADH) and retinol dehydrogenases (RDH) enzymes (Napoli 1986; Parés *et al.* 2008). The second step comprises the conversion of retinaldehyde to RA, an irreversible reaction mediated by the retinaldehyde dehydrogenase (RALDH) enzyme (Duester 2008). Then, cytosolic RA can associate with cellular RA binding protein (CRABP)-I for degradation by cytochrome P450 family 26 (CYP26) enzymes, occurring RA inactivation and the recruitment of the nuclear co-repressor complex NCOR/Sin3A/HDAC to inhibit transcription activation (Petkovic 2001; Vilhais-Neto and Pourquié 2008; Thatcher *et al.* 2009). Additionally, cytoplasmic RA can interact with CRABPII or fatty acid-binding protein type 5 (FABP5), mediating its transport to the nucleus (Dong *et al.* 1999) (Figure 1.4). Lastly, cytosol RA can activate kinase cascades (Al Tanoury *et al.* 2013); for example, RA interacts with Gαq proteins to activate the p38 MAPK or with PI3K to activate p42/p44 (ERK) MAPK (Masiá *et al.* 2007). Once activated, MAPK translocates to the nucleus and phosphorylates nuclear receptors. In the nucleus, RA exerts most of its effects on gene regulation by binding to different nuclear receptors, namely RA receptors (RAR) or peroxisome proliferator-activated receptor β/δ (PPARβ/δ). In a cell type expressing high CRABP-II and low FABP5, RA activates RAR, while in the presence of the opposite ratio (low CRABP-II and high FABP5), RA activates PPARβ/δ (Michalik and Wahli 2007). Once activated, these nuclear receptors heterodimerize with retinoid X receptors (RXR) and bind to specific DNA sequences called RA-response element (RARE) in the promoter regions of retinoid-responsive genes, inducing the transcription of target genes (Bastien and Rochette-Egly 2004). In both situations, RXR is an essential coregulator for the efficient binding of the nuclear receptor to the DNA (Germain *et al.* 2002). Additionally, coactivators (namely the p160 subfamily of steroid

receptor coactivators (SRC)) or corepressors (namely the nuclear receptor corepressor - NCoR or silencing mediator of RA and thyroid hormone receptor - SMRT) are needed to induce the activity of RAR and PPAR β/δ and, consequently, the transcriptional output of many gene networks (Al Tanoury *et al.* 2013). Since the disruption of the normal function of coregulators contributes to physiological abnormalities and diseases, these biomolecules have been explored as therapeutic targets to develop new drugs for treating or preventing nuclear receptor-related diseases (Hsia *et al.* 2010). Ultimately, RA functions were also implicated by its interaction with RA receptor-related orphan receptors (Stehlin-Gaon *et al.* 2003), which mediate inflammation, metabolism, circadian rhythms, autoimmune diseases, and immune cell differentiation (Jetten 2009).

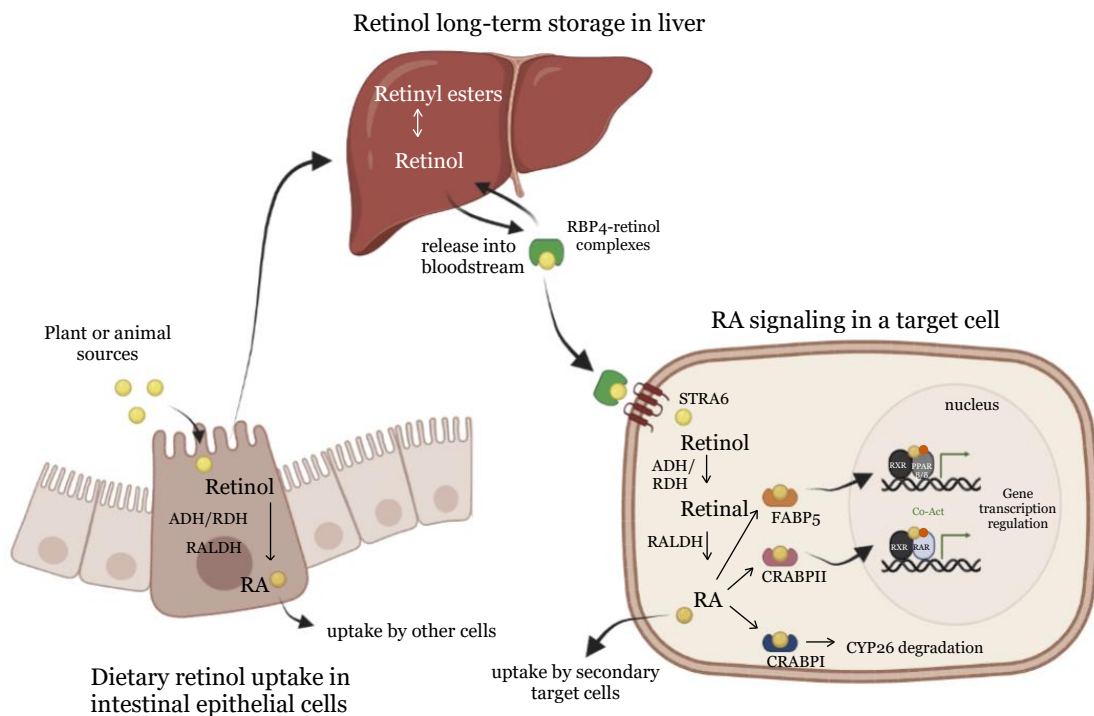


Figure 1.4 – RA metabolism and signaling pathway. The dietary retinol is absorbed by intestinal epithelial cells, metabolized into RA, and uptaken by other cells. Then, it can be transferred to the liver in form of retinyl esters for long-term storage. RBP-bound retinol complexes are released into the bloodstream and circulate to target cells. Once translocated into the cytosol of the target cell via STRA6, retinol is metabolized to retinal by the enzymes ADH and RDH (in a reversible manner) and then, to RA by the enzyme RALDH (in an irreversible manner). Cytosolic RA associates with cellular RA binding protein CRABPI for degradation by CYP26 enzymes, and with CRABPII or FABP5 for function as a ligand of nuclear receptor complexes, initiating target gene transcription. Abbreviations: ADH, alcohol dehydrogenase; CRABP, cellular RA binding protein; CYP26, cytochrome P450 family 26 enzymes; FABP5, fatty acid-binding protein type 5; PPAR β/δ , peroxisome proliferator-activated receptor β/δ ; RA, retinoic acid; RALDH, retinal dehydrogenase; RAR, RA receptor; RBP, serum retinol-binding protein; RDH, retinol dehydrogenase; RXR, retinoic X receptor; STRA, RA signaling receptor. (Adapted from Saeed *et al.* 2017 and Michalik and Wahli 2007).

Despite RA signaling regulates over 500 reported genes, including enzymes, receptors, and signaling molecules (Lane and Bailey 2005; Blomhoff R and Blomhoff HK 2006), it remains unknown whether Ago2 is one of the RA targets, an interaction further explored in the present Thesis. Since RAR is widely expressed in the brain, RA is involved in countless functions in the

CNS (Tafti and Ghyselinck 2007), where it is also crucial for the anteroposterior and dorsoventral patterning of the neural tube (Maden 2002). Other RA functions include the improvement of learning and memory through the hippocampal long-term potentiation/depression (Misner *et al.* 2001), neurogenesis (Bonnet *et al.* 2008), homeostatic plasticity (Aoto *et al.* 2008), neurite outgrowth (Corcoran and Maden 1999), axon outgrowth (Maden 2007), and neuronal differentiation (Jacobs *et al.* 2006). In accordance, RA can ameliorate aging-associated cognitive deficits (learning and memory deficits), by reversing the loss of the expression of age-related genes (Enderlin *et al.* 1997). Importantly, these effects highlight the use of RA as a promising therapeutic for the most common CNS disorders, which commonly affect elders (including stroke, neuropathy, Alzheimer's disease, and Parkinson's disease). Despite being a crucial neuronal differentiation factor in the CNS, this pleiotropic molecule is implicated in the regulation of oxidative damage and neuroinflammation (Ahlemeyer *et al.* 2000; Ahlemeyer *et al.* 2001; Jiang *et al.* 2018), BBB differentiation and integrity (Mizee *et al.* 2013), and endothelial proliferation and tubule formation (Ferreira *et al.* 2016). The effects of RA in angiogenesis and neuroinflammation (mechanisms assessed in the present Thesis) are explored in the following subchapter.

1.4.2 Effects of RA in brain angiogenesis and neuroinflammation

The role of RA in brain angiogenesis still needs to be elucidated. However, RA mediates various mechanisms in the CNS vasculature crucial for a proper angiogenic process in the brain, namely BEC proliferation, tight junction formation, BBB integrity, and pericyte stabilization (Adair and Montani 2010). Accordingly, the first evidence demonstrating that RA signaling induces BBB development and integrity was reported by Mizee and colleagues, in 2013. In this study, the authors showed that RA (5 μ M for 48 hours) enhances BBB integrity by promoting the expression of the tight proteins VE-cadherin, occludin, and ZO-1, in a human brain endothelial cell line HCMEC/D3 (an alternative to primary BEC). In the same study, it was observed that RA also regulates BBB integrity by increasing the gene expression of the efflux transporter P-glycoprotein and the glucose transporter isoform 1/Slc2a1 (GLUT1) (Mizee *et al.* 2013). GLUT1 is crucial for the development of angiogenic process and restores endothelial proliferation during sprouting angiogenesis (human brain microvasculature) (Veys *et al.* 2020). Increased expression of GLUT1 and tight junction proteins are mediated through the isoform β of RAR, while increased P-glycoprotein expression is likely regulated by other isoforms of RAR (α or γ) or by other nuclear receptors (Mizee *et al.* 2013). Additionally, the expression of RAR β in endothelial cells was reported in the fetal development of the CNS (Liao *et al.* 2005), suggesting that RA is also critical for the development of CNS vascular milieu. To reinforce this idea, others reported a regulatory role of RA in Notch signaling during spinal cord development (Paschaki *et al.* 2012), a signaling pathway involved in vessel integrity and BBB function and stability in the mammalian vasculature (Cai *et al.* 2016). Lastly, RA-mediated regulation of vascular WNT signaling prevents the over-recruitment of pericytes needed for proper brain vessel stability in mice with targeted deletions

of *Rdh10* gene (Bonney *et al.* 2018). Considering these evidence, RA was used as a promising approach to prevent early BBB dysfunction in a rat model of MCAO. The authors demonstrated that pre-treatment with RA (5 µg/g; for 4 consecutive days before the occlusion, followed by 2 injections of RA after the onset) increased ZO-1 and VE-cadherin levels. In this context, the RA effects were mediated through the isoform α of RAR (Kong *et al.* 2015), suggesting that RAR is the preferred nuclear receptor for RA-induced protective effects in this context. Importantly, the work developed in this Thesis provides expanded knowledge on the effect of RA in brain angiogenesis in stroke, a mechanism poorly explored so far.

Additionally, RA is a potent candidate to prevent neuroinflammation in CNS diseases, by downregulating the expression of cytokines and inflammatory molecules through multiple pathways. In Alzheimer's model disease, RA (20 µg/g trice a week for 4 weeks) prevents microglial activation in the mouse hippocampus through the upregulation of RAR β and TGF- β , which in turn, decreases the activity of nuclear factor- κ B and attenuates the synthesis of the inflammatory mediators iNOS and TNF- α (Takamura *et al.* 2017). Interestingly, in this context, RA may inhibit oxidative damage by mitigating ROS levels. Others reported that under staurosporine challenge (an inducer of oxidative stress by promoting ROS accumulation), RA (0.1 µM for 24 hours) restores the expression of antioxidant enzymes responsible for mitigating ROS, namely the superoxide dismutase-1 and manganese superoxide dismutase-2, which, consequently, inhibits neuronal apoptosis (primary cultures from neonatal rat hippocampus) (Ahlemeyer *et al.* 2000; Ahlemeyer *et al.* 2001). Altogether, these mechanisms can contribute to the positive effect of RA on learning and memory in mice (Ding *et al.* 2008; Chakrabarti *et al.* 2016). In stroke, RA is a well-established anti-inflammatory mediator. In a mouse model of MCAO, RA (1 µg/g; pre-treatment 1 day before occlusion, followed by 1 injection per day for 3 consecutive days) attenuates neural inflammation through the suppression of STAT1 signaling (Cai *et al.* 2019). Additionally, in a rat model of MCAO, RA (5 µg/g; for 4 consecutive days before occlusion) regulates the ubiquitin-proteasome system and restores the expression of ubiquitin thioesterase OTUB1 (Kang *et al.* 2022), which, in turn, may inhibit astrocyte activation by inhibiting IFN- γ levels (Wang *et al.* 2019). Despite the promising prophylactic and restorative effects of RA in the CNS, its administration is challenging due to the undesirable properties of this molecule. RA is rapidly degraded under physiological conditions (few hours lifetime) and after light exposure, has low solubility in the aqueous phase (0.21 µM at pH 7.3), and requires a defined range of concentrations to exert its protective effects (Szuts and Harosi 1991; Fiorella and Napoli 1994). Therefore, RA delivery systems have been developed as an alternative to circumvent these undesired side effects.

1.4.3 RA delivery systems for brain repair

RA delivery systems were designed to improve the therapeutic effectiveness of RA by enhancing its lifetime in the bloodstream, reducing its cytotoxicity, increasing cell targeting, and its capacity to cross the BBB. Accordingly, considerable improvements (e.g., rearrangements in the particle size, composition, amount of RA loaded, and its degradation and delivery profile) led to the development of promising systems. Although still face some problems to reach the brain and efficiently cross the BBB, polymeric NP are the most common systems used so far for brain repair (Ferreira *et al.* 2020). Indeed, our group demonstrated the promising effects of polymeric RA-containing NP in the Parkinson's disease context (Esteves *et al.* 2015), in an *in vitro* model of inflammation (Machado-Pereira *et al.* 2017), and in cerebral ischemia (Ferreira *et al.* 2016; Machado-Pereira *et al.* 2017). Additionally, Zhang and colleagues reported the effects of another polymeric RA-containing NP in the context of Alzheimer's disease (Zhang *et al.* 2016). The RA delivery system developed by our group (termed RA-NP in this Thesis) was prepared through electrostatic interaction of polyethylenimine (PEI, polycation) with RA and dextran sulfate (DS, polyanion), having an approximate diameter of 220 nm, positive net charge (zeta potential ~16 mV), and a DS/PEI ratio of 0.2. Importantly, RA-NP disassemble preferentially at acidic pH values (Maia *et al.* 2011), which reflects the pH values into the ischemic (von Hanwehr *et al.* 1986) and inflammatory-damaged tissue (Dong *et al.* 2013). RA-NP uptake can occur by endocytosis, micropinocytosis, or phagocytosis, and once internalized, RA is gradually released by desorption, diffusion, or nanoparticle erosion in a pH-dependent manner (Maia *et al.* 2011). Firstly, in an *in vitro* model of inflammation (LPS challenge), PEI RA-NP outstood as a glial anti-inflammatory agent by inducing a protective phenotype in a microglial cell line derived from adult murine brain (Machado-Pereira *et al.* 2017). Secondly, in an *in vitro* model of OGD mimicking ischemia, this formulation emerged as a vasculotropic and neurogenic agent by enhancing vascular regulation of neural stem cell survival and differentiation via endothelial cues. Here, RA-NP also enhanced the proliferation of human endothelial progenitor cells isolated from stroke patients (Ferreira *et al.* 2016). These cells constitute an endogenous mechanism of vascular regeneration and repair, via their enriched secretome containing trophic factors, cytokines, and chemokines, that improve BBB permeability in cerebral ischemia (Di Santo *et al.* 2014; Sargento-Freitas *et al.* 2018). Similarly, in a prenatal model of brain ischemia, RA-NP revealed safety for systemic use with a promising prophylactic effect in the neurovascular function. Thirdly, in an animal model of Parkinson's disease, PEI RA-NP arose as an innovative strategy to halt the progression of Parkinson's disease pathogenesis by protecting nigral dopaminergic neurons in the striatum via the transcription factors Nurr1 and Pitx3 (Esteves *et al.* 2015). Lastly, in the context of Alzheimer's disease, pHEMA RA/siSOX9-NP were used to efficiently deliver RA and siSOX9 to promote neural stem cell differentiation in transgenic mice. In this study, the authors demonstrated that RA inhibited oxidative damage, inflammation, and mitochondrial dysfunction which, collectively, improved cognition and memory (Zhang *et al.* 2016). Although further studies are needed to understand RA-NP pharmacokinetics, biodistribution, clearance, and toxicology, the use of these

systems is a powerful strategy to deliver RA in the brain and ensure protection in several CNS diseases.

1.5 Aims

Stroke is a major public health problem that requires effective and safety therapies to reverse the disability in patients. The only approved therapeutic approach is thrombolysis, however, it has limited efficacy due to a narrow therapeutic window under which it can be used without inducing hemorrhage transformations (Bhaskar *et al.* 2018). Neuroprotective or neurorestorative strategies aiming to modulate endogenous mechanisms have emerged as alternatives to thrombolysis, nevertheless, none was approved so far (Matei *et al.* 2021; Ghozy *et al.* 2022; Lin *et al.* 2022). In this Thesis, it was proposed, for the first time, the modulation of the Ago2 endogenous mechanism to enhance the brain vascular function compromised by cerebral ischemia. Accordingly, a repaired cerebrovasculature will contribute to full parenchymal recovery after a stroke. Among the multitude of events that occur following a stroke, inflammation plays an important role in brain tissue damage and repair, contributing to short-term mortality and long-term disability in patients.

Thus, the first main goal of this Thesis is to reveal the potential of Ago2 to revert detrimental post-stroke inflammatory mechanisms. Furthermore, this work aims to dictate the follow-up for the ischemic setting. Therefore, to successfully achieve these purposes, the main objectives of this experimental work were:

- 1) To characterize Ago2 expression and its modulatory role in the inflammatory responses elicited by brain endothelial and glial cells under LPS challenge, an *in vitro* model of inflammation.
- 2) To disclose the modulatory role of Ago2 in the endothelial-glial crosstalk under LPS challenge.
- 3) To evaluate the potential of the Ago2 exogenous application to protect the NVU from damage caused by systemic inflammation, in an inflammatory LPS animal model, an *in vivo* model of systemic inflammation.

These objectives were accomplished and are fully detailed in Chapter 3. Then, the focus of this work was directed to the ischemic damage, with the following objective:

- 4) To characterize Ago2 expression and its role on BEC function exposed to OGD followed by a recovery period (OGD/R), in an *in vitro* model of stroke.

This goal was achieved and is fully described in Chapter 4. Lastly, the results obtained led us to study the effects of the controlled delivery of retinoic acid (RA-NP) as the alternative and therapeutic approach to modulate the endogenous Ago2 and induce neuroprotection. Thus, the following aims were:

5) To assess the potential of RA-NP to enhance Ago2 expression in BEC exposed to OGD/R and determine the interaction between RA and Ago2.

6) To evaluate the neurovascular and inflammatory recovery induced by the systemic injection of RA-NP, after transient MCAO, an *in vivo* model of stroke.

These goals are described in Chapter 4. Altogether, these results represent a novelty in post-stroke recovery approaches, whose modulation of the endogenous Ago2 mechanism will be the starting point to full parenchymal recovery. Additionally, this work will also pave the way to decipher molecular interactions between Ago2 and RA signaling.

Chapter 2

Materials and Methods

2.1 Primary brain cultures

2.1.1 Primary brain endothelial cell cultures

Mouse brain endothelial cells (BEC) were isolated using a protocol adapted from (Wu *et al.* 2003; Chapter 3 of the present Thesis, Machado-Pereira *et al.* 2022). Briefly, the cortices of 3-7 days old C57BL/6J pups were isolated, minced, and resuspended in 0.25% trypsin (Gibco, Barcelona, Spain). Then, the tissue suspension was centrifuged at 350 g for 5 minutes. The pellet was filtered through a 70 μm nylon cell strainer (Falcon, Corning Incorporated, NY, USA) to retain the microvessel fraction, which was seeded onto 0.5% gelatin-coated surfaces (Sigma, MO, USA). Puromycin (0.4 $\mu\text{g}/\text{ml}$; Sigma) was added for selective endothelial cell growth. BEC were maintained at 37°C in a 95% atmospheric air and 5% carbon dioxide (CO₂) humidified atmosphere in Eagle's Minimum Essential Medium (Lonza, MD, USA) supplemented with 100 U/ml penicillin and 100 $\mu\text{g}/\text{ml}$ streptomycin (Life Technologies, Barcelona, Spain), 10% fetal bovine serum (Millipore, Berlin, Germany), 10% horse serum (Thermo Fisher Scientific, MA, USA), 10 $\mu\text{g}/\text{ml}$ EGF (Invitrogen, CA, USA), 100 $\mu\text{g}/\text{ml}$ heparin sodium salt (PanReac AppliChem, Barcelona, Spain) and 2 mM glutamine (Sigma) (protocol depicted in Figure 2.1).

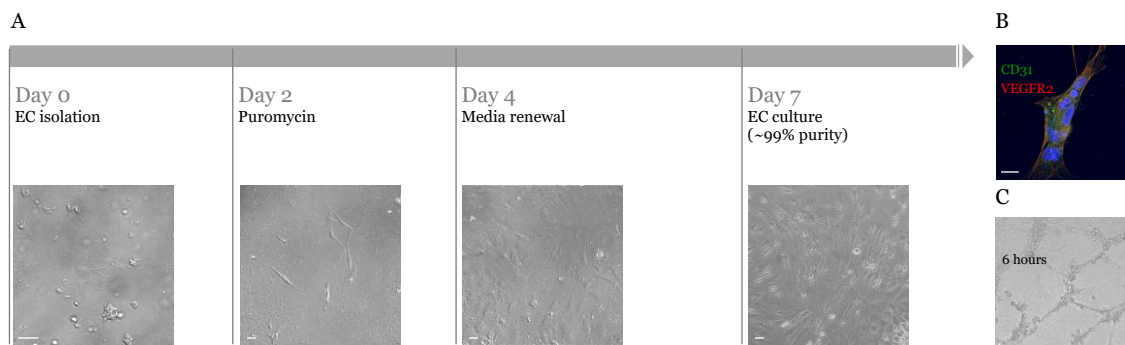


Figure 2.1 – Characterization of primary brain endothelial cell cultures. Purified endothelial cells were obtained after 7 days in culture (A), with a purity above 99% measured by immunocytochemistry (B). Capillary-like tube formation on a matrigel matrix was achieved after 6 hours (C). The differential interference contrast (DIC) images were acquired using an Olympus SP-500 UZ digital camera coupled to an Axiobserver Z1 microscope (Carl Zeiss, Oberkochen, Germany).

Cells were plated at a density of 1×10^5 cells per well in 6-well trays (Griess and enzyme-linked immunosorbent (ELISA) assays, and western blot (WB) analysis), 3×10^4 cells per well in growth factor-reduced Matrigel™ (BD Biosciences, CA, USA)-coated 48-well trays in conditioned-

medium (DIC images) (Ferreira *et al.* 2014), 2.5×10^4 cells per well in 24-well trays (immunocytochemical studies), or 7.5×10^3 cells per well in 96-well trays (cell viability and cell membrane damage assays). Untreated cells were used as the control condition (CTR). After cell treatments (described in the sections below), endothelial-cell-conditioned media (EC-CM) were collected and clarified by centrifugation at 14,000 g for 20 minutes to remove cell debris and stored at -80°C before use. Media were used for quantifying inflammatory mediators (Griess and ELISA assays) and for assessing the impact of the endothelial secretome on microglia cell death and activation (described in a section below).

2.1.2 Primary brain glial cell cultures

Microglial cells and astrocytes were isolated using a protocol adapted from (Cristóvão *et al.* 2010; Chapter 3 of the present Thesis, Machado-Pereira *et al.* 2022). Briefly, the brains of 3-5 days old C57BL/6J pups were isolated, stripped of meninges, minced, and resuspended in Dulbecco's Modified Eagle's Medium-high glucose (DMEM-HG; Sigma), with 100 U/ml penicillin and 100 $\mu\text{g}/\text{ml}$ streptomycin (Life Technologies), and 10% fetal bovine serum (Millipore). The tissue was mechanically dissociated and filtered through a 70 μm nylon cell filter (Falcon) and centrifuged at 250 g for 10 minutes. Cells were then seeded onto 0.01% poly-D-lysine-coated flasks. The medium was changed every 2 days. After approximately 10 days, cultures were shaken overnight to recover the microglia cell fraction, which was centrifuged at 230 g for 8 minutes, leaving astrocytes in the adherent monolayer. To recover astrocytes, 0.25% trypsin (Gibco) was added, and the detached cell fraction was collected and centrifuged at 230 g for 8 minutes and resuspended in DMEM-HG. The medium was changed the next day and then every 2 days. Microglial culture purity is approximately 95%, measured by immunocytochemistry (protocol depicted in the Figure 2.2).

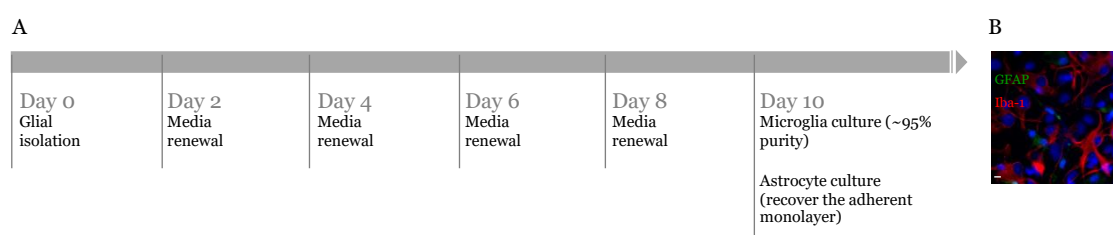


Figure 2.2 – Characterization of primary brain glial cell cultures. Purified microglial cells were obtained after 10 days in culture (A), with a purity above 95% measured by immunocytochemistry (B). Astrocytes were recovered in the adherent monolayer after 10 days in culture.

Microglial cells and astrocytes were seeded separately onto 0.01% poly-D-lysine-coated plates (Sigma) at a density of 2×10^4 cells per well in 24-well trays (immunocytochemical and silencing studies), 5×10^5 cells per well in 6-well trays (Griess assay, ELISA assays, and WB analysis) or 7.5×10^3 cells per well in 96-well trays (cell viability assays). Cells were maintained at 37°C , in 5% CO_2 and 95% atmospheric humidified air in DMEM-HG, supplemented with 100 U/ml penicillin

and 100 µg/ml streptomycin, and 10% fetal bovine serum. Cell treatments are described in the sections below. Control cells were left untreated. These cultures were implemented, characterized and optimized by Raquel Ferreira and Ana Clara Cristóvão and allow the reduction of the number of animals used in the experiments described herein.

2.2 *In vitro* models

2.2.1 *In vitro* model of inflammation

After seven and twelve days in culture, BEC and glial cells, respectively, were stimulated with lipopolysaccharide (LPS; from *Escherichia coli* O55:B5; 100 ng/ml for 24 hours; Sigma) to mimic the inflammatory process.

2.2.2 *In vitro* model of ischemia

After seven days in culture, BEC were either exposed to oxygen and glucose deprivation (OGD) alone to mimic ischemia (0.5 hours to 3 hours) or to OGD followed by a recovery period (24 hours) with the reintroduction of oxygen and nutrients (OGD/R), which mimics the ischemia-reperfusion period. Control cells (CTR) were not exposed to OGD and remained untreated. Cell treatments were performed during the recovery period. To induce OGD, cells were placed in 0.15 M phosphate-buffered saline (PBS) inside a MIC-101 modulator incubator chamber (Billups-Rothenberg Inc., Del Mar, CA, USA) and maintained at 37 °C in a 5% CO₂ and 95% nitrogen (N₂) gas environment (0.1% oxygen (O₂)).

2.3 Animal models

2.3.1 Animal model of inflammation

All experiments were performed in accordance with the National Institutes of Health and European Convention for the Protection of Vertebrate Animals Used for Experimental and Other Scientific Purposes (European Union directive number 2010/63/EU) for the care and use of laboratory animals. Mice were kept in appropriate cages under temperature-controlled conditions with a fixed 12 hours light/dark cycle, with free access to food and water. All efforts were made to reduce the number of animals and to minimize suffering. There were no signs of discomfort or significant loss of weight until the end of the experiments. A total of 26 adult C57BL6 male mice (20-week-old; 26.9 ± 0.5 g) were used in this study. Mice were housed in similar cages in the same experimental room under a controlled environment: 12 hours light/dark cycle at 22°C and ad libitum access to water and food. No animals died during this study. Mice were first injected intraperitoneally with LPS (2 mg/kg; Sigma) (Cazareth *et al.* 2014; Saraiva *et al.* 2019), followed by three daily intraperitoneal injections of Argonaute (Ago)-2. Control groups included animals injected with saline alone (sham controls) or injected with Ago2 alone (described in a section below). The day after the injection protocol was completed, animals were euthanized, and brains

were removed for WB analysis. For the immunohistochemistry protocol, mice were anesthetized with an intraperitoneal injection of xylazine (10 mg/kg of mouse weight; Rompun 2%, Bayer, Germany) and ketamine (90 mg/kg of mouse weight; Imalgene 1000, Merial, France) and then, euthanized by transcardial perfusion with 0.9% sodium chloride (NaCl), followed by perfusion with 4% paraformaldehyde (PFA; Sigma). Brains were removed, fixed overnight with 4% PFA, and immersed in a 30% sucrose solution. Finally, tissues were cryopreserved, and 40 µm-thick coronal sections were obtained using a freezing cryostat-microtome (Leica CM 3050S, Leica Microsystems, Nussloch, Germany). The experimental protocol is depicted in the figure below (Figure 2.3).

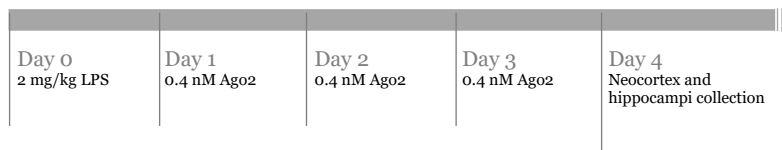


Figure 2.3 – Schematic representation of the experimental setup used in the animal model of inflammation.

2.3.2 Animal model of ischemia

All experiments were performed in accordance with the National Institutes of Health and European Convention for the Protection of Vertebrate Animals Used for Experimental and Other Scientific Purposes (European Union directive number 2010/63/EU) for the care and use of laboratory animals, the Ethics Committee for Animal Experimentation of the Vall d’Hebron Research Institute, in accordance with the Spanish legislation. The animal model of ischemia was performed by Alba Grayston at the Vall d’Hebron Institut de Recerca of the Universitat Autònoma de Barcelona, under the collaboration established with Anna Rosell (leader of the NeuroRepair L3, Neurovascular Research Laboratory, Vall d’Hebron Institut de Recerca group, Barcelona). A total of 89 C57BL/6Ncr1 adult male mice (23.4 ± 2.0 g, 8-week-old; Charles River Laboratories, Les Oncins, France) were used in this study. Mice were housed in the same experimental room under a controlled environment: 12 hours light/dark cycle at 22°C and ad libitum access to water and food. The cerebral ischemia surgery, behavioral tests, infarct volume measurements, and statistical analysis were conducted prespecified and in a blinded and randomized manner for treatment allocation. At the end of this study, a total of 11 animals were excluded: one animal died after the surgery, 9 animals died due to complications during the experimental procedure, and one based on exclusion criteria of the experimental model (no brain infarction). Transient MCAO was induced by mechanically occluding the middle cerebral artery with an intraluminal filament, as described in detail by others (Grayston *et al.* 2022). Mice were anesthetized with isoflurane via facemask (5% for induction, 1.5% for maintenance in air, 79% N₂: 21% O₂). Mouse body temperature was maintained at 37°C throughout surgery, with the use of a self-regulated heating pad connected to a rectal probe and an ophthalmic lubricating ointment (Lipolac™; Angelini Farmaceutica, Barcelona, Spain) was used to prevent eye dryness. To minimize animal pain and

discomfort, analgesia (0.1 µg/g buprenorphine; Divasa Farma-Vic S.A., Barcelona, Spain) was administered subcutaneously before surgeries. Additionally, in the seven days protocol, analgesia and 0.9 ml of saline were daily administered subcutaneously until the end of the protocol to support post-surgical recovery. Also, nutritionally fortified water gel (DietGel Recovery®, ClearH2O®, Portland, ME, USA) was given to this set of animals one week prior to surgeries for habituation and was available ad libitum after surgery. In brief, the surgery started with the exposure of the right common carotid artery (CCA) bifurcation into the external carotid artery (ECA) and the internal carotid artery (ICA), a silicone-coated monofilament (reference number: 602256PK10Re; Docol Corporation, Sharon, MA, USA) was introduced through the ECA and directed towards the ICA to occlude the middle cerebral artery (MCA). Cortical cerebral blood flow (CBF) was measured by laser Doppler flowmetry using a flexible fiber-optic probe (Moor Instruments, Devon, UK), and occlusion was confirmed by the decrease of the registered CBF over 80%. After 45 minutes of occlusion, the monofilament was removed to allow reperfusion. Only animals recovering over 80% of CBF after monofilament removal were considered for the study. Sham animals underwent the same surgical procedure except for the occlusion of the MCA with the filament. Skin wounds were closed with silk sutures and properly disinfected with povidone-iodine. Animals were allowed to recover from anesthesia under visual supervision in recovery cages with a heating pad to prevent hypothermia. The results were evaluated at three days (3-day protocol), and seven days (7-day protocol), unless stated otherwise, after cerebral ischemia. Blood and organs (brain, heart, lungs, liver, spleen, and kidneys) were collected for analysis. The experimental protocol is depicted in the figure below (Figure 2.4).

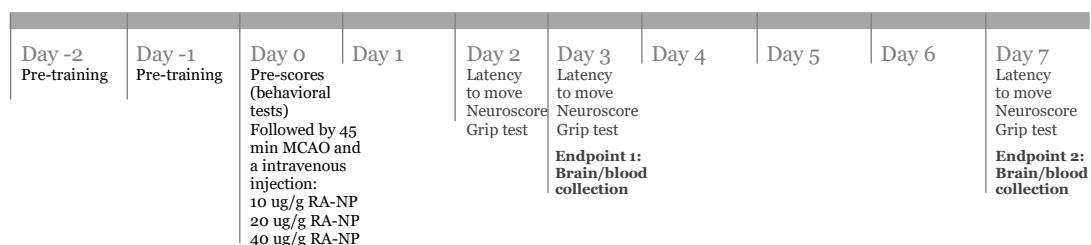


Figure 2.4 – Schematic representation of the experimental setup used in the animal model of ischemia.

2.4 Cell viability assays

Cell viability was measured using the cell counting kit-8 assay (CCK-8; Dojindo Laboratories, Kunamoto, Japan). A solution of 0.5% CCK-8 was added to cells, three hours before the endpoint of each experimental setup. Cell viability was determined in all experimental set-ups by measuring the optical density at 450 nm in an ELISA plate reader (SpectraMax® 384 Plus, Molecular Devices). Data were normalized to the control condition (untreated or vehicle-treated, where applicable).

2.5 Cell membrane damage assays

Cell membrane damage was assessed through the activity of lactate dehydrogenase (LDH) measured in cell culture media using the CytoTox 96[®] non-radioactive cytotoxicity assay (Promega Corporation, MA, USA). The degree of cell membrane damage levels was calculated according to the manufacturer's instructions and normalized to the control condition. Optical density was measured at 492 nm in an ELISA plate reader (SpectraMax[®] 384 Plus, Molecular Devices, CA, USA).

2.6 Autophagy assays

Autophagy was measured using a VIVAdetect AutophluxTM Kit (Viva Bioscience, SIG, Gyeonggi-do, South Korea). Bafilomycin A1 (bafA1; 100 nM) was added in the last hour of treatment to inhibit lysosome-dependent degradation. Then, BEC were lysed and the expression of ubiquitin-binding autophagy substrate receptor (p62) (Yoshii and Mizushima 2017) was evaluated by western blotting.

2.7 Griess assays

NO production was determined through the formation and accumulation of the stable metabolite product nitrite (NO₂). Accordingly, Griess reagents were added to each well: 0.1% N-1-naphthylenediamine dihydrochloride and 1% sulfanilamide in 5% phosphoric acid (Promega, WI, USA). Optical density was measured at 540 nm in an ELISA plate reader (SPECTRA max 384 Plus, Molecular Devices) and the total amount of protein, used for normalization, was quantified using the BCA assay (Thermo Fisher Scientific).

2.8 Ago2 treatments and injections

For the *in vitro* studies, cell treatments included Ago2 administration (0.4 nM; Abcam, Cambridge, UK) alone for 24 hours and Ago2 administration in combination with LPS stimulation for 24 hours and/or BafA1 treatment for 3 hours. For Ago2 silencing, cells were first treated for 6 hours (microglial cells and astrocytes) or for 5 hours (BEC) with lipofectamine-delivered (2 µg/ml; Invitrogen) siAgo2 (50 ng/ml; Ambion, Inc, Thermo Fisher Scientific) or a scrambled miRNA sequence (50 nmol/l; Thermo Scientific), according to the manufacturer's instructions. Ago2 downregulation was confirmed by western blotting (Machado-Pereira *et al.* 2022). After Ago2 silencing, cells were washed with PBS and were either exposed to LPS or left unexposed for activation (Chapter 3 experiments), or exposed to RA-NP or free RA (Chapter 4 experiments), for 24 hours in complete media. For Ago2 inhibition assays, BEC were treated with BCI-137 alone (100 nM for 24 hours; Merck Millipore, Darmstadt, Germany) or with BCI-137 in combination with retinoic acid (RA)-loaded nanoparticles (RA-NP) and free RA (Chapter 4 experiments). BCI-

137 was prepared as described by others (Masciarelli *et al.* 2014). Briefly, the inhibitor of Ago2 activity was dissolved in DMSO and then diluted in 4-(2-hydroxyethyl)-1-piperazineethanesulfonic acid (HEPES)-buffered saline (10 mM HEPES; 150 mM NaCl; 0.005% surfactant P20).

For the *in vivo* studies, adult mice were injected intraperitoneally with LPS, followed by three daily intraperitoneal injections of Ago2 (0.4 nM; Abcam) prepared in saline, as described by us and others (Ferreira *et al.* 2014; Danilov *et al.* 2020).

2.9 RA-NP synthesis

RA-NP were prepared as previously described by us (Maia *et al.* 2011). Briefly, RA-NP were prepared by adding all-*trans* RA (2% w/v in dimethyl sulfoxide (DMSO)) to polyethylenimine (PEI; 1% w/v in borate buffer, pH 8.0). Then, dextran sulfate solution (1% w/v) and 1 M zinc sulfate were added. Nanoparticles were centrifuged 3 times in 5% mannitol solution at 14,000 g for 20 minutes. RA-NP were conjugated with fluorescein isothiocyanate (FITC; 10 µg/ml) for *in vitro* cellular tracking. Then, the resulting nanoparticles (220 nm average diameter and zeta potential of +16 mV) were lyophilized for 4 days and stored at 4°C. This procedure was kindly carried out by Carlos Boto (collaborator of our group). For the *in vivo* biodistribution studies (described in a section below), RA-NP (40 µg/ml) were conjugated with the dye Cyanine5 N-hydroxysuccinimide ester (Cy5; 6.325 µg/ml; Lumiprobe GmbH, Hannover, Germany; calculated by a calibration curve from a known concentration of free Cy5, linear regression equation $y = 0.9227x$, $R^2 = 0.9965$) (220 nm average diameter and zeta potential of +16 mV). This procedure was kindly carried out by Vitor Francisco (collaborator of our group and co-author of the work conducted in Chapter 4). Blank nanoparticles (blank NP) were prepared following the same procedure, without RA. The amount of RA contained in 3, 10, and 30 µg/ml RA-NP is equivalent to 0.12, 0.40, and 1.20 µM free RA, respectively (Maia *et al.* 2011). These procedures were implemented at Lino Ferreira's laboratory (leader of the Advanced Therapies Research group, Cantanhede), collaborator of our group and co-author of the work.

2.10 RA-NP treatments and injections

For the *in vitro* studies, RA or RA-NP were added and maintained throughout the recovery period (24 hours after OGD). An additional control included DMSO in the percentage used to dissolve the highest concentration of free RA that was tested.

For the *in vivo* studies, RA-NP suspensions (10, 20, and 40 µg/g animal) were intravenously administered via the retro-orbital vascular sinus using a 30G needle (with the bevel down, at an angle of approximately 30°), as described (Yardeni *et al.* 2011). A total of 100 µl were administered (50 µl per retro-orbital sinus) (Grayston *et al.* 2022), after MCA reperfusion and under anesthesia, to the groups of mice as follows. This procedure was kindly carried out by Alba Grayston (co-

author of the work conducted in Chapter 4). For the 3-day protocol, 5 sham, 10 vehicle, 7 RA-NP (10 µg/g), 9 RA-NP (20 µg/g), and 8 RA-NP (40 µg/g) were treated. For the 7-day protocol, 4 sham, 16 mice vehicle, and 16 RA-NP (20 µg/g) were treated. The results were evaluated at three days and seven days after cerebral ischemia.

2.11 Immunostaining analysis

2.11.1 Immunocytochemistry analysis

Cell cultures were fixed with 2% paraformaldehyde (PFA; Sigma), washed with PBS, and blocked with a solution of 3% bovine serum albumin and 0.1% Tween 20 (Sigma) for 20 minutes at room temperature to prevent nonspecific binding. Cells were incubated with the primary antibody for 30 minutes at room temperature followed by overnight incubation at 4°C. Incubation with the respective secondary antibody was performed at room temperature for 2 hours. The antibodies used are detailed in the table below (Table 2.1). The nuclei were stained with Hoechst 33342 (4 µg/mL; Molecular Probes, OR, USA). Cell preparations were mounted in Dakocytomation fluorescent medium (Dakocytomation Inc., CA, USA) and images were acquired with AxioImager A1 microscope (Carl Zeiss, Gottingen, Germany).

Table 2.1 – List of primary and secondary antibodies, and dilutions used for immunocytochemistry.

Primary antibody	Company	Host	Dilution
Argonaute-2 (Ago2)	Cell Signaling, MA, USA	Rabbit	1:200
Cluster of differentiation-31 (CD31)	Novocastra, Leica Biosystems, Nussloch GmbH, Germany	Mouse	1:500
Glial fibrillary acidic protein (GFAP)	BD Biosciences, CA, USA	Mouse	1:500
Ionized calcium-binding adapter molecule-1 (Iba-1)	FujiFilm Wako Chemicals, VA, USA	Rabbit	1:500
Neuropilin-1 (NRP1)	BD Biosciences, CA, USA	Rabbit	1:200
Vascular endothelial growth factor receptor-2 (VEGFR2)	Abcam, Cambridge, UK	Rabbit	1:500
Secondary antibody	Company	Host	Dilution
Anti-mouse Alexa Fluor 488	Life Technologies, Carlsbad, CA, USA	Donkey	1:200
Anti-mouse Alexa Fluor 594	Abcam, Cambridge, UK	Donkey	1:200
Anti-rabbit Alexa Fluor 546	Life Technologies, Carlsbad, CA, USA	Donkey	1:200

2.11.2 Immunohistochemistry analysis

The immunoassays were conducted as described by our group (Machado-Pereira *et al.* 2022). Briefly, brains were removed, fixed with 4% PFA, and immersed in a 30% sucrose solution.

Finally, tissues were cryopreserved, and 40 μm -thick coronal slices were obtained in a freezing cryostat-microtome (Leica CM 3050S, Leica Microsystems, Nussloch, Germany). Afterwards, slices were incubated in a blocking solution containing 2% of horse serum (Thermo Fisher Scientific) and 0.3% Triton X-100 (Thermo Fisher Scientific) diluted in 0.1 M PBS for 2 hours at room temperature. Then, slices were incubated overnight at 4°C with the primary antibodies diluted in the blocking solution. After that, sections were rinsed in 0.1 M PBS and incubated with respective secondary antibodies and Hoechst-33342 (1:1000; Life Technologies) diluted in a solution containing 0.3% Triton X-100 in 0.1 M PBS for 2 hours at room temperature. Finally, tissue sections were rinsed in 0.1 M PBS and mounted in Fluoroshield Mounting Medium (Abcam Plc., Cambridge, UK). The primary and respective secondary antibodies are detailed in Supplementary Table I. Representative images were acquired in the peri-infarct area and corresponding area in the contralateral hemispheres using an AxioObserver LSM 710 confocal microscope (Carl Zeiss) under a 40 \times oil immersion objective. The antibodies used are detailed in the table below (Table 2.2).

Table 2.2 – List of primary and secondary antibodies, and dilutions used for immunohistochemistry.

Primary antibody	Company	Host	Dilution
Argonaute-2 (Ago2)	Cell Signaling, MA, USA	Rabbit	1:100
Beta-III tubulin (β -III tubulin)	Cell Signaling, MA, USA	Rabbit	1:500
Cluster of differentiation-31 (CD31)	Novocastra, Leica Biosystems, Nussloch GmbH, Germany	Mouse	1:500
Cluster of differentiation molecule 11b (CD11b)	AbD Serotec, Oxfordshire, UK	Rat	1:500
Glial fibrillary acidic protein (GFAP)	BD Biosciences, CA, USA	Mouse	1:1000
Microtubule-associated protein 2 (MAP2)	Merck Millipore, Darmstadt, Germany	Rabbit	1:500
Neuronal nuclear protein (NeuN)	Merck Millipore, Darmstadt, Germany	Mouse	1:500
Secondary antibody	Company	Host	Dilution
Anti-mouse Alexa Fluor 488	Life Technologies, Carlsbad, CA, USA	Donkey	1:200
Anti-mouse Alexa Fluor 594	Abcam, Cambridge, UK	Donkey	1:200
Anti-rabbit Alexa Fluor 546	Life Technologies, Carlsbad, CA, USA	Donkey	1:200
Anti-rabbit Alexa Fluor 594	Life Technologies, Carlsbad, CA, USA	Donkey	1:200
Anti-rat Alexa Fluor 488	Life Technologies, Carlsbad, CA, USA	Donkey	1:200

2.12 Vessel density analysis

To stain perfused blood vessels, a retro-orbital injection of a total of 40 µg of fluorescent lectin (Vector Laboratories, CA, United States) was performed 10 minutes prior to euthanasia. Brain slices were obtained as described in the previous subsection (2.11.2 Immunohistochemistry analysis). Afterwards, slices were permeabilized with 0.3% Triton X-100 (Thermo Fisher Scientific) in 0.1 M PBS for 30 minutes and rinsed in PBS and incubated with Hoechst-33342 (1:1000; Life Technologies) diluted in a solution containing 0.3% Triton X-100 in 0.1 M PBS for 2 hours at room temperature. Finally, tissue sections were rinsed in 0.1 M PBS and mounted in Fluoroshield Mounting Medium (Abcam Plc., Cambridge, UK). The corresponding images were kindly acquired by Luisa Cortes (Head of Microscopy Core Facility at the Center for Neuroscience and Cell Biology) using an automatic Slide Scanner (Carl Zeiss) under a 20x objective. Vessel density was measured in the peri-infarct area, i.e., the area surrounding the infarct/lesion, and normalized to each contralateral hemisphere, in 30 mid-brain slices obtained +0.25 mm in the anteroposterior axis measured from the bregma (Franklin and Paxinos 1997; Taylor *et al.* 2021). Briefly, six images (within the cortex and striatum) of the peri-infarct area in the ipsilateral and corresponding area in the contralateral hemispheres were acquired. Finally, a total of 12 fields, including different areas, were used to calculate the mean vessel density. All images were processed for background correction and unequivocal intensity signal per vessel network. All analyses were performed randomly using the open-source image processing program ImageJ software (National Institutes of Health).

2.13 WB analysis

Cell cultures and animal tissue were lysed using RIPA lysis buffer (0.15 M NaCl, 0.05 M Tris, 5 mM ethylene glycol tetraacetic acid, 1% Triton X-100, 0.5% deoxycholic acid, 0.1% sodium dodecyl sulphate, and 10 mM dichlorodiphenyltrichloroethane), with a cocktail of proteinase inhibitors (Roche Diagnostics Ltd., Mannheim, Germany). Total protein concentration was determined using the BCA assay (Thermo Scientific). The samples were separated in an 8%, 10% or 12.5% acrylamide gel (Applichem, Darmstadt, Germany), by sodium dodecyl sulphate-polyacrylamide gel electrophoresis (Mini-PROTEAN® Tetra Handcast, Bio-Rad, CA, USA), in a Tris-glycine running solution (pH 8.3; Acros Organics, Geel, Belgium) at room temperature and were transferred onto a polyvinylidene difluoride membrane (GE Healthcare, Little Chalfont, UK) for 60 or 100 minutes. Membranes were blocked for 1 hour in 0.1% gelatin (Sigma) or 5% (w/v) non-fat milk solution diluted in tris-buffered saline containing 0.05% Tween 20 (TBS-T; Sigma) and incubated overnight with the primary antibodies. After that, membranes were incubated with secondary antibodies. Protein expression was normalized with housekeeping targets. The antibodies used are detailed in the table below (Table 2.3). Proteins were detected by enhanced chemiluminescence exposure (Chemidoc™ MP imaging system (BioRad Laboratories, CA, USA), and levels were determined by densitometric analysis using the open-source image processing program ImageJ software (National Institutes of Health).

Table 2.3 – List of primary, secondary, and housekeeping antibodies used for WB analysis.

Primary antibody	Company	Host	Dilution
Argonaute-2 (Ago2)	Cell Signaling, MA, USA	Rabbit	1:500
Beta-III tubulin (β -III tubulin)	Cell Signaling, MA, USA	Rabbit	1:500
cAMP-response element binding protein (CREB)	Cell Signaling, MA, USA	Rabbit	1:1000
Cluster of differentiation molecule 11b (CD11b)	St John's Laboratory, London, UK	Rabbit	1:500
Endothelial nitric oxide synthase (eNOS)	BD Biosciences, CA, USA	Mouse	1:1000
Glial fibrillary acidic protein (GFAP)	BD Biosciences, CA, USA	Mouse	1:1000
Glial cell line-derived neurotrophic factor (GDNF)	Santa Cruz Biotechnology, CA, USA	Rabbit	1:250
Inducible nitric oxide synthase (iNOS)	BD Biosciences, CA, USA	Rabbit	1:1000
Ionized calcium-binding adapter molecule-1 (Iba-1)	Santa Cruz Biotechnology, CA, USA	Mouse	1:200
Microtubule-associated protein 2 (MAP2)	Santa Cruz Biotechnology, CA, USA	Rabbit	1:1000
NADPH oxidase 2 (Nox2)	BD Biosciences, CA, USA	Mouse	1:1000
Neuronal nuclear protein (NeuN)	Merck Millipore, Darmstadt, Germany	Mouse	1:500
Neuropilin-1 (NRP1)	Origene, MD, USA	Rabbit	1:500
Phosphorylated p38 (Pp38)	Cell Signaling, MA, USA	Rabbit	1:1000
Phosphorylated-Akt (pAkt) (Thr308)	Cell Signaling, MA, USA	Rabbit	1:1000
Postsynaptic density protein 95 (PSD-95)	Merck Millipore, Darmstadt, Germany	Mouse	1:1000
NADPH oxidase cytosolic protein p47phox (p47phox)	St John's Laboratory, London, UK	Rabbit	1:1000
Ubiquitin-binding autophagy substrate receptor (p62)	Santa Cruz Biotechnology, CA, USA	Mouse	1:1000
S100 calcium-binding protein B (S100B)	BD Biosciences, CA, USA	Mouse	1:5000
Total p38	Cell Signaling, MA, USA	Rabbit	1:1000
Tumor necrosis factor receptor-associated factor 6 (TRAF6)	Thermo Fisher Scientific, MA, USA	Rabbit	1:1000
Vascular endothelial (VE)-cadherin	St John's Laboratory, London, UK	Rabbit	1:1000

(table continues on the next page)

Secondary antibody	Company	Host	Dilution
Anti-mouse	Santa Cruz Biotechnology, CA, USA	Goat	1:5000
Anti-rabbit	Santa Cruz Biotechnology, CA, USA	Goat	1:5000
Housekeeping genes	Company	Host	Dilution
Actin	BD Biosciences, CA, USA	Mouse	1:5000
Glyceraldehyde 3-phosphate dehydrogenase (GAPDH)	Merck Millipore, Darmstadt, Germany	Mouse	1:5000
Tubulin	Sigma, MO, USA	Mouse	1:5000

2.14 Neurological scores and sensorimotor tests

The neurobehavioral outcome was evaluated at two, three, and seven days after MCAO using neurological scores and sensorimotor tests (grip strength and latency to move) (Morancho *et al.* 2012; Grayston *et al.* 2022). Briefly, neurological function was evaluated based on a 39-point scoring scale that assessed general deficits [0-13] (hair [0-2], ears [0-2], eyes [0-3], posture [0-3], and spontaneous activity [0-3]) and focal deficits [0-26] (body symmetry [0-2], gait [0-4], climbing on a surface held at 45° [0-3], circling behavior [0-3], forelimb symmetry [0-4], compulsory circling [0-3], whisker response [0-4], gripping test of the forepaws [0-3]). Additionally, the forelimb force was assessed using a grid with an angle of 30° (Bioseb, Chaville, France); herein, six measurements were taken for each mouse. Latency measures (time the mouse takes, in seconds, to move one body length) were also assessed at the same time points. Mice were pre-trained three days prior to the surgeries and a pre-MCAO measure (baseline) was obtained for the forelimb force analysis and latency measurements.

2.15 Infarct volume analysis

At the end of the 3-day protocol, mice were euthanized under deep anesthesia by exsanguination by cardiac puncture followed by transcardial perfusion with cold saline. Brains were obtained, freshly sliced into 1 mm thick coronal sections, and stained with 2,3,5-triphenyltetrazolium chloride (TTC; Sigma, St. Louis, MO, USA) in saline at room temperature for 15 minutes. Images were acquired using a CanoScan 4200F scanner (Canon USA Inc., NY, USA). Infarct volumes were quantified using the open-source image processing program ImageJ software (National Institutes of Health) (Morancho *et al.* 2012). Briefly, the infarct volume was calculated by integration of the lesion areas and considering the average of anterior and posterior views. Infarct volumes were then corrected for the edema index, which was determined as the area of the whole ipsilateral hemisphere divided by the area of the contralateral hemisphere. Infarct percentage was defined as the infarct volume divided by the total hemisphere volume.

2.16 Hemorrhage transformation analysis

Hemorrhagic transformation was assessed by measuring the total intracerebral hemorrhage volume, following the same protocol as for the infarct volume quantification described in the previous subsection (subsection 2.15 Infarct volume analysis).

2.17 Biodistribution studies

Fluorescent molecular imaging was performed to assess the RA-NP biodistribution *in vivo* and *ex vivo* using an IVIS Lumina LT Series III imaging system (PerkinElmer, Waltham, MA). Briefly, for *in vivo* image acquisitions, mice were anesthetized with isoflurane via facemask (5% for induction, 1.5% for maintenance in 95% O₂), and images were acquired at one hour after injection with RA-NP-Cy5 (40 µg/ml; $\lambda_{ex}/\lambda_{em} = 640/732$ nm). After *in vivo* acquisition, mice were euthanized by cervical dislocation after collecting blood samples by cardiac puncture, and organs (brain, heart, lungs, liver, spleen, kidneys) were dissected for the *ex vivo* imaging of the whole organs. Then, coronal brain slices were obtained for a more detailed analysis of the RA-NP biodistribution. All the images were acquired in the dorsal and ventral body/organ position. For quantification purposes, delimited regions of interest (ROI) were manually drawn surrounding the fluorescence signal. RA-NP fluorescent signal was obtained based on the total radiant efficiency value (TRE; [photons/s]/[µW/cm²]) using the Living Image software (PerkinElmer, Waltham, MA) and corrected by the TRE obtained from the corresponding ROI of the control animal serving as background signal. The background control animal did not receive nanoparticle administration and was imaged *in vivo* and *ex vivo* for background purposes. For *in vivo* data acquisitions, brain and abdominal ROI were drawn, and for *ex vivo* data acquisitions, ROI including the whole dissected organ were drawn.

2.18 Biochemical analysis/toxicity studies

Plasma collection was described in the ELISA section in the present Chapter. Systemic toxicity was evaluated based on plasma enzyme levels related to renal, liver, and pancreas function, namely alanine aminotransferase (ALT), aspartate aminotransferase (AST), creatine kinase (CK), lipase, creatinine, urea, sodium, and α -amylase using an Olympus AU5800 clinical chemistry analyzer. For each analyte, the respective unit/concentration is in the Table 4.1 (Chapter 4). Data were acquired by the Department of Clinical Biochemistry, Clinical Laboratories, Vall d'Hebron University Hospital, Barcelona, under the collaboration established with Anna Rosell (leader of the NeuroRepair L3, Neurovascular Research Laboratory, Vall d'Hebron Institut de Recerca group, Barcelona).

2.19 ELISA

For *in vitro* studies, cell culture media were collected and centrifuged (14,000 g for 20 minutes) to remove cell debris and contaminating nanoparticles. These samples were stored at -80°C until used without dilution. Total protein concentration was assessed using the BCA assay (Thermo Fisher Scientific) and was used for normalization. Samples were analyzed for Ago2 levels using a human Ago2 ELISA kit (MyBioSource, CA, USA), and for IL-1 β , IL-6, and TNF- α levels using a mouse IL-1 β ELISA kit, mouse IL-6 ELISA kit, and mouse TNF- α ELISA kit (BD Biosciences, CA, USA), respectively, according to the manufacturer's instructions.

For *in vivo* studies, venous blood was collected from the right ventricle into ethylenediamine tetraacetic acid 3K tubes (Everest-Tecnovet, Barcelona, Spain) and centrifuged (1,500 g for 10 minutes at 4°C) to obtain plasma. Brain homogenates were centrifuged (14,000 g for 20 minutes at 4°C) to collect supernatants. These plasma samples and brain supernatants were also stored at -80°C until use. All samples were analyzed for Ago2 levels using a mouse Ago2 ELISA kit (MyBioSource, CA, USA) according to the manufacturer's instructions. In addition, plasma samples were analyzed for systemic toxicity. Brain supernatant data were expressed as the ratio of ipsilateral to contralateral hemispheres.

2.20 Data analysis

Statistical analysis was performed using GraphPad Prism 8.1 (GraphPad Software, CA, USA). Statistical significance was determined using one-way ANOVA, followed by Dunnett's post-comparisons test and Bonferroni's post-comparisons test assuming normal or non-normal distribution, according to the comparison under analysis. Other analysis performed using the Student's t-test were detailed in each respective figure legend, when applicable. Statistical significance was considered relevant for p values <0.05. Data are expressed as mean \pm standard error of mean (SEM), determined from at least three independent experiments (numbers indicated in graph bars), performed in duplicate, except for western blotting experiments (no duplicates).

Chapter 3

Argonaute-2 protects the neurovascular unit from damage caused by systemic inflammation

Data from this Chapter were published in: Machado-Pereira M, Saraiva C, Bernardino L, Cristóvão AC, Ferreira R. Argonaute-2 protects the neurovascular unit from damage caused by systemic inflammation. *Journal of neuroinflammation*. 2022. 19(1): 17.

3.1 Abstract

The brain vasculature plays a pivotal role in the inflammatory process by modulating the interaction between blood cells and the neurovascular unit. Ago2 has been suggested as essential for endothelial survival but its role in the brain vasculature or in the endothelial-glia crosstalk has not been addressed. Thus, our aim was to clarify the significance of Ago2 in the inflammatory responses elicited by these cell types. Mouse primary cultures of BEC, astrocytes and microglia were used to evaluate cellular responses to the modulation of Ago2. Exposure of microglia to endothelial cell-conditioned media was used to assess the potential for *in vivo* studies. Adult mice were injected intraperitoneally with LPS (2 mg/kg) followed by three daily intraperitoneal injections of Ago2 (0.4 nM) to assess markers of endothelial disruption, glial reactivity and neuronal function. Herein, we demonstrated that LPS activation disturbed the integrity of adherens junctions and downregulated Ago2 in primary BEC. Exogenous treatment recovered intracellular Ago2 above control levels and recuperated vascular endothelial-cadherin expression, while downregulating LPS-induced NO release. Primary astrocytes did not show a significant change in Ago2 levels or response to the modulation of the Ago2 system, although endogenous Ago2 was shown to be critical in the maintenance of tumor necrosis factor- α basal levels. LPS-activated primary microglia overexpressed Ago2, and Ago2 silencing contained the inflammatory response to some extent, preventing IL-6 and NO release. Moreover, the secretome of Ago2-modulated BEC had a protective effect over microglia. The intraperitoneal injection of LPS impaired BBB and neuronal function, while triggering inflammation, and the subsequent systemic administration of Ago2 reduced or normalized endothelial, glial, and neuronal markers of LPS damage. This outcome likely resulted from the direct action of Ago2 over the brain endothelium, which reestablished glial and neuronal function. Ago2 could be regarded as a putative therapeutic agent, or target, in the recuperation of the neurovascular unit in inflammatory conditions.

3.2 Introduction

The brain vasculature exhibits unique properties that are required to coordinate parenchymal homeostasis and provide protection from circulating pathological elements (e.g., viruses, bacteria, toxins). The inner walls of blood vessels are lined by endothelial cells, which mediate the interactions between the bloodstream and neural cells, becoming a key component in BBB function and integrity (Daneman and Prat 2015). Understanding these cellular interactions is pivotal to disclose the mechanisms behind BBB disruption occurring in brain disorders and pathologies, and to promote vascular recovery. Cell activation unleashed by systemic inflammation is conducive to the generation of a pool of circulating mediators, i.e., cytokines, growth factors and vasoactive molecules that stimulate cell recruitment and adhesion, and sustain further cell activation, which may impair BBB function and aggravate tissue damage (Machado-Pereira *et al.* 2017; Varatharaj and Galea 2017). Considering that a major anti-angiogenic factor is inflammation, we focused on the endothelial-glia crosstalk, using the endotoxin LPS as the inflammatory cue. LPS has a direct effect on endothelial cells, namely on vasoregulation, vascular permeability, leukocyte recruitment and adhesion, with most work focusing on cell lines and/or peripheral vessels (Dauphinee and Karsan 2006). LPS is a classical inducer of Toll-like receptor 4 (TLR4) signaling (Akira *et al.* 2004). The TLR4 pro-inflammatory pathway requires tight control to avoid cytokine-related cell death and tissue damage and, in that sense, uses miR as a mechanism for negative regulation (O'Neill *et al.* 2011). These small but impactful noncoding molecules interact with messenger RNA and repress protein synthesis (Fabian *et al.* 2010; Bartel 2018). Ago2 is one of the key participants in the canonical biogenesis of miR, with the assistance of chaperones heat shock cognate protein 70 and heat shock protein 90 (Liu *et al.* 2004). Although there are other members of the Argonaute family, Ago2 is the only human Ago protein with endonuclease activity. In other mammals, the non-catalytic Ago proteins (Ago1, Ago3, and Ago4) can act redundantly to some extent (Meister 2013). Additionally, it operates as a natural carrier: most miR in the human plasma circulate in Ago2 ribonucleoprotein complexes (Arroyo *et al.* 2011; Boon and Vickers 2013), suggesting both intracellular and extracellular levels of Ago2 matter. Indeed, Ago2 knockdown directly correlates with a decrease in the expression of mature miR (Schmitter *et al.* 2006), while its upregulation is associated with a global increase (Winter and Diederichs 2011; Martinez and Gregory 2013). In a non-pathological vascular context, Ago2 knockdown per se compromised cell survival and the formation of tubules (primitive vascular network) by human umbilical vein endothelial cells (HUVEC) (Asai *et al.* 2008), indicating a role in angiogenesis. Moreover, Ago2 downregulation specifically decreased VEGF expression and signaling in hepatocellular carcinoma cell lines (Huh7 and SMMC-7721). The infection with a recombinant adenovirus expressing Ago2 restored VEGF expression and release in these cells (Ye ZL *et al.* 2015). Finally, we reported that Ago2 facilitates miR-18a entry into human and mouse BEC *in vitro* and *in vivo* (Ferreira *et al.* 2014), respectively. We found that BEC were highly permissive to miR uptake compared to other cell types, and uptake depended on Ago2 concentration. Extracellular Ago2 can be internalized through NRP1 (Prud'homme *et al.* 2016). Neuropilins (NRP) also bind to other ligands, such as class III semaphorins and members of the

VEGF family (Dueck *et al.* 2012). However, we did not discriminate against the impact of specific levels of Ago2 on BEC under pathological or inflammatory conditions. In this work, our aim was to clarify the role of Ago2 in (i) BEC and glia function under inflammatory conditions induced systemically, and (ii) in the repair of inflammation-afflicted neural tissue.

Herein, we demonstrated that LPS downregulated Ago2 and increased permeability of BEC *in vitro*, while Ago2 treatment restored these parameters. The conditioned media from Ago2-restored endothelium preserved the activity of microglia. Activated microglia overexpressed Ago2 and Ago2 silencing partially contained the inflammatory response, but LPS challenge did not affect astrocytic Ago2. It was only necessary to maintain the basal release of TNF- α *in vitro*. *In vivo*, the administration of Ago2 in LPS-injected animals produced a protective response in the neocortex and hippocampus, by reversing endothelial activation and securing normal glial and neuronal function. Therefore, Ago2 could be used as a potential agent for intravascular therapies, or a target for deactivating microglia, in an inflammatory setting. Considering the importance of inflammation in neuropathological contexts, further studies should explore the role of Ago2 in the CNS.

3.3 Results

3.3.1 LPS induces Ago2 downregulation and endothelial activation

Primary BEC were exposed to LPS (100 ng/ml) to mimic contact with an inflammatory environment (Ferreira *et al.* 2010; Ferreira *et al.* 2011; Ferreira *et al.* 2012; Machado-Pereira *et al.* 2018). These cells express Ago2 and its receptor, NRP1 (Prud'homme *et al.* 2016) (Figure 3.1A). Exposure to LPS significantly downregulated Ago2 intracellular levels (LPS = $41.9 \pm 7.5\%$, ** $p < 0.01$), similarly to the effect observed with Ago2 silencing (siAgo2 = $35.7 \pm 3.5\%$, ** $p < 0.01$) (Figure 3.1B). We have shown that a concentration of 50 ng/ml siRNA knockdowns intracellular Ago2 (Ferreira *et al.* 2014). In contrast, Ago2 silencing did not change the expression levels of NRP1 (siAgo2 = $105.9 \pm 7.6\%$), while LPS exposure significantly decreased the expression levels of NRP1 (LPS = $12.5 \pm 2.3\%$, **** $p < 0.0001$) (Figure 3.1C). Ago2 silencing compromised cell survival (siAgo2 = $64.8 \pm 4.9\%$, * $p < 0.05$) (Figure 3.1D) and induced necrosis or late apoptosis, as suggested by the release of LDH through the disrupted plasma membrane (LPS = $170.5 \pm 3.2\%$, **** $p < 0.0001$) (Figure 3.1E). We measured the extracellular levels of Ago2 by ELISA, but values were below the detection range and sensitivity threshold value (data not shown). Thus, we considered that Ago2 was not released. LPS had no effect on cell viability nor caused toxicity (Figure 3.1D and 3.1E), but significantly decreased total protein content (Figure 3.1F). Conversely, intracellular Ago2 levels were increased upon Ago2 exogenous co-application (0.4 nM) (LPS+Ago2 = $138.5 \pm 15.8\%$, **** $p < 0.0001$) (Figure 3.1G). This concentration ensures maximum miR delivery to primary BEC (Ferreira *et al.* 2014), to secure RISC activity. The application of Ago2 alone did not change Ago2 intracellular levels (Ago2 = $72.3 \pm 9.2\%$) (Figure 3.1B) nor affected cell viability, toxicity, or protein content (Figure 3.1D, 3.1E and 3.1F); however, it

increased NRP1 (Ago2 = 148.5 ± 6.4%, ***p<0.001) (Figure 3.1C). Then, we evaluated the contribution of a protein-degrading mechanism, autophagy, by treating cells with a late-stage inhibitor of this process, BafA1. The treatment with BafA1 for 3 hours increased intracellular Ago2 (LPS+BafA1 = 138.5 ± 13.9%, ###p < 0.0001) (Figure 3.1G). We tested other periods of incubation with BafA1, albeit with no effect on Ago2 levels (data not shown). Using the same experimental conditions, we measured the release of NO (Figure 3.1H). NO is a vasoregulator that inhibits platelet aggregation and leukocyte adhesion (Prud'homme *et al.* 2016). While LPS increased NO levels (LPS = 186.5 ± 15.7%, ***p<0.001), as expected (Dauphinee and Karsan 2006), Ago2 treatment inhibited NO release (LPS+Ago2 = 41.7 ± 15.0%, ###p<0.0001). Autophagy inhibition failed to change the NO response to LPS (LPS+BafA1 = 219.5 ± 32.8%, ***p<0.001) (Figure 3.1H). LPS downregulated the expression of VE-cadherin (LPS = 63.5 ± 22.5%, p=0.0307), which is responsible for the assembly of adherens junctions and BBB integrity (Vestweber 2008). Ago2 treatment recuperated VE-cadherin expression (LPS+Ago2 = 134.6 ± 22.5%, *p<0.05) (Figure 3.1I) and the inhibition of autophagy resulted in VE-cadherin levels similar to untreated cells, as well (LPS+BafA1 = 100.1 ± 22.7%) (Figure 3.1I). LPS administration enhanced the release of cytokines involved in angiogenesis, TNF-α (LPS = 225.0 ± 28.9%, *p < 0.05) and IL-6 (LPS = 319.9 ± 37.7%, ****p < 0.0001), as expected (Sainson *et al.* 2008; Gopinathan *et al.* 2015), but Ago2 treatment failed to produce a significant effect (Figures 3.1J and 3.1K, respectively). In sum, the loss of Ago2 appears to be correlated with specific markers of endothelial activation.

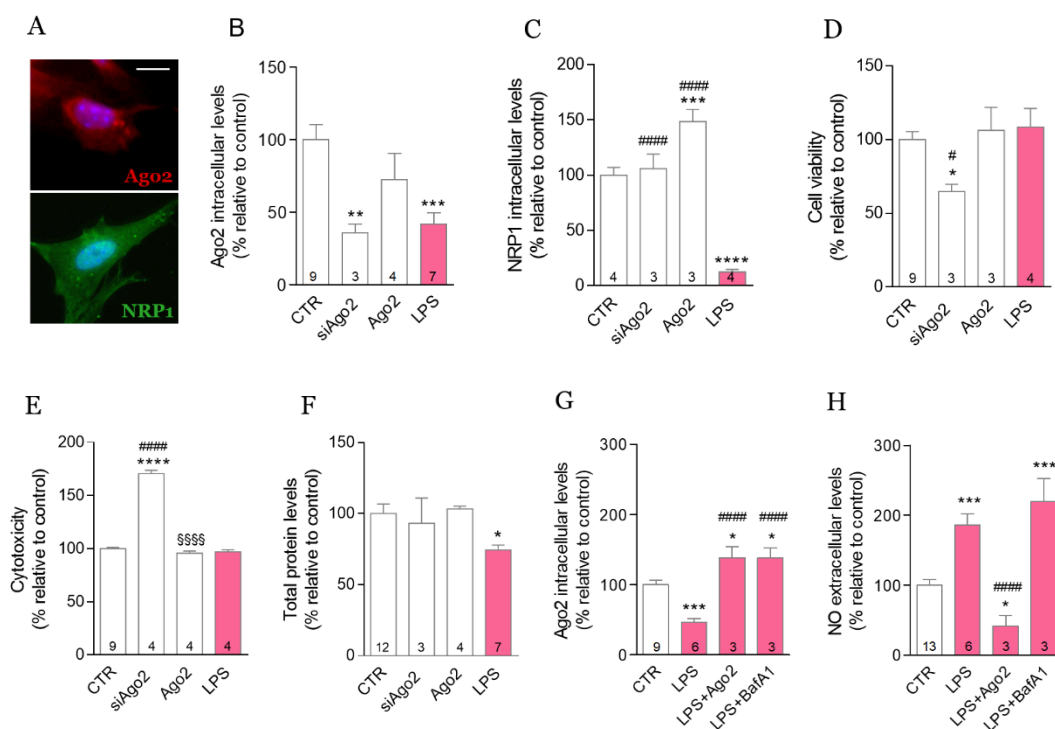


(figure continues on the next page)

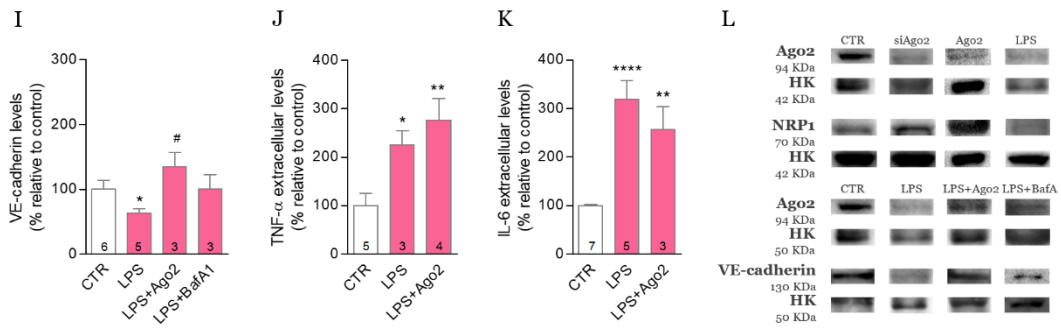


Figure 3.1 – LPS-induced Ago2 downregulation correlates with loss of endothelial function. Mouse primary BEC express Ago2 and NRP1, assessed by immunocytochemistry (A); scale bar 10 μ m. BEC stimulated with LPS (100 ng/ml for 24 hours) exhibited endogenous Ago2 levels significantly lower than untreated cells (CTR). This effect was similarly obtained with Ago2 silencing (0.05 μ M). Ago2 treatment per se did not change intracellular levels (B). While siAgo2 had no effect on NRP1 expression, the receptor was downregulated by LPS and upregulated by Ago2 treatment alone (C). Ago2 silencing compromised cell survival (D) and induced cytotoxicity (E). LPS only caused loss of protein content (F). Ago2 treatment had no effect on any of these parameters associated to cell survival (D-F) Ago2 co-treatment (0.4 nM) restored its intracellular levels in LPS-activated endothelial cells. The same result was produced by autophagy inhibition with bafA1 (100 nM), measured by WB (G). LPS-activated cells released NO and Ago2 treatment significantly reverted LPS-induced increase of NO levels, measured by Griess assay (H). LPS-activated cells showed a decrease in VE-cadherin expression and Ago2 treatment maintained the levels of this intercellular junction protein, measured by WB (I). LPS-activated BEC released pro-inflammatory factors, such as TNF- α and IL-6, the replenishment of Ago2 intracellular levels failed to normalize the levels of these cytokines (J and K, respectively), measured by ELISA. Representative protein bands obtained from western blotting experiments (L). Data are expressed as the mean \pm SEM of the indicated number of repeats and as a percentage relative to untreated controls (*p < 0.05, **p < 0.01, ***p < 0.001, ****p < 0.0001 compared to untreated controls; #p < 0.05, ##p < 0.01, ###p < 0.001, ####p < 0.0001 compared to LPS-activated cells; one-way ANOVA for all figures; in Figure 3.1I, Student's t test was used for the comparison between CTR and LPS).

3.3.2 Microglial, but not astrocytic Ago2, is necessary for LPS-induced cell activation

Astrocytes are physically associated with, and significantly contribute to regulate blood vessel function (Macvicar and Newman 2015). Contrary to BEC, primary astrocytes did not reveal significant differences in Ago2 expression after LPS exposure. While Ago2 silencing per se reduced Ago2 levels (siAgo2 = 45.7 \pm 16.1%, *p < 0.05), Ago2 expression was maintained and slightly increased following LPS stimulation (LPS+siAgo2 = 130.3 \pm 9.4%) (Figure 3.2A), and reproduced the same results as LPS alone in the following panels. The astrocytic population did not demonstrate significant changes in cell viability (Figure 3.2B). Astrocytes were activated by LPS exposure, as observed by increased expression of GFAP (LPS = 145.2 \pm 4.7%, **p < 0.01) (Figure 3.2C), TNF- α release (LPS = 302.9 \pm 15.5%, ****p < 0.001) (Figure 3.2E) and expression of glial cell-derived neurotrophic factor (GDNF) (LPS = 208.3 \pm 34.2%, *p < 0.05) (Figure 3.2F). However, we did not register any changes in NO levels (Figure 3.2D). Ago2 silencing alone only resulted in a significant decrease regarding the basal release of TNF- α (siAgo2 = 64.0 \pm 14.0%, p = 0.0271) (Figure 3.2E). Microglia participate in the inflammatory response and contribute to the maintenance of BBB integrity (Machado-Pereira *et al.* 2016). Contrary to BEC, under

inflammatory conditions, microglia overexpressed Ago2 (LPS = $352.0 \pm 15.2\%$, $***p < 0.001$) (Figure 3.2A), with no impact on cell viability (Figure 3.2B).

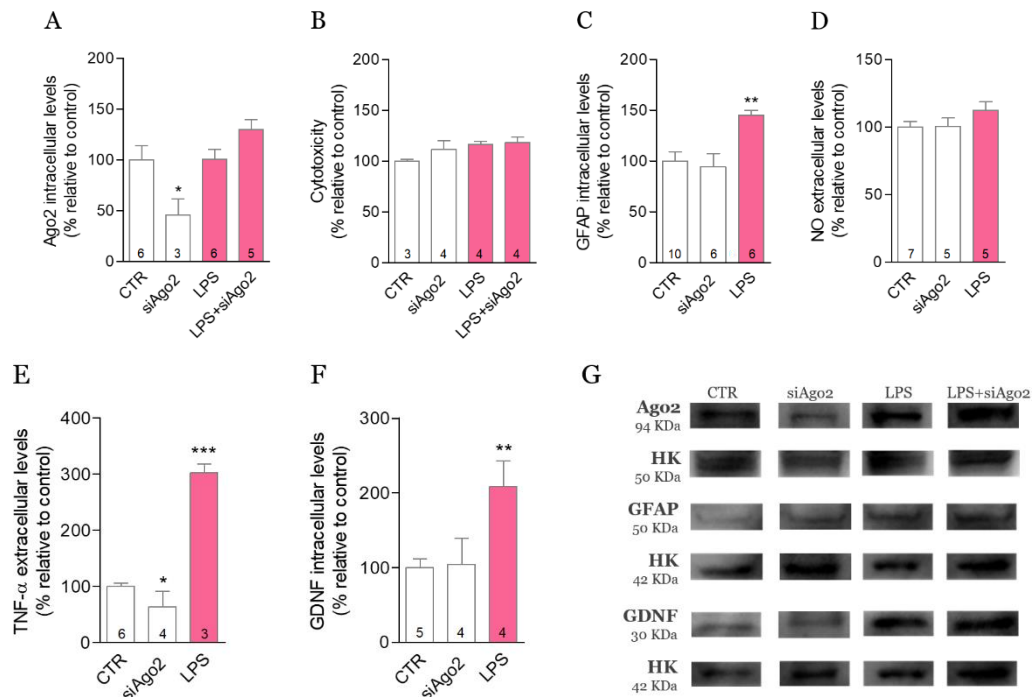


Figure 3.2 – Ago2 is not involved in LPS-induced astrocyte activation. Direct exposure to LPS (100 ng/ml) did not change Ago2 levels (A) or caused cytotoxicity in primary astrocytes (B). LPS-activated primary astrocytes overexpressed GFAP (C) and GDNF (F), measured by WB, and released TNF- α (E), measured by ELISA. Ago2 silencing decreased Ago2 levels (A) and lowered the basal release of TNF- α (E). No effect was observed on NO (D). Representative protein bands obtained from western blotting experiments (G). Data are expressed as the mean \pm SEM of the indicated number of repeats and as a percentage relative to untreated controls (* $p < 0.05$, ** $p < 0.01$, *** $p < 0.0001$ compared to untreated controls; one-way ANOVA for all figures; in Figure 3.2E, Student's t test was used for the comparison between CTR and siAgo2).

In microglia, Ago2 silencing alone ($0.05 \mu\text{M}$) lowered Ago2 intracellular levels (siAgo2 = $34.0 \pm 12.7\%$, $***p < 0.001$) as well as in the presence of LPS (LPS+siAgo2 = $30.0 \pm 2.7\%$, $***p < 0.001$) (Figure 3.3A), highlighting important differences with astrocytes. Only in the latter condition, cell toxicity was induced (LPS+siAgo2 = $137.9 \pm 18.5\%$, $*p < 0.05$) (Figure 3.3B). However, in these conditions, Ago2 silencing lowered the release of NO (LPS+siAgo2 = $122.4 \pm 3.9\%$, $##p < 0.01$) (Figure 3.3C) and normalized IL-6 (LPS+siAgo2 = $88.4 \pm 5.5\%$, $###p < 0.001$) (Figure 3.3E). The opposite effect was obtained regarding the expression of TRAF6 (LPS+siAgo2 = $88.5 \pm 5.9\%$, $#p < 0.05$) (Figure 3.3F) versus the decrease induced after LPS stimulation (LPS = $71.9 \pm 2.9\%$, $**p < 0.01$). TRAF6 is a regulator of the immune response (Yang FM *et al.* 2018). No changes were produced by Ago2 silencing on LPS-stimulated TNF- α release (Figure 3.3D).

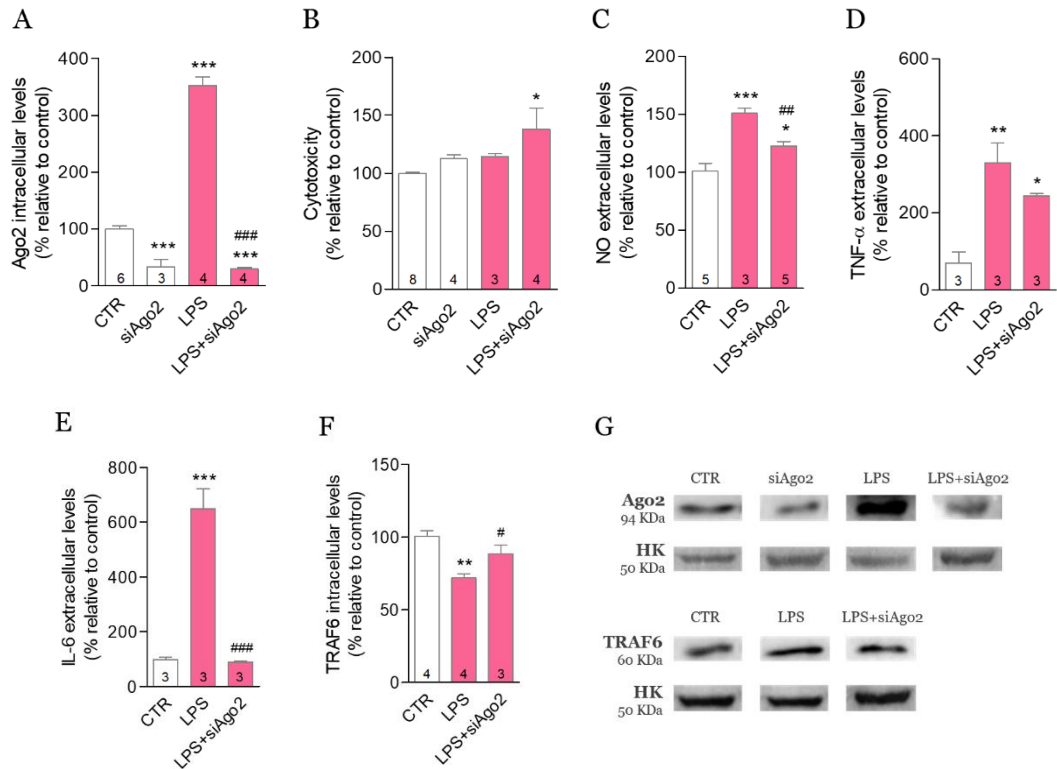


Figure 3.3 – Ago2 silencing reduces microglial inflammatory responses. LPS (100 ng/ml) increased Ago2 intracellular levels in primary microglia, while the transfection with 0.05 μ M of Ago2 siRNA reduced the intracellular levels of Ago2, even after LPS stimulation, measured by western blotting (A). Ago2 silencing was cytotoxic only in conjunction with LPS (B). Ago2-silenced microglial revealed lower levels of NO (C) and IL-6 (E), but not TNF- α (D), in an inflammatory environment, measured by ELISA. TRAF6 expression was reduced after LPS challenge but Ago2 silencing counteracted this effect, measured by western blotting (F). Representative protein bands obtained from western blotting experiments (G). Data are expressed as the mean \pm SEM of the indicated number of repeats and as a percentage relative to untreated controls (* p < 0.05, ** p < 0.01; *** p < 0.001, compared to untreated controls; # p < 0.05, ## p < 0.01, ### p < 0.001, compared to LPS-activated cells; one-way ANOVA for all figures; in Figure 3.3D, Student's t test was used for the comparison between CTR and LPS).

3.3.3 Ago2-restored endothelium reduces microglia activation

The endothelial secretome shapes microglia responses and endothelial-activated microglial cells adopt a neurotoxic profile (Xing *et al.* 2018). We exposed primary microglia to the conditioned media of primary BEC (EC-CM) previously stimulated with LPS alone (100 ng/ml) ((LPS EC)-CM) or treated with Ago2 (0.4 nM) ((LPS+Ago2 EC)-CM), or left untreated (CTR EC)-CM (Figure 3.4A). (CTR EC)-CM significantly reduced microglial basal cell death, but this effect was lost with (LPS EC)-CM ((CTR EC)-CM = 68.7 \pm 3.9%, *** p < 0.001); (LPS EC)-CM = 95.0 \pm 4.0%, § p < 0.05). Ago2 treatment retained the protective quality of (CTR EC)-CM ((LPS+Ago2 EC)-CM = 73.5 \pm 3.1%, * p < 0.05; § p < 0.05) (Figure 3.4B). Microglia exposed to (LPS+Ago2 EC)-CM presented CD11b levels similar to cells either left untreated or exposed to (CTR EC)-CM, and significantly different from cells exposed to (LPS EC)-CM, suggesting a strong attempt to prevent cell activation ((CTR EC)-CM = 104.1 \pm 4.2%; (LPS EC)-CM = 313.9 \pm 14.6%, *** p < 0.001, §§ p < 0.01; (LPS+Ago2 EC)-CM = 136.7 \pm 8.4%, \$\$\$ p < 0.05)) (Figure 3.4C). Ago2 silencing in the presence of LPS also prevented CD11b overexpression (LPS+siAgo2 = 51.6 \pm 32.1%, ### p < 0.001),

although this condition raised cell death (LPS+siAgo2 = 127.7 ± 12.2%, *p<0.05 (Figure 3.4B). Lastly, IL-1β levels were not significant changed by any of the EC-CM, although cells were responsive to LPS stimulation (LPS = 196.1 ± 64.6%, *p=0.0484) (Figure 3.4D). On the other hand, (CTR EC)-CM and (LPS+Ago2 EC)-CM efficiently reduced NO below the levels obtained by untreated cells or cells exposed to (LPS EC)-CM ((CTR EC)-CM = 55.2 ± 5.2%, ****p<0.0001; (LPS EC)-CM = 104.5 ± 14.6%, §§§§p<0.0001; (LPS+Ago2 EC)-CM = 43.8 ± 2.4%, §§§§p<0.0001) (Figure 3.4E). Hence, the secretome of either Ago2-restored endothelium or normal BEC shared the same properties.

A

Brain endothelial cells

No treatment (CTR)
LPS
LPS + Ago2

EC-CM collection
(after 24 hours)

(CTR EC)-CM
(LPS EC)-CM
(LPS + Ago2)-CM

Microglia

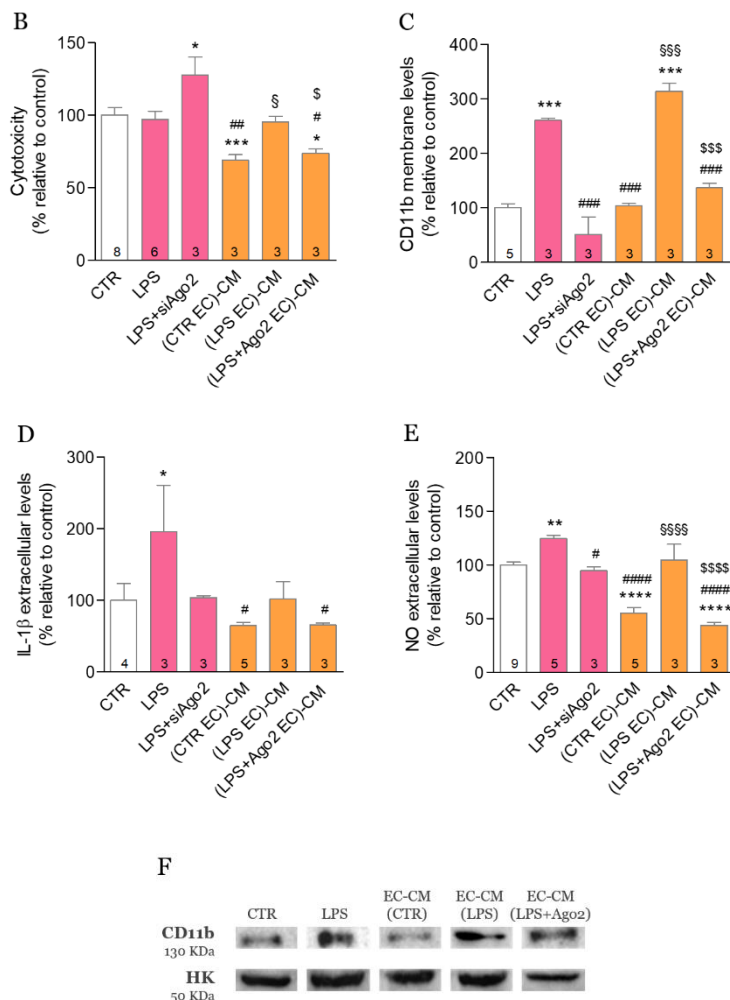
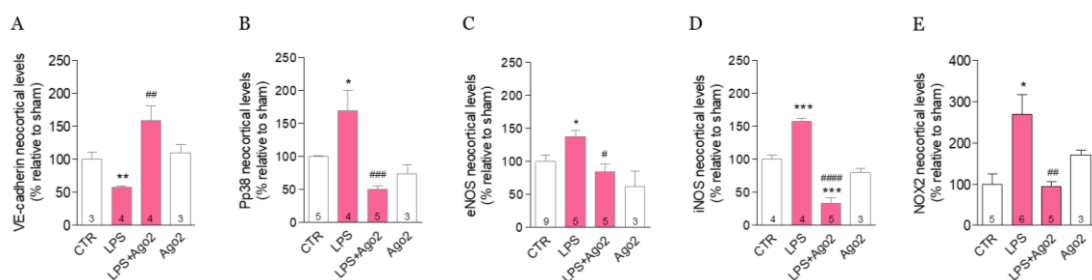


Figure 3.4 – Ago2-restored endothelium normalizes microglia response. Schematic representation of the experimental setup (A). Endothelial cell-conditioned media (EC-CM) from cells exposed to LPS and treated with Ago2 (0.4 nM) ((LPS+Ago2 EC)-CM) reproduced the protective effect of EC-CM collected from healthy endothelial cells ((CTR EC)-CM), measured by LDH activity assay (B). Microglial cells exposed to (LPS+Ago2 EC)-CM presented CD11b levels similar to untreated cells (CTR) and cells exposed to (CTR EC)-CM,

measured by WB, while (LPS EC)-CM had the same effect as the LPS treatment (C). EC-CM had no significant effect over IL-1 β release (D), but (CTR EC)-CM and (LPS+Ago2 EC)-CM decreased NO below control levels (E). Representative protein bands obtained from western blotting experiments (F). Data are expressed as the mean \pm SEM of the indicated number of repeats and as a percentage relative to untreated controls (*p < 0.05, **p < 0.01, ***p < 0.001, ****p < 0.0001, compared to untreated controls; #p < 0.05, ##p < 0.01, ###p < 0.001, ####p < 0.0001, compared to LPS-activated cells; §p < 0.05, §§§p < 0.001, §§§§p < 0.0001, compared to (CTR EC)-CM; §p < 0.05, §§§p < 0.001, §§§§p < 0.0001, compared to (LPS EC)-CM; one-way ANOVA; in Figure 3.4D, Student's t test was used for the comparison between CTR and LPS)).

3.3.4 Systemic administration of Ago2 normalizes endothelial and glial activation in the mouse cortex

Mice were injected intraperitoneally with LPS (2 mg/kg) to induce BBB disruption and brain tissue inflammation (Xing *et al.* 2018; Saraiva *et al.* 2019). Then, mice received daily intraperitoneal injections of Ago2 (0.4 nM), as published by us and others (Ferreira *et al.* 2014; Danilov *et al.* 2020) (Figure 3.5M) and we evaluated markers associated to LPS activation of endothelial and glial cells, namely VE-cadherin, Pp38, eNOS, iNOS, NOX2, p47phox, Iba-1, GFAP and S100B (Figures 3.5A to 3.5J). As expected, all markers with the exception of VE-cadherin and p47phox were increased upon LPS administration (LPS = 57.4 \pm 2.3%, **p = 0.0030 (VE-cadherin); LPS = 169.0 \pm 31.3%, *p < 0.05 (Pp38); LPS = 137.7 \pm 9.6%, *p = 0.0117 (eNOS); LPS = 157.2 \pm 5.3%, ***p < 0.001 (iNOS); LPS = 270.2 \pm 47.3%, *p < 0.05 (NOX 2); LPS = 65.6 \pm 9.2%, *p = 0.0113 (p47phox); LPS = 211.5 \pm 36.4%, *p = 0.05 (Iba-1); LPS = 378.6 \pm 14.5%, ***p < 0.001 (GFAP); LPS = 191.3 \pm 13.5%, **p < 0.01 (S100B)). No changes were produced on NRP1 levels (LPS = 116.7 \pm 10.4%). Ago2 treatment (0.4 nM) normalized the expression of all markers with the exception of iNOS, which was decreased below control levels, and NRP1, which was upregulated (LPS+Ago2 = 109.9 \pm 12.6%, ##p < 0.01 (VE-cadherin); LPS+Ago2 = 50.8 \pm 4.9%, ###p < 0.001 (Pp38); LPS+Ago2 = 84.6 \pm 11.8%, #p < 0.05 (eNOS); LPS+Ago2 = 33.2 \pm 8.7%, ***p < 0.001 (iNOS); LPS+Ago2 = 94.33 \pm 11.1%, ##p < 0.01 (NOX2); LPS+Ago2 = 123.4 \pm 13.2%, #p < 0.05 (p47phox); LPS+Ago2 = 70.7 \pm 9.0%, #p < 0.05 (Iba-1); LPS+Ago2 = 95.4 \pm 11.4%, ###p < 0.001 (GFAP); LPS+Ago2 = 95.9 \pm 9.3%, ##p < 0.01 (S100B); (LPS+Ago2 = 170.3 \pm 18.9%, *p < 0.05)). Ago2 injection per se did not produce any significant changes in these markers or over Ago2 tissue levels (Figure 3.5J). These data, summarized in Figure 3.5M, support the hypothesis of an anti-inflammatory effect produced by Ago2 via the deactivation of inflamed brain endothelium.



(figure continues on the next page)

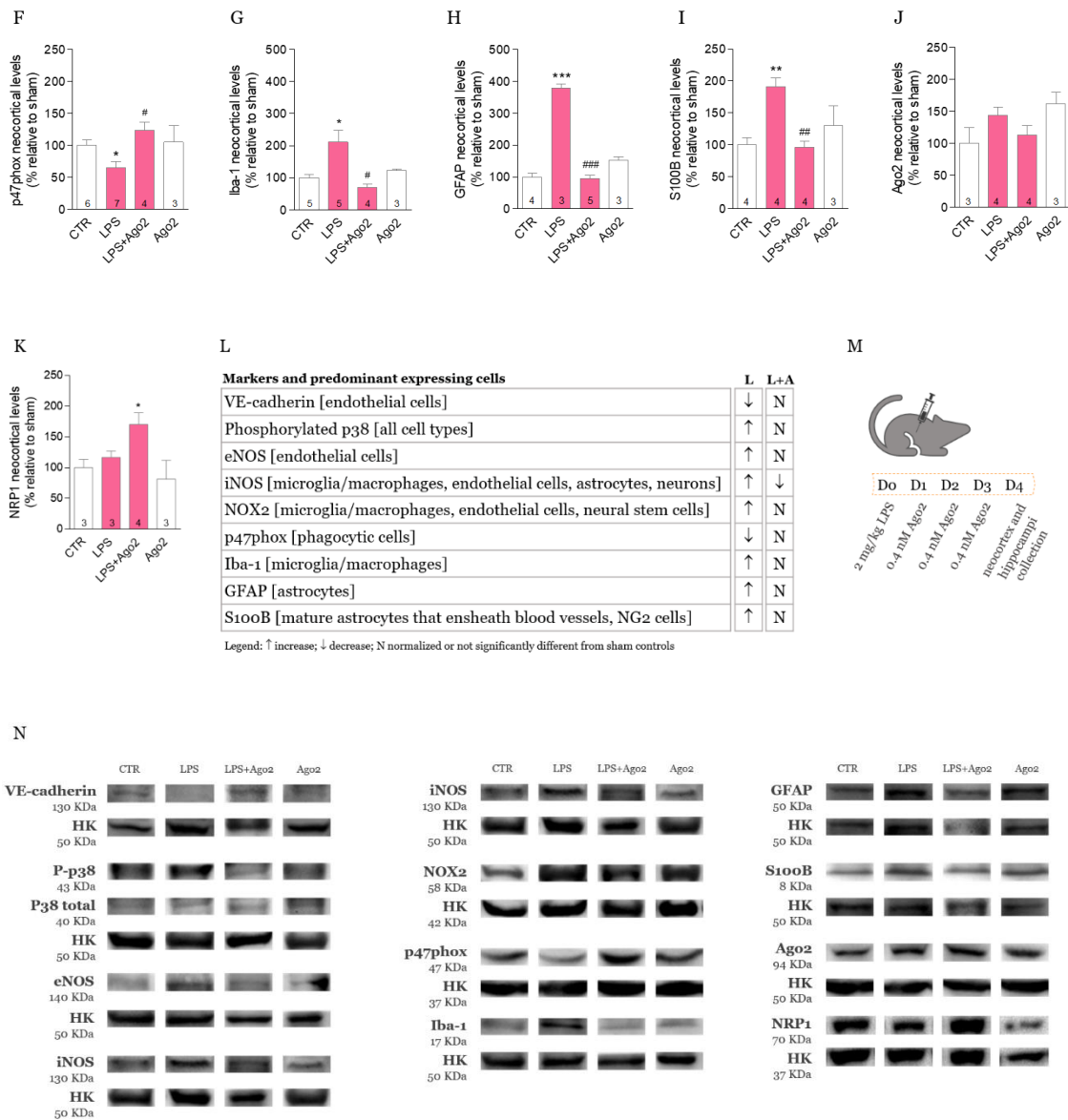
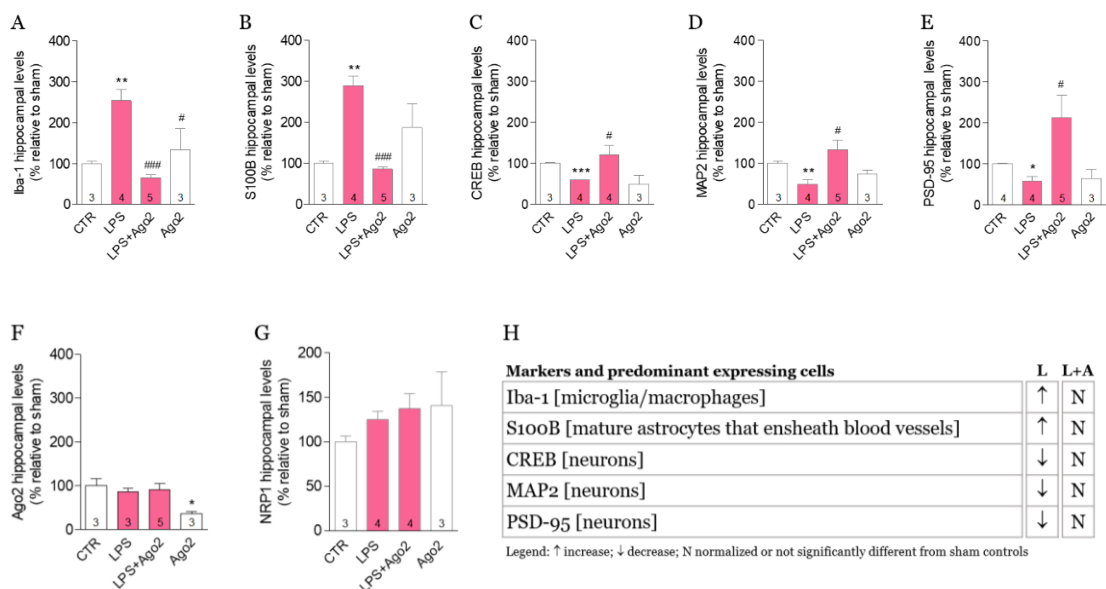


Figure 3.5 – Systemic administration of Ago2 restores endothelial barrier function and normalizes glial activation in the cortex. Mice injected intraperitoneally with LPS (2 mg/kg) showed the activation of p38 signaling pathway i.e., increased Pp38 (B) and produced higher levels of eNOS (C), iNOS (D), NOX2 (E), Iba-1 (G), GFAP (H) and S100B (I), and lower levels of VE-cadherin (A) and p47phox (F). LPS-injected mice treated with Ago2 (0.4 nmol/L) had marker levels similar to sham controls (animals injected with PBS, CTR), with the exception of the Pp38 and iNOS markers. The same pattern of reduction below control levels was obtained with Ago2 injection in sham controls. Ago2 cortical levels did not change significantly in any of the experimental conditions (J). The levels of NRP1 were only raised in LPS-injected mice treated with Ago2 (K). The table summarizes data from these experiments (L). Schematic representation of the experimental setup used herein (and in the Figure 3.6) (M). Representative protein bands obtained from western blotting experiments (N). Data are expressed as the mean \pm SEM of the indicated number of repeats and as a percentage relative to sham controls (*p < 0.05, **p < 0.01, ***p < 0.001, ****p < 0.0001 compared to sham controls; #p < 0.05, ##p < 0.01, ###p < 0.0001 compared to LPS-injected animals; one-way ANOVA; in Figure 3.5A, 3.5C and 3.5F, Student's t test was used for the comparison between CTR and LPS).

3.3.5 Systemic administration of Ago2 normalizes inflammatory response and induces neuroprotection in the mouse hippocampus.

We measured the expression of microglial marker Iba-1 and astrocyte marker S100B, which identifies astrocytes in direct contact with blood vessels, to evaluate whether Ago2 could reverse the glial and neuronal LPS-induced damage in the hippocampus (Sánchez *et al.* 2000). As expected, glial markers were increased upon LPS administration (LPS = 254.3 ± 27.9% (Iba-1); LPS = 290.2 ± 22.5% (S100B); **p<0.01 (Figures 3.6A to 3.6B)). Ago2 treatment (0.4 nM) restored the expression of Iba-1 (LPS+Ago2 = 64.8 ± 7.5%, ###p<0.001) and S100B (LPS+Ago2 = 85.8 ± 5.7%, ###p < 0.0001). No changes were produced on NRP1 levels (LPS = 125.4 ± 9.2%; LPS+Ago2 = 137.6 ± 16.8%). To disclose if the normalized inflammatory response was accompanied by an effect over neuronal function and synaptic activity, we evaluated the expression of CREB, MAP2, and PSD-95 (Sánchez *et al.* 2000; Kim and Sheng 2004; Alberini 2009). Herein, as expected, we observed a reduction in the expression of CREB, MAP2 and PSD-95 upon LPS administration (LPS = 59.0 ± 1.2%, ***p < 0.001 (CREB); LPS = 49.2 ± 10.3%, **p=0057 (MAP2); LPS = 58.1 ± 10.7%, *p = 0.0109 (PSD-95) (Figures 3.6C to 3.6E)). Ago2 treatment normalized the expression of these markers (LPS+Ago2 = 120.5 ± 22.8% (CREB); LPS+Ago2 = 132.6 ± 23.8% (MAP2); LPS+Ago2 = 211.9 ± 56.0% (PSD-95); #p<0.05. Ago2 per se did not have an effect (Figures 3.6A to 3.6E). Finally, the Ago2 hippocampus levels did not change in the experimental conditions, except for the Ago2-injected mice, in which a decrease was observed (Ago2 = 36.8 ± 4.5%, *p<0.05) (Figure 3.6F). The table summarized data that support the hypothesis that Ago2 may positively impact neuronal activity upon inflammatory challenge (Figure 3.6H).



(figure continues on the next page)

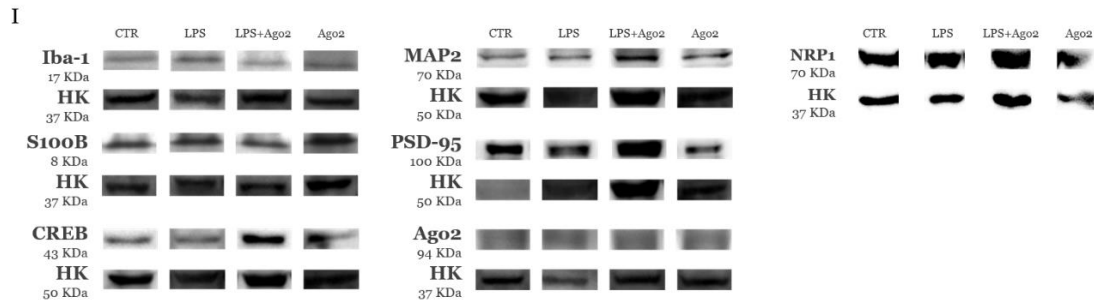


Figure 3.6 – Systemic administration of Ago2 normalizes inflammatory activation and induces neuroprotection in the hippocampus. LPS-injected mice (LPS, 2 mg/kg) produced higher levels of Iba-1 (A) and S100B (B), and lower levels of CREB (C), MAP2 (D), and PSD-95 (E). Mice treated with Ago2 (0.4 nmol/L) had marker levels similar to sham controls (animals injected with PBS, CTR), with the exception of the Iba-1 marker. Similar to the mouse cortex, the Ago2 hippocampus levels did not change significantly in the experimental conditions, with the exception of the Ago2-injected mice, in which a decrease of Ago2 levels occurred (F). NRP1 levels did not change significantly in any of the experimental conditions (G). The table summarizes data from these experiments (H). Representative protein bands obtained from western blotting experiments (I). Data are expressed as the mean \pm SEM of the indicated number of repeats and as a percentage relative to sham controls (* p < 0.05, ** p < 0.01, *** p < 0.001, **** p < 0.0001 compared to sham controls; # p < 0.05, ## p < 0.001, ### p < 0.0001 compared to LPS-injected animals; one-way ANOVA; in Figure 3.6C to 3.6E, Student's t test was used for the comparison between CTR and LPS).

Ultimately, LPS injection slightly increased Ago2 detection in the neocortex (Figure 3.5J) albeit not significantly. We hypothesized that microglia, which have higher density in the neocortex, and overexpress Ago2 *in vitro* and *in vivo*, are likely contributing to this effect (in comparison with the hippocampus; Figure 3.7).

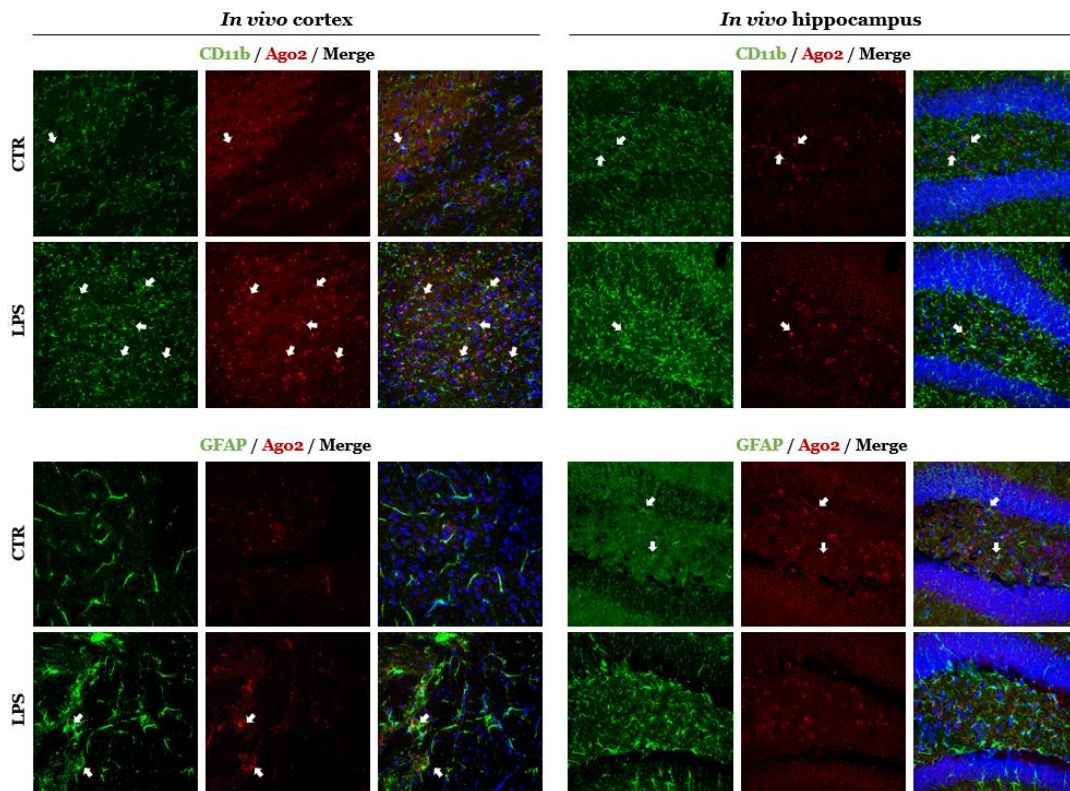


Figure 3.7 – Representative confocal images of GFAP, CD11b (green) and Ago2 (red) obtained in cortex and hippocampal slices from mice injected with saline (CTR) and 2 mg/kg LPS.

3.4 Discussion

The role of the brain endothelium in inflammation-induced barrier loss and parenchymal damage remains poorly explored, despite being a key target for intravascular therapies addressing injury in the CNS (Machado-Pereira *et al.* 2018). The first report exploring Ago2 in vascular function showed that silencing this protein alone inhibited proliferation, enhanced apoptosis, and suppressed the formation of tubules of HUVEC (Asai *et al.* 2008). Thus, our first aim was to clarify the role of Ago2 in brain endothelial cells (BEC) and identify changes in function, via Ago2, when exposed to an inflammatory cue, i.e., LPS. LPS stimulation alters the expression of junctional proteins and triggers the production of several inflammatory mediators (*in vitro* models) and disrupts the BBB (*in vivo* models) (Varatharaj and Galea 2017).

Our data showed that LPS-activated BEC expressed lower Ago2 levels, an effect reproduced with Ago2 silencing. However, only the latter specifically compromised cell survival, in accordance with the work of Asai and colleagues (Asai *et al.* 2008). The exogenous application of Ago2 increased intracellular levels, likely via NRP1-mediated internalization (Prud'homme *et al.* 2016). NRP1 is the main Ago2 receptor (whether Ago2 is carrying miR or not) although it can also bind to multiple ligand families such as class III semaphorins and the VEGF family (Dueck *et al.* 2012). Neuronal, endothelial, and epithelial cells are the main cell types expressing NRP1 and are thus responsive to extracellular Ago2 (Wild *et al.* 2012), which is particularly relevant for understanding the outcomes of our *in vivo* model. In endothelial cells, NRP1 is essential for normal vascular development (Gu *et al.* 2003): NRP1-deficient mice die during the embryo stage with abnormalities in the vasculature, heart, and nervous system (Kitsukawa *et al.* 1997; Kawasaki *et al.* 1999). Interestingly, LPS stimulation downregulated NRP1 in primary endothelial cells, an effect that was shown by others to provide positive signals for cell survival (e.g., HUVEC) through the regulation of growth factor receptor (Bae *et al.* 2008). The reduction of NRP1 expression could be a consequence of the protein-degrading mechanism autophagy, which occurs in the inflamed endothelium (Reglero-Real *et al.* 2021), possibly to maintain cell viability. In primary macrophages, LPS (100 ng/ml for 12 hours) also mediated NRP1 suppression through the activation of TLR4–NF- κ B p50 and p65 pathways. TLR4 can be activated by either exogenous (e.g., LPS) or endogenous (e.g., HSP60) ligands, inducing downstream signals (MyD88-dependent and MyD88-independent signals) and promoting cytokine and chemokine production (Sun *et al.* 2015). However, this result is not consistently observed in all cells exposed to LPS (e.g., mouse embryonic fibroblasts, rat fibroblasts, HUVEC, and human vascular smooth muscle cells), suggesting a difference in the regulation of NRP1 depending on cell type, cell location, cell immortalization, and their different response and/or sensibilization to LPS administration (Dai *et al.* 2017). In contrast, NRP1 expression was maintained with Ago2 silencing, as a likely compensatory mechanism to maintain endothelial function through VEGF interactions (Bielenberg *et al.* 2007). The exogenous application and subsequent internalization of Ago2, in the presence of LPS, may imply other forms of Ago2 internalization, such as vesicular structures (Geekiyange *et al.* 2020) or a different NRP receptor. Bae and colleagues also showed that,

although hypoxia and nutrient deprivation decreased NRP1 expression, it did not change NRP2 levels (Bae *et al.* 2008). Ago2 alone upregulated NRP1; this is possibly a response to the rise in available ligand, i.e., exogenous Ago2 (which is not naturally present in cell culture medium) as a cue to promote internalization. However, healthy cells did not internalize Ago2, or alternatively, were able to degrade it, maintaining their intracellular levels constant. Since Ago2 was not released, we hypothesized that the LPS-induced decrease of intracellular Ago2 occurred by autophagy (Schaaf *et al.* 2019), an essential mechanism to maintain brain homeostasis. Accordingly, the inhibition of autophagy in the presence of LPS increased Ago2 levels similarly to Ago2 supplementation. Changes in Ago2 levels influence miR availability and delivery, and autophagy-mediated degradation of Ago2 during LPS challenge could decrease miR processing and facilitate the translation of inflammatory targets. Contrary to Ago2 treatment (maintained over a period of 24 hours), the inhibition of autophagy, which also increased intracellular Ago2 (within 3 hours), did not reduce LPS-induced NO release. Exogenously administered Ago2 possibly maintains the processing of Ago2-miR complexes in the cell cytoplasm (Bartel 2018) for a longer period of time, shutting translation off for targets involved in the NO signaling pathway. Recently, NO release from endothelial cells was found considerably decreased when miR-195 and miR-582 were up-regulated (Wang *et al.* 2012). The target of these miR is eNOS and we showed that Ago2 reduced eNOS and iNOS expression in the LPS-injected mice, further supporting a modulatory role of Ago2 in this pathway. Thus, our results revealed that, under inflammatory conditions, Ago2 can be considered, indirectly, a pro-angiogenic factor since low NO levels are deemed pro-angiogenic while high amounts are anti-angiogenic. Since excessive NO levels also correlate with higher VE-cadherin complex disruption in murine microvascular endothelial cells (González *et al.* 2003), Ago2-induced reduction of NO could have contributed to normalize VE-cadherin levels. VE-cadherin is crucial for proper vessel growth and vascular lumen development (Carmeliet *et al.* 1999). The inhibition of autophagy recuperated the loss of VE-cadherin caused by LPS. LPS triggers a series of events leading to tyrosine phosphorylation of VE-cadherin, its disassembly from the adherens junction, and lysosomal degradation (Chan *et al.* 2020). Others have shown that a different autophagy inhibitor (3-methyladenine) prevented the cleavage and consequent loss of VE-cadherin at adherens junctions, in a model of acute lung injury (Slavin *et al.* 2018). Ago2 treatment did not affect the release of TNF- α , or IL-6 induced by LPS in BEC. Most authors agree on a pro-angiogenic effect *in vivo* and an anti-angiogenic role *in vitro* for TNF- α . However, Sainson and colleagues described a temporal effect: TNF- α initially blocks signaling through VEGFR2, but once inflammation is resolved, it induces a tip cell phenotype (Sainson *et al.* 2008). Ago2 did not appear to regulate TNF- α , but the maintenance of high levels of TNF- α during LPS stimulation and Ago2 co-treatment suggests a pro-angiogenic purpose. Lowering the release of IL-6 could be beneficial to vascular activity since high expression can promote defective angiogenesis (Gopinathan *et al.* 2015), but no significant reduction of IL-6 release induced by Ago2 was observed.

Then, we assessed the role of Ago2 in primary astrocytes. These are crucial regulators of CNS homeostasis and BBB function (Abbott 2002). *In vitro*, the full range of astrocytic activation can

be limited in pure cultures; the presence of contaminating microglia enhances the response to LPS (Chen *et al.* 2015), which may account for the tamer response regarding NO release. Moreover, LPS did not change Ago2 levels and was able to overcome Ago2 silencing, suggesting a compensatory mechanism. LPS-activated astrocytes exhibited GDNF overexpression and higher TNF- α release. Exogenous TNF- α can induce the astrocytic expression and secretion of GDNF *in vitro* and *in vivo*, while the disruption of TNFR1 signaling cancels this effect. Accordingly, Ago2 silencing lowered the basal release of TNF- α and maintained GDNF levels similar to control, as described *in vitro* and *in vivo* by Brambilla and colleagues (Brambilla *et al.* 2016). Thus, astrocytic Ago2 does not appear to play a role in LPS-induced inflammation.

We then characterized the role of Ago2 in primary microglial cultures stimulated with LPS. Contrary to BEC, intracellular Ago2 levels were upregulated in activated microglia. Microglial Ago2 does not seem relevant for cell survival since silencing did not produce significant cell death (only in combination with LPS stimulation). Ago2 accumulation was accompanied by higher levels of IL-6, TNF- α and NO. The effect of LPS (1 ng/ml) on Ago2 has been addressed on peripheral macrophages (Mazumder *et al.* 2013), which share functional similarities with microglia. In that study, the early response to LPS caused Ago2 phosphorylation and miR dissociation, thus shutting down miR-mediated repression and enhancing cytokine synthesis. Authors then showed that a prolonged exposure to LPS reversed the process. In their work, no changes in Ago2 intracellular levels or localization were reported; moreover, Ago2 was found to be the most abundant Ago protein in their model (RAW 264.7 cells). Ago2 is commonly perceived as the most relevant family member given its slicer activity and its higher relative abundance in the cell. In our work, Ago2 silencing did not change TNF- α levels but reduced LPS-induced release of IL-6 and NO, suggesting an important and specific role of Ago2 in these pathways. Others have reported that the four Ago proteins can function redundantly and, upon Ago2 downregulation, Ago1 and Ago3 can become functional substitutes *in vitro* (Ferreira *et al.* 2012; Guo and Geller 2014; Leonov *et al.* 2015), maintaining to some degree RISC activity and translation off. Accordingly, we found that TRAF6 levels were similar to control cells upon Ago2 silencing. TRAF6 downregulation occurs after prolonged LPS stimulation to avoid excessive immune response (Liew *et al.* 2005; Yang FM *et al.* 2018). Since the release of IL-6 and NO was prevented, this mechanism could have been delayed to some extent. Moreover, if RISC is compromised because of Ago2 silencing, miR-146a-, or miR14b-, or miR-124-dependent degradation of TRAF6 may not occur (Walsh *et al.* 2015), which should have led to sustained inflammatory release in the presence of LPS (it only occurred for TNF- α). These observations further fuel the idea that the role of Ago2 is complex, and it modulates cell responses differently. To clarify the process of endothelial regulation, via Ago2, we evaluated microglial activation induced by endothelial cell-conditioned media. BEC are a trophic vault for factors that regulate immune responses and parenchymal regeneration (Machado-Pereira *et al.* 2016). While media from healthy endothelial cells reduced basal cell death by likely enhancing survival/proliferation or slowing down cell death processes (Iannucci *et al.* 2020), media obtained from LPS-stimulated endothelial cells abolished this effect. Conversely, Ago2 treatment modulated this pool of factors, secreted by endothelial

cells, increasing again cell survival and favoring a surveying microglial state. While we did not observe a significant impact on the release of microglial IL-1 β , conditioned media from healthy or Ago2-treated activated BEC greatly reduced NO below control levels. If the microenvironment favors proliferation, microglia lower NO, by decreasing iNOS expression and protein kinase G signaling, which results in increased cell division (Maksoud *et al.* 2020).

Lastly, we used a recombinant protein to assess the specific role of Ago2 in the endothelial secretome, but Ago2 may be acting alone or in a ribonucleoprotein complex with miR (secreted by cells and/or that are already present in cell media). Recently, the content of small non-coding RNA contaminants was evaluated in FBS, vesicle-depleted FBS and serum-free media. None were found to be free of small non-coding RNA contaminants (Mannerström *et al.* 2019). To add complexity to the matter, the positive outcomes observed in the *in vivo* studies can also be a result of Ago2 possibly being delivered in vesicular structures that can transport lipids and other proteins that could hypothetically contribute to the observed results on endothelial cells, and consequently on the composition of their secretome (Weaver and Patton 2020). Above all, the conditioned media from both healthy and activated BEC treated with Ago2 had similar properties, and both elicited different responses than the media from activated endothelial cells.

A systemic challenge with 2 mg/kg LPS disrupts the BBB and results in significant glial activation (Varatharaj and Galea 2017; Saraiva *et al.* 2019), which is best assessed by examining both pro- and anti-inflammatory markers (Hoogland *et al.* 2015). Since LPS minimally penetrates the murine brain (about 0.025%) and BBB disruption does not enhance LPS uptake (Banks and Robinson 2010), this model induces a local effect on blood vessels (reproducing the *in vitro* data obtained with BEC). It is also unlikely that Ago2 crosses the BBB, given its high molecular size (nearly 100 kDa). In light of our *in vitro* data, Ago2 is likely internalized by the BEC that constitute the BBB, via NRP1, reestablishing vascular function, with consequent normalizing actions on neuronal and glial cells. In addition, our *in vivo* data indicated that there was no direct correlation between changes in Ago2 measured in the tissue lysates and the injection of Ago2 (alone or after LPS). In the neocortex, Ago2 levels remained unchanged and, in the hippocampus, Ago2 was either similar to sham animal levels or reduced. Considering the *in vitro* data, we first confirmed that LPS lowered VE-cadherin expression and then focused on a signaling pathway responsive to stress stimuli (p38 mitogen-activated protein kinases), enzymes that are involved in NO synthesis (eNOS and iNOS), oxidative stress (NOX2 and the cytosolic Nox2 organizer p47phox), and markers for glial activation (Iba-1, GFAP and S100B) (Bode *et al.* 2012; Trevelin *et al.* 2020).

The systemic administration of Ago2 normalized targets associated with vascular function and immune cell activity, and decreased iNOS levels, possibly because of its broader cellular expression (or Ago2 specificity on this pathway). Along the same lines as our *in vitro* data, others have identified miR-939 and miR-26a as blockers of iNOS protein synthesis (Guo and Geller 2014). By making Ago2 available again, Ago2-miR complexes can reassemble and perform their function. Recently, Carbonell and Gomes extensively reviewed the relationship between cellular redox status and miR expression, listing several molecules that inhibit NOX2 expression, such as

miR-448-3p, miR-124-5p, and miR-652 (Carbonell and Gomes 2020). Finally, miR-451 levels depend on the maintenance of Ago2 levels. Yet, Ago2 expression was found to be reduced in p47phox-deficient macrophages, impairing miR-451 processing (data obtained in near anoxic conditions) (Ranjan *et al.* 2015). In a macrophage cell line, LPS (100 ng/ml; the same concentration used by us *in vitro*) also induced a time-dependent decrease in p47phox expression (Wang *et al.* 2017), thus possibly reducing Ago2 expression. Indeed, few studies have focused on the role of Ago2 in inflammation-induced brain injury. A study conducted on peripheral blood mononuclear cells from post-traumatic stress disorder patients concluded that the chronic inflammation observed in these individuals could be triggered by downregulation of Ago2 and Dicer1, which impairs the generation of mature miR (Bam *et al.* 2017). The miR-132-mediated Ago2 suppression in human dermal lymphatic endothelial cells affected the levels of miR-221 and miR146a, which are involved in angiogenesis and inflammation, respectively (Leonov *et al.* 2015). Hence, certain Ago2-miR complexes operate as key regulators of the inflammatory process (de Kerckhove *et al.* 2018). In other contexts, miR-145-5p induces post-transcriptionally Ago2 expression, dictating miR-145-5p tumor suppressor activity (breast carcinoma cell lines) (Bellissimo *et al.* 2019). Conversely, the impairment of Ago2/miR-185-3p axis may promote colorectal cancer metastasis in colorectal cancer tissues (Liu *et al.* 2021). In sum, Ago2 expression and/or effects may be conditioned by different miR, which are in turn expressed differently in terms of cell type and their response to a stimulus. It would be interesting to explore in the future which set of miR preferably binds to Ago2 and are internalized by BEC, under inflammatory conditions, to assess if there are specific molecules responsible for the observed effects. Ago2 normalized the expression of GFAP and S100B. Elevated levels of S100B and GFAP are considered markers for astrocytic damage or dysfunction but S100B could be a more interesting target during the angiogenic process since it identifies astrocytes that ensheath blood vessels (Steiner *et al.* 2007). S100B can also be secreted and exhibit a cytokine-like activity, coordinating glia-glia and glia-neuron interactions (Donato 2001). Donato and colleagues postulated that these effects were achieved by the contact between S100B and the receptor for advanced glycation end products (RAGE), a multiligand receptor that propagates inflammatory stimuli and affects several neurotrophic and neurotoxic factors in inflammatory disorders.

LPS injection slightly increased Ago2 detection in the neocortex, albeit not significantly. Microglia, which overexpress Ago2 *in vitro* and *in vivo* (Figure 3.7) are likely contributing to this effect; there is also a higher microglial density in this brain region than in the hippocampus (Savchenko *et al.* 1997). Ago2 overexpression is found in cancerous tissue and cell lines (Ye Z *et al.* 2015). In this context, conflicting reports claim that Ago2 upregulation does not exert any effect on cell proliferation or migration (Parisi *et al.* 2011), has an inhibitory effect on migration (Zhang *et al.* 2013), or promotes invasiveness (Adams *et al.* 2009; Cheng *et al.* 2013). LPS administration induces hippocampal microglia reactivity, which in turn secrete cytokines that may induce astrocytic activation (Liddelow *et al.* 2017). Herein, these effects were normalized after the systemic injection of Ago2, similarly to what we had observed in the neocortex.

LPS-induced systemic inflammation negatively affects cognitive function (Arai *et al.* 2001; Noh *et al.* 2014), and our results demonstrated a significant decrease in the expression of CREB, MAP2, and PSD-95. CREB is critical for axonal outgrowth, synaptic plasticity, and memory formation (Alberini 2009). MAP2 is involved in synaptic plasticity and neuronal cell death (Sánchez *et al.* 2000). PSD-95 influences synaptic transmission and plasticity, learning, and memory (Kim and Sheng 2004). Ago2 injection caused the normal expression of these markers as a likely consequence of the previously described normalizing actions on glial cells.

The Ago2 injection per se may have resulted in lower Ago2 than sham animals, possibly via a mechanism of negative regulation to counteract the trend towards elevated NRP1 expression in the hippocampus and stabilize signaling. Batassa and colleagues have reported that Ago2 silencing in the mouse hippocampus can alter RISC activity, which can affect learning and memory processes in these animals (Batassa *et al.* 2010).

3.5 Conclusions

Considering these results, we propose that Ago2 regulation of the neurovascular unit occurs as depicted in the figure below (Figure 3.8). In sum, LPS activation of the p38 signaling pathway in BEC promotes the transcription of mRNA related to pro-inflammatory mediators and the disruption of the VE-cadherin complex. The translation of these transcripts (e.g., IL-6, TNF- α) is facilitated by low Ago2 levels and triggers glial activation. The exogenous application and internalization of Ago2, via NRP1, reduce eNOS expression and NO levels, restoring barrier integrity, and granting glial and neuronal protection.

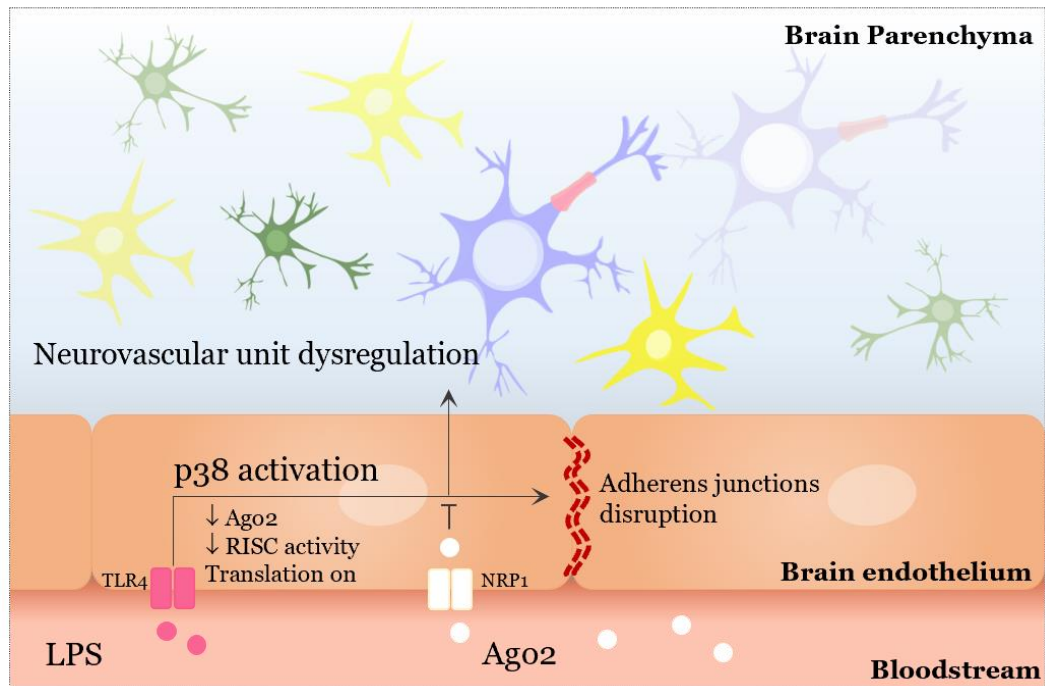


Figure 3.8 – Proposed model for Ago2 regulation of the endothelial and glial crosstalk. LPS activation of the p38 signaling pathway promotes VE-cadherin downregulation and the transcription of mRNA related to pro-inflammatory mediators (e.g., cytokines). The translation of these transcripts is facilitated by low Ago2 levels and low RISC activity. These events trigger the activation of microglia and astrocytes associated with blood vessels, and cause neuronal damage. The exogenous application and internalization of Ago2, via NRP1, recuperates RISC activity, which is conducive to eNOS degradation and low NO, reducing glial activation and protecting neuronal cells.

Chapter 4

Retinoic acid-loaded nanoparticles promote neurovascular protection in stroke

Part of the data from this Chapter was published in: Machado-Pereira M, Grayston A, Garcia-Gabilondo M, Francisco V, Cristóvão AC, Marto JP, Vieira H, Viana-Baptista M, Ferreira L, Bernardino L, Rosell A, Ferreira R. Retinoic Acid-Loaded Nanoparticles Promote Neurovascular Protection in Stroke. *Stroke*. 2023. 54(4):e149-e151.

4.1 Abstract

Ischemic stroke is a leading cause of disability that requires urgent therapies that can complement current reperfusion approaches to enhance sequelae-free neurologic recovery. Treatment efficacy can be enhanced by targeting blood-brain barrier (BBB) deregulation and inflammation-induced barrier loss. Retinoic acid (RA) is one of the most powerful signaling molecules regulating these processes. To boost its therapeutic potential, we developed polymeric nanoparticles enriched with RA (RA-NP) able to induce protective and regenerative effects with the advantage of carrying a lower RA concentration. However, the therapeutic effects and molecular changes induced by RA-NP in relevant stroke models have not yet been described. Our aim was to determine the pro-angiogenic mechanisms underlying RA interaction with Argonaute (Ago)-2, herein described for the first time. Ago2 is the main coordinator of microRNA trafficking and activity and a putative regulator of vascular function, which is altered under hypoxia. Yet, it is unclear whether the restoration of the Ago-2 expression in the stroke area would reverse BBB deregulation and promote neurovascular repair. In this work, our *in vitro* results showed that in mouse primary cultures of brain endothelial cells subjected to oxygen and glucose deprivation (OGD), RA-NP (not soluble RA) treatment not only restored Ago2 levels but also required it to improve vascular function compromised by OGD, an effect mediated through the nitric oxide pathway. *In vivo*, adult mice subjected to transient middle cerebral artery occlusion (MCAO) followed by a single intravenous injection of RA-NP showed reduced infarct size and normalized acute inflammatory response (until the third-day post-injury). In the subacute phase (seven days post-injury), RA-NP promoted neuronal protection and exhibited a promising pro-angiogenic effect in the peri-infarct region. Thus, RA-NP could be envisioned as a safe and promising approach for stroke therapy and for other CNS vascular and/or inflammatory injuries.

4.2 Introduction

Ischemic stroke is a major cause of death and disability worldwide with life-saving approved medical therapies (e.g., pharmacological or mechanical vessel recanalization) that must meet strict clinical criteria before administration, thus limiting the number of patients that can be effectively treated (Virani *et al.* 2020). To date, there are no approved neuroprotective nor neurorestorative treatments that can reduce infarct extension and repair the surrounding damaged tissue (Lin *et al.* 2022), supporting the quest for new repairing molecules or agents. Retinoic acid (RA) is one of the most powerful and promising signaling molecules therapy-wise, despite its limitations (e.g., poor solubility, broad side effects, photosensitivity). To overcome these shortcomings, delivery formulations (e.g., polymeric scaffolds, nanoparticles, microparticles) have been developed (Ferreira *et al.* 2020). Accordingly, we have shown the protective effects of all-trans RA-containing polymeric nanoparticles (RA-NP) in an *in vitro* model of ischemia. Specifically, RA-NP (3 to 10 $\mu\text{g}/\text{ml}$ of the formulation, i.e., the equivalent to 0.12 to 0.40 μM of free RA) enhanced the proliferation and tube formation of endothelial cell lines exposed to oxygen and glucose deprivation (OGD), and promoted the proliferation of endothelial progenitor cells isolated from ischemic stroke patients (Ferreira *et al.* 2016). We have also injected mouse pups intravenously with the same RA-NP formulation (10 $\mu\text{g}/\text{g}$) and obtained significant protection of the neurovascular unit from ensuing ischemic injury (Machado-Pereira *et al.* 2018). Others have recently found a significant inverse correlation between the risk of a stroke and blood circulating retinol (RA precursor) (Guo *et al.* 2021). RA signaling was first found to be important for blood-brain barrier (BBB) formation in the developing mouse brain by Mizze and colleagues (Mizze *et al.* 2013). Others injected RA (5 $\mu\text{g}/\text{g}$) for four consecutive days prior to the MCAO (rat model of stroke) and obtained an increase in zonula occludens-1 and vascular endothelial (VE)-cadherin expression, crucial components of the BBB structure (Kong *et al.* 2015). The same concentration of RA (5 μM) used by Mizze and colleagues also enhanced vascular endothelial growth factor (VEGF) mRNA and protein levels in glioma cells, while a higher dose (40 μM) had the opposite effect (both in normoxic and hypoxic conditions) (Liang *et al.* 2014). Thus, the actions of RA on angiogenesis are complex, time- and concentration-dependent (Ferreira *et al.* 2020). In fact, a lower concentration of RA (1 μM) was shown to decrease Argonaute-2 (Ago2) levels (Long *et al.* 2015), which appears counterintuitive considering the role that this protein appears to have in angiogenesis. Ago2 is the only human Ago protein with endonuclease activity, forming ribonucleoprotein complexes with microRNA (miR) thus enabling their trafficking and activity (Diederichs and Haber 2007). The functions of the other Ago family members (Ago1, Ago3, and Ago4) in the human brain remain poorly understood (Chu *et al.* 2010). Recently, we showed that Ago2 and VE-cadherin are significantly downregulated in primary brain endothelial cells (BEC) challenged by an inflammatory cue (lipopolysaccharide, LPS). Moreover, the systemic administration of Ago2 *per se* (0.4 nM) in LPS-injected mice normalized markers linked to vascular, neuronal, and glial function (Machado-Pereira *et al.* 2022), further suggesting a key role for Ago2 in the central nervous system (CNS) injury. Therefore, we aimed to determine the mechanisms underlying RA/RA-NP-mediated regulation of Ago2, and clarify its pro-angiogenic

role, in brain endothelial function challenged by ischemia to set the foundation for a potential therapy for stroke.

Our results showed that oxygen and glucose deprivation (*in vitro* model of ischemia) compromised endothelial viability and induced autophagic Ago2 degradation *in vitro*. The formulated RA not only recovered Ago2 levels but also required it to recover the vascular function compromised by ischemia, and this effect was mediated through the nitric oxide (NO) pathway. *In vivo*, a single intravenous injection of RA-NP post-injury reduced infarct size and normalized the acute inflammatory response (up to three days post-injury). In the subacute phase (seven days post-injury), RA-NP improved neuronal survival and exhibited increased vessel density in the peri-infarct region. Therefore, RA-NP could be envisioned as a potential therapeutic agent that can be used systemically in the context of cerebral ischemia by regulating injury-related vascular and inflammation mechanisms.

4.3 Results

4.3.1 OGD compromises endothelial viability and induces autophagic Ago2 degradation

Primary BEC were either exposed to OGD alone (Figures 4.1B to 4.1G) or to OGD followed by a 24-hour recovery period (OGD/R) (Figures 4.2A to 4.2K), following the experimental design depicted in Figure 4.1A. One hour of OGD markedly decreased cell viability (1h OGD = $73.6 \pm 7.7\%$, * $p < 0.05$), and this effect was maintained after a longer exposure time (3h OGD = $63.7 \pm 7.0\%$, *** $p < 0.001$), as observed using the CCK-8 assay (Figure 4.1B). Likewise, loss of total protein content began after 1 hour and continued up to 3 hours (3h OGD = $56.4 \pm 6.8\%$, *** $p < 0.001$) (Figure 4.1C). To fully demonstrate the impact of this effect, we analyzed LDH leakage, an indicator of cell membrane damage (Chen 2005). BEC became significantly compromised after 3 hours of OGD (3h OGD = $136.7 \pm 15.3\%$, ** $p < 0.01$) (Figure 4.1D). At this timepoint, there was a significant decrease of intracellular Ago2 (3h OGD = $55.7 \pm 8.5\%$, ** $p < 0.01$) (Figure 4.1E); but OGD did not induce Ago2 release (Figure 4.1F). In parallel, 3 hours of OGD reduced the expression of the Ago2 membrane receptor, NRP1 (3h OGD = $11.7 \pm 6.5\%$, ** $p < 0.01$) (Figure 4.1G).

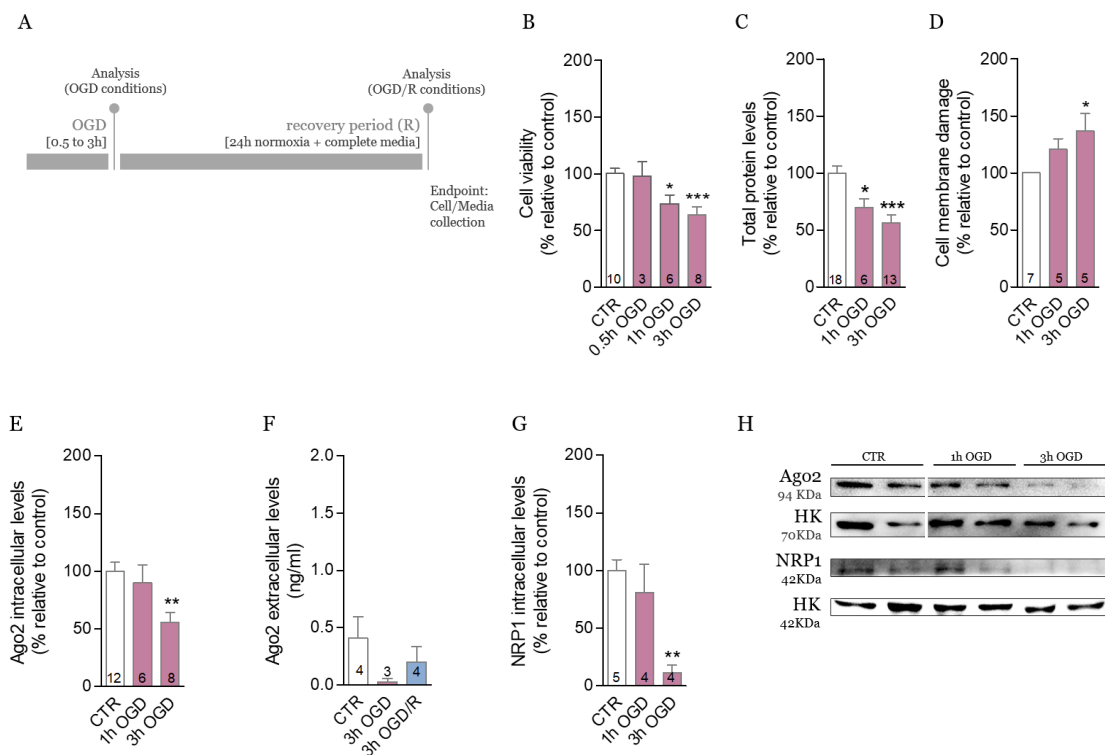


Figure 4.1 – Ischemia compromised BEC viability and downregulated Ago2. Mouse primary BEC were either exposed to OGD alone or to OGD followed by a 24-hour recovery period (OGD/R). The experimental design used *in vitro* is depicted herein (A). Three hours of OGD compromised endothelial cell viability (B), measured by CCK-8. Total protein content decreased after 1 hour of OGD exposure (C), measured by BCA assay. Three hours of OGD induced cell membrane damage (D), measured by LDH assays. After 3 hours of OGD, Ago2 levels significantly lowered in comparison with untreated cells (control, CTR) (E), measured by western blotting. In these conditions, Ago2 was not released (F), measured by ELISA. NRP1 levels also decreased after 3 hours of OGD (G), measured by western blotting. Representative protein bands obtained from western blotting experiments (H). Data were expressed as the mean \pm SEM of the indicated number of repeats and as a percentage relative to untreated controls (* $p < 0.05$, ** $p < 0.01$, *** $p < 0.001$ compared to untreated controls; one-way ANOVA for all figures). Abbreviations: Ago2, argonaute-2; OGD, oxygen and glucose deprivation; OGD/R, OGD followed by a 24-hour recovery period; NRP1, neuropilin-1; R, recovery period.

Next, we investigated whether the restoration of oxygen and nutrients (mimicking the clinical reperfusion), could alter the observed changes. Three hours of OGD/R also reduced cell viability (3h OGD/R = $69.0 \pm 7.4\%$, * $p < 0.05$) (Figure 4.2A) and increased cell membrane damage (3h OGD/R = $175.9 \pm 36.2\%$, * $p < 0.05$) (Figure 4.2B), albeit with no impact on protein levels (Figure 4.2C). The longest recovery period was also ineffective in the restitution of Ago2 (3h OGD/R = $40.2 \pm 13.9\%$, * $p < 0.05$) (Figure 4.2D) and NRP1 (3h OGD/R = $49.9 \pm 14.7\%$, * $p < 0.05$) (Figure 4.2E). Once again, we confirmed that Ago2 was not released (Figure 4.1F). Since cerebral ischemia triggers autophagy to ensure molecule recycling (Chen 2005), the expression of an autophagy-associated protein (p62) was evaluated to establish a correlation with the decreased levels of Ago2 and NRP1 under OGD/R. The effect of a lysosome inhibitor, bafilomycin A1 (bafA1), was also analyzed (Campbell *et al.* 2019; Balch *et al.* 2020). As expected, 3 hours of OGD/R decreased p62

protein levels (3h OGD/R = $31.4 \pm 13.2\%$), confirming that autophagy was induced, and bafA1 (100 nM) prompted the accumulation of p62 (3h OGD/R + bafA1 = $61.9 \pm 4.1\%$) (Figure 4.2F) (Yoshii and Mizushima 2017). BafA1 also recuperated the levels of Ago2 (3h OGD/R + bafA1 = $126.9 \pm 26.3\%$, # $p < 0.05$) (Figure 4.2G) and NRP1 (3h OGD/R + bafA1 = $110.8 \pm 16.1\%$, # $p < 0.05$) (Figure 4.2H). Ago2 and NRP1 staining confirmed these results (Figure 4.2I). Although the inhibition of autophagy restored Ago2 and NRP1 levels, it failed to improve cell viability (Figure 4.2K). It did, however, reverse the degree of membrane damage (Figure 4.2K). Once we determined the timepoint at which Ago2 levels were decreased, we moved to evaluate the protective role of RA/RA-NP and its relationship with Ago2.

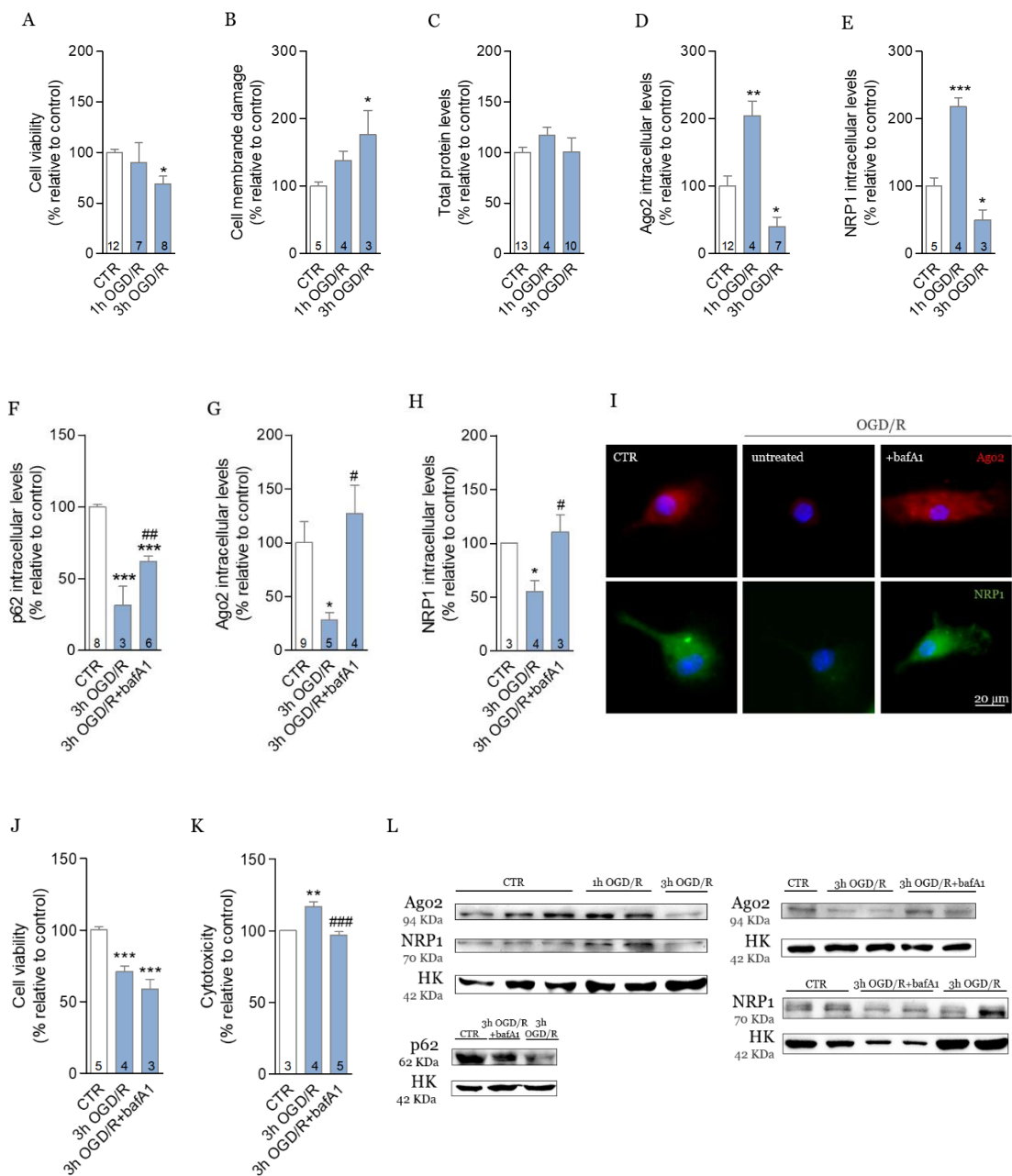
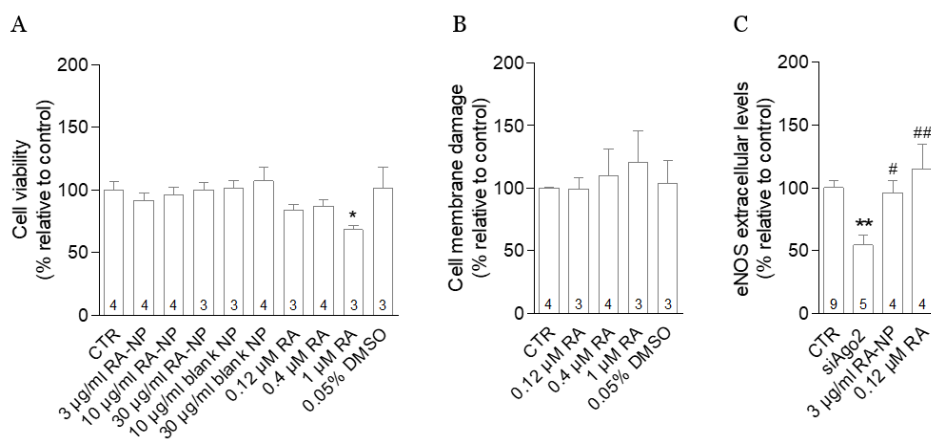


Figure 4.2 – (figure legend continues on the next page)

Figure 4.2 – Ischemia following a recovery period compromised BEC viability and induced autophagic Ago2 degradation. Three hours of OGD/R led to reduced cell viability (A) and integrity (B). OGD/R had no impact on total protein levels (C). Ago2 (D) and NRP1 (E) levels remained decreased following 3h OGD/R. Three hours of OGD/R decreased p62 protein levels confirming that autophagy was induced, and bafA1 prompted the accumulation of p62 (F), measured by western blotting. The inhibition of autophagy through BafA1 treatment, recuperated the levels of Ago2 (G) and NRP1 (H). Representative images depicting the quantitative data were provided (I). Although the BafA1 treatment failed to recuperate cell viability (J), it reversed the degree of cytotoxicity (K). Representative protein bands obtained from western blotting experiments (L). Data were expressed as the mean \pm SEM of the indicated number of repeats and as a percentage relative to untreated controls (* p < 0.05, ** p < 0.01, *** p < 0.001 compared to untreated controls; # p < 0.05, ### p < 0.001 compared to 3h OGD/R-exposed cells; one-way ANOVA for all figures). Abbreviations: Ago2, argonaute-2; BafA1, bafilomycin A1; OGD, oxygen and glucose deprivation; OGD/R, OGD followed by a 24-hour recovery period; NRP1, neuropilin-1; p62, ubiquitin-binding autophagy substrate receptor; R, recovery period.

4.3.2 RA-NP require Ago2 to recover vascular function compromised by ischemia

We have previously shown that RA-NP treatment (10 μ g/ml) significantly has a protective effect and partially restores the proliferation of an endothelial cell line exposed to OGD (Ferreira *et al.* 2016). Thus, we started by evaluating the therapeutic potential of RA-NP, and the free agent (RA) in equivalent concentrations, on our primary cell cultures (Figures 4.3 and 4.4). First, we confirmed that the basal viability of healthy BEC was not compromised by RA-NP treatments and concentrations up to 30 μ g/ml of either RA-NP or blank NP were tested. As for treatments with free RA, only 1 μ M of free RA reduced cell viability (1 μ M RA = $68.2 \pm 3.1\%$, * p < 0.05) (Figure 4.3A). Still, this concentration had no evident impact on cell membrane damage (Figure 4.3B). In addition, free RA did not affect markers of vascular function, namely endothelial nitric oxide synthase (eNOS) and NO (Figures 4.3C and 4.3D, respectively), in comparison with untreated cells.



(figure continues on the next page)

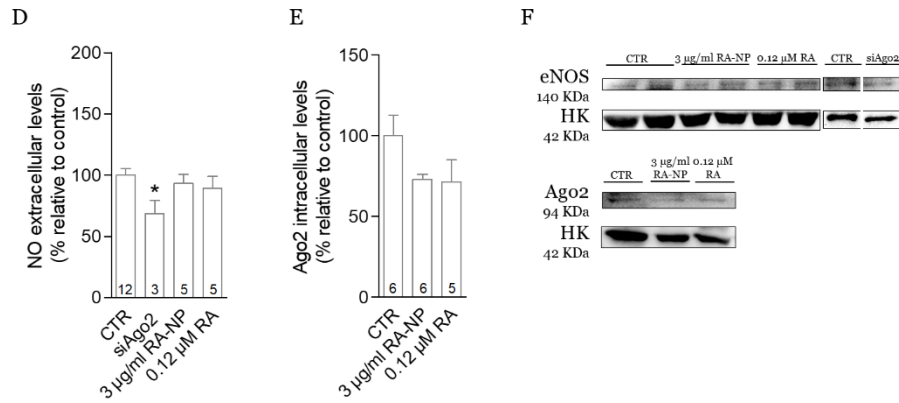
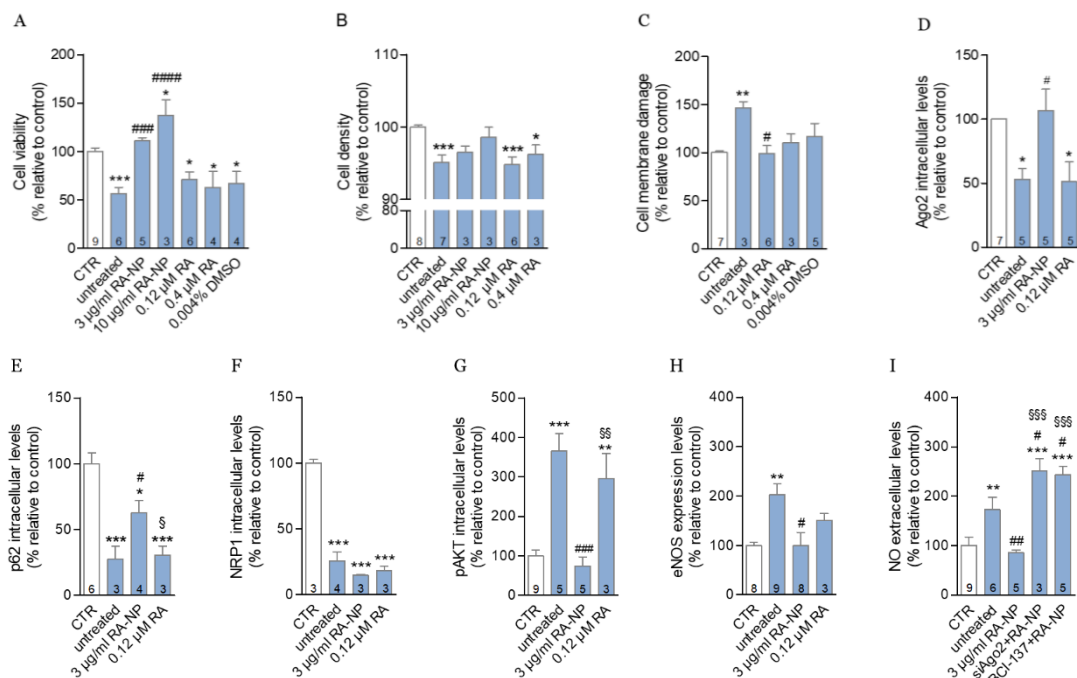


Figure 4.3 – Basal BEC viability, eNOS, NO, and Ago2 expression levels after RA-NP treatment. RA-NP (concentrations up to 30 µg/ml) did not change BEC viability and only 1 µM of free RA reduced cell viability (A). Nonetheless, free RA (1 µM) had no impact on cell membrane damage (B), measured by CCK-8 and LDH assays, respectively. Under basal conditions, Ago2 silencing decreased eNOS levels (C) and consequently NO release (D). RA-NP and free RA had no effect in Ago2 levels (E). Representative protein bands obtained from western blotting experiments (F). Data were expressed as the mean ± SEM of the indicated number of repeats and as a percentage relative to untreated controls (*p < 0.05, **p < 0.01 compared to untreated cells; #p < 0.05, ##p < 0.01 compared to siAgo2-treated cells; one-way ANOVA for all figures). Abbreviations: Ago2, argonaute-2; DMSO, dimethyl sulfoxide; eNOS, endothelial nitric oxide synthetase; NO, nitric oxide; RA, retinoic acid; RA-NP, retinoic acid-loaded nanoparticles.

Afterwards, RA-NP treatment was tested under 3 hours of OGD/R, and 3 µg/ml RA-NP normalized BEC viability (untreated = 56.5 ± 6.4%, ***p < 0.001; 3 µg/ml RA-NP = 110.8 ± 3.3%, ***p < 0.001), while 10 µg/ml RA-NP significantly increased viability above control levels (10 µg/ml RA-NP = 137.5 ± 15.9%, *p < 0.05) (Figure 4.4A), likely due to some degree of recovery in cell numbers or changes in cell metabolism induced by this concentration (Figure 4.4B). In contrast, blank NP (10 µg/ml blank NP = 65.9 ± 22.8%, *p < 0.05) and free RA (0.12 µM RA = 70.9 ± 7.9%, *p < 0.05; 0.4 µM RA = 62.9 ± 16.7%, *p < 0.05) had no effect on the viability of untreated cells subjected to OGD/R (Figure 4.4A). Nevertheless, 0.12 µM free RA (concentration equivalent to 3 µg/ml RA-NP) counteracted the loss of membrane damage (untreated = 146.3 ± 6.7%, **p < 0.01; 0.12 µM RA = 99.0 ± 8.1%, #p < 0.05) (Figure 4.4C). Considering these data, we focused on the effect of 3 µg/ml RA-NP and 0.12 µM free RA, and analyzed Ago2 expression after 3 hours OGD/R. Western blotting revealed that intracellular Ago2 was normalized with 3 µg/ml RA-NP (3 µg/ml RA-NP = 106.8 ± 16.6%, #p < 0.05), while its equivalent dose of RA had no effect (untreated = 52.8 ± 8.8%, *p < 0.05; 0.12 µM RA = 51.3 ± 15.4%, *p < 0.05) (Figure 4.4D). This effect was obtained because, in these conditions, free RA also failed to inhibit autophagy (0.12 µM RA = 30.8 ± 6.8%; §p < 0.05) (Figure 4.4E), a process previously implicated in the loss of Ago2 (Figure 4.2G). The low expression of NRP1 caused by OGD/R remained unaffected by RA-NP and free RA treatments (untreated = 25.6 ± 7.3 %, ***p < 0.001; 3 µg/ml RA-NP = 14.9 ± 0.7%, ***p < 0.001; 0.12 µM RA = 18.4 ± 3.3%, ***p < 0.001) (Figure 4.4F), suggesting that RA-NP formulation may act therapeutically by preventing the loss of intracellular Ago2. In response to changes in blood flow (e.g., ischemia), the endothelium responds by producing vasoactive substances, primarily nitric oxide (NO) (Krupinski *et al.* 1994; Bai and Lyden 2015), via Akt

phosphorylation and consequent eNOS activation (Hayashi *et al.* 2003; Buga *et al.* 2014). Accordingly, three hours of OGD/R induced Akt phosphorylation (untreated = 365.3 ± 45.0%, ***p<0.001), but only RA-NP normalized this process (3 µg/ml RA-NP = 74.8 ± 22.2%, ###p<0.001) (Figure 4.4G). Similarly, three hours of OGD/R induced the expression of eNOS (untreated = 202.4 ± 22.0%, **p<0.01) and, similarly, 3 µg/ml RA-NP normalized eNOS to control condition (3 µg/ml RA-NP = 81.58 ± 13.5%, #p<0.05) (Figure 4.4H). The free agent had no effect on eNOS (Figure 4.4I) since it still maintained increased Akt phosphorylated during ischemia (Figure 4.4J). Therefore, we focused on the role of the formulated RA over NO release. In accordance, RA-NP normalized NO production induced by ischemia (untreated = 172.4 ± 25.1%, **p<0.01; 3 µg/ml RA-NP = 85.8 ± 5.2%, ##p<0.01) (Figure 4.4K). To assess a role for Ago2 in the process of NO regulation, we silenced Ago2 (siAgo2 treatment) or inhibited Ago2 activity (BCI-137 treatment, 100 nM). We showed that a concentration of 50 ng/ml siRNA for 5 hours silences approximately 65% of intracellular Ago2 in BEC (Machado-Pereira *et al.* 2022), while Masciarelli and colleagues reported that BCI-137 interfered with Ago2-nuclei acid interaction thus inhibiting Ago2 binding to miR (Masciarelli *et al.* 2014). In both cases, NO levels were significantly higher than those induced by ischemia alone (siAgo2+RA-NP = 250.7 ± 25.7%, #p<0.05; BCI-137+RA-NP = 243.1 ± 17.0%, #p<0.05) (Figure 4.4I). Since inducible nitric oxide synthase (iNOS) can also contribute to NO production, we confirmed that both treatments caused the overexpression of iNOS (siAgo2+RA-NP = 281.0 ± 56.1%, ###p<0.001; BCI-137+RA-NP = 241.5 ± 9.3%, ###p<0.001) (Figure 4.4K). Importantly, RA-NP only prevented cell membrane damage only when Ago2 expression and/or activity was preserved (3 µg/ml RA-NP = 105.5 ± 2.5%, #p<0.05) (Figure 4.4J). Accordingly, Ago2 silencing, or inhibition also contributed to increased toxicity (siAgo2+RA-NP = 240.2 ± 3.1%, **p<0.01; BCI-137+RA-NP = 186.0 ± 23.5%, *p<0.05).



(figure continues on the next page)

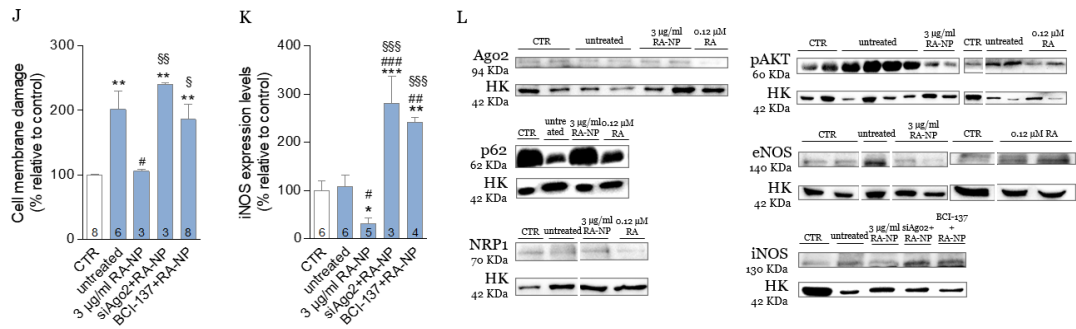


Figure 4.4 – RA-NP required Ago2 to recover vascular function compromised by ischemia. Under 3 hours of OGD/R, RA-NP (3 µg/ml) normalized BEC viability, and free RA had no effect on ischemic cell viability (A). Under 3h OGD/R, RA-NP (3 µg/ml) did not alter cell number in comparison with untreated cells (B). Nonetheless, free RA (0.12 µM) counteracted the loss of membrane damage (C). Intracellular Ago2 levels were normalized with RA-NP (3 µg/ml), while its equivalent dose of free RA was unsuccessful (D), measured by western blotting. In the same conditions, RA-NP inhibited autophagy, while free RA failed (E), measured by western blotting. NRP1 levels were not recuperated after RA-NP or free RA treatments (F). RA-NP (3 µg/ml) normalized ischemia-induced-Akt phosphorylation (G). Similarly, RA-NP normalized eNOS levels induced by ischemia (H) and, consequently, the NO release (I). RA-NP only prevented NO release (I) and cytotoxicity (J) when Ago2 expression and/or activity was preserved. When Ago2 expression and/or activity was decreased, RA-NP and free RA overexpressed iNOS (K). Representative protein bands obtained from western blotting experiments (L). Data were expressed as the mean ± SEM of the indicated number of repeats and as a percentage relative to untreated controls (*p < 0.05, **p < 0.01, ***p < 0.001 compared to untreated cells; #p < 0.05, ##p < 0.05, ###p < 0.001, ####p < 0.0001 compared to 3h OGD/R-exposed cells; §p < 0.05, §§p < 0.01, §§§p < 0.001 compared to RA-NP treated cells; one-way ANOVA for all figures; in Figure 4.4G, Student's t test was used for the comparison between RA-NP and free RA). Abbreviations: Ago2, argonaute-2; DMSO, dimethyl sulfoxide; eNOS, endothelial nitric oxide synthetase; NO, nitric oxide; NRP1, neuropilin-1; pAkt, phosphorylated-Akt; p62, ubiquitin-binding autophagy substrate receptor; RA, retinoic acid; RA-NP, retinoic acid-loaded nanoparticles.

Real-time imaging of BEC confirmed our quantitative data (Figure 4.5). In sum, formulated RA regulated the Akt/eNOS/NO pathway via Ago2, thus recovering the vascular function compromised by ischemia.

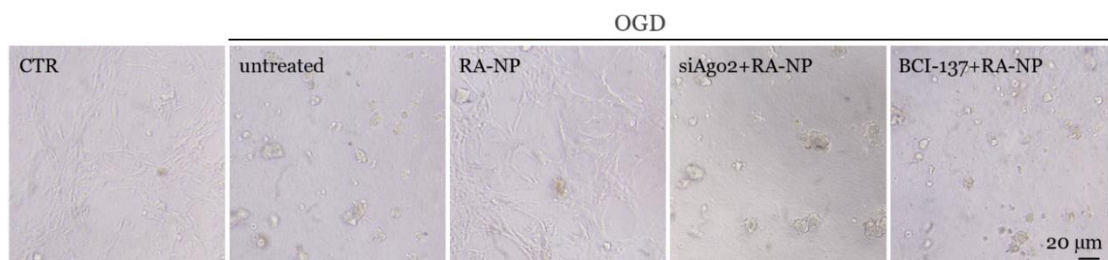


Figure 4.5 – Real-time imaging of BEC after treatments. Representative images confirmed the quantitative data, assessed in a digital camera coupled to a microscope. Scale bar 20 µm. Abbreviations: Ago2, argonaute-2; OGD, oxygen and glucose deprivation; RA-NP, retinoic acid-loaded nanoparticles.

4.3.3 Treatment with intravenous RA-NP protects from brain injury but does not restore functional outcome after ischemia

Mice were subjected to transient MCAO followed by intravenous single doses of RA-NP after reperfusion (experimental design in Figure 4.6A). First, biodistribution studies confirmed that one-hour post-administration of RA-NP-Cy5 (40 $\mu\text{g/g}$) in a MCAO-subjected animal, the formulation effectively reached the brain, as observed by the detection of the fluorescent signal *in vivo* (TRE brain = 13.4×10^9 (p/sec/cm²/sr)/($\mu\text{W/cm}^2$)) and *ex vivo* (TRE brain = 3.3×10^{10} (p/sec/cm²/sr)/($\mu\text{W/cm}^2$)) (Figure 4.6B). The mortality rate and body weight were similar among all groups.

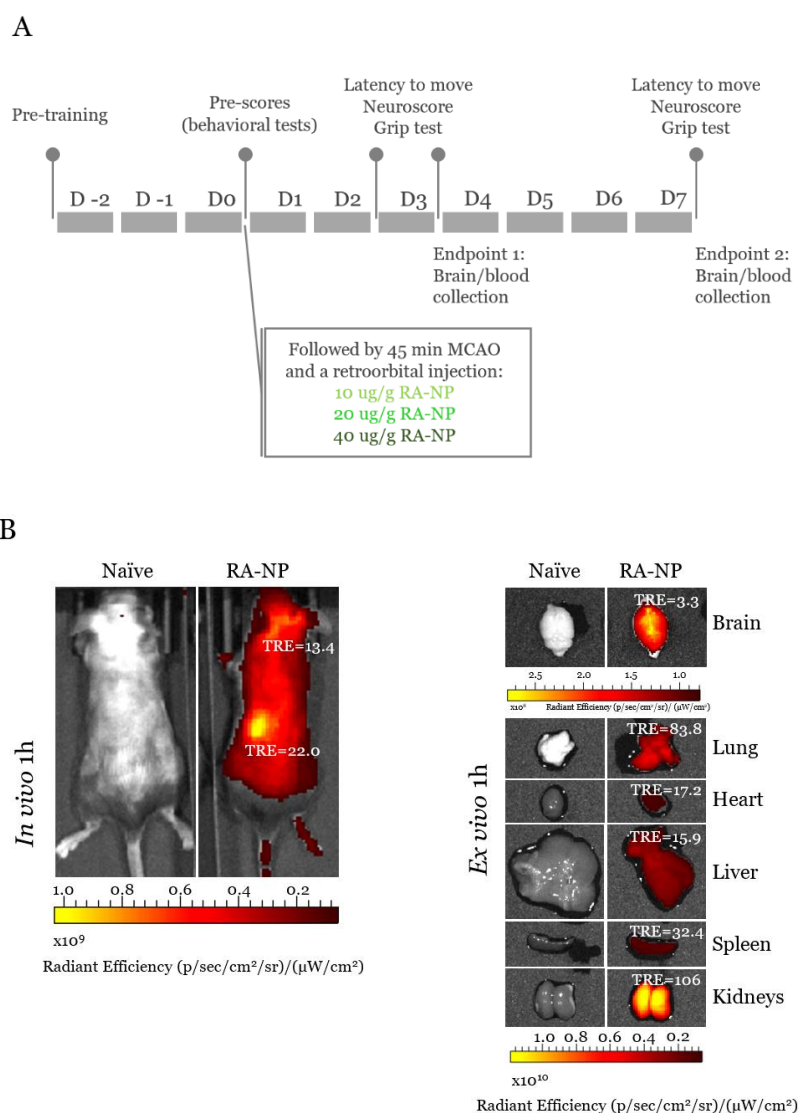


Figure 4.6 – Schematic representation of the experimental setup used herein and biodistribution analysis. Mice were subjected to transient MCAO (45 minutes occlusion) followed by intravenous administration of single doses of RA-NP (10, 20, and 40 $\mu\text{g/g}$) (A). One-hour post-administration in a MCAO-subjected animal, RA-NP effectively reached the brain *in vivo* and *ex vivo* (B), measured by fluorescent molecular imaging. Abbreviations: h, hour; p, photons; RA-NP, retinoic acid-loaded nanoparticles; sec, seconds; TRE, total radiant efficiency value.

Three days after MCAO, we analyzed the volume of striatal and cortical infarct lesions after the administration of different doses of RA-NP (10, 20, and 40 $\mu\text{g/g}$) (Figures 4.7A to 4.7F) to determine the effect on neuroprotection and decide on the most promising dose for the long-term analysis (7-day protocol). We observed a *quasi*-significant reduction in the total infarct percentage in the 20 $\mu\text{g/g}$ RA-NP treated group, compared to the vehicle group (vehicle = $62.9 \pm 3.1\%$; 20 $\mu\text{g/g}$ RA-NP = $56.2 \pm 1.6\%$, $p=0.0692$) (Figure 4.7A). This dose significantly reduced the percentage of infarct in the cortex (vehicle = $46.3 \pm 2.9\%$; 20 $\mu\text{g/g}$ RA-NP = $39.5 \pm 1.3\%$, $\#p<0.05$) (Figure 4.7B), but the same protective effect was not observed in the sub-cortex (vehicle = $16.6 \pm 0.9\%$; 20 $\mu\text{g/g}$ RA-NP = $16.7 \pm 0.7\%$, $p=0.89$) (Figure 4.7C). The 20 $\mu\text{g/g}$ RA-NP treatment significantly decreased the corrected total volume (20 $\mu\text{g/g}$ RA-NP = $88.8 \pm 2.1\%$, $\#p<0.05$) (Figure 4.7D), the corrected cortex volume (20 $\mu\text{g/g}$ RA-NP = $61.8 \pm 1.7\%$, $\#p<0.05$) (Figure 4.7E), and the corrected striatum volume (20 $\mu\text{g/g}$ RA-NP = $24.5 \pm 1.1\%$, $\#p<0.05$) (Figure 4.7F), in comparison with vehicle group. A representative set of images depicting TTC staining is shown in Figure 4.7G.

Importantly, no significant differences in cerebral hemorrhagic transformations were observed (Figure 4.7H). The dose showing neuroprotection (20 $\mu\text{g/g}$) was chosen for the 7-day protocol.

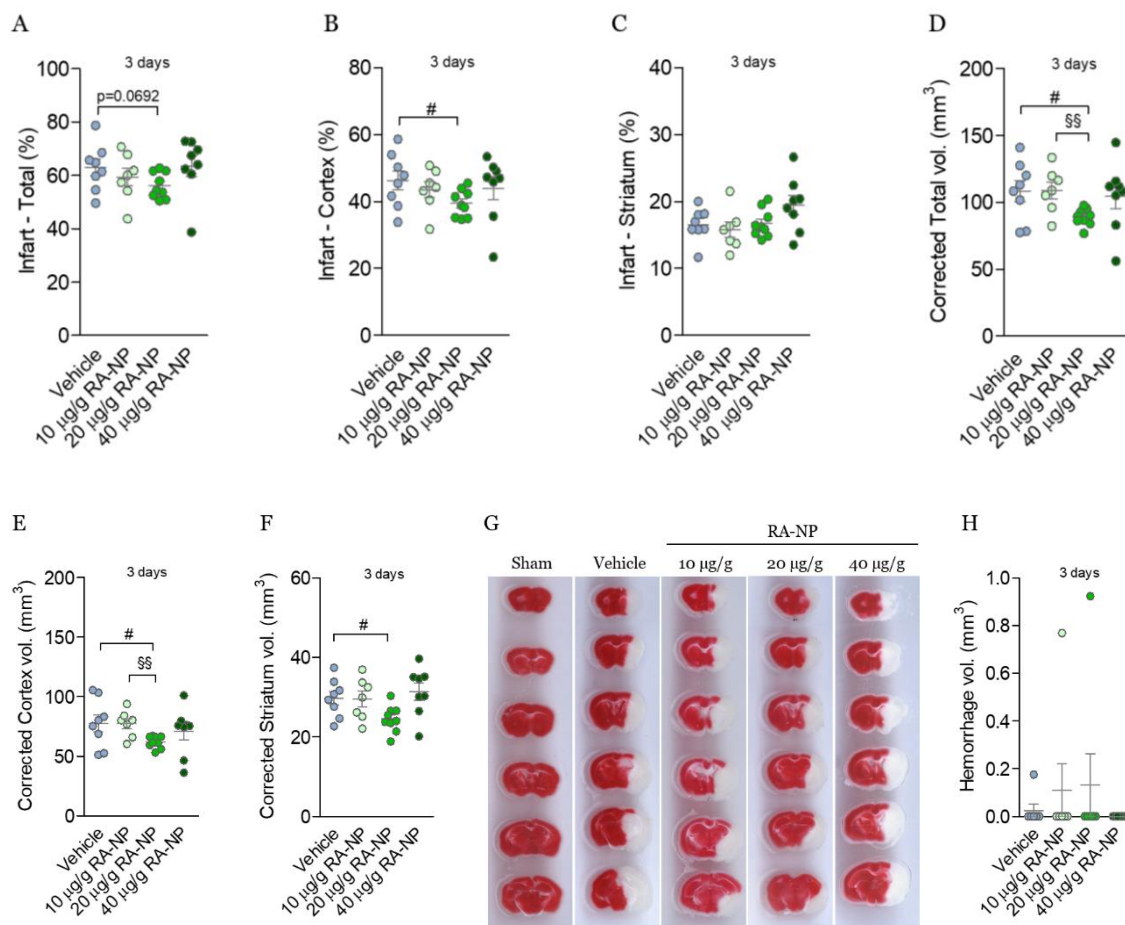


Figure 4.7 – Intravenous injection of RA-NP enhanced tissue survival in MCAO-subjected animals. Three days after MCAO, RA-NP (20 $\mu\text{g/g}$) slightly reduced the percentage of total infarct, measured via TTC staining (A). This dose significantly reduced the percentage of infarct in the cortex (B) but not in the striatum

(C). RA-NP (20 $\mu\text{g/g}$) decreased the corrected total volume (D), the corrected cortex volume (E), and the corrected striatum volume (F) in comparison with the vehicle group. Representative TTC staining images used for analysis were provided (G). No significant differences in hemorrhagic transformations were obtained (H). Data were expressed as the mean \pm SEM of the indicated number of repeats and as a percentage relative to untreated controls ($^{\#}p < 0.05$ compared to vehicle mice; $^{\text{ss}}p < 0.01$ compared to RA-NP (10 $\mu\text{g/g}$); Student's t test for all figures). Abbreviations: RA-NP, retinoic acid-loaded nanoparticles; TTC, 2,3,5-triphenyltetrazolium chloride; vol, volume.

In this regard, our data did not reveal significant differences in functional outcomes, including latency to move (Figure 4.8A), neuroscore (Figure 4.8B), and forelimb grip strength (Figure 4.8C) at three days post-administration. However, seven days post-RA-NP administration (20 $\mu\text{g/g}$) mice showed higher grip strength force than vehicle-treated mice (vehicle = $65.5 \pm 3.3\%$; 20 $\mu\text{g/g}$ RA-NP = $76.4 \pm 3.0\%$, $^{\#}p < 0.05$) (Figure 4.8C).

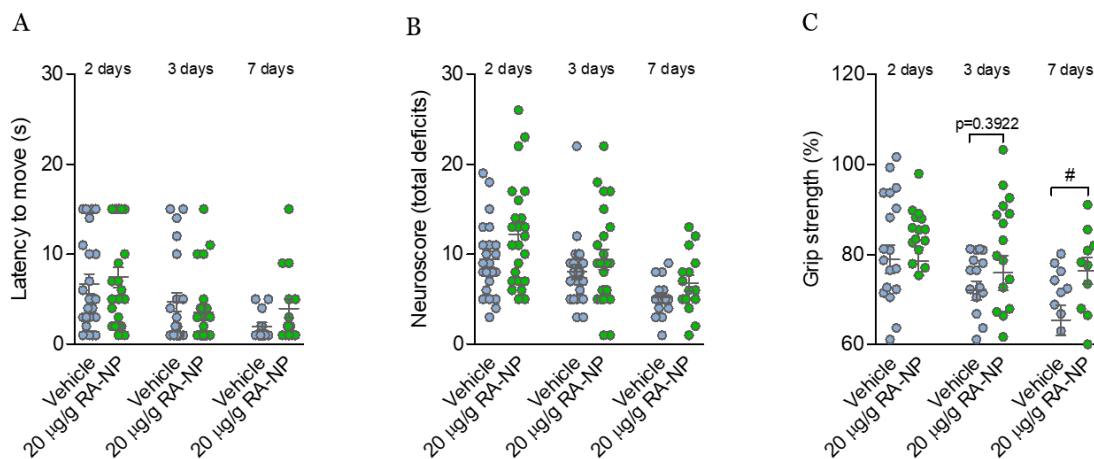


Figure 4.8 – Intravenous injection of RA-NP did not complete functional outcome in MCAO-subjected animals. Three days after MCAO, RA-NP did not reveal significant differences in functional outcomes, including latency to move (A), neuroscore (B), and forelimb grip strength (C). No significant changes were observed in the latency to move and neuroscore, but seven days post-RA-NP injection, mice showed higher grip strengths than vehicle mice. Data were expressed as the mean \pm SEM of the indicated number of repeats and as a percentage relative to untreated controls ($^{\#}p < 0.05$ compared to vehicle mice; in Figures 4.8C, Student's t test was used for the comparison between vehicle and RA-NP). Abbreviations: RA-NP, retinoic acid-loaded nanoparticles; s, seconds.

We also evaluated the safety of the nanoformulation, considering that it could accumulate in off-target peripheral organs. We assessed the systemic toxicity of RA-NP treatment (10, 20, and 40 $\mu\text{g/g}$) at three and seven days by measuring the levels of analytes related to hepatic (ALT), muscle (AST, CK, sodium), renal (urea) and pancreatic (lipase and α -amylase) (dys)function (Table 4.1). First, no significant differences in the levels of systemic enzymes were observed between sham and the vehicle group ($p > 0.05$ for all enzymes) after three days. Three days after MCAO, lipase was significantly lowered after administration with RA-NP (sham = 38.00 ± 1.00 ; 40 $\mu\text{g/g}$ RA-NP = 30.20 ± 1.83 , $p = 0.0023$) but remained above vehicle levels (vehicle = 25.00 ± 4.00). Regarding α -amylase, enzyme levels were enhanced after administration with RA-NP albeit not

significantly from vehicle (sham = 1354.00 ± 67.50; vehicle = 1561.00 ± 187.50; 10 µg/g RA-NP = 1646.00 ± 27.72, p=0.0041, in comparison with the sham group). Seven days after MCAO, the levels of AST (vehicle = 407.50 ± 26.11, p=0.0003), CK (vehicle = 2770.00 ± 475.40, p=0.0229), and lipase (vehicle = 40.82 ± 2.08, p=0.0376) were decreased. The nanoformulation did not aggravate the effect over AST or lipase, and reestablished CK levels (sham = 7189.00 ± 2947.00; 10 µg/g RA-NP = 3398.00 ± 737.10, p=0.0852). Urea levels after nanoparticle injection were similar to ischemic injury alone (vehicle = 44.20 ± 2.90; 10 µg/g RA-NP = 50.57 ± 3.97, p=0.0397), in comparison with the sham group. Overall, our results indicate that RA-NP were able to accumulate in the brain without inducing visible systemic toxicity. The results further show that the RA-NP decreased infarct size but had little impact in animal functional recovery (only at day 7 post-infarct).

Table 4.1 – Serum levels of ALT, AST, CK, urea, sodium, lipase, and α-amylase measured three and seven days post-MCAO. Gray cells indicate significant differences in comparison with sham mice and/or vehicle mice. Data were represented as mean ± SEM. Abbreviations: ALT, alanine aminotransferase; AST, aspartate aminotransferase; CK, creatine kinase; RA-NP, retinoic acid-loaded nanoparticles.

Timeline		Sham	Vehicle	10 µg/g RA-NP	20 µg/g RA-NP	40 µg/g RA-NP
3 days						
ALT (IU/l)	Mean ± SEM	35.80 ± 9.39	42.00 ± 4.16	40.67 ± 2.72	51.40 ± 12.28	37.60 ± 9.78
	pSham	-	0.6475	0.6016	0.3426	0.8977
	pVehicle	-	-	0.7901	0.5930	0.7536
AST (IU/l)	Mean ± SEM	268.8 ± 75.01	422.30 ± 96.99	433.50 ± 56.63	659.20 ± 115.4	317.60 ± 57.82
	pSham	-	0.2569	0.1078	0.0220	0.6203
	pVehicle	-	-	0.9178	0.3557	0.2116
CK (IU/l)	Mean ± SEM	972.30 ± 484.40	1029.00 ± 18.50	1793.00 ± 533.9	1621.00 ± 150.80	1167.00 ± 341.8
	pSham	-	0.9341	0.3629	0.2944	0.7473
	pVehicle	-	-	0.4626	0.4088	0.8183
Urea (mg/dl)	Mean ± SEM	40.67 ± 3.18	48.00 ± 9.00	56.17 ± 4.74	64.20 ± 8.33	57.00 ± 7.33
	pSham	-	0.4199	0.0698	0.0833	0.1550
	pVehicle	-	-	0.4295	0.3214	0.5243
Sodium (mmol/l)	Mean ± SEM	146.10 ± 1.25	145.50 ± 3.74	146.70 ± 2.89	142.50 ± 3.35	148.0 ± 2.61
	pSham	-	0.8607	0.8790	0.3457	0.5304
	pVehicle	-	-	0.8256	0.5881	0.5948
Lipase (IU/l)	Mean ± SEM	38.00 ± 1.00	25.00 ± 4.00	30.83 ± 3.20	37.25 ± 6.61	30.20 ± 1.83
	pSham	-	0.0876	0.2670	0.9435	0.0023
	pVehicle	-	-	0.3785	0.2967	0.0502
α-Amylase (IU/l)	Mean ± SEM	1354.00 ± 67.50	1561.00 ± 187.50	1646.00 ± 27.72	1567.00 ± 88.06	1616.00 ± 221.90
	pSham	-	0.4080	0.0041	0.1849	0.4780
	pVehicle	-	-	0.4703	0.9748	0.8829

(table continue continues on the next page)

7 days						
ALT (IU/l)	Mean ± SEM	52.67 ± 3.84	44.07 ± 3.83	-	48.71 ± 5.48	-
	pSham	-	0.3349	-	0.7514	-
	pVehicle	-	-	-	0.4937	-
AST (IU/l)	Mean ± SEM	821.50 ± 155.30	407.50 ± 26.11	-	494.80 ± 50.88	-
	pSham	-	0.0003	-	0.0178	-
	pVehicle	-	-	-	0.1445	-
CK (IU/l)	Mean ± SEM	7189.00 ± 2947.00	2770.00 ± 475.40	-	3398.00 ± 737.10	-
	pSham	-	0.0229	-	0.0852	-
	pVehicle	-	-	-	0.4744	-
Urea (mg/dl)	Mean ± SEM	33.50 ± 1.66	44.20 ± 2.90	-	50.57 ± 3.97	-
	pSham	-	0.0822	-	0.0397	-
	pVehicle	-	-	-	0.2015	-
Sodium (mmol/l)	Mean ± SEM	140.10 ± 0.79	142.30 ± 0.87	-	145.2 ± 1.52	-
	pSham	-	0.2264	-	0.1103	-
	pVehicle	-	-	-	0.1107	-
Lipase (IU/l)	Mean ± SEM	50.67 ± 2.03	40.82 ± 2.08	-	39.27 ± 2.44	-
	pSham	-	0.0376	-	0.0386	-
	pVehicle	-	-	-	0.6355	-
α-Amylase (IU/l)	Mean ± SEM	1508.00 ± 54.86	1508.00 ± 28.72	-	1448.00 ± 53.08	-
	pSham	-	0.9928	-	0.5690	-
	pVehicle	-	-	-	0.3092	-

4.3.4 Treatment with intravenous RA-NP promotes neuronal survival

To investigate the potential of RA-NP treatment (20 µg/g) in containing neuronal damage, we evaluated changes in neuronal nuclear protein (NeuN), microtubule-associated protein 2 (MAP2), and class III beta-tubulin (βIII-tubulin) (Buscemi *et al.* 2019). Three days after MCAO, NeuN levels decreased in both hemispheres (vehicle = 26.5 ± 13.3% (contralateral hemisphere); vehicle = 22.3 ± 11.1%; *p<0.05 (ipsilateral hemisphere)), in comparison with the sham group (Figure 4.9A), but RA-NP treatment did not reverse this effect (20 µg/g RA-NP = 5.9 ± 2.0%, *p<0.05, ###p<0.001 (contralateral hemisphere); 20 µg/g RA-NP = 31.4 ± 16.3%, *p<0.05 (ipsilateral hemisphere)), in comparison with the sham group. In the subacute phase (7-day protocol), the loss of NeuN levels in vehicle-treated ischemic mice only reached significance in the ipsilateral hemisphere at 3 days and in the contralateral hemisphere at 7 days (vehicle = 3.8 ± 1.0% (contralateral hemisphere); ***p<0.001; vehicle = 68.9 ± 17.3%; ***p<0.001 (ipsilateral hemisphere)). Nonetheless, NeuN levels were significantly recovered after the RA-NP injection in comparison with the vehicle group, in the contralateral hemisphere (20 µg/g RA-NP = 37.5 ± 5.1%, ###p<0.001 (contralateral hemisphere)). No significant effects were observed in the ipsilateral hemisphere seven days after MCAO (vehicle = 68.9 ± 17.3%; 20 µg/g RA-NP = 109.7 ± 35.8%), alluding to some degree of spontaneous recovery. Representative fluorescence images depicting the quantitative data are shown in Figure 4.9B. Three days after MCAO, MAP2

expression decreased (vehicle = $64.4 \pm 8.6\%$; $*p < 0.05$ (contralateral hemisphere)), in comparison with the sham group. MAP2 expression was maintained similarly to sham values in the ipsilateral hemisphere (vehicle = $109.3 \pm 25.2\%$ (ipsilateral hemisphere)). RA-NP significantly increased MAP2 levels in both hemispheres, compared with both sham and vehicle groups (20 $\mu\text{g/g}$ RA-NP = $686.3 \pm 121.5\%$, $***p < 0.001$, $###p < 0.001$ (contralateral hemisphere); 20 $\mu\text{g/g}$ RA-NP = $672.0 \pm 163.9\%$, $**p < 0.01$, $##p < 0.01$ (ipsilateral hemisphere)) (Figure 4.9C). No significant effects were observed in the subacute phase (20 $\mu\text{g/g}$ RA-NP = $82.2 \pm 45.9\%$, $***p < 0.001$, $###p < 0.001$ (contralateral hemisphere); 20 $\mu\text{g/g}$ RA-NP = $152.8 \pm 100.4\%$, $**p < 0.01$, $##p < 0.01$ (ipsilateral hemisphere)). Representative fluorescence images depicting the quantitative data are shown in Figure 4.9D. Regarding $\beta\text{III-tubulin}$ expression, three days after MCAO, no differences were observed in the contralateral hemisphere, even after the RA-NP injection (vehicle = $89.5 \pm 39.3\%$; 20 $\mu\text{g/g}$ RA-NP = $41.5 \pm 11.6\%$), in comparison with the sham group (Figure 4.9E). In contrast, in the ipsilateral hemisphere, we observed a significant decrease in $\beta\text{III-tubulin}$ levels (vehicle = $55.9 \pm 7.0\%$; $*p < 0.05$), in comparison with the sham group, which were not counteracted by RA-NP (20 $\mu\text{g/g}$ RA-NP = $37.1 \pm 11.6\%$; $*p < 0.05$). In the subacute phase, we observed a significant reduction in $\beta\text{III-tubulin}$ levels in both hemispheres (vehicle = $37.3 \pm 13.3\%$, $*p < 0.05$, $###p < 0.001$ (contralateral hemisphere); vehicle = $57.3 \pm 8.4\%$, $**p < 0.01$ (ipsilateral hemisphere)), in comparison with the sham group. Although RA-NP did not significantly revert this effect, $\beta\text{III-tubulin}$ levels were similar to sham values (20 $\mu\text{g/g}$ RA-NP = $65.1 \pm 14.0\%$ (contralateral hemisphere); 20 $\mu\text{g/g}$ RA-NP = $78.3 \pm 11.7\%$ (ipsilateral hemisphere)). Representative fluorescence images depicting the quantitative data are shown in Figure 4.9F. Taken together, our results support the neuroprotective potential of RA-NP after stroke.

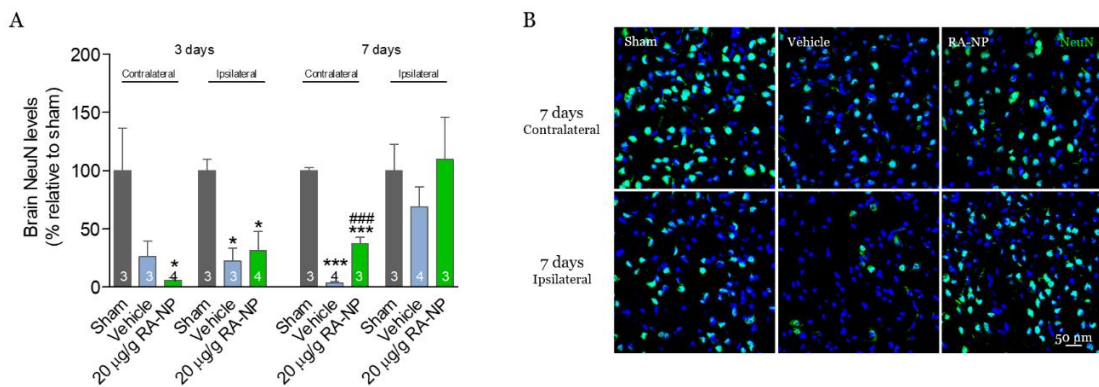


(figure continues on the next page)

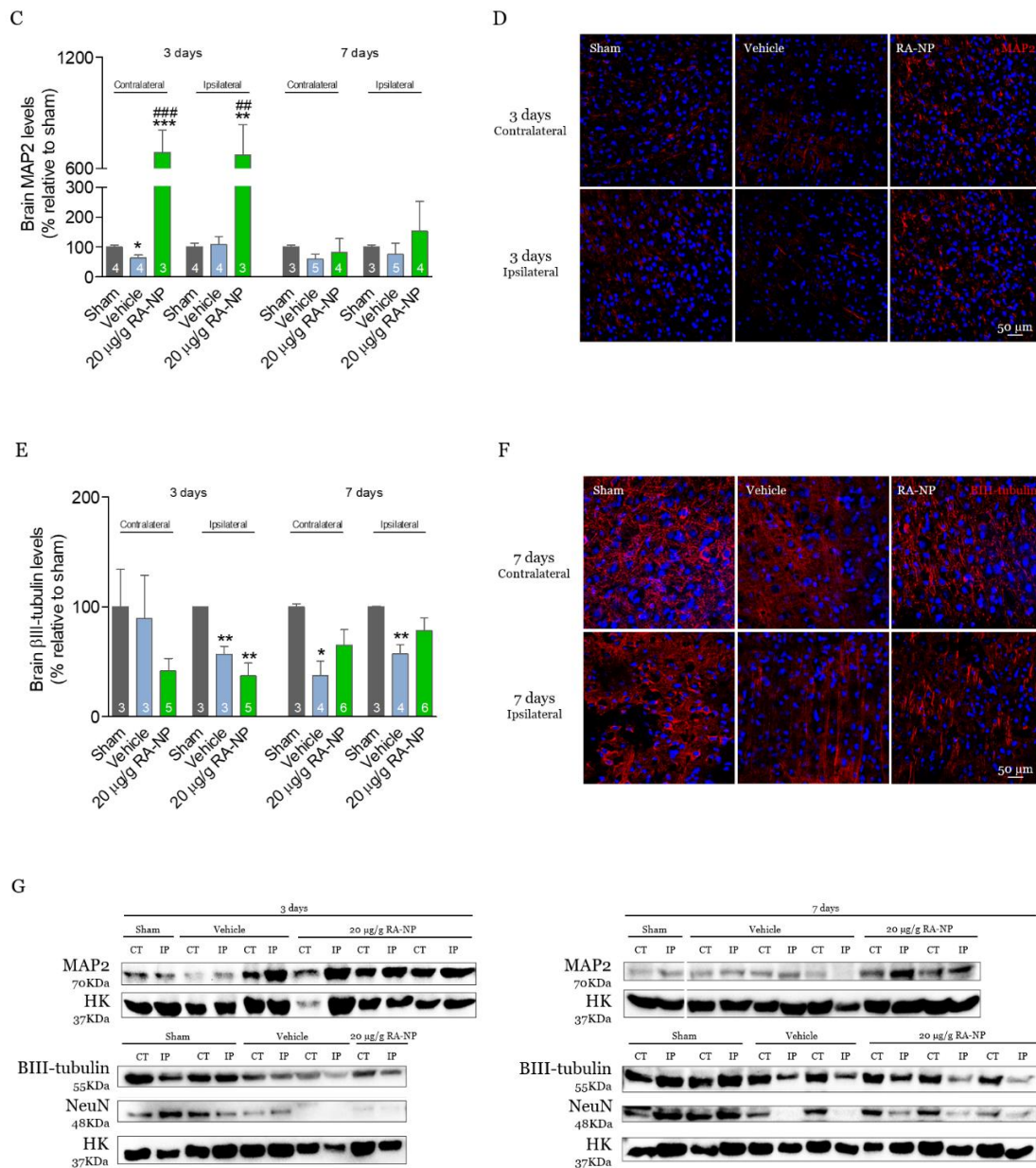
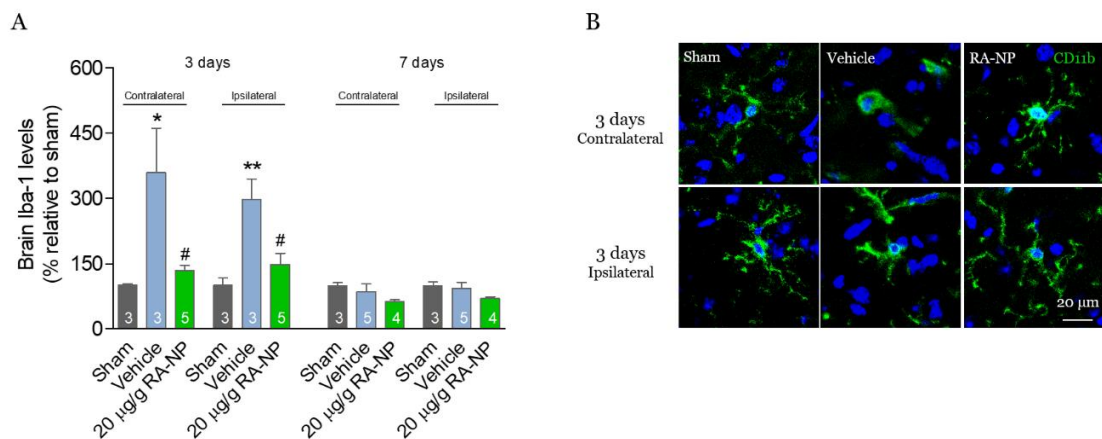


Figure 4.9 – RA-NP increased neuronal survival after brain ischemia. In the acute phase, RA-NP (20 µg/g) did not affect the loss of NeuN-positive neurons induced by MCAO, but after seven days, the formulation was significantly effective in the contralateral hemisphere (A). Three days after MCAO, RA-NP significantly increased MAP2 levels in both hemispheres, but no effect was observed in the subacute phase, in any of the hemispheres (C). In the acute phase, βIII-tubulin-positive cells decreased in the ipsilateral hemisphere, but RA-NP did not change protein levels. In the subacute phase, βIII-tubulin levels induced RA-NP treatment did not significantly differ from sham or vehicle (E), measured by western blotting. Representative images of NeuN (B) MAP2 (D), and βIII-tubulin (F) staining after RA-NP injection, assessed by immunohistochemistry. Representative protein bands obtained from western blotting experiments (G). Data were expressed as the mean ± SEM of the indicated number of repeats and as a percentage relative to untreated controls (*p < 0.05, **p < 0.01, ***p < 0.001 compared to sham mice; #p < 0.01, ###p < 0.001 compared to vehicle mice, one-way ANOVA for all figures; in Figure 4.9C, Student's t test was used for the comparison between sham and vehicle in the contralateral hemisphere three days after MCAO, and in Figure 4.9E, Student's t test was used for the comparison between sham and vehicle in the ipsilateral hemisphere three and seven days after MCAO). Abbreviations: MAP2, microtubule-associated protein 2; NeuN, neuronal nuclear protein; RA-NP, retinoic acid-loaded nanoparticles; βIII-tubulin, class III beta-tubulin.

4.3.5 Treatment with intravenous RA-NP normalizes the inflammatory response acutely after cerebral ischemia

In the acute phase (three days post-injury), glial cells are critical players in the progression of the neuroinflammatory process, contributing to brain tissue damage (Yoshimura and Ito 2020). Thus, we evaluated the expression of markers associated with inflammation (microglial marker, Iba-1, and astrocyte marker, GFAP). As expected, microglia activation marker Iba-1 was increased after MCAO (vehicle = $359.6 \pm 101.9\%$, * $p < 0.05$ (contralateral hemisphere); vehicle = $298.3 \pm 46.82\%$, ** $p < 0.01$ (ipsilateral hemisphere)) in comparison with sham group, three days after MCAO (Figure 4.10A). RA-NP (20 $\mu\text{g/g}$) efficiently decreased Iba-1 levels in both hemispheres (20 $\mu\text{g/g}$ RA-NP = $133.6 \pm 12.7\%$, # $p < 0.05$ (contralateral hemisphere); 20 $\mu\text{g/g}$ RA-NP = $148.1 \pm 25.7\%$, # $p < 0.05$ (ipsilateral hemisphere)) towards basal levels (Figure 4.10A). In contrast, we did not observe microglia activation seven days after MCAO. Also, astrocyte activation marker GFAP was increased in the acute phase after ischemia (vehicle = $184.2 \pm 35.9\%$, * $p < 0.05$ (contralateral hemisphere); vehicle = $231.8 \pm 76.9\%$ (ipsilateral hemisphere)) (Figure 4.10C). RA-NP (20 $\mu\text{g/g}$) significantly decreased GFAP expression (20 $\mu\text{g/g}$ RA-NP = $55.3 \pm 3.3\%$, ### $p < 0.001$ (contralateral hemisphere); 20 $\mu\text{g/g}$ RA-NP = $87.2 \pm 20.6\%$, # $p < 0.05$ (ipsilateral hemisphere)). This effect of RA-NP in the astrocytic population was not maintained subacutely (20 $\mu\text{g/g}$ RA-NP = $181.6 \pm 12.5\%$ (contralateral hemisphere); 20 $\mu\text{g/g}$ RA-NP = $111.3 \pm 10.6\%$ (ipsilateral hemisphere)) (figure 4.10C). Representative fluorescence images depicting morphological changes of glial cells after RA-NP treatment are shown in Figures 4.10B and 4.10D. Overall, RA-NP treatment induced a clear anti-inflammatory profile in astrocytes (acute phase) and in microglial cells (subacute phase).



(figure continues on the next page)

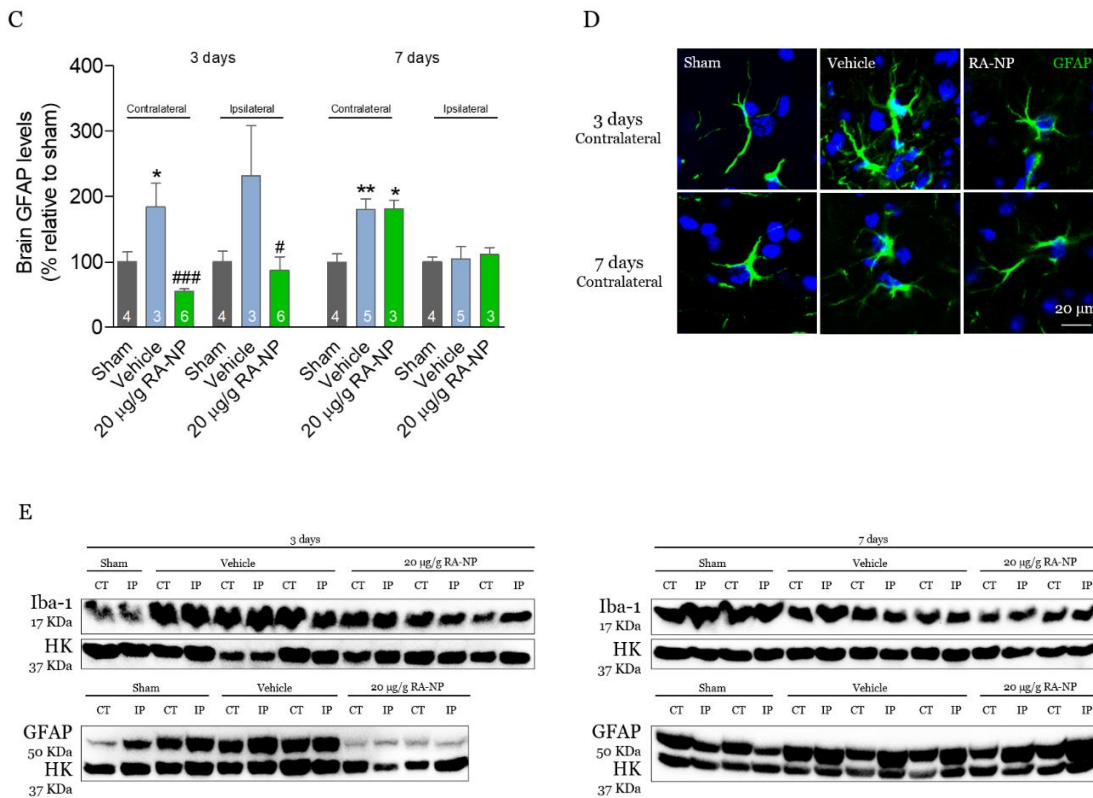
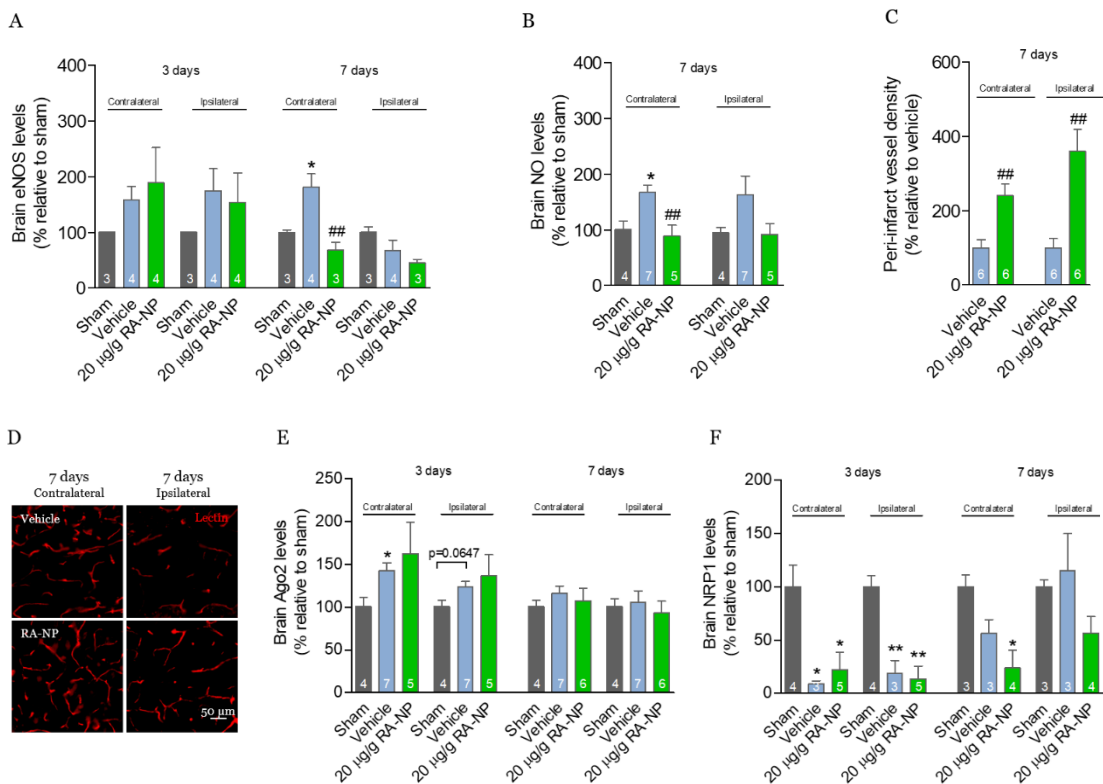


Figure 4.10 – RA-NP normalized the acute inflammatory response after cerebral ischemia. In the acute phase (up to 72 hours post-MCAO), RA-NP (20 µg/g) decreased Iba-1 (A) and GFAP (C) levels in both hemispheres, measured by western blotting. In the subacute phase, no significant changes were observed except for GFAP overexpression in the contralateral hemisphere after MCAO (A and C). Representative images of microglial (B) and astrocytic (D) morphology after RA-NP were obtained by immunohistochemistry. Representative protein bands obtained from western blotting experiments (E). Data were expressed as the mean ± SEM of the indicated number of repeats and as a percentage relative to untreated controls (* $p < 0.05$, ### $p < 0.001$ compared to vehicle mice, one-way ANOVA for all figures). Abbreviations: GFAP, glial fibrillary acidic protein; Iba-1, ionized calcium-binding adaptor molecule 1; RA-NP, retinoic acid-loaded nanoparticles.

4.3.6 Treatment with intravenous RA-NP stimulates angiogenesis in the subacute phase

Lastly, we assessed parameters involved in vascular function. We began by evaluating the expression of eNOS, as an important mediator of the VEGF angiogenic effect; particularly, its deregulated expression not only has a negative impact on angiogenesis, but also decreases neurogenesis and aggravates neurological functional recovery after stroke (Chen 2005). We observed that eNOS levels were increased after MCAO, but this effect was only significant in the subacute phase (seven days after MCAO) in the contralateral hemisphere (vehicle = $181.3 \pm 23.9\%$, * $p < 0.05$). In these same conditions, RA-NP (20 µg/g) were able to counteract this effect (20 µg/g RA-NP = $68.4 \pm 13.7\%$, ### $p < 0.01$ (contralateral hemisphere)) (Figure 4.11A). Considering the significant effect of RA-NP in eNOS regulation subacutely, we next evaluated NO release at this time-point. We observed a significant increase in NO production (vehicle = 167.1 ± 12.7 , * $p < 0.05$), in comparison with the sham group, but RA-NP normalized NO production (20

$\mu\text{g/g RA-NP} = 89.1 \pm 19.3\%$, $\#p < 0.01$ in the contralateral hemisphere (Figure 4.11B). Accordingly, we evaluated brain vessel density at this time-point and observed a significant increase in the percentage of the peri-infarct vessel density after RA-NP treatment, when compared to vehicle group ($20 \mu\text{g/g RA-NP} = 240.0 \pm 31.8\%$, $**p < 0.01$ (contralateral hemisphere); $20 \mu\text{g/g RA-NP} = 359.7 \pm 59.5\%$, $**p < 0.01$ (ipsilateral hemisphere)) (Figure 4.11C). Representative images of peri-infarct lectin-positive vessels are depicted in Figure 4.11D. Finally, to establish a connection with the *in vitro* data, we assessed the Ago2 levels in the mouse brain. We observed that these were increased three days after MCAO (vehicle = $142.1 \pm 9.2\%$, $*p < 0.05$ (contralateral hemisphere)), but were unaffected by RA-NP treatment ($20 \mu\text{g/g RA-NP} = 162.3 \pm 36.9\%$). Seven days after MCAO, we did not observe any changes in brain Ago2 levels (Figure 4.11E). Then, we assessed the expression of the Ago2 membrane receptor, NRP1. Three days after MCAO we observed a significant loss of NRP1 expression levels (vehicle = $8.7 \pm 3.1\%$, $*p < 0.05$ (contralateral hemisphere); vehicle = $19.1 \pm 11.9\%$, $**p < 0.01$ (ipsilateral hemisphere)). This effect was not recovered through the RA-NP injection ($20 \mu\text{g/g RA-NP} = 22.3 \pm 16.4\%$, $*p < 0.05$ (contralateral hemisphere); $20 \mu\text{g/g RA-NP} = 13.6 \pm 12.0\%$, $**p < 0.01$ (ipsilateral hemisphere). In the subacute phase, NRP1 levels remained decreased after RA-NP injection, in the contralateral hemisphere ($20 \mu\text{g/g RA-NP} = 23.8 \pm 16.6\%$, $**p < 0.05$), in comparison with the sham group. In the ipsilateral hemisphere, we did not observe significant changes (Figure 4.11F). Altogether, our results showed that the RA-NP treatment normalized eNOS and NO production, and increased peri-infarct vessel density.



(figure continues on the next page)

G

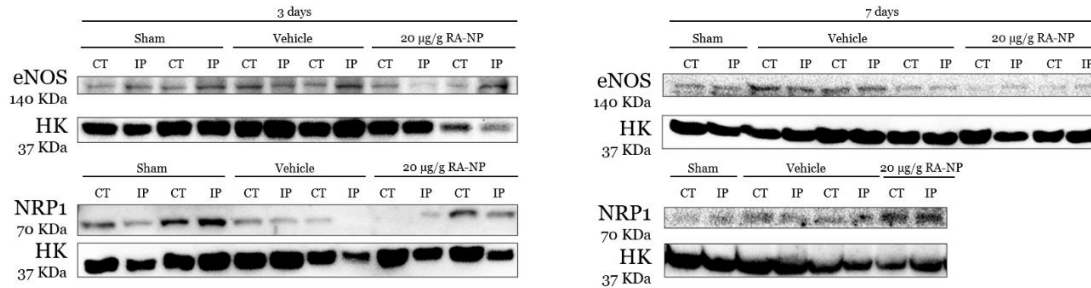


Figure 4.11 – RA-NP ameliorated vascular function in the subacute phase. In the acute phase, no alterations were observed in the eNOS levels. In the subacute phase, in the contralateral hemisphere, RA-NP (20 µg/g) were able to counteract the ischemia-induced eNOS expression (A). Similarly, RA-NP normalized NO release in the contralateral hemisphere (B). At this time-point, RA-NP significantly increased the percentage of the peri-infarct vessel density in comparison with vehicle mice (C), measured by lectin staining. Representative images of peri-infarct lectin-positive vessels were provided (D). Ago2 levels were increased three days after MCAO but were unaffected by RA-NP, measured by ELISA. No changes were observed in the subacute phase (E). Ago2 membrane receptor was significantly decreased three days after MCAO; RA-NP injection failed to recuperate NRP1 levels. Seven days after MCAO, NRP1 levels were only significantly changed by RA-NP in the contralateral hemisphere, measured by western blotting (F). Representative protein bands obtained from western blotting experiments (G). Data were expressed as the mean \pm SEM of the indicated number of repeats and as a percentage relative to untreated controls (* p < 0.05 compared to sham mice; ** p < 0.01 compared to vehicle mice, one-way ANOVA for all figures; in Figure 4.11E Student's t test was used for the comparison between vehicle and RA-NP). Abbreviations: Ago2, argonaute-2; eNOS, endothelial nitric oxide synthase; NO, nitric oxide; NRP1, neuropilin-1; RA-NP, retinoic acid-loaded nanoparticles.

4.4 Discussion

Life-saving reperfusion therapies for ischemic stroke follow strict clinical criteria, which strongly limit the number of patients that can benefit from them. The complex pathophysiology of stroke further complicates the effective translation of therapies (Marto *et al.* 2016), which should target multiple injury and repair mechanisms. Repairing blood vessels and/or promoting the formation of new functional ones (i.e., angiogenesis) could serve as a therapeutic target to improve post-stroke recovery (Bai and Lyden 2015; Campbell *et al.* 2019). The work of Krupinski and colleagues showed a positive correlation between a higher number of blood vessels and prolonged patient survival (Krupinski *et al.* 1994). Active angiogenesis was later associated with reduced cognitive and motor function loss in stroke (Hayashi *et al.* 2003; Buga *et al.* 2014; Eldahshan *et al.* 2021). Hence, we aimed to identify a therapeutic strategy to promote the neurovascular unit's protection after significant ischemic damage. VEGF and other pro-angiogenic factors (e.g., fibroblast growth factor, hepatocyte growth factor) have been studied for this purpose. Still, these molecules are involved in complex signaling pathways, and clinical translation has proven challenging. Slow-release strategies, neutralization of inhibitory factors, and cell-based approaches have also shown promising data in preclinical studies (Rust 2020). Herein, we show that, *in vitro*, RA-NP recovered the vascular function compromised by ischemia via Ago2. *In vivo*, the intravenous administration of RA-NP reduced the infarct volume and attenuated the neuro-inflammatory

response in the acute phase. In the subacute phase, RA-NP potentiated peri-infarct angiogenesis and revealed a promising trend to obtain a functional outcome in forepaw grip strength. In line, we have previously demonstrated the therapeutic benefits of RA-NP in ischemic conditions. In particular, we reported this polymeric formulation promoted the proliferation of mouse and human endothelial cells and rescued them from ischemic death *in vitro* (Ferreira *et al.* 2016; Machado-Pereira *et al.* 2018); also, the secretome of RA-NP-treated ischemic endothelial cells enhanced neural stem cell survival and proliferation (Ferreira *et al.* 2016). The intravenous injection of RA-NP in mouse pups induced a preventive effect on organotypic slice cultures exposed to OGD (Machado-Pereira *et al.* 2018). We have also described the repairing role of Ago2 in the brain endothelium exposed to inflammatory conditions *in vitro* and *in vivo*, with a protective effect on all components of the neurovascular unit (Machado-Pereira *et al.* 2022). For these reasons, the potential of RA-NP to simultaneously promote neurovascular repair and enhance the Ago2 endogenous mechanism was explored in the present study.

First, we confirmed that OGD, a well-established *in vitro* model of stroke (Andjelkovic *et al.* 2003), lowered cell viability after a recovery period (OGD/R). OGD induces rapid changes in microvessels (Shi *et al.* 2016), which leads to endothelial hyperpermeability (Förstermann and Münzel 2006) and, ultimately, to cell death (Chavakis and Dimmeler 2002). Although protocols differ (e.g., time of exposure, the origin of endothelial cells, species, and cell immortalization), others have reported similar findings. Ku and colleagues obtained a marked reduction of mouse brain microvascular endothelial cell (bEnd.3) viability (decreased by approximately 70%) after 16 hours of OGD (Ku *et al.* 2016). Liao and colleagues found a significant reduction in cell survival (about 50%) of primary vascular endothelial cells, human umbilical vein endothelial cells (HUVEC), and bEnd.3 cells after OGD/R (4 hours of OGD followed by 24 hours of recovery) (Liao *et al.* 2016). After 3 hours, both OGD and OGD/R caused cell membrane damage and the loss of Ago2. Indeed, Ago2 knockdown increased HUVEC death and impaired tubule formation (Asai *et al.* 2008), suggesting an association between cell survival and Ago2. Although OGD/R did not change the total protein content, Ago2 and NRP1 were significantly reduced. NRP1 mediates the internalization of extracellular Ago2 (Prud'homme *et al.* 2016). In addition to neuronal and epithelial cells, this receptor is mainly expressed by endothelial cells and plays a key role in angiogenesis (loss of NRP1 compromises this process). NRP1 enhances vascular endothelial growth factor 165 (VEGF165) binding to its receptor and promotes extracellular matrix signaling in endothelial cells (Issitt *et al.* 2019). Our results showed that a shorter period of OGD (1 hour) followed by recovery increased both Ago2 and NRP1, which could be the result of a compensation mechanism (no significant cell death or cell membrane damage occurred in those conditions). We have shown that normalizing intracellular Ago2 replenishes NRP1 expression in an inflammatory context (Machado-Pereira *et al.* 2022), highlighting the relevance of Ago2 expression and its maintenance at the intracellular level. Ago2 overexpression was reported to drive vessel formation in an *in vitro* model of myeloma angiogenesis: proangiogenic let-7 family members and miR-17/92 cluster members were positively regulated by Ago2, whereas anti-angiogenic miR-145 and miR-361 were negatively regulated (Wu *et al.* 2014). Conversely, Ago2 knockdown increased

apoptosis and impaired tube formation of an endothelial cell line (Asai *et al.* 2008) and decreased VEGF expression and signaling in hepatocellular carcinoma cell lines (Ye ZL *et al.* 2015). In addition, both endothelial and cancer cell lines used in different models of hypoxia and nutrient deprivation showed the loss of NRP1, while chloroquine and bafA1 prevented this effect (Bae *et al.* 2008). Considering the last-mentioned results and our previous work (Machado-Pereira *et al.* 2022), we hypothesized that Ago2 was degraded through autophagy under ischemic conditions. Indeed, autophagy is a complex process that can serve as a pro-survival or pro-death function (Nikoletopoulou *et al.* 2013) and is triggered in endothelial cells exposed to ischemia to secure macromolecule recycling (Schaaf *et al.* 2019). Accordingly, we confirmed that autophagy was activated in OGD/R conditions since the p62 levels dropped. The inhibition of autophagy via BafA1 (Yoshii and Mizushima 2017) promoted the accumulation of p62 and rescued Ago2 levels. Others also observed this result in different cell types: Ago2 accumulation was reversed by autophagy in a neurodegenerative context (Schaaf *et al.* 2019), while Ago2 increased in autophagy-deficient autophagy related 5^{-/-} and autophagy related 16^{-/-} mouse embryonic fibroblast cells (Sibony *et al.* 2015). In our study, autophagy inhibition did not affect viability, leading us to explore other approaches to recover both Ago2 intracellular levels and consequent cell survival.

Inline, and based on our previous results showing a good therapeutic effect of RA-NP on ischemic endothelial cell survival (Ferreira *et al.* 2016; Machado-Pereira *et al.* 2018), we proceeded to investigate the role of RA-NP on primary BEC exposed to ischemic injury *in vitro* and dissect its link to Ago2. Our screening under physiological conditions first showed that the nanoformulation and the free RA (below 1 μ M) were harmless to primary BEC. Under basal conditions, both RA-NP and the equivalent dose of free RA showed a trend towards decreased Ago2 levels, albeit not statistically significant. In ischemic conditions, and aligned with our previous work, 3 μ g/ml RA-NP reestablished cell survival, while the equivalent concentration of the free agent (0.12 μ M RA) had no effect. Moreover, RA-NP recuperated Ago2 levels after ischemia by inhibiting autophagy. The equivalent concentration of free RA did not affect autophagy, suggesting that the controlled release of formulated RA likely ensures a more efficient and stable intracellular internalization and processing. The role of RA in autophagy is still ambiguous since others using higher doses (1 to 5 μ M) have shown RA to trigger autophagy (Zhou *et al.* 2018), again reinforcing the concentration-dependent actions of this molecule (Ferreira *et al.* 2020). Also, the differential expression of miR induced by RA (Wang *et al.* 2020) may dictate the autophagy response (Akkoc and Gozuacik 2020). We previously established a connection between Ago2 and the NO pathway by showing that Ago2 treatment *in vitro* and *in vivo* normalized NO release promoted by LPS, *in vitro* and *in vivo* (Machado-Pereira *et al.* 2022). Additionally, others have alluded to significant crosstalk between the RA and NO signaling pathways (Achan *et al.* 2002; Cho *et al.* 2005; Tao *et al.* 2018; Caccavale *et al.* 2021), which led us to clarify these possible interactions in our experimental settings. NO and eNOS, the enzyme responsible for most of the vascular NO production, are crucial for proper endothelial function (Förstermann and Münzel 2006). The overexpression of eNOS is linked to endothelial dysfunction (Zhao *et al.* 2015). Moreover, OGD/R

induces the overexpression of eNOS (rat focal ischemia model) (Zhang *et al.* 1993; Veltkamp *et al.* 2002), associating this effect with the Akt pathway, which can activate eNOS. Fulton and colleagues showed that activated Akt increased NO release from endothelial cells, while activation-deficient Akt lessened NO production (Fulton *et al.* 1999). In the current work, under physiological conditions, neither RA-NP nor free RA interfered with eNOS expression and NO production. Still, after OGD/R, RA-NP treatment normalized the phosphorylation levels of Akt, the expression of eNOS, and the consequent production of NO. Others have shown that a higher RA concentration (1 μM) enhances eNOS activity and NO production in murine endothelioma cells (sEnd.1), albeit with no changes in eNOS mRNA (Achan *et al.* 2002), while eNOS expression was reduced by 0.01 μM RA in human tracheobronchial epithelial cells (Norford *et al.* 1998). Herein, we decide to assess whether the regulation of eNOS/NO levels by RA-NP was dependent on Ago2, using two approaches: Ago2 protein silencing (siAgo2 treatment) and Ago2 activity inhibition (BCI-137 treatment). Herein, RA-NP were shown to require Ago2 to reduce the levels of NO induced by ischemia. In both scenarios, NO production increased significantly over the levels induced by ischemia, suggesting the involvement of Ago2 in the modulatory effect of RA-NP in the NO signaling pathway, as we previously described (Machado-Pereira *et al.* 2022). This outcome entailed the participation of iNOS in the NO overexpression. Ago2 silencing may potentiate RA-induced expression of transglutaminase type-II (TGase-II) (Iosue *et al.* 2013), which in turn may enhance iNOS expression (inflammatory context) (Lee *et al.* 2004). Noteworthy, under physiological conditions (i.e., no stimulus and no treatment), Ago2 silencing alone also significantly changed NO signaling by decreasing eNOS levels and, consequently, NO production, adding complexity to the matter. NO can be used in the clinic at low concentrations, and its sustained release via methoxy PEG-PLGA nanoparticles enhanced tube formation (Yang C *et al.* 2018). Accordingly, we found that endothelial cell adhesion and growth were impaired when Ago2 expression or activity was inhibited. Others have reported in human trophoblast and endothelial cells in the placenta that the negative regulation of Ago2 can also inhibit tube formation under LPS challenge (Ming Yanga *et al.* 2016). Overall, our *in vitro* data support a regenerative role for RA-NP by regulating the Akt/eNOS/NO pathway via Ago2, an effect further explored *in vivo* using a transient model of MCAO.

We have previously tested the intravenous administration of RA-NP in mouse pups and observed that 10 $\mu\text{g/g}$ of the formulation significantly protected organotypic hippocampal slice cultures from ischemic damage (Machado-Pereira *et al.* 2018). Herein, we explored the therapeutic potential of the systemic administration of RA-NP in a mouse model of cerebral ischemia. The seminal work by Plane and colleagues had previously demonstrated the benefits of RA in stroke (Plane *et al.* 2008). In their work, rats subjected to transient MCAO (90 minutes occlusion) were fed an RA-enriched diet and exposed to an enriched environment, later exhibiting enhanced post-stroke striatal neurogenesis and decreased infarct volume. However, their approach failed to induce functional recovery. Using a similar stroke model (transient MCAO), Kong and colleagues showed that 5 $\mu\text{g/g}$ RA administered shortly after occlusion and approximately 10 hours after rt-PA administration and reperfusion led to a decrease in hemorrhage and improved neurological

deficits 24 hours after stroke (Kong *et al.* 2015). In our model, we did not observe major hemorrhagic events after MCAO and/or RA-NP administration, evidencing the safety of our study. Furthermore, to conduct the *in vivo* studies, we conjugated a different imaging moiety (Cy5 instead of FITC) to the polymeric formulation to allow signal acquisition. RA-NP-Cy5 nanoparticles are physically similar to FITC-conjugated nanoparticles (similar particle size and zeta potential) used *in vitro* herein and in our previous work (Maia *et al.* 2011; Ferreira *et al.* 2016; Machado-Pereira *et al.* 2017; Machado-Pereira *et al.* 2018). This change did not alter the properties of the nanoformulation adding to the reproducibility of the effects elicited by the polymeric formulation. Nanoparticles with 200 nm average diameter injected intravenously or intraperitoneally preferentially accumulate in the liver and spleen (Rosenholm *et al.* 2012; Blanco *et al.* 2015). Herein, the RA-NP fluorescence signal accumulated in central organs such as the kidney, lung, and liver 1-hour post-injection but was also visibly detected in the brain. Regarding systemic toxicity data, three days after MCAO, no enzyme alterations were observed (20 µg/g RA-NP), supporting the safety of this treatment in the acute phase. In the subacute phase, the model likely changed some parameters (e.g., surgical procedure, systemic alterations after ischemia): a decrease in AST and lipase levels. Lower AST levels are related to the absence of intraoperative complications (human retrospective studies) (Woo *et al.* 2017), and low lipase levels could be associated with reduced food intake. The formulation did increase urea levels but only compared to the sham, suggesting the effect could also be attributed to the model. Overall, the data support that RA-NP can be administered systemically and safely.

It was reported that ischemic mice (60 minutes MCAO) injected intraperitoneally with 1 µg/g RA two hours after the lesion showed a reduced infarct volume and improved neurological score in the following 24 hours (Cai *et al.* 2019). In our *in vivo* study, we tested three doses of RA-NP (10, 20, and 40 µg/g) equivalent to 0.123, 0.246, and 0.492 µg/g free RA, respectively, representing lower RA concentrations than those used by other works mentioned previously. The lowest and highest doses appeared ineffective, while the 20 µg/g dose significantly reduced the infarct area, possibly due to RA's narrow therapeutic window of action (Ferreira *et al.* 2020). Considering that the concentration herein used was low, we assume that in future studies multiple RA injections could be necessary to sustain the effect of RA and observe a functional animal recovery. Since we observed a recovery in grip strength, we examined whether any neuronal repair or regeneration supported these data. The efficacy of RA-NP in promoting neuroprotection was also assessed through the expression of three neuronal markers (NeuN, MAP2, and βIII-tubulin). NeuN is expressed in post-mitotic mature neurons, and its loss directly correlates with neuronal death (Buscemi *et al.* 2019). Herein, a single injection of RA-NP rescued approximately half of the lost neuronal population in the subacute phase (ipsilateral hemisphere). This is in accordance of a previous study from our group, showing that the stereotaxic injection of the same formulation promotes the survival of dopaminergic cells injured by 1-methyl-4-phenyl-1, 2, 3, 6-tetrahydropyridine (MPTP) in an *in vivo* model of Parkinson's disease, in a similar timeframe after lesion (Esteves *et al.* 2015). Indeed, RA is a modulator of several signaling pathways, such as cyclic AMP response element binding protein (CREB), known to promote neuronal survival

(Walton and Dragunow 2000). We also examined another marker for mature neurons, MAP2, a cytoskeletal protein that signals early neuronal damage after stroke (Mages *et al.* 2021), and that is linked to neurite outgrowth and dendrite development (Sánchez *et al.* 2000). The contralateral hemisphere exhibited a loss of MAP2-positive neurons three days post-injury, but a remarkable upregulation of this marker in both hemispheres after RA-NP injection, suggestive of neurite outgrowth. In fact, others have shown that RA (10 μ M) can induce neurite outgrowth via MAP2 upregulation, in a neuroblastoma cell line, after three and seven days of incubation. However, this RA concentration did not change the levels of β III-tubulin, a protein that contributes to microtubule stability (Paik *et al.* 2019). This marker identifies some mitotically active neuronal precursors, newly generated immature postmitotic neurons, and differentiated neurons (von Bohlen und Halbach 2007). Therefore, the effect we observed in the subacute phase (seven days post-MCAO) reflects the actions of RA-NP on these cell subpopulations, meaning that the trend towards sham levels could indicate neuroprotection of resident cells and/or some contribution of migrating immature neurons to the penumbra area. We have shown that RA-NP induces the differentiation of subventricular zone-derived neural stem cells via the upregulation of β III-tubulin (Maia *et al.* 2011). An adjusted experimental design and timeline should be explored in future studies to clarify the contribution of RA-NP to this process in stroke context.

Given the anti-inflammatory potential of RA in stroke, we hypothesized that the reduction of infarct volume could have resulted from the inhibition of neuroinflammatory response (Cai *et al.* 2018). Accordingly, in the acute phase, the systemic injection of RA-NP normalized microglial Iba-1 and astrocytic GFAP levels in both hemispheres when the inflammatory process is more exacerbated (Cai *et al.* 2018). The overexpression of GFAP in the subacute phase could be related to the astrocyte-mediated regeneration occurring in other brain regions (not discernable in the brain homogenates used for western blotting). In fact, and in alignment with our *in vitro* data, RA may attenuate inflammation by several mechanisms, including the downregulation of L-arginine/NO pathway through the inhibition of iNOS expression (LPS-activated mesangial cells) (Datta and Lianos 1999) or the inhibition of the release of proinflammatory cytokines by the activated microglial and astrocyte cells (Dheen *et al.* 2005; Xu *et al.* 2006). Thus, our data contribute to expanding the knowledge on the effect of RA in the acute phase post-stroke, which has been poorly explored so far. Then we examined whether RA-NP could improve vascular function. The expression of eNOS peaks at seven days post-stroke (rat MCAO model) (Lapi *et al.* 2015), which follows our model (contralateral hemisphere). RA-NP normalized eNOS expression and NO production in the contralateral hemisphere in the subacute phase, which is also in agreement with our *in vitro* data and with reports by others: RA inhibits eNOS mRNA level and NO synthesis (porcine oocyte) (Hattori *et al.* 2001). Consequently, RA-NP also increased peri-infarct vessel density in both hemispheres, and this effect was sustained for up to seven days of analysis.

Regarding the interaction between RA and Ago2, our *in vivo* data did not reveal a direct correlation between the outcome of RA-NP treatment and Ago2 levels in the brain. We only observed a significant increase in Ago2 expression in the contralateral hemisphere three days

after stroke, possibly due to the microglial activation. We demonstrated that LPS-activated microglia overexpressed Ago2 *in vitro* and *in vivo* (Machado-Pereira *et al.* 2022). Moreover, RA-NP treatment did not normalize these values. Although NRP1 expression dropped significantly in the acute phase (a potential consequence of neuronal and vessel loss), RA-NP did not recuperate the loss of the Ago2 receptor, which is in alignment with our *in vitro* data. More studies should be considered to obtain an accurate Ago2 expression profiling across various brain areas and in different cell populations. Additionally, since ischemia can change miR signature (Pignataro 2021), future studies should investigate Ago2-specific miR load as well. The absence of genetic models poses an added challenge since Ago2-deficient mice display developmental abnormalities and high mortality rates in early development stages (Morita *et al.* 2007). There are some limitations that should be considered for future studies. Like in other brain injuries, our results revealed more robust responses in the contralateral hemisphere based on the crossed anatomy of motor and sensory systems. The absence of a full functional recovery also indicates that multiple RA-NP injections or other protocol modifications, such as administration route or time point of injection, should be considered.

4.5 Conclusions

Considering these results, we propose that RA-NP regulation of the brain vasculature under ischemia occurs as depicted in the figure below (Figure 4.12). Accordingly, the present study revealed the therapeutic and safety potential of the intravenous administration of RA-NP in the acute phase of stroke. We observed a reduction in cortical infarct size, mediated at least partially by the inhibition of post-stroke cerebral inflammation. In the subacute phase, RA-NP also showed a good pro-angiogenic effect in the peri-infarct region. In sum, RA-NP could be envisioned as a potential therapeutic agent for systemic therapies aimed at treating neurovascular and/or neuroinflammatory conditions.

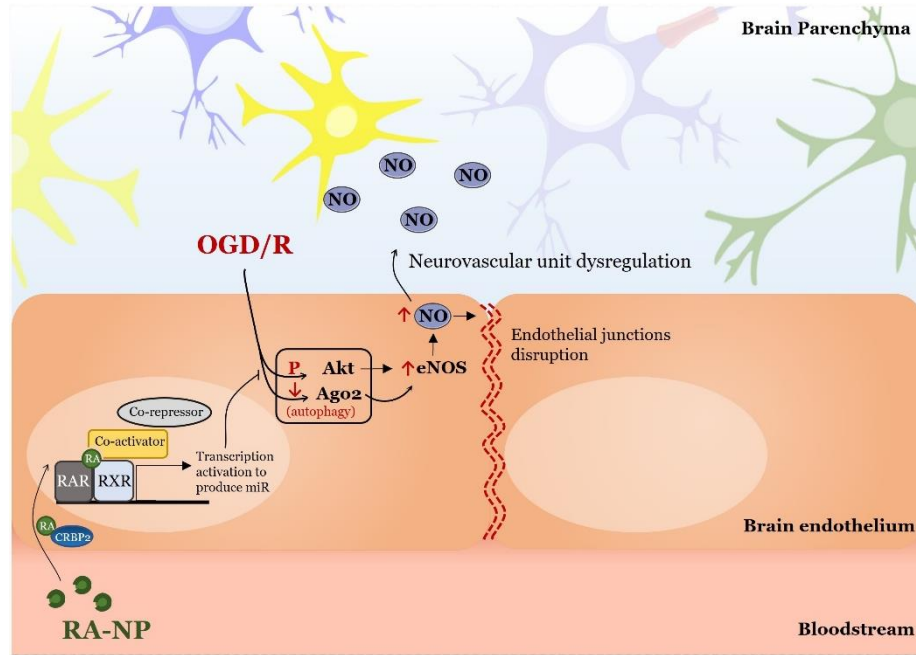


Figure 4.12 – Proposed model for RA-NP regulation of the brain vascular function, via Ago2, under ischemia. OGD/R induced autophagic Ago2 degradation and promoted Akt phosphorylation, leading to eNOS activation and consequent release of high amounts of NO. These events compromise endothelial viability. The exogenous application of RA-NP activated the expression of certain miR that regulated the Akt/eNOS/NO pathway via Ago2, thus recovering the vascular function compromised by OGD/R.

Chapter 5

General discussion

Life-threatening medical conditions, dementia, and economic burden still dominate current discussions about stroke, which remains a leading cause of disability in Portugal and worldwide, lacking effective therapies. The development of strategies aiming to modulate endogenous neuroprotective mechanisms (e.g., neurogenesis, angiogenesis, axonal sprouting, and synaptogenesis) emerged as a safer alternative to thrombolysis (which has a short time window) and opened new insights in stroke therapies (Matei *et al.* 2021; Ghozy *et al.* 2022). Although some of these strategies have shown significant preclinical advances (Bliss *et al.* 2006; Hicks *et al.* 2007; Kolb *et al.* 2007; Erlandsson *et al.* 2011; Zhang *et al.* 2011; Eckert *et al.* 2013), they undervalue the importance of cerebral vasculature in post-stroke recovery. Indeed, a favorable outcome (i.e., higher survival and higher recovery rates) in stroke patients is correlated with increased serum levels of pro-angiogenic factors (Slevin *et al.* 2000; Lee *et al.* 2010; Navarro-Sobrinho *et al.* 2011) and higher vascular densities in the peri-infarct region (Krupinski *et al.* 1994). Moreover, collateral circulation (recruitment of vascular networks to maintain CBF in the ischemic region) may improve clinical outcome in patients (Bang *et al.* 2011; Malhotra and Liebeskind 2020) and the effectiveness of the thrombolytic therapies (Uniken Venema *et al.* 2022), highlighting the active role and the importance of the vasculature to induce neuroprotection. Therefore, therapeutic targeting of dysregulated cerebral vasculature constitutes a promising strategy for brain repair and, consequently, to improve clinical outcomes following a stroke. The endonucleolytic activity (Liu *et al.* 2004; Boon and Vickers 2013), along with the protective and pro-angiogenic abilities of Ago2 in the peripheral vasculature (Asai *et al.* 2008; Ye ZL *et al.* 2015), make it a strong candidate to induce neurovascular repair following cerebral ischemia. Moreover, our group previously demonstrated that Ago2 functions as a biocompatible and non-invasive miR delivery vehicle to human and mouse brain endothelial cells *in vitro* and *in vivo* (Ferreira *et al.* 2014), which may be highly relevant in the context of stroke since miR play a vital role in the infarct-sparing effect (Pignataro 2021). In that sense, in this work, the therapeutic effects of Ago2 in the ischemic cerebral vasculature were investigated. To achieve the proposed goals, *in vitro* (OGD/R) and *in vivo* (transient MCAO) models were used.

Due to the limited knowledge regarding the Ago2 functions on dysregulated brain vasculature, the purpose of the first study (Chapter 3) was to uncover whether Ago2 could protect the brain endothelium and the NVU from inflammatory conditions (LPS challenge). After ischemia onset, inflammatory cells are activated and accumulate within the brain parenchyma, leading to inflammatory injury (Wang *et al.* 2007), which exacerbates the prognosis and symptoms in the context of stroke (Yoshimura and Ito 2020). *In vitro* and *in vivo* data revealed that Ago2 protected the entire NVU from damage caused by systemic inflammation by normalizing a set of factors

secreted by endothelial cells, which in turn favors glial and neuronal state. Furthermore, the data fueled the notion that the role of Ago2 is complex and modulates NVU cell responses differently, possibly as a compensatory mechanism to keep the injury from producing further damage. Interestingly, *in vivo* data highlighted that Ago2 may potentially restore the BBB integrity by preserving the essential component of the endothelial junction, namely the VE-cadherin (Vestweber 2008), suggesting a promising therapeutic value to induce brain angiogenesis. Also, in this pathological setting, *in vivo* data showed that Ago2 could modulate the eNOS expression levels towards the baseline (and possibly the NO levels, despite not being evaluated in this study). Others reported that proper NO levels are required for VE-cadherin stability, preventing BBB hyperpermeability (González *et al.* 2003; Di Lorenzo *et al.* 2013; Ninchoji *et al.* 2021). Thus, it was hypothesized that Ago2-preserved VE-cadherin expression occurred by balancing NO levels. Interestingly, the effect of Ago2 to promote basal NO levels was also observed in the ischemic setting (Chapter 4), suggesting a strong correlation between Ago2/NO signaling and BBB integrity. Having this in mind, a deeper understanding of the precise molecular mechanisms by which NO modulates VE-cadherin expression and stability via Ago2 is needed. In line, others reported that the stability of VE-cadherin is achieved due to its actin cytoskeleton binding partners, namely β -catenin and p120-catenin (Li *et al.* 2018). Additionally, Thibeault and colleagues stated that the β -catenin is a substrate for S-nitrosylation Cys619 by NO in mouse lung endothelial cells, promoting its dissociation from VE-cadherin and, consequently, its disassembly and increased endothelial permeability (Thibeault *et al.* 2010). Accordingly, it would be important to investigate the effect of Ago2-modulated NO levels on β -catenin S-nitrosylation by (i) confirming that NO induces S-nitrosylation of β -catenin in ischemic brain endothelial cells using the biotin-switch assay (Jaffrey and Snyder 2001); (ii) investigating whether Ago2 can induce S-nitrosylation of β -catenin, using siAgo2 and performing the biotin-switch assay; and (iii) assessing the cysteine residues of β -catenin that are substrates for modifications by NO in ischemic brain endothelial cells by mass spectrometric analyses. Likewise, it would be interesting to examine the S-nitrosylation of p120-catenin using the same approach. These results will provide novel insights to explain the Ago2 effect on the stability of intercellular junctions between BEC and, consequently, on BBB integrity. Besides ischemic stroke, these evidence may have therapeutic value to other CNS diseases with a disrupted BBB function (e.g., hemorrhagic stroke, multiple sclerosis, epilepsy, and Alzheimer's disease).

In addition, in this first work, a possible link between the endogenous Ago2 mechanism and an improved cognitive function in the animals was investigated by evaluating markers pertaining to neuronal function. Accordingly, in the *in vivo* model of systemic inflammation, Ago2 induced a neuroprotective effect in the hippocampus by restoring key proteins of the neuronal function, namely CREB, MAP2, and PSD-95, anticipating a promising role for Ago2 in cognitive function. Despite not being explored in this Thesis, additional studies (e.g., novel object recognition test and the Morris water maze) should be conducted to assess spatial learning and memory *in vivo*.

Based on the previous data, the therapeutic potential of Ago2 protein in cerebral ischemia was further explored using a nanotechnology-based RA delivery system (RA-NP) in an attempt to

increase Ago2 intracellular levels in brain endothelium and restore its protective functions (Chapter 4). RA-NP were used due to their capability to deliver intracellularly RA (Ferreira *et al.* 2016; Machado-Pereira *et al.* 2017; Machado-Pereira *et al.* 2018), an anti-inflammatory, pro-survival, and pro-angiogenic agent (Choi *et al.* 2005; Dheen *et al.* 2005; Saito *et al.* 2007). The use of RA-NP in this Thesis, in addition to their preclinical application in an animal stroke model, represents a novelty for the retinoid family by unveiling another target of the RA signaling pathway never explored so far (the Ago2 protein). *In vitro* data demonstrated that RA-NP restored the Ago2 intracellular levels by inhibiting autophagy in brain endothelial cells, which ultimately protected the brain endothelium from ischemic damage. Although data suggested that the protective role of RA-NP was achieved by the regulation of the Akt/eNOS/NO signaling via Ago2, additional studies are needed to dissect the interaction between Ago2 and RA. Firstly, and in line with the obtained data, it could be hypothesized that RA induces the expression of certain miR capable of inhibiting autophagy. In fact, it is widely described that RA regulates the expression of several miR to perform its biological functions (Wang *et al.* 2020). Among other mechanisms, miR are key regulators of the autophagic process in response to stress signals (e.g., starvation, energy demand crisis, and growth factor deprivation) (Akkoc and Gozuacik 2020). For instance, RA increases the expression of miR-34a in myocardial cells from ischemia-reperfusion injury (Welch *et al.* 2007; Shao *et al.* 2017) and miR-30 in gastric cancer cells (Abbasi *et al.* 2022), which exert their effects by inhibiting autophagy. Thus, reverse transcription polymerase chain reaction or RNA sequencing studies elucidating miR expression signature in ischemic brain endothelium treated with RA-NP may increase the understanding of the interaction between RA and Ago2 and its impact on brain protection. Secondly, it could be hypothesized that RA-NP induce Ago2 post-translation modifications, increasing its stability and activity. Previous studies have found that Ago2 hydroxylation increases Ago2 stability and activity and increases miR levels, and this process is highly mediated by C-P4H (Qi *et al.* 2008; Wu *et al.* 2011). Thus, to determine whether RA-NP may promote Ago2 stability, it would be interesting to assess the Ago2 hydroxylation status in brain endothelial cells through real-time reverse transcription-polymerase chain reaction analysis of C-P4H α / β mRNA (the two subunits of C-P4H). A better understanding of Ago2 post-translational modifications will be promising in providing novel avenues for highly effective approaches to modulating the role of Ago2 and miR homeostasis. Additionally, predicting protein interaction networks based on genetic models of Ago2 loss-of-function provides valuable insights under pathological contexts. However, their use for the current study can be challenging. Ago2-deficient mice display developmental abnormalities and high mortality rates early in development (Morita *et al.* 2007). An additional challenge is posed by models in which RA production is ablated since these models require exogenous RA application to ensure successful conception and embryonic CNS development (Ghyselinck *et al.* 1997) and to avoid lethality at this stage through multiple defects (e.g., shortened anteroposterior axis, absent limb buds, enlarged heart, and lack of organized extraembryonic vessels in the yolk sac) (Niederreither *et al.* 1999).

Then, once confirmed the relevance of the endogenous Ago2 mechanism to recover vascular function after ischemia and defined RA-NP as a promising tool to improve this mechanism, it was hypothesized that the systemic injection of RA-NP has therapeutic value in an animal model of stroke, by promoting tissue survival and functional outcome. *In vivo* data corroborated part of the previous hypothesis, and an amelioration of the inflammatory response was observed in the acute phase, together with neuronal survival and neurovascular repair in the subacute phase after stroke. Importantly, in the subacute phase, a robust pro-angiogenic effect was observed in the peri-infarct region. In light of these preliminary results and the existing literature, the modulation of the endogenous Ago2 system might be a promising alternative to VEGF administration in the hyperacute phase after stroke. VEGF, while increasing angiogenesis, also increases vascular permeability, leading to edema formation and increased bleeding risk, which can have life-threatening consequences for patients (Zhang *et al.* 2000). In future studies, and since angiogenesis may function as a gateway for macrophage infiltration after stroke (Rust 2020), the angiogenic process should be closely monitored to ensure a safe modulation of the endogenous Ago2 mechanism.

Finally, these observations were extended and it was investigated whether the modulation of endogenous Ago2 mechanism through RA-NP may induce sensorimotor function in the animals. Although there are no guidelines for the selection of behavioral tests, the selection of animal experiments is a challenging issue in preclinical stroke research since it has to combine the animal's condition with the functional results. In this sense, the sensorimotor tests neuroscore, grip strength, and latency time were defined as reliable procedures to predict the effectiveness of RA-NP following stroke. Against the initial hypothesis, a single systemic injection of RA-NP after stroke could not promote significant functional outcome in mice, despite a promising trend in the grip strength in the subacute phase. Although RA-NP seemed to reach the brain parenchyma (as tracked *in vivo* and *ex vivo* by IVIS Lumina LT Series III) and had been uptaken (as confirmed by the enhanced tissue survival, acute inflammatory restitution, and subacute neurovascular protection), data suggest that there was a low bioavailability of the formulation, which negatively impacts on intracellular brain Ago2 levels (unchanged in the subacute phase) and in sensorimotor results. Thus, future studies should consider multiple injections in an attempt to observe a functional outcome. Alternatively, physicochemical changes of the RA-NP could be considered, including their coating with transferrin to facilitate their passage through the brain parenchyma (Yemisci *et al.* 2015) or with PEG to prolong the circulation time and reduce particle clearance by the reticuloendothelial system (Schroeder *et al.* 1998; Tang *et al.* 2019).

Lastly, the use of healthy, adult, and male animals in this study requires explanation since preclinical stroke research should attempt to mimic the complexity of human trials by including models that incorporate aging and comorbidities, studying both genders and long-term sequelae (according to STAIR recommendations). Nonetheless, the present study represents an exploratory investigation aiming to assess the potential of modulating an endogenous mechanism to enhance neurovascular repair and inflammatory restitution in stroke. For standardization purposes, future studies should deliberately combine animals of different ages, sex, and genetic

backgrounds. Indeed, the molecular mechanisms of ischemic cell death and the stroke outcome in males and females are different due to the estrus cycle in female mice (estrogen protects the brain in numerous models of experimental brain injury by altering endothelium-dependent NO and prostacyclin-mediated responses of mesenteric arteries) (Liu *et al.* 2009). Similarly, aging is also an adverse prognosticator of stroke outcomes (Hecht *et al.* 2012). However, it is important to note that randomization, blinding, and data analysis protocols were considered whenever possible in the current research work.

Altogether, this Thesis provided strong evidence that Ago2 represents an endogenous mechanism that can be targeted to recover cerebrovascular function compromised by cerebral ischemia and, consequently, to induce homeostasis to brain parenchyma. Lastly, research to develop innovative strategies to enhance this endogenous system may have therapeutic value for post-stroke recovery.

Chapter 6

Conclusions

The burden of stroke is a substantial public health issue rapidly expanding worldwide, requiring safer and more effective therapies. Additionally, strategies aiming to modulate endogenous protective mechanisms have been proposed as promising alternatives for intravenous thrombolysis therapies, despite undervaluing the importance of cerebral vasculature. Indeed, a proper cerebrovascular function is pivotal to mitigate the detrimental effects of stroke and correlates with higher survival rates and long-term improvement of neurological function in patients. Considering these evidence, a major innovative aspect of this Thesis is the demonstration of Ago2 protein as a promising endogenous mechanism to improve brain vascular function compromised after a stroke and, consequently, to full parenchymal recovery.

Ago2 reveals a key protein to protect the NVU from damage caused by systemic inflammation (LPS challenge), one of the most critical post-stroke pathological events contributing to a poor prognosis in stroke patients. Noteworthy, in Chapter 3, it was demonstrated that LPS activation downregulated Ago2 intracellular levels in primary BEC, with detrimental effects for all elements of the NVU. The exogenous Ago2 treatment recovered the intracellular baseline levels of this protein, reestablishing the expression of the main component of the endothelial junction (VE-cadherin), an effect mediated through the NO pathway. In adult mice intraperitoneally injected with LPS, the exogenous Ago2 application restored endothelial integrity, previously disrupted by the inflammatory process, which, in turn, provided support for proper glial and neuronal function. Likewise, this Thesis revealed that Ago2 endogenous mechanism is compromised in the ischemic cerebral vasculature (highlighted by decreased expression levels of this protein). For that reason, in Chapter 4, it was proposed a novel strategy to modulate Ago2 mechanism and improve brain vascular function, based on the controlled release of an anti-inflammatory and pro-angiogenic signaling molecule. In particular, it was explored the therapeutic effect of RA-NP to enhance Ago2 intracellular levels in primary BEC under ischemia (OGD/R). It was shown that RA-NP restored Ago2 intracellular levels and required this protein to induce vascular protection compromised by OGD/R (an effect mediated through the NO pathway). In adult mice subjected to transient MCAO, a single systemic administration of RA-NP reduced infarct size and normalized acute inflammatory response (three days post-injury). In the subacute phase (seven days post-injury), RA-NP promoted neuronal protection and exhibited a good proangiogenic effect in the peri-infarct region. Nonetheless, an absence of a full functional recovery in MCAO-subjected mice was observed. Although RA-NP could be envisioned as a safe and promising approach aiming to potentiate Ago2 endogenous mechanism and protect brain injury following a stroke, further studies still need to be conducted to attain a functional outcome and depict the interaction between RA and Ago2 as well.

In sum, the original data presented in this Thesis cover novel functions of Ago2 in the CNS and opens new insights for developing safer and more effective therapies for stroke by targeting the Ago2 endogenous mechanism.

Chapter 7

References

Abbasi A, Hosseinpourfeizi M, Safaralizadeh R. All-trans retinoic acid-mediated miR-30a up-regulation suppresses autophagy and sensitizes gastric cancer cells to cisplatin. *Life Sci.* 2022 Aug 13;307:120884. doi: 10.1016/j.lfs.2022.120884.

Abbott NJ. Astrocyte-endothelial interactions and blood-brain barrier permeability. *J Anat.* 2002 Jun;200(6):629-38. doi: 10.1046/j.1469-7580.2002.00064.x.

Achan V, Tran CT, Arrigoni F, et al. all-trans-Retinoic acid increases nitric oxide synthesis by endothelial cells: a role for the induction of dimethylarginine dimethylaminohydrolase. *Circ Res.* 2002 Apr 19;90(7):764-9. doi: 10.1161/01.res.0000014450.40853.2b.

Achilike S, Beauchamp JES, Cron SG, et al. Caregiver Burden and Associated Factors Among Informal Caregivers of Stroke Survivors. *J Neurosci Nurs.* 2020 Dec;52(6):277-283. doi: 10.1097/JNN.0000000000000552.

Adair TH, Montani JP. *Angiogenesis.* San Rafael (CA): Morgan & Claypool Life Sciences; 2010.

Adams BD, Claffey KP, White BA. Argonaute-2 expression is regulated by epidermal growth factor receptor and mitogen-activated protein kinase signaling and correlates with a transformed phenotype in breast cancer cells. *Endocrinology.* 2009 Jan;150(1):14-23. doi: 10.1210/en.2008-0984.

Ahlemeyer B, Bauerbach E, Plath M, et al. Retinoic acid reduces apoptosis and oxidative stress by preservation of SOD protein level. *Free Radic Biol Med.* 2001 May 15;30(10):1067-77. doi: 10.1016/s0891-5849(01)00495-6.

Ahlemeyer B, Hühne R, Kriegstein J. Retinoic acid potentiated the protective effect of NGF against staurosporine-induced apoptosis in cultured chick neurons by increasing the trkA protein expression. *J Neurosci Res.* 2000 Jun 15;60(6):767-78. doi: 10.1002/1097-4547(20000615)60:6<767::AID-JNR9>3.0.CO;2-6.

Akira S, Takeda K. Toll-like receptor signalling. *Nat Rev Immunol.* 2004 Jul;4(7):499-511. doi: 10.1038/nri1391.

Akkoc Y, Gozuacik D. MicroRNAs as major regulators of the autophagy pathway. *Biochim Biophys Acta Mol Cell Res.* 2020 May;1867(5):118662. doi: 10.1016/j.bbamcr.2020.118662.

Al Tanoury Z, Piskunov A, Rochette-Egly C. Vitamin A and retinoid signaling: genomic and nongenomic effects. *J Lipid Res.* 2013 Jul;54(7):1761-75. doi: 10.1194/jlr.R030833.

Alberini CM. Transcription factors in long-term memory and synaptic plasticity. *Physiol Rev.* 2009 Jan;89(1):121-45. doi: 10.1152/physrev.00017.2008.

Alisch RS, Jin P, Epstein M, et al. Argonaute2 is essential for mammalian gastrulation and proper mesoderm formation. *PLoS Genet.* 2007 Dec 28;3(12):e227. doi: 10.1371/journal.pgen.0030227.

Allen NJ, Bennett ML, Foo LC, et al. Astrocyte glypicans 4 and 6 promote formation of excitatory synapses via GluA1 AMPA receptors. *Nature.* 2012 May 27;486(7403):410-4. doi: 10.1038/nature11059.

Aoto J, Nam CI, Poon MM, et al. Synaptic signaling by all-trans retinoic acid in homeostatic synaptic plasticity. *Neuron.* 2008 Oct 23;60(2):308-20. doi: 10.1016/j.neuron.2008.08.012.

Arai K, Matsuki N, Ikegaya Y, et al. Deterioration of spatial learning performances in lipopolysaccharide-treated mice. *Jpn J Pharmacol.* 2001 Nov;87(3):195-201. doi: 10.1254/jjp.87.195.

Archie SR, Al Shoyaib A, Cucullo L. Blood-Brain Barrier Dysfunction in CNS Disorders and Putative Therapeutic Targets: An Overview. *Pharmaceutics.* 2021 Oct 26;13(11):1779. doi: 10.3390/pharmaceutics13111779.

Arroyo JD, Chevillet JR, Kroh EM, et al. Argonaute2 complexes carry a population of circulating microRNAs independent of vesicles in human plasma. *Proc Natl Acad Sci U S A.* 2011 Mar 22;108(12):5003-8. doi: 10.1073/pnas.1019055108.

Asai T, Suzuki Y, Matsushita S, et al. Disappearance of the angiogenic potential of endothelial cells caused by Argonaute2 knockdown. *Biochem Biophys Res Commun.* 2008 Apr 4;368(2):243-8. doi: 10.1016/j.bbrc.2008.01.074.

Atochin DN, Huang PL. Endothelial nitric oxide synthase transgenic models of endothelial dysfunction. *Pflugers Arch.* 2010 Nov;460(6):965-74. doi: 10.1007/s00424-010-0867-4.

Austin SA, Santhanam AV, Hinton DJ, et al. Endothelial nitric oxide deficiency promotes Alzheimer's disease pathology. *J Neurochem.* 2013 Dec;127(5):691-700. doi: 10.1111/jnc.12334.

Avraham HK, Lee TH, Koh Y, et al. Vascular endothelial growth factor regulates focal adhesion assembly in human brain microvascular endothelial cells through activation of the focal adhesion kinase and related adhesion focal tyrosine kinase. *J Biol Chem.* 2003 Sep 19;278(38):36661-8. doi: 10.1074/jbc.M301253200.

Bae D, Lu S, Taglienti CA, et al. Metabolic stress induces the lysosomal degradation of neuropilin-1 but not neuropilin-2. *J Biol Chem.* 2008 Oct 17;283(42):28074-80. doi: 10.1074/jbc.M804203200.

Bai J, Lyden PD. Revisiting cerebral postischemic reperfusion injury: new insights in understanding reperfusion failure, hemorrhage, and edema. *Int J Stroke.* 2015 Feb;10(2):143-52. doi: 10.1111/ijss.12434.

Balch MHH, Nimjee SM, Rink C, et al. Beyond the Brain: The Systemic Pathophysiological Response to Acute Ischemic Stroke. *J Stroke.* 2020 May;22(2):159-172. doi: 10.5853/jos.2019.02978. Erratum in: *J Stroke.* 2020 Sep;22(3):424.

Bam M, Yang X, Zumbrun EE, et al. Decreased AGO2 and DCR1 in PBMCs from War Veterans with PTSD leads to diminished miRNA resulting in elevated inflammation. *Transl Psychiatry.* 2017 Aug 29;7(8):e1222. doi: 10.1038/tp.2017.185.

Bang OY, Saver JL, Kim SJ, et al. Collateral flow predicts response to endovascular therapy for acute ischemic stroke. *Stroke.* 2011 Mar;42(3):693-9. doi: 10.1161/STROKEAHA.110.595256.

Banks WA, Robinson SM. Minimal penetration of lipopolysaccharide across the murine blood-brain barrier. *Brain Behav Immun.* 2010 Jan;24(1):102-9. doi: 10.1016/j.bbi.2009.09.001.

Bartel DP. Metazoan MicroRNAs. *Cell.* 2018 Mar 22;173(1):20-51. doi: 10.1016/j.cell.2018.03.006.

Bastien J, Rochette-Egly C. Nuclear retinoid receptors and the transcription of retinoid-target genes. *Gene.* 2004 Mar 17;328:1-16. doi: 10.1016/j.gene.2003.12.005.

Batassa EM, Costanzi M, Saraulli D, et al. RISC activity in hippocampus is essential for contextual memory. *Neurosci Lett.* 2010 Mar 8;471(3):185-8. doi: 10.1016/j.neulet.2010.01.038.

Bavelloni A, Ramazzotti G, Poli A, et al. MiRNA-210: A Current Overview. *Anticancer Res.* 2017 Dec;37(12):6511-6521. doi: 10.21873/anticancer.12107.

Beishon L, Panerai RB. The Neurovascular Unit in Dementia: An Opinion on Current Research and Future Directions. *Front Aging Neurosci.* 2021 Jul 28;13:721937. doi: 10.3389/fnagi.2021.721937.

Bellissimo T, Tito C, Ganci F, et al. Argonaute 2 drives miR-145-5p-dependent gene expression program in breast cancer cells. *Cell Death Dis.* 2019 Jan 8;10(1):17. doi: 10.1038/s41419-018-1267-5.

Belov Kirdajova D, Kriska J, Tureckova J, et al. Ischemia-Triggered Glutamate Excitotoxicity From the Perspective of Glial Cells. *Front Cell Neurosci*. 2020 Mar 19;14:51. doi: 10.3389/fncel.2020.00051.

Bernardo-Castro S, Sousa JA, Brás A, et al. Pathophysiology of Blood-Brain Barrier Permeability Throughout the Different Stages of Ischemic Stroke and Its Implication on Hemorrhagic Transformation and Recovery. *Front Neurol*. 2020 Dec 9;11:594672. doi: 10.3389/fneur.2020.594672.

Bhaskar S, Stanwell P, Cordato D, Attia J, et al. Reperfusion therapy in acute ischemic stroke: dawn of a new era? *BMC Neurol*. 2018 Jan 16;18(1):8. doi: 10.1186/s12883-017-1007-y.

Bhattacharyya SN, Habermacher R, Martine U, et al. Relief of microRNA-mediated translational repression in human cells subjected to stress. *Cell*. 2006 Jun 16;125(6):1111-24. doi: 10.1016/j.cell.2006.04.031.

Bible E, Qutachi O, Chau DY, et al. Neo-vascularization of the stroke cavity by implantation of human neural stem cells on VEGF-releasing PLGA microparticles. *Biomaterials*. 2012 Oct;33(30):7435-46. doi: 10.1016/j.biomaterials.2012.06.085.

Bielenberg DR, Klagsbrun M. Targeting endothelial and tumor cells with semaphorins. *Cancer Metastasis Rev*. 2007 Dec;26(3-4):421-31. doi: 10.1007/s10555-007-9097-4.

Blanco E, Shen H, Ferrari M. Principles of nanoparticle design for overcoming biological barriers to drug delivery. *Nat Biotechnol*. 2015 Sep;33(9):941-51. doi: 10.1038/nbt.3330.

Bliss TM, Kelly S, Shah AK, et al. Transplantation of hNT neurons into the ischemic cortex: cell survival and effect on sensorimotor behavior. *J Neurosci Res*. 2006 May 1;83(6):1004-14. doi: 10.1002/jnr.20800.

Blomhoff R, Blomhoff HK. Overview of retinoid metabolism and function. *J Neurobiol*. 2006 Jun;66(7):606-30. doi: 10.1002/neu.20242.

Bodak M, Cirera-Salinas D, Luitz J, et al. The Role of RNA Interference in Stem Cell Biology: Beyond the Mutant Phenotypes. *J Mol Biol*. 2017a May 19;429(10):1532-1543. doi: 10.1016/j.jmb.2017.01.014.

Bodak M, Cirera-Salinas D, Yu J, et al. Dicer, a new regulator of pluripotency exit and LINE-1 elements in mouse embryonic stem cells. *FEBS Open Bio*. 2017b Jan 11;7(2):204-220. doi: 10.1002/2211-5463.12174.

Bode JG, Ehltling C, Häussinger D. The macrophage response towards LPS and its control through the p38(MAPK)-STAT3 axis. *Cell Signal*. 2012 Jun;24(6):1185-94. doi: 10.1016/j.cellsig.2012.01.018.

- Bohmert K, Camus I, Bellini C, et al. AGO1 defines a novel locus of Arabidopsis controlling leaf development. *EMBO J.* 1998 Jan 2;17(1):170-80. doi: 10.1093/emboj/17.1.170.
- Bollmann SR, Press CM, Tyler BM, et al. Expansion and Divergence of Argonaute Genes in the Oomycete Genus *Phytophthora*. *Front Microbiol.* 2018 Nov 30;9:2841. doi: 10.3389/fmicb.2018.02841.
- Bonnet E, Touyarot K, Alfos S, et al. Retinoic acid restores adult hippocampal neurogenesis and reverses spatial memory deficit in vitamin A deprived rats. *PLoS One.* 2008;3(10):e3487. doi: 10.1371/journal.pone.0003487.
- Bonney S, Dennison BJC, Wendlandt M, et al. Retinoic Acid Regulates Endothelial β -catenin Expression and Pericyte Numbers in the Developing Brain Vasculature. *Front Cell Neurosci.* 2018 Dec 5;12:476. doi: 10.3389/fncel.2018.00476.
- Boon RA, Vickers KC. Intercellular transport of microRNAs. *Arterioscler Thromb Vasc Biol.* 2013 Feb;33(2):186-92. doi: 10.1161/ATVBAHA.112.300139.
- Brambilla L, Guidotti G, Martorana F, et al. Disruption of the astrocytic TNFR1-GDNF axis accelerates motor neuron degeneration and disease progression in amyotrophic lateral sclerosis. *Hum Mol Genet.* 2016 Jul 15;25(14):3080-3095. doi: 10.1093/hmg/ddw161.
- Braun LJ, Zinnhardt M, Vockel M, et al. VE-PTP inhibition stabilizes endothelial junctions by activating FGD5. *EMBO Rep.* 2019 Jul;20(7):e47046. doi: 10.15252/embr.201847046.
- Bronevetsky Y, Villarino AV, Eisley CJ, et al. T cell activation induces proteasomal degradation of Argonaute and rapid remodeling of the microRNA repertoire. *J Exp Med.* 2013 Feb 11;210(2):417-32. doi: 10.1084/jem.20111717.
- Brouns R, De Deyn PP. The complexity of neurobiological processes in acute ischemic stroke. *Clin Neurol Neurosurg.* 2009 Jul;111(6):483-95. doi: 10.1016/j.clineuro.2009.04.001.
- Brown LS, Foster CG, Courtney JM, et al. Pericytes and Neurovascular Function in the Healthy and Diseased Brain. *Front Cell Neurosci.* 2019 Jun 28;13:282. doi: 10.3389/fncel.2019.00282.
- Buga AM, Margaritescu C, Scholz CJ, et al. Transcriptomics of post-stroke angiogenesis in the aged brain. *Front Aging Neurosci.* 2014 Mar 18;6:44. doi: 10.3389/fnagi.2014.00044.
- Buscemi L, Price M, Bezzi P, et al. Spatio-temporal overview of neuroinflammation in an experimental mouse stroke model. *Sci Rep.* 2019 Jan 24;9(1):507. doi: 10.1038/s41598-018-36598-4.

Caccavale F, Annona G, Subirana L, et al. Crosstalk between nitric oxide and retinoic acid pathways is essential for amphioxus pharynx development. *Elife*. 2021 Aug 25;10:e58295. doi: 10.7554/eLife.58295.

Cai W, Liu S, Hu M, et al. Post-stroke DHA Treatment Protects Against Acute Ischemic Brain Injury by Skewing Macrophage Polarity Toward the M2 Phenotype. *Transl Stroke Res*. 2018 Dec;9(6):669-680. doi: 10.1007/s12975-018-0662-7.

Cai W, Wang J, Hu M, et al. All trans-retinoic acid protects against acute ischemic stroke by modulating neutrophil functions through STAT1 signaling. *J Neuroinflammation*. 2019 Aug 31;16(1):175. doi: 10.1186/s12974-019-1557-6.

Cai Z, Zhao B, Deng Y, et al. Notch signaling in cerebrovascular diseases (Review). *Mol Med Rep*. 2016 Oct;14(4):2883-98. doi: 10.3892/mmr.2016.5641.

Campbell BCV, De Silva DA, Macleod MR, et al. Ischaemic stroke. *Nat Rev Dis Primers*. 2019 Oct 10;5(1):70. doi: 10.1038/s41572-019-0118-8.

Carbonell T, Gomes AV. MicroRNAs in the regulation of cellular redox status and its implications in myocardial ischemia-reperfusion injury. *Redox Biol*. 2020 Sep;36:101607. doi: 10.1016/j.redox.2020.101607.

Carmeliet P, Lampugnani MG, Moons L, et al. Targeted deficiency or cytosolic truncation of the VE-cadherin gene in mice impairs VEGF-mediated endothelial survival and angiogenesis. *Cell*. 1999 Jul 23;98(2):147-57. doi: 10.1016/s0092-8674(00)81010-7.

Carmell MA, Xuan Z, Zhang MQ, et al. The Argonaute family: tentacles that reach into RNAi, developmental control, stem cell maintenance, and tumorigenesis. *Genes Dev*. 2002 Nov 1;16(21):2733-42. doi: 10.1101/gad.1026102.

Carmignoto G, Gómez-Gonzalo M. The contribution of astrocyte signalling to neurovascular coupling. *Brain Res Rev*. 2010 May;63(1-2):138-48. doi: 10.1016/j.brainresrev.2009.11.007.

Carmona MA, Murai KK, Wang L, et al. Glial ephrin-A3 regulates hippocampal dendritic spine morphology and glutamate transport. *Proc Natl Acad Sci U S A*. 2009 Jul 28;106(30):12524-9. doi: 10.1073/pnas.0903328106.

Casey MC, Prakash A, Holian E, et al. Quantifying Argonaute 2 (Ago2) expression to stratify breast cancer. *BMC Cancer*. 2019 Jul 19;19(1):712. doi: 10.1186/s12885-019-5884-x.

Cazareth J, Guyon A, Heurteaux C, et al. Molecular and cellular neuroinflammatory status of mouse brain after systemic lipopolysaccharide challenge: importance of CCR2/CCL2 signaling. *J Neuroinflammation*. 2014 Jul 28;11:132. doi: 10.1186/1742-2094-11-132.

- Chakrabarti M, McDonald AJ, Will Reed J, et al. Molecular Signaling Mechanisms of Natural and Synthetic Retinoids for Inhibition of Pathogenesis in Alzheimer's Disease. *J Alzheimers Dis.* 2016;50(2):335-52. doi: 10.3233/JAD-150450.
- Chan PH. Reactive oxygen radicals in signaling and damage in the ischemic brain. *J Cereb Blood Flow Metab.* 2001 Jan;21(1):2-14. doi: 10.1097/00004647-200101000-00002.
- Chan YH, Harith HH, Israf DA, et al. Differential Regulation of LPS-Mediated VE-Cadherin Disruption in Human Endothelial Cells and the Underlying Signaling Pathways: A Mini Review. *Front Cell Dev Biol.* 2020 Jan 6;7:280. doi: 10.3389/fcell.2019.00280.
- Chavakis E, Dimmeler S. Regulation of endothelial cell survival and apoptosis during angiogenesis. *Arterioscler Thromb Vasc Biol.* 2002 Jun 1;22(6):887-93. doi: 10.1161/01.atv.0000017728.55907.a9.
- Cheloufi S, Dos Santos CO, Chong MM, et al. A dicer-independent miRNA biogenesis pathway that requires Ago catalysis. *Nature.* 2010 Jun 3;465(7298):584-9. doi: 10.1038/nature09092.
- Chen J, Zacharek A, Zhang C, et al. Endothelial nitric oxide synthase regulates brain-derived neurotrophic factor expression and neurogenesis after stroke in mice. *J Neurosci.* 2005 Mar 2;25(9):2366-75. doi: 10.1523/JNEUROSCI.5071-04.2005.
- Chen JH, Hong CT, Chung CC, et al. Safety and efficacy of endovascular thrombectomy in acute ischemic stroke treated with anticoagulants: a systematic review and meta-analysis. *Thromb J.* 2022 Jun 21;20(1):35. doi: 10.1186/s12959-022-00394-y.
- Chen SH, Oyarzabal EA, Sung YF, et al. Microglial regulation of immunological and neuroprotective functions of astroglia. *Glia.* 2015 Jan;63(1):118-31. doi: 10.1002/glia.22738.
- Cheng H, Yang B, Ke T, et al. Mechanisms of Metal-Induced Mitochondrial Dysfunction in Neurological Disorders. *Toxics.* 2021 Jun 17;9(6):142. doi: 10.3390/toxics9060142.
- Cheng N, Li Y, Han ZG. Argonaute2 promotes tumor metastasis by way of up-regulating focal adhesion kinase expression in hepatocellular carcinoma. *Hepatology.* 2013 May;57(5):1906-18. doi: 10.1002/hep.26202.
- Cho DH, Choi YJ, Jo SA, et al. Retinoic acid decreases nitric oxide production in endothelial cells: a role of phosphorylation of endothelial nitric oxide synthase at Ser(1179). *Biochem Biophys Res Commun.* 2005 Jan 28;326(4):703-10. doi: 10.1016/j.bbrc.2004.11.099.
- Choi WH, Ji KA, Jeon SB, et al. Anti-inflammatory roles of retinoic acid in rat brain astrocytes: Suppression of interferon-gamma-induced JAK/STAT phosphorylation. *Biochem Biophys Res Commun.* 2005 Apr 1;329(1):125-31. doi: 10.1016/j.bbrc.2005.01.110.

Christopherson KS, Ullian EM, Stokes CC, et al. Thrombospondins are astrocyte-secreted proteins that promote CNS synaptogenesis. *Cell*. 2005 Feb 11;120(3):421-33. doi: 10.1016/j.cell.2004.12.020.

Chu CY, Rana TM. Translation repression in human cells by microRNA-induced gene silencing requires RCK/p54. *PLoS Biol*. 2006 Jul;4(7):e210. doi: 10.1371/journal.pbio.0040210.

Chu Y, Yue X, Younger ST, et al. Involvement of argonaute proteins in gene silencing and activation by RNAs complementary to a non-coding transcript at the progesterone receptor promoter. *Nucleic Acids Res*. 2010 Nov;38(21):7736-48. doi: 10.1093/nar/gkq648.

Conger AK, Martin EC, Yan TJ, et al. Argonaute 2 Expression Correlates with a Luminal B Breast Cancer Subtype and Induces Estrogen Receptor Alpha Isoform Variation. *Noncoding RNA*. 2016 Sep 21;2(3):8. doi: 10.3390/ncrna2030008.

Cook RL, Householder KT, Chung EP, et al. A critical evaluation of drug delivery from ligand modified nanoparticles: Confounding small molecule distribution and efficacy in the central nervous system. *J Control Release*. 2015 Dec 28;220(Pt A):89-97. doi: 10.1016/j.jconrel.2015.10.013.

Corbett D, Nguemeni C, Gomez-Smith M. How can you mend a broken brain? Neurorestorative approaches to stroke recovery. *Cerebrovasc Dis*. 2014;38(4):233-9. doi: 10.1159/000368887.

Corcoran J, Maden M. Nerve growth factor acts via retinoic acid synthesis to stimulate neurite outgrowth. *Nat Neurosci*. 1999 Apr;2(4):307-8. doi: 10.1038/7214.

Correa-Paz C, da Silva-Candal A, Polo E, et al. New Approaches in Nanomedicine for Ischemic Stroke. *Pharmaceutics*. 2021 May 20;13(5):757. doi: 10.3390/pharmaceutics13050757.

Coull AJ, Lovett JK, Rothwell PM. Oxford Vascular Study. Population based study of early risk of stroke after transient ischaemic attack or minor stroke: implications for public education and organisation of services. *BMJ*. 2004 Feb 7;328(7435):326. doi: 10.1136/bmj.37991.635266.44.

Cristóvão AC, Saavedra A, Fonseca CP, et al. Microglia of rat ventral midbrain recovers its resting state over time *in vitro*: let microglia rest before work. *J Neurosci Res*. 2010 Feb 15;88(3):552-62. doi: 10.1002/jnr.22219.

Dai X, Okon I, Liu Z, et al. A novel role for myeloid cell-specific neuropilin 1 in mitigating sepsis. *FASEB J*. 2017 Jul;31(7):2881-2892. doi: 10.1096/fj.201601238R.

Daneman R, Prat A. The blood-brain barrier. *Cold Spring Harb Perspect Biol*. 2015 Jan 5;7(1):a020412. doi: 10.1101/cshperspect.a020412.

- Danilov CA, Gu Y, Punj V, et al. Intravenous delivery of microRNA-133b along with Argonaute-2 enhances spinal cord recovery following cervical contusion in mice. *Spine J.* 2020 Jul;20(7):1138-1151. doi: 10.1016/j.spinee.2020.02.019.
- Datta PK, Lianos EA. Nitric oxide induces heme oxygenase-1 gene expression in mesangial cells. *Kidney Int.* 1999 May;55(5):1734-9. doi: 10.1046/j.1523-1755.1999.00429.x.
- Dauphinee SM, Karsan A. Lipopolysaccharide signaling in endothelial cells. *Lab Invest.* 2006 Jan;86(1):9-22. doi: 10.1038/labinvest.3700366.
- de Kerckhove M, Tanaka K, Umehara T, et al. Targeting miR-223 in neutrophils enhances the clearance of *Staphylococcus aureus* in infected wounds. *EMBO Mol Med.* 2018 Oct;10(10):e9024. doi: 10.15252/emmm.201809024.
- Dheen ST, Jun Y, Yan Z, et al. Retinoic acid inhibits expression of TNF-alpha and iNOS in activated rat microglia. *Glia.* 2005 Apr 1;50(1):21-31. doi: 10.1002/glia.20153.
- Di Lorenzo A, Lin MI, Murata T, et al. eNOS-derived nitric oxide regulates endothelial barrier function through VE-cadherin and Rho GTPases. *J Cell Sci.* 2013 Dec 15;126(Pt 24):5541-52. doi: 10.1242/jcs.115972. Epub 2013 Sep 17. Erratum in: *J Cell Sci.* 2014 May 1;127(Pt 9):2120.
- Di Masi A, Leboffe L, De Marinis E, et al. Retinoic acid receptors: from molecular mechanisms to cancer therapy. *Mol Aspects Med.* 2015 Feb;41:1-115. doi: 10.1016/j.mam.2014.12.003.
- Di Santo S, Seiler S, Fuchs AL, et al. The secretome of endothelial progenitor cells promotes brain endothelial cell activity through PI3-kinase and MAP-kinase. *PLoS One.* 2014 Apr 22;9(4):e95731. doi: 10.1371/journal.pone.0095731.
- Diederichs S, Haber DA. Dual role for argonautes in microRNA processing and posttranscriptional regulation of microRNA expression. *Cell.* 2007 Dec 14;131(6):1097-108. doi: 10.1016/j.cell.2007.10.032.
- Diener HC, Hankey GJ. Primary and Secondary Prevention of Ischemic Stroke and Cerebral Hemorrhage: JACC Focus Seminar. *J Am Coll Cardiol.* 2020 Apr 21;75(15):1804-1818. doi: 10.1016/j.jacc.2019.12.072.
- Ding Y, Qiao A, Wang Z, et al. Retinoic acid attenuates beta-amyloid deposition and rescues memory deficits in an Alzheimer's disease transgenic mouse model. *J Neurosci.* 2008 Nov 5;28(45):11622-34. doi: 10.1523/JNEUROSCI.3153-08.2008.
- Donato R. S100: a multigenic family of calcium-modulated proteins of the EF-hand type with intracellular and extracellular functional roles. *Int J Biochem Cell Biol.* 2001 Jul;33(7):637-68. doi: 10.1016/s1357-2725(01)00046-2.

Dong D, Ruuska SE, Levinthal DJ, et al. Distinct roles for cellular retinoic acid-binding proteins I and II in regulating signaling by retinoic acid. *J Biol Chem*. 1999 Aug 20;274(34):23695-8. doi: 10.1074/jbc.274.34.23695.

Dong L, Li Z, Leffler NR, et al. Acidosis activation of the proton-sensing GPR4 receptor stimulates vascular endothelial cell inflammatory responses revealed by transcriptome analysis. *PLoS One*. 2013 Apr 16;8(4):e61991. doi: 10.1371/journal.pone.0061991.

Dong X. Current Strategies for Brain Drug Delivery. *Theranostics*. 2018 Feb 5;8(6):1481-1493. doi: 10.7150/thno.21254.

Drouin-Ouellet J, Sawiak SJ, Cisbani G, et al. Cerebrovascular and blood-brain barrier impairments in Huntington's disease: Potential implications for its pathophysiology. *Ann Neurol*. 2015 Aug;78(2):160-77. doi: 10.1002/ana.24406.

Dudvarski Stankovic N, Teodorczyk M, Ploen R, et al. Microglia-blood vessel interactions: a double-edged sword in brain pathologies. *Acta Neuropathol*. 2016 Mar;131(3):347-63. doi: 10.1007/s00401-015-1524-y.

Dueck A, Ziegler C, Eichner A, et al. microRNAs associated with the different human Argonaute proteins. *Nucleic Acids Res*. 2012 Oct;40(19):9850-62. doi: 10.1093/nar/gks705.

Duester G. Retinoic acid synthesis and signaling during early organogenesis. *Cell*. 2008 Sep 19;134(6):921-31. doi: 10.1016/j.cell.2008.09.002.

Duong CN, Vestweber D. Mechanisms Ensuring Endothelial Junction Integrity Beyond VE-Cadherin. *Front Physiol*. 2020 May 21;11:519. doi: 10.3389/fphys.2020.00519.

Eckert MA, Vu Q, Xie K, et al. Evidence for high translational potential of mesenchymal stromal cell therapy to improve recovery from ischemic stroke. *J Cereb Blood Flow Metab*. 2013 Sep;33(9):1322-34. doi: 10.1038/jcbfm.2013.91.

Eldahshan W, Sayed MA, Awad ME, et al. Stimulation of angiotensin II receptor 2 preserves cognitive function and is associated with an enhanced cerebral vascular density after stroke. *Vascul Pharmacol*. 2021 Dec;141:106904. doi: 10.1016/j.vph.2021.106904.

Enderlin V, Pallet V, Alfos S, et al. Age-related decreases in mRNA for brain nuclear receptors and target genes are reversed by retinoic acid treatment. *Neurosci Lett*. 1997 Jun 27;229(2):125-9. doi: 10.1016/s0304-3940(97)00424-2.

Erlandsson A, Lin CH, Yu F, et al. Immunosuppression promotes endogenous neural stem and progenitor cell migration and tissue regeneration after ischemic injury. *Exp Neurol*. 2011 Jul;230(1):48-57. doi: 10.1016/j.expneurol.2010.05.018.

- Esteves M, Cristóvão AC, Saraiva T, et al. Retinoic acid-loaded polymeric nanoparticles induce neuroprotection in a mouse model for Parkinson's disease. *Front Aging Neurosci.* 2015 Mar 6;7:20. doi: 10.3389/fnagi.2015.00020.
- Eulalio A, Behm-Ansmant I, Schweizer D, et al. P-body formation is a consequence, not the cause, of RNA-mediated gene silencing. *Mol Cell Biol.* 2007 Jun;27(11):3970-81. doi: 10.1128/MCB.00128-07.
- Fabian MR, Sonenberg N, Filipowicz W. Regulation of mRNA translation and stability by microRNAs. *Annu Rev Biochem.* 2010;79:351-79. doi: 10.1146/annurev-biochem-060308-103103.
- Fagerberg L, Hallström BM, Oksvold P, et al. Analysis of the human tissue-specific expression by genome-wide integration of transcriptomics and antibody-based proteomics. *Mol Cell Proteomics.* 2014 Feb;13(2):397-406. doi: 10.1074/mcp.M113.035600.
- Farina M, Vieira LE, Buttari B, et al. The Nrf2 Pathway in Ischemic Stroke: A Review. *Molecules.* 2021 Aug 18;26(16):5001. doi: 10.3390/molecules26165001.
- Feigin VL, Brainin M, Norrving B, et al. World Stroke Organization (WSO): Global Stroke Fact Sheet 2022. *Int J Stroke.* 2022 Jan;17(1):18-29. doi: 10.1177/17474930211065917. Erratum in: *Int J Stroke.* 2022 Apr;17(4):478.
- Feigin VL, Stark BA, Johnson CO, et al. Global, regional, and national burden of stroke and its risk factors, 1990-2019: a systematic analysis for the Global Burden of Disease Study 2019. *Lancet Neurol.* 2021 Oct;20(10):795-820. doi: 10.1016/S1474-4422(21)00252-0.
- Feng B, Hu P, Lu SJ, et al. Increased argonaute 2 expression in gliomas and its association with tumor progression and poor prognosis. *Asian Pac J Cancer Prev.* 2014;15(9):4079-83. doi: 10.7314/apjcp.2014.15.9.4079.
- Ferreira R, Bernardino L. Nanotechnology for intracellular delivery and targeting, In: *Nanoengineered Biomaterials for Advanced Drug Delivery*, Elsevier 2020, pp 683-696, ISBN9780081029855. <https://doi.org/10.1016/B978-0-08-102985-5.00027-9>.
- Ferreira R, Fonseca MC, Santos T, et al. Retinoic acid-loaded polymeric nanoparticles enhance vascular regulation of neural stem cell survival and differentiation after ischaemia. *Nanoscale.* 2016 Apr 21;8(15):8126-37. doi: 10.1039/c5nr09077f.
- Ferreira R, Napoli J, Enver T, et al. Advances and challenges in retinoid delivery systems in regenerative and therapeutic medicine. *Nat Commun.* 2020 Aug 26;11(1):4265. doi: 10.1038/s41467-020-18042-2.

Ferreira R, Santos T, Amar A, et al. Argonaute-2 promotes miR-18a entry in human brain endothelial cells. *J Am Heart Assoc.* 2014 May 16;3(3):e000968. doi: 10.1161/JAHA.114.000968.

Ferreira R, Santos T, Amar A, et al. MicroRNA-18a improves human cerebral arteriovenous malformation endothelial cell function. *Stroke.* 2014 Jan;45(1):293-7. doi: 10.1161/STROKEAHA.113.003578.

Ferreira R, Santos T, Cortes L, et al. Neuropeptide Y inhibits interleukin-1 beta-induced microglia motility. *J Neurochem.* 2012 Jan;120(1):93-105. doi: 10.1111/j.1471-4159.2011.07541.x.

Ferreira R, Santos T, Viegas M, et al. Neuropeptide Y inhibits interleukin-1 β -induced phagocytosis by microglial cells. *J Neuroinflammation.* 2011 Dec 2;8:169. doi: 10.1186/1742-2094-8-169.

Ferreira R, Xapelli S, Santos T, et al. Neuropeptide Y modulation of interleukin-1 β (IL-1 β)-induced nitric oxide production in microglia. *J Biol Chem.* 2010 Dec 31;285(53):41921-34. doi: 10.1074/jbc.M110.164020.

Filková M, Jüngel A, Gay RE, et al. MicroRNAs in rheumatoid arthritis: potential role in diagnosis and therapy. *BioDrugs.* 2012 Jun 1;26(3):131-41. doi: 10.2165/11631480-000000000-00000.

Fiorella PD, Napoli JL. Microsomal retinoic acid metabolism. Effects of cellular retinoic acid-binding protein (type I) and C18-hydroxylation as an initial step. *J Biol Chem.* 1994 Apr 8;269(14):10538-44.

Fluri F, Schuhmann MK, Kleinschnitz C. Animal models of ischemic stroke and their application in clinical research. *Drug Des Devel Ther.* 2015 Jul 2;9:3445-54. doi: 10.2147/DDDT.S56071.

Foley CP, Rubin DG, Santillan A, et al. Intra-arterial delivery of AAV vectors to the mouse brain after mannitol mediated blood brain barrier disruption. *J Control Release.* 2014 Dec 28;196:71-78. doi: 10.1016/j.jconrel.2014.09.018. Epub 2014 Sep 28. PMID: 25270115; PMCID: PMC4268109.

Förstermann U, Closs EI, Pollock JS, et al. Nitric oxide synthase isozymes. Characterization, purification, molecular cloning, and functions. *Hypertension.* 1994 Jun;23(6 Pt 2):1121-31. doi: 10.1161/01.hyp.23.6.1121.

Förstermann U, Münzel T. Endothelial nitric oxide synthase in vascular disease: from marvel to menace. *Circulation.* 2006 Apr 4;113(13):1708-14. doi: 10.1161/CIRCULATIONAHA.105.602532.

Frank F, Hauver J, Sonenberg N, et al. Arabidopsis Argonaute MID domains use their nucleotide specificity loop to sort small RNAs. *EMBO J.* 2012 Aug 29;31(17):3588-95. doi: 10.1038/emboj.2012.204.

- Franklin K and Paxinos G. The mouse brain in stereotaxic coordinates. 6th ed. Academic Press. 1997.
- Fredericks WR, Rapoport SI. Reversible osmotic opening of the blood-brain barrier in mice. *Stroke*. 1988 Feb;19(2):266-8. doi: 10.1161/01.str.19.2.266.
- Fukuta T, Asai T, Yanagida Y, et al. Combination therapy with liposomal neuroprotectants and tissue plasminogen activator for treatment of ischemic stroke. *FASEB J*. 2017 May;31(5):1879-1890. doi: 10.1096/fj.201601209R.
- Fulton D, Gratton JP, McCabe TJ, et al. Regulation of endothelium-derived nitric oxide production by the protein kinase Akt. *Nature*. 1999 Jun 10;399(6736):597-601. doi: 10.1038/21218. Erratum in: *Nature* 1999 Aug 19;400(6746):792.
- Gallego I, Villate-Beitia I, Saenz-Del-Burgo L, et al. Therapeutic Opportunities and Delivery Strategies for Brain Revascularization in Stroke, Neurodegeneration, and Aging. *Pharmacol Rev*. 2022 Apr;74(2):439-461. doi: 10.1124/pharmrev.121.000418.
- Garbuzova-Davis S, Saporta S, Sanberg PR. Implications of blood-brain barrier disruption in ALS. *Amyotroph Lateral Scler*. 2008 Dec;9(6):375-6. doi: 10.1080/17482960802160990.
- Garnett A, Ploeg J, Markle-Reid M, et al. Factors impacting the access and use of formal health and social services by caregivers of stroke survivors: an interpretive description study. *BMC Health Serv Res*. 2022 Apr 1;22(1):433. doi: 10.1186/s12913-022-07804-x.
- Gasche Y, Copin JC, Sugawara T, et al. Matrix metalloproteinase inhibition prevents oxidative stress-associated blood-brain barrier disruption after transient focal cerebral ischemia. *J Cereb Blood Flow Metab*. 2001 Dec;21(12):1393-400. doi: 10.1097/00004647-200112000-00003.
- Geekiyana H, Rayatpisheh S, Wohlschlegel JA, et al. Extracellular microRNAs in human circulation are associated with miRISC complexes that are accessible to anti-AGO2 antibody and can bind target mimic oligonucleotides. *Proc Natl Acad Sci U S A*. 2020 Sep 29;117(39):24213-24223. doi: 10.1073/pnas.2008323117.
- Germain P, Iyer J, Zechel C, et al. Co-regulator recruitment and the mechanism of retinoic acid receptor synergy. *Nature*. 2002 Jan 10;415(6868):187-92. doi: 10.1038/415187a.
- Ghozy S, Reda A, Varney J, et al. Neuroprotection in Acute Ischemic Stroke: A Battle Against the Biology of Nature. *Front Neurol*. 2022 May 31;13:870141. doi: 10.3389/fneur.2022.870141.
- Ghyselinck NB, Dupé V, Dierich A, et al. Role of the retinoic acid receptor beta (RARbeta) during mouse development. *Int J Dev Biol*. 1997 Jun;41(3):425-47.

Giannotta M, Trani M, Dejana E. VE-cadherin and endothelial adherens junctions: active guardians of vascular integrity. *Dev Cell*. 2013 Sep 16;26(5):441-54. doi: 10.1016/j.devcel.2013.08.020.

Giorgi C, Cogoni C, Catalanotto C. From transcription to translation: new insights in the structure and function of Argonaute protein. *Biomol Concepts*. 2012 Dec;3(6):545-59. doi: 10.1515/bmc-2012-0024.

Girouard H, Iadecola C. Neurovascular coupling in the normal brain and in hypertension, stroke, and Alzheimer disease. *J Appl Physiol* (1985). 2006 Jan;100(1):328-35. doi: 10.1152/jappphysiol.00966.2005.

Global Health Estimates 2019. Accessed on 10 October 2022. <https://www.who.int/data/gho/data/themes/mortality-and-global-health-estimates>.

Gomez CR. Editorial: Time is brain! *J Stroke Cerebrovasc Dis*. 1993;3(1):1-2. doi: 10.1016/S1052-3057(10)80125-9.

Gómez-Casati ME, Murtie JC, Rio C, et al. Nonneuronal cells regulate synapse formation in the vestibular sensory epithelium via erbB-dependent BDNF expression. *Proc Natl Acad Sci U S A*. 2010 Sep 28;107(39):17005-10. doi: 10.1073/pnas.1008938107.

Gonzales-Portillo GS, Sanberg PR, Franzblau M, et al. Mannitol-enhanced delivery of stem cells and their growth factors across the blood-brain barrier. *Cell Transplant*. 2014;23(4-5):531-9. doi: 10.3727/096368914X678337.

González D, Herrera B, Beltrán A, et al. Nitric oxide disrupts VE-cadherin complex in murine microvascular endothelial cells. *Biochem Biophys Res Commun*. 2003 Apr 25;304(1):113-8. doi: 10.1016/s0006-291x(03)00546-1.

Gopinathan G, Milagre C, Pearce OM, et al. Interleukin-6 Stimulates Defective Angiogenesis. *Cancer Res*. 2015 Aug 1;75(15):3098-107. doi: 10.1158/0008-5472.CAN-15-1227.

Goyal M, Menon BK, van Zwam WH, et al. Endovascular thrombectomy after large-vessel ischaemic stroke: a meta-analysis of individual patient data from five randomised trials. *Lancet*. 2016 Apr 23;387(10029):1723-31. doi: 10.1016/S0140-6736(16)00163-X.

Grayston A, Zhang Y, Garcia-Gabilondo M, et al. Endovascular administration of magnetized nanocarriers targeting brain delivery after stroke. *J Cereb Blood Flow Metab*. 2022 Feb;42(2):237-252. doi: 10.1177/0271678X211028816.

Green AR, Shuaib A. Therapeutic strategies for the treatment of stroke. *Drug Discov Today*. 2006 Aug;11(15-16):681-93. doi: 10.1016/j.drudis.2006.06.001.

- Gu C, Rodriguez ER, Reimert DV, et al. Neuropilin-1 conveys semaphorin and VEGF signaling during neural and cardiovascular development. *Dev Cell*. 2003 Jul;5(1):45-57. doi: 10.1016/s1534-5807(03)00169-2.
- Gu Y, Dee CM, Shen J. Interaction of free radicals, matrix metalloproteinases and caveolin-1 impacts blood-brain barrier permeability. *Front Biosci (Schol Ed)*. 2011 Jun 1;3(4):1216-31. doi: 10.2741/222.
- Guo L, Huang Y, Wan R, et al. Increased Blood Retinol Levels Are Associated With a Reduced Risk of TIA or Stroke in an Adult Population: Lifestyle Factors- and CVDs-Stratified Analysis. *Front Cardiovasc Med*. 2021 Nov 16;8:744611. doi: 10.3389/fcvm.2021.744611.
- Guo Z, Geller DA. microRNA and human inducible nitric oxide synthase. *Vitam Horm*. 2014;96:19-27. doi: 10.1016/B978-0-12-800254-4.00002-7.
- Hale A, Lee C, Annis S, et al. An Argonaute 2 switch regulates circulating miR-210 to coordinate hypoxic adaptation across cells. *Biochim Biophys Acta*. 2014 Nov;1843(11):2528-42. doi: 10.1016/j.bbamcr.2014.06.012.
- Hankey GJ, Blacker DJ. Is it a stroke? *BMJ*. 2015 Jan 15;350:h56. doi: 10.1136/bmj.h56.
- Hankey GJ. Stroke. *Lancet*. 2017 Feb 11;389(10069):641-654. doi: 10.1016/S0140-6736(16)30962-X.
- Hao R, Sun B, Yang L, et al. RVG29-modified microRNA-loaded nanoparticles improve ischemic brain injury by nasal delivery. *Drug Deliv*. 2020 Dec;27(1):772-781. doi: 10.1080/10717544.2020.1760960.
- Harrison EH. Mechanisms involved in the intestinal absorption of dietary vitamin A and provitamin A carotenoids. *Biochim Biophys Acta*. 2012 Jan;1821(1):70-7. doi: 10.1016/j.bbaliip.2011.06.002.
- Hartsock A, Nelson WJ. Adherens and tight junctions: structure, function and connections to the actin cytoskeleton. *Biochim Biophys Acta*. 2008 Mar;1778(3):660-9. doi: 10.1016/j.bbamem.2007.07.012.
- Haskell H, Natarajan M, Hecker TP, et al. Focal adhesion kinase is expressed in the angiogenic blood vessels of malignant astrocytic tumors in vivo and promotes capillary tube formation of brain microvascular endothelial cells. *Clin Cancer Res*. 2003 Jun;9(6):2157-65.
- Hattori MA, Takesue K, Kato Y, et al. Expression of endothelial nitric oxide synthase in the porcine oocyte and its possible function. *Mol Cell Biochem*. 2001 Mar;219(1-2):121-6. doi: 10.1023/a:1010830507846.

Hauptmann J, Schraivogel D, Bruckmann A, et al. Biochemical isolation of Argonaute protein complexes by Ago-APP. *Proc Natl Acad Sci U S A*. 2015 Sep 22;112(38):11841-5. doi: 10.1073/pnas.1506116112.

Hawkins RD, Son H, Arancio O. Nitric oxide as a retrograde messenger during long-term potentiation in hippocampus. *Prog Brain Res*. 1998;118:155-72. doi: 10.1016/S0079-6123(08)63206-9.

Hayashi T, Noshita N, Sugawara T, et al. Temporal profile of angiogenesis and expression of related genes in the brain after ischemia. *J Cereb Blood Flow Metab*. 2003 Feb;23(2):166-80. doi: 10.1097/01.WCB.0000041283.53351.CB.

He J, Liu J, Huang Y, et al. Oxidative Stress, Inflammation, and Autophagy: Potential Targets of Mesenchymal Stem Cells-Based Therapies in Ischemic Stroke. *Front Neurosci*. 2021 Feb 26;15:641157. doi: 10.3389/fnins.2021.641157.

Hébert M, Lesept F, Vivien D, et al. The story of an exceptional serine protease, tissue-type plasminogen activator (tPA). *Rev Neurol (Paris)*. 2016 Mar;172(3):186-97. doi: 10.1016/j.neurol.2015.10.002.

Hecht N, He J, Kremenetskaia I, et al. Cerebral hemodynamic reserve and vascular remodeling in C57/BL6 mice are influenced by age. *Stroke*. 2012 Nov;43(11):3052-62. doi: 10.1161/STROKEAHA.112.653204.

Hemmerich K, Suschek CV, Lerzynski G, et al. iNOS activity is essential for endothelial stress gene expression protecting against oxidative damage. *J Appl Physiol (1985)*. 2003 Nov;95(5):1937-46. doi: 10.1152/jappphysiol.00419.2003.

Hersh DS, Wadajkar AS, Roberts N, et al. Evolving Drug Delivery Strategies to Overcome the Blood Brain Barrier. *Curr Pharm Des*. 2016;22(9):1177-1193. doi: 10.2174/1381612822666151221150733.

Herson PS, Traystman RJ. Animal models of stroke: translational potential at present and in 2050. *Future Neurol*. 2014 Sep;9(5):541-551. doi: 10.2217/fnl.14.44.

Hertz L. Bioenergetics of cerebral ischemia: a cellular perspective. *Neuropharmacology*. 2008 Sep;55(3):289-309. doi: 10.1016/j.neuropharm.2008.05.023.

Hicks AU, Hewlett K, Windle V, et al. Enriched environment enhances transplanted subventricular zone stem cell migration and functional recovery after stroke. *Neuroscience*. 2007 Apr 25;146(1):31-40. doi: 10.1016/j.neuroscience.2007.01.020.

Höck J, Meister G. The Argonaute protein family. *Genome Biol*. 2008;9(2):210. doi: 10.1186/gb-2008-9-2-210.

Holloway PM, Gavins FN. Modeling Ischemic Stroke In Vitro: Status Quo and Future Perspectives. *Stroke*. 2016 Feb;47(2):561-9. doi: 10.1161/STROKEAHA.115.011932.

Hoogland IC, Houbolt C, van Westerloo DJ, et al. Systemic inflammation and microglial activation: systematic review of animal experiments. *J Neuroinflammation*. 2015 Jun 6;12:114. doi: 10.1186/s12974-015-0332-6.

Horman SR, Janas MM, Litterst C, et al. Akt-mediated phosphorylation of argonaute 2 downregulates cleavage and upregulates translational repression of MicroRNA targets. *Mol Cell*. 2013 May 9;50(3):356-67. doi: 10.1016/j.molcel.2013.03.015.

Howells DW, Porritt MJ, Rewell SS, et al. Different strokes for different folks: the rich diversity of animal models of focal cerebral ischemia. *J Cereb Blood Flow Metab*. 2010 Aug;30(8):1412-31. doi: 10.1038/jcbfm.2010.66.

Hsia EY, Goodson ML, Zou JX, et al. Nuclear receptor coregulators as a new paradigm for therapeutic targeting. *Adv Drug Deliv Rev*. 2010 Oct 30;62(13):1227-37. doi: 10.1016/j.addr.2010.09.016.

Hu X, Pan J, Li Y, et al. Extracellular vesicles from adipose-derived stem cells promote microglia M2 polarization and neurological recovery in a mouse model of transient middle cerebral artery occlusion. *Stem Cell Res Ther*. 2022 Jan 20;13(1):21. doi: 10.1186/s13287-021-02668-0.

Huang V, Li LC. Demystifying the nuclear function of Argonaute proteins. *RNA Biol*. 2014;11(1):18-24. doi: 10.4161/rna.27604.

Hutvagner G, Simard MJ. Argonaute proteins: key players in RNA silencing. *Nat Rev Mol Cell Biol*. 2008 Jan;9(1):22-32. doi: 10.1038/nrm2321.

Hynes RO. Integrins: bidirectional, allosteric signaling machines. *Cell*. 2002 Sep 20;110(6):673-87. doi: 10.1016/s0092-8674(02)00971-6.

Iannucci J, Rao HV, Grammas P. High Glucose and Hypoxia-Mediated Damage to Human Brain Microvessel Endothelial Cells Induces an Altered, Pro-Inflammatory Phenotype in BV-2 Microglia *In vitro*. *Cell Mol Neurobiol*. 2022 May;42(4):985-996. doi: 10.1007/s10571-020-00987-z.

Iosue I, Quaranta R, Masciarelli S, et al. Argonaute 2 sustains the gene expression program driving human monocytic differentiation of acute myeloid leukemia cells. *Cell Death Dis*. 2013 Nov 21;4(11):e926. doi: 10.1038/cddis.2013.452.

Issitt T, Bosseboeuf E, De Winter N, et al. Neuropilin-1 Controls Endothelial Homeostasis by Regulating Mitochondrial Function and Iron-Dependent Oxidative Stress. *iScience*. 2019 Jan 25;11:205-223. doi: 10.1016/j.isci.2018.12.005.

Jacobs S, Lie DC, DeCicco KL, et al. Retinoic acid is required early during adult neurogenesis in the dentate gyrus. *Proc Natl Acad Sci U S A*. 2006 Mar 7;103(10):3902-7. doi: 10.1073/pnas.0511294103.

Jaffrey SR, Snyder SH. The biotin switch method for the detection of S-nitrosylated proteins. *Sci STKE*. 2001 Jun 12;2001(86):pl1. doi: 10.1126/stke.2001.86.pl1.

Jakymiw A, Ikeda K, Fritzler MJ, et al. Autoimmune targeting of key components of RNA interference. *Arthritis Res Ther*. 2006;8(4):R87. doi: 10.1186/ar1959.

Jakymiw A, Lian S, Eystathioy T, et al. Disruption of GW bodies impairs mammalian RNA interference. *Nat Cell Biol*. 2005 Dec;7(12):1267-74. doi: 10.1038/ncb1334. Epub 2005 Nov 13. Erratum in: *Nat Cell Biol*. 2006 Jan;8(1):100.

Jang M, Gould E, Xu J, et al. Oligodendrocytes regulate presynaptic properties and neurotransmission through BDNF signaling in the mouse brainstem. *Elife*. 2019 Apr 18;8:e42156. doi: 10.7554/eLife.42156.

Jetten AM. Retinoid-related orphan receptors (RORs): critical roles in development, immunity, circadian rhythm, and cellular metabolism. *Nucl Recept Signal*. 2009;7:e003. doi: 10.1621/nrs.07003.

Jiang CT, Wu WF, Deng YH, et al. Modulators of microglia activation and polarization in ischemic stroke (Review). *Mol Med Rep*. 2020 May;21(5):2006-2018. doi: 10.3892/mmr.2020.11003.

Jiang W, Guo M, Gong M, et al. Vitamin A bio-modulates apoptosis via the mitochondrial pathway after hypoxic-ischemic brain damage. *Mol Brain*. 2018 Mar 13;11(1):14. doi: 10.1186/s13041-018-0360-0.

Jiao H, Wang Z, Liu Y, et al. Specific role of tight junction proteins claudin-5, occludin, and ZO-1 of the blood-brain barrier in a focal cerebral ischemic insult. *J Mol Neurosci*. 2011 Jun;44(2):130-9. doi: 10.1007/s12031-011-9496-4.

Jiao S, Miller PJ, Lapchak PA. Enhanced delivery of [125I]glial cell line-derived neurotrophic factor to the rat CNS following osmotic blood-brain barrier modification. *Neurosci Lett*. 1996 Dec 20;220(3):187-90. doi: 10.1016/s0304-3940(96)13265-1.

Jickling GC, Sharp FR. Improving the translation of animal ischemic stroke studies to humans. *Metab Brain Dis*. 2015 Apr;30(2):461-7. doi: 10.1007/s11011-014-9499-2.

Jin P, Zarnescu DC, Ceman S, et al. Biochemical and genetic interaction between the fragile X mental retardation protein and the microRNA pathway. *Nat Neurosci*. 2004 Feb;7(2):113-7. doi: 10.1038/nn1174.

- Jin RC, Loscalzo J. Vascular Nitric Oxide: Formation and Function. *J Blood Med.* 2010 Aug 1;2010(1):147-162. doi: 10.2147/JBM.S7000.
- Jonas S, Izaurralde E. Towards a molecular understanding of microRNA-mediated gene silencing. *Nat Rev Genet.* 2015 Jul;16(7):421-33. doi: 10.1038/nrg3965.
- Ju R, Wen Y, Gou R, et al. The experimental therapy on brain ischemia by improvement of local angiogenesis with tissue engineering in the mouse. *Cell Transplant.* 2014;23 Suppl 1:S83-95. doi: 10.3727/096368914X684998.
- Kahles T, Luedike P, Endres M, et al. NADPH oxidase plays a central role in blood-brain barrier damage in experimental stroke. *Stroke.* 2007 Nov;38(11):3000-6. doi: 10.1161/STROKEAHA.107.489765.
- Kanai M, Raz A, Goodman DS. Retinol-binding protein: the transport protein for vitamin A in human plasma. *J Clin Invest.* 1968 Sep;47(9):2025-44. doi: 10.1172/JCI105889.
- Kang JB, Shah MA, Park DJ, et al. Retinoic acid regulates the ubiquitin-proteasome system in a middle cerebral artery occlusion animal model. *Lab Anim Res.* 2022 May 13;38(1):13. doi: 10.1186/s42826-022-00123-6.
- Karatas H, Aktas Y, GURSOY-OZDEMIR Y, et al. A nanomedicine transports a peptide caspase-3 inhibitor across the blood-brain barrier and provides neuroprotection. *J Neurosci.* 2009 Nov 4;29(44):13761-9. doi: 10.1523/JNEUROSCI.4246-09.2009.
- Kawaguchi R, Yu J, Honda J, et al. A membrane receptor for retinol binding protein mediates cellular uptake of vitamin A. *Science.* 2007 Feb 9;315(5813):820-5. doi: 10.1126/science.1136244.
- Kawasaki T, Kitsukawa T, Bekku Y, et al. A requirement for neuropilin-1 in embryonic vessel formation. *Development.* 1999 Nov;126(21):4895-902. doi: 10.1242/dev.126.21.4895.
- Khanna A, Kahle KT, Walcott BP, et al. Disruption of ion homeostasis in the neurogliovascular unit underlies the pathogenesis of ischemic cerebral edema. *Transl Stroke Res.* 2014 Feb;5(1):3-16. doi: 10.1007/s12975-013-0307-9.
- Kim E, Sheng M. PDZ domain proteins of synapses. *Nat Rev Neurosci.* 2004 Oct;5(10):771-81. doi: 10.1038/nrn1517.
- Kim JY, Park J, Lee JE, et al. NOX Inhibitors - A Promising Avenue for Ischemic Stroke. *Exp Neurobiol.* 2017 Aug;26(4):195-205. doi: 10.5607/en.2017.26.4.195.
- Kitsukawa T, Shimizu M, Sanbo M, et al. Neuropilin-semaphorin III/D-mediated chemorepulsive signals play a crucial role in peripheral nerve projection in mice. *Neuron.* 1997 Nov;19(5):995-1005. doi: 10.1016/s0896-6273(00)80392-x.

Kleindorfer DO, Towfighi A, Chaturvedi S, et al. 2021 Guideline for the Prevention of Stroke in Patients With Stroke and Transient Ischemic Attack: A Guideline From the American Heart Association/American Stroke Association. *Stroke*. 2021 Jul;52(7):e364-e467. doi: 10.1161/STR.0000000000000375. Erratum in: *Stroke*. 2021 Jul;52(7):e483-e484.

Kleinschnitz C, Grund H, Wingler K, et al. Post-stroke inhibition of induced NADPH oxidase type 4 prevents oxidative stress and neurodegeneration. *PLoS Biol*. 2010 Sep 21;8(9):e1000479. doi: 10.1371/journal.pbio.1000479.

Knecht T, Story J, Liu J, et al. Adjunctive Therapy Approaches for Ischemic Stroke: Innovations to Expand Time Window of Treatment. *Int J Mol Sci*. 2017 Dec 19;18(12):2756. doi: 10.3390/ijms18122756.

Koester SK, Dougherty JD. A Proposed Role for Interactions between Argonautes, miRISC, and RNA Binding Proteins in the Regulation of Local Translation in Neurons and Glia. *J Neurosci*. 2022 Apr 20;42(16):3291-3301. doi: 10.1523/JNEUROSCI.2391-21.2022.

Koizumi J, Yoshida Y, Nakazawa T, et al. Experimental studies of ischemic brain edema, I: a new experimental model of cerebral embolism in rats in which recirculation can be introduced in the ischemic area. *Jpn J Stroke*. 1986; 8:1-8.

Kolb B, Morshead C, Gonzalez C, et al. Growth factor-stimulated generation of new cortical tissue and functional recovery after stroke damage to the motor cortex of rats. *J Cereb Blood Flow Metab*. 2007 May;27(5):983-97. doi: 10.1038/sj.jcbfm.9600402.

Kong L, Wang Y, Wang XJ, et al. Retinoic acid ameliorates blood-brain barrier disruption following ischemic stroke in rats. *Pharmacol Res*. 2015 Sep;99:125-36. doi: 10.1016/j.phrs.2015.05.014.

Kortekaas R, Leenders KL, van Oostrom JC, et al. Blood-brain barrier dysfunction in parkinsonian midbrain in vivo. *Ann Neurol*. 2005 Feb;57(2):176-9. doi: 10.1002/ana.20369.

Krupinski J, Kaluza J, Kumar P, et al. Role of angiogenesis in patients with cerebral ischemic stroke. *Stroke*. 1994 Sep;25(9):1794-8. doi: 10.1161/01.str.25.9.1794.

Ku JM, Taher M, Chin KY, et al. Characterisation of a mouse cerebral microvascular endothelial cell line (bEnd.3) after oxygen glucose deprivation and reoxygenation. *Clin Exp Pharmacol Physiol*. 2016 Aug;43(8):777-86. doi: 10.1111/1440-1681.12587.

Kulkarni M, Ozgur S, Stoecklin G. On track with P-bodies. *Biochem Soc Trans*. 2010 Feb;38(Pt 1):242-51. doi: 10.1042/BST0380242.

Kuriakose D, Xiao Z. Pathophysiology and Treatment of Stroke: Present Status and Future Perspectives. *Int J Mol Sci*. 2020 Oct 15;21(20):7609. doi: 10.3390/ijms21207609.

- Kusakabe TG, Takimoto N, Jin M, et al. Evolution and the origin of the visual retinoid cycle in vertebrates. *Philos Trans R Soc Lond B Biol Sci.* 2009 Oct 12;364(1531):2897-910. doi: 10.1098/rstb.2009.0043.
- Kwak PB, Tomari Y. The N domain of Argonaute drives duplex unwinding during RISC assembly. *Nat Struct Mol Biol.* 2012 Jan 10;19(2):145-51. doi: 10.1038/nsmb.2232.
- Lane MA, Bailey SJ. Role of retinoid signalling in the adult brain. *Prog Neurobiol.* 2005 Mar;75(4):275-93. doi: 10.1016/j.pneurobio.2005.03.002.
- Lapi D, Colantuoni A. Remodeling of Cerebral Microcirculation after Ischemia-Reperfusion. *J Vasc Res.* 2015;52(1):22-31. doi: 10.1159/000381096.
- Lapi D, Vagnani S, Sapio D, et al. Effects of bone marrow mesenchymal stem cells (BM-MSCs) on rat pial microvascular remodeling after transient middle cerebral artery occlusion. *Front Cell Neurosci.* 2015 Aug 25;9:329. doi: 10.3389/fncel.2015.00329.
- Lee H, Pienaar IS. Disruption of the blood-brain barrier in Parkinson's disease: curse or route to a cure? *Front Biosci (Landmark Ed).* 2014 Jan 1;19(2):272-80. doi: 10.2741/4206.
- Lee J, Kim YS, Choi DH, et al. Transglutaminase 2 induces nuclear factor-kappaB activation via a novel pathway in BV-2 microglia. *J Biol Chem.* 2004 Dec 17;279(51):53725-35. doi: 10.1074/jbc.M407627200.
- Lee SC, Lee KY, Kim YJ, et al. Serum VEGF levels in acute ischaemic strokes are correlated with long-term prognosis. *Eur J Neurol.* 2010 Jan;17(1):45-51. doi: 10.1111/j.1468-1331.2009.02731.x.
- Lee SS, Min H, Ha JY, et al. Dysregulation of the miRNA biogenesis components DICER1, DROSHA, DGCR8 and AGO2 in clear cell renal cell carcinoma in both a Korean cohort and the cancer genome atlas kidney clear cell carcinoma cohort. *Oncol Lett.* 2019 Oct;18(4):4337-4345. doi: 10.3892/ol.2019.10759.
- Leonov G, Shah K, Yee D, et al. Suppression of AGO2 by miR-132 as a determinant of miRNA-mediated silencing in human primary endothelial cells. *Int J Biochem Cell Biol.* 2015 Dec;69:75-84. doi: 10.1016/j.biocel.2015.10.006.
- Leung AK, Calabrese JM, Sharp PA. Quantitative analysis of Argonaute protein reveals microRNA-dependent localization to stress granules. *Proc Natl Acad Sci U S A.* 2006 Nov 28;103(48):18125-30. doi: 10.1073/pnas.0608845103.
- Leung AK, Sharp PA. Quantifying Argonaute proteins in and out of GW/P-bodies: implications in microRNA activities. *Adv Exp Med Biol.* 2013;768:165-82. doi: 10.1007/978-1-4614-5107-5_10.

Li AD, Tong L, Xu N, et al. miR-124 regulates cerebromicrovascular function in APP/PS1 transgenic mice via C1ql3. *Brain Res Bull.* 2019 Nov;153:214-222. doi: 10.1016/j.brainresbull.2019.09.002.

Li J, Zheng M, Shimoni O, et al. Development of Novel Therapeutics Targeting the Blood-Brain Barrier: From Barrier to Carrier. *Adv Sci (Weinh).* 2021 Aug;8(16):e2101090. doi: 10.1002/advs.202101090.

Li L, Yu C, Gao H, et al. Argonaute proteins: potential biomarkers for human colon cancer. *BMC Cancer.* 2010 Feb 10;10:38. doi: 10.1186/1471-2407-10-38.

Li L, Zhou J, Han L, et al. The Specific Role of Reactive Astrocytes in Stroke. *Front Cell Neurosci.* 2022 Mar 7;16:850866. doi: 10.3389/fncel.2022.850866.

Li W, Chen Z, Chin I, et al. The Role of VE-cadherin in Blood-brain Barrier Integrity Under Central Nervous System Pathological Conditions. *Curr Neuropharmacol.* 2018;16(9):1375-1384. doi: 10.2174/1570159X16666180222164809.

Li Y, Song YH, Li F, et al. MicroRNA-221 regulates high glucose-induced endothelial dysfunction. *Biochem Biophys Res Commun.* 2009 Mar 27;381(1):81-3. doi: 10.1016/j.bbrc.2009.02.013.

Li Y, Zhang J. Animal models of stroke. *Animal Model Exp Med.* 2021 Sep 15;4(3):204-219. doi: 10.1002/ame2.12179.

Lian L, Zhang Y, Liu L, et al. Neuroinflammation in Ischemic Stroke: Focus on MicroRNA-mediated Polarization of Microglia. *Front Mol Neurosci.* 2021 Jan 7;13:612439. doi: 10.3389/fnmol.2020.612439.

Liang C, Guo S, Yang L. Effects of all-trans retinoic acid on VEGF and HIF-1 α expression in glioma cells under normoxia and hypoxia and its anti-angiogenic effect in an intracerebral glioma model. *Mol Med Rep.* 2014 Nov;10(5):2713-9. doi: 10.3892/mmr.2014.2543.

Liao J, Li Y, Luo Y, et al. Recent Advances in Targeted Nanotherapies for Ischemic Stroke. *Mol Pharm.* 2022 Sep 5;19(9):3026-3041. doi: 10.1021/acs.molpharmaceut.2c00383.

Liao LX, Zhao MB, Dong X, et al. TDB protects vascular endothelial cells against oxygen-glucose deprivation/reperfusion-induced injury by targeting miR-34a to increase Bcl-2 expression. *Sci Rep.* 2016 Nov 25;6:37959. doi: 10.1038/srep37959.

Liao WL, Wang HF, Tsai HC, et al. Retinoid signaling competence and RARbeta-mediated gene regulation in the developing mammalian telencephalon. *Dev Dyn.* 2005 Apr;232(4):887-900. doi: 10.1002/dvdy.20281.

- Liddelow SA, Guttenplan KA, Clarke LE, et al. Neurotoxic reactive astrocytes are induced by activated microglia. *Nature*. 2017 Jan 26;541(7638):481-487. doi: 10.1038/nature21029.
- Liew FY, Xu D, Brint EK, et al. Negative regulation of toll-like receptor-mediated immune responses. *Nat Rev Immunol*. 2005 Jun;5(6):446-58. doi: 10.1038/nri1630.
- Lin X, Li N, Tang H. Recent Advances in Nanomaterials for Diagnosis, Treatments, and Neurorestoration in Ischemic Stroke. *Front Cell Neurosci*. 2022 Jun 28;16:885190. doi: 10.3389/fncel.2022.885190.
- Lingen MW, Polverini PJ, Bouck NP. Inhibition of squamous cell carcinoma angiogenesis by direct interaction of retinoic acid with endothelial cells. *Lab Invest*. 1996 Feb;74(2):476-83.
- Liu J, Carmell MA, Rivas FV, et al. Argonaute2 is the catalytic engine of mammalian RNAi. *Science*. 2004 Sep 3;305(5689):1437-41. doi: 10.1126/science.1102513.
- Liu J, Rivas FV, Wohlschlegel J, et al. A role for the P-body component GW182 in microRNA function. *Nat Cell Biol*. 2005b Dec;7(12):1261-6. doi: 10.1038/ncb1333. Epub 2005 Nov 13. Erratum in: *Nat Cell Biol*. 2006 Jan;8(1):100.
- Liu J, Valencia-Sanchez MA, Hannon GJ, et al. MicroRNA-dependent localization of targeted mRNAs to mammalian P-bodies. *Nat Cell Biol*. 2005a Jul;7(7):719-23. doi: 10.1038/ncb1274.
- Liu J, Wang Y, Akamatsu Y, et al. Vascular remodeling after ischemic stroke: mechanisms and therapeutic potentials. *Prog Neurobiol*. 2014 Apr;115:138-56. doi: 10.1016/j.pneurobio.2013.11.004.
- Liu M, Dziennis S, Hurn PD, et al. Mechanisms of gender-linked ischemic brain injury. *Restor Neurol Neurosci*. 2009;27(3):163-79. doi: 10.3233/RNN-2009-0467.
- Liu R, Yuan H, Yuan F, et al. Neuroprotection targeting ischemic penumbra and beyond for the treatment of ischemic stroke. *Neurol Res*. 2012 May;34(4):331-7. doi: 10.1179/1743132812Y.0000000020.
- Liu S, Levine SR, Winn HR. Targeting ischemic penumbra: part I - from pathophysiology to therapeutic strategy. *J Exp Stroke Transl Med*. 2010 Mar 15;3(1):47-55. doi: 10.6030/1939-067x-3.1.47.
- Liu WY, Wang ZB, Wang Y, et al. Increasing the Permeability of the Blood-brain Barrier in Three Different Models *in vivo*. *CNS Neurosci Ther*. 2015 Jul;21(7):568-74. doi: 10.1111/cns.12405.
- Liu X, Meng X, Peng X, et al. Impaired AGO2/miR-185-3p/NRP1 axis promotes colorectal cancer metastasis. *Cell Death Dis*. 2021 Apr 12;12(4):390. doi: 10.1038/s41419-021-03672-1.

Lochhead JJ, Thorne RG. Intranasal delivery of biologics to the central nervous system. *Adv Drug Deliv Rev.* 2012 May 15;64(7):614-28. doi: 10.1016/j.addr.2011.11.002.

Longa EZ, Weinstein PR, Carlson S, et al. Reversible middle cerebral artery occlusion without craniectomy in rats. *Stroke.* 1989 Jan;20(1):84-91. doi: 10.1161/01.str.20.1.84.

Lopez-Orozco J, Pare JM, Holme AL, et al. Functional analyses of phosphorylation events in human Argonaute 2. *RNA.* 2015 Dec;21(12):2030-8. doi: 10.1261/rna.053207.115.

Lyden P, Buchan A, Boltze J, et al; STAIR XI Consortium*. Top Priorities for Cerebroprotective Studies-A Paradigm Shift: Report From STAIR XI. *Stroke.* 2021 Aug;52(9):3063-3071. doi: 10.1161/STROKEAHA.121.034947.

Ma JB, Ye K, Patel DJ. Structural basis for overhang-specific small interfering RNA recognition by the PAZ domain. *Nature.* 2004 May 20;429(6989):318-322. doi: 10.1038/nature02519.

Machado-Pereira M, Santos T, Bernardino L, et al. Vascular inter-regulation of inflammation: molecular and cellular targets for CNS therapy. *J Neurochem.* 2017 Mar;140(5):692-702. doi: 10.1111/jnc.13914.

Machado-Pereira M, Santos T, Ferreira L, et al. Anti-Inflammatory Strategy for M2 Microglial Polarization Using Retinoic Acid-Loaded Nanoparticles. *Mediators Inflamm.* 2017;2017:6742427. doi: 10.1155/2017/6742427.

Machado-Pereira M, Santos T, Ferreira L, et al. Challenging the great vascular wall: Can we envision a simple yet comprehensive therapy for stroke? *J Tissue Eng Regen Med.* 2018 Jan;12(1):e350-e354. doi: 10.1002/term.2427.

Machado-Pereira M, Santos T, Ferreira L, et al. Intravenous administration of retinoic acid-loaded polymeric nanoparticles prevents ischemic injury in the immature brain. *Neurosci Lett.* 2018 Apr 23;673:116-121. doi: 10.1016/j.neulet.2018.02.066.

Machado-Pereira M, Saraiva C, Bernardino L, et al. Argonaute-2 protects the neurovascular unit from damage caused by systemic inflammation. *J Neuroinflammation.* 2022 Jan 6;19(1):11. doi: 10.1186/s12974-021-02324-7.

MacVicar BA, Newman EA. Astrocyte regulation of blood flow in the brain. *Cold Spring Harb Perspect Biol.* 2015 Mar 27;7(5):a020388. doi: 10.1101/cshperspect.a020388.

Maden M. Retinoic acid in the development, regeneration and maintenance of the nervous system. *Nat Rev Neurosci.* 2007 Oct;8(10):755-65. doi: 10.1038/nrn2212.

Maden M. Retinoid signalling in the development of the central nervous system. *Nat Rev Neurosci.* 2002 Nov;3(11):843-53. doi: 10.1038/nrn963.

- Mages B, Fuhs T, Aleithe S, et al. The Cytoskeletal Elements MAP2 and NF-L Show Substantial Alterations in Different Stroke Models While Elevated Serum Levels Highlight Especially MAP2 as a Sensitive Biomarker in Stroke Patients. *Mol Neurobiol*. 2021 Aug;58(8):4051-4069. doi: 10.1007/s12035-021-02372-3.
- Maia J, Santos T, Aday S, et al. Controlling the neuronal differentiation of stem cells by the intracellular delivery of retinoic acid-loaded nanoparticles. *ACS Nano*. 2011 Jan 25;5(1):97-106. doi: 10.1021/nn101724r.
- Maksoud MJE, Tellios V, Xiang YY, et al. Nitric oxide signaling inhibits microglia proliferation by activation of protein kinase-G. *Nitric Oxide*. 2020 Jan 1;94:125-134. doi: 10.1016/j.niox.2019.11.005.
- Malhotra K, Liebeskind D. Collaterals in ischemic stroke. *Brain Hemorrhages*. 2020 Jan; 1(1),6-12. doi: <https://doi.org/10.1016/j.hebst.2019.12.003>.
- Mannerström B, Paananen RO, Abu-Shahba AG, et al. Extracellular small non-coding RNA contaminants in fetal bovine serum and serum-free media. *Sci Rep*. 2019 Apr 2;9(1):5538. doi: 10.1038/s41598-019-41772-3. Erratum in: *Sci Rep*. 2020 Jan 23;10(1):1369.
- Martinez NJ, Gregory RI. Argonaute2 expression is post-transcriptionally coupled to microRNA abundance. *RNA*. 2013 May;19(5):605-12. doi: 10.1261/rna.036434.112.
- Marto JP, Borbinha C, Calado S, et al. The Stroke Chronometer-A New Strategy to Reduce Door-to-Needle Time. *J Stroke Cerebrovasc Dis*. 2016 Sep;25(9):2305-7. doi: 10.1016/j.jstrokecerebrovasdis.2016.05.023.
- Masciarelli S, Quaranta R, Iosue I, et al. A small-molecule targeting the microRNA binding domain of argonaute 2 improves the retinoic acid differentiation response of the acute promyelocytic leukemia cell line NB4. *ACS Chem Biol*. 2014 Aug 15;9(8):1674-9. doi: 10.1021/cb500286b.
- Masiá S, Alvarez S, de Lera AR, et al. Rapid, nongenomic actions of retinoic acid on phosphatidylinositol-3-kinase signaling pathway mediated by the retinoic acid receptor. *Mol Endocrinol*. 2007 Oct;21(10):2391-402. doi: 10.1210/me.2007-0062.
- Mauch DH, Nägler K, Schumacher S, et al. CNS synaptogenesis promoted by glia-derived cholesterol. *Science*. 2001 Nov 9;294(5545):1354-7. doi: 10.1126/science.294.5545.1354.
- Mazumder A, Bose M, Chakraborty A, et al. A transient reversal of miRNA-mediated repression controls macrophage activation. *EMBO Rep*. 2013 Nov;14(11):1008-16. doi: 10.1038/embor.2013.149.

- McCabe C, Arroja MM, Reid E, et al. Animal models of ischaemic stroke and characterisation of the ischaemic penumbra. *Neuropharmacology*. 2018 May 15;134(Pt B):169-177. doi: 10.1016/j.neuropharm.2017.09.022.
- McColl B, Howells D, Rothwell N, et al. Modeling risk factors and confounding effects in stroke. In: Dirnagl U, editor. *Rodent Models of Stroke. Neuromethods, Vol 120*. New York, NY: Humana Press (2016). p. 93–122. doi: 10.1007/978-1-4939-5620-3_9.
- McConnell HL, Kersch CN, Woltjer RL, et al. The Translational Significance of the Neurovascular Unit. *J Biol Chem*. 2017 Jan 20;292(3):762-770. doi: 10.1074/jbc.R116.760215.
- McKenzie AJ, Hoshino D, Hong NH, et al. KRAS-MEK Signaling Controls Ago2 Sorting into Exosomes. *Cell Rep*. 2016 May 3;15(5):978-987. doi: 10.1016/j.celrep.2016.03.085.
- Meister G, Landthaler M, Patkaniowska A, et al. Human Argonaute2 mediates RNA cleavage targeted by miRNAs and siRNAs. *Mol Cell*. 2004 Jul 23;15(2):185-97. doi: 10.1016/j.molcel.2004.07.007.
- Meister G. Argonaute proteins: functional insights and emerging roles. *Nat Rev Genet*. 2013 Jul;14(7):447-59. doi: 10.1038/nrg3462.
- Merali Z, Huang K, Mikulis D, et al. Evolution of blood-brain-barrier permeability after acute ischemic stroke. *PLoS One*. 2017 Feb 16;12(2):e0171558. doi: 10.1371/journal.pone.0171558.
- Michalik L, Wahli W. Guiding ligands to nuclear receptors. *Cell*. 2007 May 18;129(4):649-51. doi: 10.1016/j.cell.2007.05.001.
- Misner DL, Jacobs S, Shimizu Y, et al. Vitamin A deprivation results in reversible loss of hippocampal long-term synaptic plasticity. *Proc Natl Acad Sci U S A*. 2001 Sep 25;98(20):11714-9. doi: 10.1073/pnas.191369798.
- Mizee MR, Wooldrik D, Lakeman KA, et al. Retinoic acid induces blood-brain barrier development. *J Neurosci*. 2013 Jan 23;33(4):1660-71. doi: 10.1523/JNEUROSCI.1338-12.2013.
- Modzelewski AJ, Holmes RJ, Hilz S, et al. AGO4 regulates entry into meiosis and influences silencing of sex chromosomes in the male mouse germline. *Dev Cell*. 2012 Aug 14;23(2):251-64. doi: 10.1016/j.devcel.2012.07.003.
- Mohammadi MT, Shid Moosavi SM, Dehghani GA. Contribution of nitric oxide synthase (NOS) activity in blood-brain barrier disruption and edema after acute ischemia/reperfusion in aortic coarctation-induced hypertensive rats. *Iran Biomed J*. 2011;15(1-2):22-30.

- Mohammadi MT. Overproduction of nitric oxide intensifies brain infarction and cerebrovascular damage through reduction of claudin-5 and ZO-1 expression in striatum of ischemic brain. *Pathol Res Pract*. 2016 Nov;212(11):959-964. doi: 10.1016/j.prp.2015.12.009.
- Mohan KM, Wolfe CD, Rudd AG, et al. Risk and cumulative risk of stroke recurrence: a systematic review and meta-analysis. *Stroke*. 2011 May;42(5):1489-94. doi: 10.1161/STROKEAHA.110.602615.
- Morancho A, García-Bonilla L, Barceló V, et al. A new method for focal transient cerebral ischaemia by distal compression of the middle cerebral artery. *Neuropathol Appl Neurobiol*. 2012 Oct;38(6):617-27. doi: 10.1111/j.1365-2990.2012.01252.x.
- Morita S, Horii T, Kimura M, et al. One Argonaute family member, Eif2c2 (Ago2), is essential for development and appears not to be involved in DNA methylation. *Genomics*. 2007 Jun;89(6):687-96. doi: 10.1016/j.ygeno.2007.01.004.
- Mosconi MG, Paciaroni M. Treatments in Ischemic Stroke: Current and Future. *Eur Neurol*. 2022 Aug 2:1-18. doi: 10.1159/000525822.
- Muldoon LL, Nilaver G, Kroll RA, et al. Comparison of intracerebral inoculation and osmotic blood-brain barrier disruption for delivery of adenovirus, herpesvirus, and iron oxide particles to normal rat brain. *Am J Pathol*. 1995 Dec;147(6):1840-51.
- Müller M, Fazi F, Ciaudo C. Argonaute Proteins: From Structure to Function in Development and Pathological Cell Fate Determination. *Front Cell Dev Biol*. 2020 Jan 22;7:360. doi: 10.3389/fcell.2019.00360.
- Musuka TD, Wilton SB, Traboulsi M, et al. Diagnosis and management of acute ischemic stroke: speed is critical. *CMAJ*. 2015 Sep 8;187(12):887-93. doi: 10.1503/cmaj.140355.
- Musumeci T, Bonaccorso A, Puglisi G. Epilepsy Disease and Nose-to-Brain Delivery of Polymeric Nanoparticles: An Overview. *Pharmaceutics*. 2019 Mar 13;11(3):118. doi: 10.3390/pharmaceutics11030118.
- Nakanishi K. Anatomy of four human Argonaute proteins. *Nucleic Acids Res*. 2022 Jun 23;50(12):6618-38. doi: 10.1093/nar/gkac519.
- Napoli JL. Retinol metabolism in LLC-PK1 Cells. Characterization of retinoic acid synthesis by an established mammalian cell line. *J Biol Chem*. 1986 Oct 15;261(29):13592-7.
- National Institute of Neurological Disorders and Stroke rt-PA Stroke Study Group. Tissue plasminogen activator for acute ischemic stroke. *N Engl J Med*. 1997 Dec 14;333(24):1581-7. doi: 10.1056/NEJM199512143332401.

Navarro-Sobrino M, Rosell A, Hernández-Guillamon M, et al. A large screening of angiogenesis biomarkers and their association with neurological outcome after ischemic stroke. *Atherosclerosis*. 2011 May;216(1):205-11. doi: 10.1016/j.atherosclerosis.2011.01.030.

Niederreither K, Subbarayan V, Dollé P, et al. Embryonic retinoic acid synthesis is essential for early mouse post-implantation development. *Nat Genet*. 1999 Apr;21(4):444-8. doi: 10.1038/7788.

Nikoletopoulou V, Markaki M, Palikaras K, et al. Crosstalk between apoptosis, necrosis and autophagy. *Biochim Biophys Acta*. 2013 Dec;1833(12):3448-3459. doi: 10.1016/j.bbamcr.2013.06.001.

Ninchoji T, Love DT, Smith RO, et al. eNOS-induced vascular barrier disruption in retinopathy by c-Src activation and tyrosine phosphorylation of VE-cadherin. *Elife*. 2021 Apr 28;10:e64944. doi: 10.7554/eLife.64944.

NINDS t-PA Stroke Study Group. Intracerebral hemorrhage after intravenous t-PA therapy for ischemic stroke. *Stroke*. 1997 Nov;28(11):2109-18. doi: 10.1161/01.str.28.11.2109.

Nogueira RG, Jadhav AP, Haussen DC, et al. DAWN Trial Investigators. Thrombectomy 6 to 24 Hours after Stroke with a Mismatch between Deficit and Infarct. *N Engl J Med*. 2018 Jan 4;378(1):11-21. doi: 10.1056/NEJMoa1706442.

Noh H, Jeon J, Seo H. Systemic injection of LPS induces region-specific neuroinflammation and mitochondrial dysfunction in normal mouse brain. *Neurochem Int*. 2014 Apr;69:35-40. doi: 10.1016/j.neuint.2014.02.008.

Norford D, Koo JS, Gray T, et al. Expression of nitric oxide synthase isoforms in normal human tracheobronchial epithelial cells *in vitro*: dependence on retinoic acid and the state of differentiation. *Exp Lung Res*. 1998 May-Jun;24(3):355-66. doi: 10.3109/01902149809041540.

Nozohouri S, Sifat AE, Vaidya B, et al. Novel approaches for the delivery of therapeutics in ischemic stroke. *Drug Discov Today*. 2020 Mar;25(3):535-551. doi: 10.1016/j.drudis.2020.01.007.

O'Neill LA, Sheedy FJ, McCoy CE. MicroRNAs: the fine-tuners of Toll-like receptor signalling. *Nat Rev Immunol*. 2011 Mar;11(3):163-75. doi: 10.1038/nri2957.

Owolabi MO, Thrift AG, Mahal A, et al. Stroke Experts Collaboration Group. Primary stroke prevention worldwide: translating evidence into action. *Lancet Public Health*. 2022 Jan;7(1):e74-e85. doi: 10.1016/S2468-2667(21)00230-9. Erratum in: *Lancet Public Health*. 2022 Jan;7(1):e14.

Paik J, Vogel S, Piantedosi R, et al. 9-cis-retinoids: biosynthesis of 9-cis-retinoic acid. *Biochemistry*. 2000 Jul 11;39(27):8073-84. doi: 10.1021/bi992152g.

- Paik S, Somvanshi RK, Kumar U. Somatostatin-Mediated Changes in Microtubule-Associated Proteins and Retinoic Acid-Induced Neurite Outgrowth in SH-SY5Y Cells. *J Mol Neurosci*. 2019 May;68(1):120-134. doi: 10.1007/s12031-019-01291-2.
- Panuganti KK, Tadi P, Lui F. Transient Ischemic Attack. 2022 Jul 18. In: StatPearls [Internet]. Treasure Island (FL): StatPearls Publishing; 2022 Jan–.
- Paolicelli RC, Bolasco G, Pagani F, et al. Synaptic pruning by microglia is necessary for normal brain development. *Science*. 2011 Sep 9;333(6048):1456-8. doi: 10.1126/science.1202529.
- Papachristou DJ, Korpetinou A, Giannopoulou E, et al. Expression of the ribonucleases Drossha, Dicer, and Ago2 in colorectal carcinomas. *Virchows Arch*. 2011 Oct;459(4):431-40. doi: 10.1007/s00428-011-1119-5.
- Pardridge WM. Blood-brain barrier drug targeting: the future of brain drug development. *Mol Interv*. 2003 Mar;3(2):90-105, 51. doi: 10.1124/mi.3.2.90.
- Pardridge WM. The blood-brain barrier: bottleneck in brain drug development. *NeuroRx*. 2005 Jan;2(1):3-14. doi: 10.1602/neurorx.2.1.3.
- Parés X, Farrés J, Kedishvili N, et al. Medium- and short-chain dehydrogenase/reductase gene and protein families: Medium-chain and short-chain dehydrogenases/reductases in retinoid metabolism. *Cell Mol Life Sci*. 2008 Dec;65(24):3936-49. doi: 10.1007/s00018-008-8591-3.
- Parisi C, Giorgi C, Batassa EM, et al. Ago1 and Ago2 differentially affect cell proliferation, motility and apoptosis when overexpressed in SH-SY5Y neuroblastoma cells. *FEBS Lett*. 2011 Oct 3;585(19):2965-71. doi: 10.1016/j.febslet.2011.08.003.
- Park MS, Phan HD, Busch F, et al. Human Argonaute3 has slicer activity. *Nucleic Acids Res*. 2017 Nov 16;45(20):11867-11877. doi: 10.1093/nar/gkx916.
- Park MS, Sim G, Kehling AC, et al. Human Argonaute2 and Argonaute3 are catalytically activated by different lengths of guide RNA. *Proc Natl Acad Sci U S A*. 2020 Nov 17;117(46):28576-28578. doi: 10.1073/pnas.2015026117.
- Parker JS, Roe SM, Barford D. Crystal structure of a PIWI protein suggests mechanisms for siRNA recognition and slicer activity. *EMBO J*. 2004 Dec 8;23(24):4727-37. doi: 10.1038/sj.emboj.7600488.
- Paschaki M, Lin SC, Wong RL, et al. Retinoic acid-dependent signaling pathways and lineage events in the developing mouse spinal cord. *PLoS One*. 2012;7(3):e32447. doi: 10.1371/journal.pone.0032447.

Patel MM, Goyal BR, Bhadada SV, et al. Getting into the brain: approaches to enhance brain drug delivery. *CNS Drugs*. 2009;23(1):35-58. doi: 10.2165/0023210-200923010-00003.

Patil S, Rossi R, Jabrah D, et al. Detection, Diagnosis and Treatment of Acute Ischemic Stroke: Current and Future Perspectives. *Front Med Technol*. 2022 Jun 24;4:748949. doi: 10.3389/fmedt.2022.748949.

Perego C, Fumagalli S, De Simoni MG. Temporal pattern of expression and colocalization of microglia/macrophage phenotype markers following brain ischemic injury in mice. *J Neuroinflammation*. 2011 Dec 10;8:174. doi: 10.1186/1742-2094-8-174.

Peters L, Meister G. Argonaute proteins: mediators of RNA silencing. *Mol Cell*. 2007 Jun 8;26(5):611-23. doi: 10.1016/j.molcel.2007.05.001.

Philips T, Rothstein JD. Oligodendroglia: metabolic supporters of neurons. *J Clin Invest*. 2017 Sep 1;127(9):3271-3280. doi: 10.1172/JCI90610.

Pignataro G. Emerging Role of microRNAs in Stroke Protection Elicited by Remote Postconditioning. *Front Neurol*. 2021 Oct 21;12:748709. doi: 10.3389/fneur.2021.748709.

Piroozian F, Bagheri Varkiyani H, Koolivand M, et al. The impact of variations in transcription of DICER and AGO2 on exacerbation of childhood B-cell lineage acute lymphoblastic leukaemia. *Int J Exp Pathol*. 2019 Jun;100(3):184-191. doi: 10.1111/iep.12316.

Plane JM, Whitney JT, Schallert T, et al. Retinoic acid and environmental enrichment alter subventricular zone and striatal neurogenesis after stroke. *Exp Neurol*. 2008 Nov;214(1):125-34. doi: 10.1016/j.expneurol.2008.08.006.

Poliseno L, Tuccoli A, Mariani L, et al. MicroRNAs modulate the angiogenic properties of HUVECs. *Blood*. 2006 Nov 1;108(9):3068-71. doi: 10.1182/blood-2006-01-012369.

Pound P, Ram R. Are researchers moving away from animal models as a result of poor clinical translation in the field of stroke? An analysis of opinion papers. *BMJ Open Sci*. 2020 Feb 24;4(1):e100041. doi: 10.1136/bmjos-2019-100041.

Profaci CP, Munji RN, Pulido RS, et al. The blood-brain barrier in health and disease: Important unanswered questions. *J Exp Med*. 2020 Apr 6;217(4):e20190062. doi: 10.1084/jem.20190062.

Prud'homme GJ, Glinka Y, Lichner Z, et al. Neuropilin-1 is a receptor for extracellular miRNA and AGO2/miRNA complexes and mediates the internalization of miRNAs that modulate cell function. *Oncotarget*. 2016 Oct 18;7(42):68057-68071. doi: 10.18632/oncotarget.10929.

Pun PB, Lu J, Moochhala S. Involvement of ROS in BBB dysfunction. *Free Radic Res*. 2009 Apr;43(4):348-64. doi: 10.1080/10715760902751902.

Qi HH, Ongusaha PP, Myllyharju J, et al. Prolyl 4-hydroxylation regulates Argonaute 2 stability. *Nature*. 2008 Sep 18;455(7211):421-4. doi: 10.1038/nature07186.

Qin C, Yang S, Chu YH, et al. Signaling pathways involved in ischemic stroke: molecular mechanisms and therapeutic interventions. *Signal Transduct Target Ther*. 2022 Jul 6;7(1):215. doi: 10.1038/s41392-022-01064-1. Erratum in: *Signal Transduct Target Ther*. 2022 Aug 12;7(1):278.

Quévillon Huberdeau M, Zeitler DM, Hauptmann J, et al. Phosphorylation of Argonaute proteins affects mRNA binding and is essential for microRNA-guided gene silencing *in vivo*. *EMBO J*. 2017 Jul 14;36(14):2088-2106. doi: 10.15252/embj.201696386.

Radermacher KA, Wingler K, Langhauser F, et al. Neuroprotection after stroke by targeting NOX4 as a source of oxidative stress. *Antioxid Redox Signal*. 2013 Apr 20;18(12):1418-27. doi: 10.1089/ars.2012.4797.

Rami A, Kögel D. Apoptosis meets autophagy-like cell death in the ischemic penumbra: Two sides of the same coin? *Autophagy*. 2008 May;4(4):422-6. doi: 10.4161/auto.5778.

Ranjan R, Lee YG, Karpurapu M, et al. p47phox and reactive oxygen species production modulate expression of microRNA-451 in macrophages. *Free Radic Res*. 2015 Jan;49(1):25-34. doi: 10.3109/10715762.2014.974037.

Rapoport SI. Advances in osmotic opening of the blood-brain barrier to enhance CNS chemotherapy. *Expert Opin Investig Drugs*. 2001 Oct;10(10):1809-18. doi: 10.1517/13543784.10.10.1809.

Rathore SS, Hinn AR, Cooper LS, et al. Characterization of incident stroke signs and symptoms: findings from the atherosclerosis risk in communities study. *Stroke*. 2002 Nov;33(11):2718-21. doi: 10.1161/01.str.0000035286.87503.31.

Reglero-Real N, Pérez-Gutiérrez L, Yoshimura A, et al. Autophagy modulates endothelial junctions to restrain neutrophil diapedesis during inflammation. *Immunity*. 2021 Sep 14;54(9):1989-2004.e9. doi: 10.1016/j.immuni.2021.07.012.

Rigby H, Gubitza G, Phillips S. A systematic review of caregiver burden following stroke. *Int J Stroke*. 2009 Aug;4(4):285-92. doi: 10.1111/j.1747-4949.2009.00289.x.

Robertson CS, Gopinath SP, Valadka AB, et al. Variants of the endothelial nitric oxide gene and cerebral blood flow after severe traumatic brain injury. *J Neurotrauma*. 2011 May;28(5):727-37. doi: 10.1089/neu.2010.1476.

Roger VL, Go AS, Lloyd-Jones DM, et al. American Heart Association Statistics Committee and Stroke Statistics Subcommittee. Heart disease and stroke statistics--2011 update: a report from

the American Heart Association. *Circulation*. 2011 Feb 1;123(4):e18-e209. doi: 10.1161/CIR.0b013e3182009701. Erratum in: *Circulation*. 2011 Feb 15;123(6):e240. Erratum in: *Circulation*. 2011 Oct 18;124(16):e426.

Rosenholm JM, Mamaeva V, Sahlgren C, et al. Nanoparticles in targeted cancer therapy: mesoporous silica nanoparticles entering preclinical development stage. *Nanomedicine (Lond)*. 2012 Jan;7(1):111-20. doi: 10.2217/nnm.11.166.

Rothwell PM, Giles MF, Chandratheva A, et al. Early use of Existing Preventive Strategies for Stroke (EXPRESS) study. Effect of urgent treatment of transient ischaemic attack and minor stroke on early recurrent stroke (EXPRESS study): a prospective population-based sequential comparison. *Lancet*. 2007 Oct 20;370(9596):1432-42. doi: 10.1016/S0140-6736(07)61448-2. Erratum in: *Lancet*. 2008 Feb 2;371(9610):386.

Rouf SA, Moo-Young M, Chisti Y. Tissue-type plasminogen activator: characteristics, applications and production technology. *Biotechnol Adv*. 1996;14(3):239-66. doi: 10.1016/0734-9750(96)00019-5.

Rüdel S, Wang Y, Lenobel R, et al. Phosphorylation of human Argonaute proteins affects small RNA binding. *Nucleic Acids Res*. 2011 Mar;39(6):2330-43. doi: 10.1093/nar/gkq1032.

Rust R. Insights into the dual role of angiogenesis following stroke. *J Cereb Blood Flow Metab*. 2020 Jun;40(6):1167-1171. doi: 10.1177/0271678X20906815.

Rybak A, Fuchs H, Hadian K, et al. The let-7 target gene mouse lin-41 is a stem cell specific E3 ubiquitin ligase for the miRNA pathway protein Ago2. *Nat Cell Biol*. 2009 Dec;11(12):1411-20. doi: 10.1038/ncb1987.

Sacco RL, Kasner SE, Broderick JP, et al. American Heart Association Stroke Council, Council on Cardiovascular Surgery and Anesthesia; Council on Cardiovascular Radiology and Intervention; Council on Cardiovascular and Stroke Nursing; Council on Epidemiology and Prevention; Council on Peripheral Vascular Disease; Council on Nutrition, Physical Activity and Metabolism. An updated definition of stroke for the 21st century: a statement for healthcare professionals from the American Heart Association/American Stroke Association. *Stroke*. 2013 Jul;44(7):2064-89. doi: 10.1161/STR.0b013e318296aeca. Erratum in: *Stroke*. 2019 Aug;50(8):e239.

Saeed A, Dullaart RPF, Schreuder TCMA, et al. Disturbed Vitamin A Metabolism in Non-Alcoholic Fatty Liver Disease (NAFLD). *Nutrients*. 2017 Dec 29;10(1):29. doi: 10.3390/nu10010029.

Sainson RC, Johnston DA, Chu HC, et al. TNF primes endothelial cells for angiogenic sprouting by inducing a tip cell phenotype. *Blood*. 2008 May 15;111(10):4997-5007. doi: 10.1182/blood-2007-08-108597.

- Saito A, Sugawara A, Uruno A, et al. All-trans retinoic acid induces in vitro angiogenesis via retinoic acid receptor: possible involvement of paracrine effects of endogenous vascular endothelial growth factor signaling. *Endocrinology*. 2007 Mar;148(3):1412-23. doi: 10.1210/en.2006-0900.
- Sánchez C, Díaz-Nido J, Avila J. Phosphorylation of microtubule-associated protein 2 (MAP2) and its relevance for the regulation of the neuronal cytoskeleton function. *Prog Neurobiol*. 2000 Jun;61(2):133-68. doi: 10.1016/s0301-0082(99)00046-5.
- Sanchez-Covarrubias L, Slosky LM, Thompson BJ, et al. Transporters at CNS barrier sites: obstacles or opportunities for drug delivery? *Curr Pharm Des*. 2014;20(10):1422-49. doi: 10.2174/13816128113199990463.
- Sand M, Skrygan M, Georgas D, et al. Expression levels of the microRNA maturing microprocessor complex component DGCR8 and the RNA-induced silencing complex (RISC) components argonaute-1, argonaute-2, PACT, TARBP1, and TARBP2 in epithelial skin cancer. *Mol Carcinog*. 2012 Nov;51(11):916-22. doi: 10.1002/mc.20861.
- Santos T, Ferreira R, Maia J, et al. Polymeric nanoparticles to control the differentiation of neural stem cells in the subventricular zone of the brain. *ACS Nano*. 2012 Dec 21;6(12):10463-74. doi: 10.1021/nn304541h.
- Saraiva C, Barata-Antunes S, Santos T, et al. Histamine modulates hippocampal inflammation and neurogenesis in adult mice. *Sci Rep*. 2019 Jun 10;9(1):8384. doi: 10.1038/s41598-019-44816-w.
- Saraiva C, Praça C, Ferreira R, et al. Nanoparticle-mediated brain drug delivery: Overcoming blood-brain barrier to treat neurodegenerative diseases. *J Control Release*. 2016 Aug 10;235:34-47. doi: 10.1016/j.jconrel.2016.05.044.
- Sargento-Freitas J, Aday S, Nunes C, et al. Endothelial progenitor cells enhance blood-brain barrier permeability in subacute stroke. *Neurology*. 2018 Jan 9;90(2):e127-e134. doi: 10.1212/WNL.0000000000004801.
- Sasaki T, Shiohama A, Minoshima S, et al. Identification of eight members of the Argonaute family in the human genome. *Genomics*. 2003 Sep;82(3):323-30. doi: 10.1016/s0888-7543(03)00129-0.
- Sato Y, Falcone-Juengert J, Tominaga T, et al. Remodeling of the Neurovascular Unit Following Cerebral Ischemia and Hemorrhage. *Cells*. 2022 Sept;11(18), 2823.
- Savchenko VL, Nikonenko IR, Skibo GG, et al. Distribution of microglia and astrocytes in different regions of the normal adult rat brain. *Neurophysiology*. 1997 Nov;29, 343-351. doi: 10.1007/BF02463354.

Schaaf MB, Houbaert D, Meçe O, et al. Autophagy in endothelial cells and tumor angiogenesis. *Cell Death Differ.* 2019 Mar;26(4):665-679. doi: 10.1038/s41418-019-0287-8.

Schirle NT, MacRae IJ. The crystal structure of human Argonaute2. *Science.* 2012 May 25;336(6084):1037-40. doi: 10.1126/science.1221551.

Schmitter D, Filkowski J, Sewer A, et al. Effects of Dicer and Argonaute down-regulation on mRNA levels in human HEK293 cells. *Nucleic Acids Res.* 2006;34(17):4801-15. doi: 10.1093/nar/gkl646.

Schreibelt G, Kooij G, Reijerkerk A, et al. Reactive oxygen species alter brain endothelial tight junction dynamics via RhoA, PI3 kinase, and PKB signaling. *FASEB J.* 2007 Nov;21(13):3666-76. doi: 10.1096/fj.07-8329com.

Schroeder U, Sommerfeld P, Ulrich S, et al. Nanoparticle technology for delivery of drugs across the blood-brain barrier. *J Pharm Sci.* 1998 Nov;87(11):1305-7. doi: 10.1021/js980084y.

Seet BT, Dikic I, Zhou MM, et al. Reading protein modifications with interaction domains. *Nat Rev Mol Cell Biol.* 2006 Jul;7(7):473-83. doi: 10.1038/nrm1960.

Seo JH, Maki T, Maeda M, et al. Oligodendrocyte precursor cells support blood-brain barrier integrity via TGF- β signaling. *PLoS One.* 2014 Jul 31;9(7):e103174. doi: 10.1371/journal.pone.0103174.

Seyedaghamiri F, Salimi L, Ghaznavi D, et al. Exosomes-based therapy of stroke, an emerging approach toward recovery. *Cell Commun Signal.* 2022 Jul 22;20(1):110. doi: 10.1186/s12964-022-00919-y.

Shao H, Yang L, Wang L, et al. MicroRNA-34a protects myocardial cells against ischemia-reperfusion injury through inhibiting autophagy via regulating TNF α expression. *Biochem Cell Biol.* 2018 Jun;96(3):349-354. doi: 10.1139/bcb-2016-0158.

Shen J, Xia W, Khotskaya YB, et al. EGFR modulates microRNA maturation in response to hypoxia through phosphorylation of AGO2. *Nature.* 2013 May 16;497(7449):383-7. doi: 10.1038/nature12080.

Shi Y, Zhang L, Pu H, et al. Rapid endothelial cytoskeletal reorganization enables early blood-brain barrier disruption and long-term ischaemic reperfusion brain injury. *Nat Commun.* 2016 Jan 27;7:10523. doi: 10.1038/ncomms10523. Erratum in: *Nat Commun.* 2020 Aug 25;11(1):4335.

Shirakami Y, Lee SA, Clugston RD, et al. Hepatic metabolism of retinoids and disease associations. *Biochim Biophys Acta.* 2012 Jan;1821(1):124-36. doi: 10.1016/j.bbali.2011.06.023.

- Shuaib A, Lees KR, Lyden P, et al. SAINT II Trial Investigators. NXY-059 for the treatment of acute ischemic stroke. *N Engl J Med*. 2007 Aug 9;357(6):562-71. doi: 10.1056/NEJMoa070240.
- Sibony M. Autophagy Regulates Expression of Argonaute 2, a Critical Regulator of the MicroRNA Silencing Pathway. 2012.
- Simard JM, Sheth KN, Kimberly WT, et al. Glibenclamide in cerebral ischemia and stroke. *Neurocrit Care*. 2014 Apr;20(2):319-33. doi: 10.1007/s12028-013-9923-1.
- Slavin SA, Leonard A, Grose V, et al. Autophagy inhibitor 3-methyladenine protects against endothelial cell barrier dysfunction in acute lung injury. *Am J Physiol Lung Cell Mol Physiol*. 2018 Mar 1;314(3):L388-L396. doi: 10.1152/ajplung.00555.2016.
- Slevin M, Krupinski J, Slowik A, et al. Serial measurement of vascular endothelial growth factor and transforming growth factor-beta1 in serum of patients with acute ischemic stroke. *Stroke*. 2000 Aug;31(8):1863-70. doi: 10.1161/01.str.31.8.1863.
- Smibert P, Yang JS, Azzam G, et al. Homeostatic control of Argonaute stability by microRNA availability. *Nat Struct Mol Biol*. 2013 Jul;20(7):789-95. doi: 10.1038/nsmb.2606.
- Sommer CJ. Ischemic stroke: experimental models and reality. *Acta Neuropathol*. 2017 Feb;133(2):245-261. doi: 10.1007/s00401-017-1667-0.
- Stamatovic SM, Keep RF, Andjelkovic AV. Brain endothelial cell-cell junctions: how to "open" the blood brain barrier. *Curr Neuropharmacol*. 2008 Sep;6(3):179-92. doi: 10.2174/157015908785777210.
- Statistics Portugal 2021. Accessed on 12 August 2022. https://www.ine.pt/xportal/xmain?xpid=INE&xpgid=ine_destaques&DESTAQUESdest_boui=458515689&DESTAQUESmodo=2.
- Stehlin-Gaon C, Willmann D, Zeyer D, et al. All-trans retinoic acid is a ligand for the orphan nuclear receptor ROR beta. *Nat Struct Biol*. 2003 Oct;10(10):820-5. doi: 10.1038/nsb979.
- Steiner J, Bernstein HG, Biela H, et al. Evidence for a wide extra-astrocytic distribution of S100B in human brain. *BMC Neurosci*. 2007 Jan 2;8:2. doi: 10.1186/1471-2202-8-2.
- Stoll G, Nieswandt B. Thrombo-inflammation in acute ischaemic stroke - implications for treatment. *Nat Rev Neurol*. 2019 Aug;15(8):473-481. doi: 10.1038/s41582-019-0221-1.
- Strbian D, Durukan A, Pitkonen M, et al. The blood-brain barrier is continuously open for several weeks following transient focal cerebral ischemia. *Neuroscience*. 2008 Apr 22;153(1):175-81. doi: 10.1016/j.neuroscience.2008.02.012.

Stroke Progress Review Group. 2001. Accessed on 15 August 2022. <https://www.ninds.nih.gov/stroke-progress-review-group>.

Sun M, Deng B, Zhao X, et al. Isoflurane preconditioning provides neuroprotection against stroke by regulating the expression of the TLR4 signalling pathway to alleviate microglial activation. *Sci Rep*. 2015 Jun 18;5:11445. doi: 10.1038/srep11445.

Sun P, Zhang K, Hassan SH, et al. Endothelium-Targeted Deletion of microRNA-15a/16-1 Promotes Poststroke Angiogenesis and Improves Long-Term Neurological Recovery. *Circ Res*. 2020 Apr 10;126(8):1040-1057. doi: 10.1161/CIRCRESAHA.119.315886.

Sweeney MD, Ayyadurai S, Zlokovic BV. Pericytes of the neurovascular unit: key functions and signaling pathways. *Nat Neurosci*. 2016 May 26;19(6):771-83. doi: 10.1038/nn.4288.

Szuts EZ, Harosi FI. Solubility of retinoids in water. *Arch Biochem Biophys*. 1991 Jun;287(2):297-304. doi: 10.1016/0003-9861(91)90482-x.

Szymborska A, Gerhardt H. Hold Me, but Not Too Tight-Endothelial Cell-Cell Junctions in Angiogenesis. *Cold Spring Harb Perspect Biol*. 2018 Aug 1;10(8):a029223. doi: 10.1101/cshperspect.a029223.

Tafti M, Ghyselinck NB. Functional implication of the vitamin A signaling pathway in the brain. *Arch Neurol*. 2007 Dec;64(12):1706-11. doi: 10.1001/archneur.64.12.1706.

Taganov KD, Boldin MP, Chang KJ, et al. NF-kappaB-dependent induction of microRNA miR-146, an inhibitor targeted to signaling proteins of innate immune responses. *Proc Natl Acad Sci U S A*. 2006 Aug 15;103(33):12481-6. doi: 10.1073/pnas.0605298103.

Takamura R, Watamura N, Nikkuni M, et al. All-trans retinoic acid improved impaired proliferation of neural stem cells and suppressed microglial activation in the hippocampus in an Alzheimer's mouse model. *J Neurosci Res*. 2017 Mar;95(3):897-906. doi: 10.1002/jnr.23843.

Tang Y, Wang X, Li J, et al. Overcoming the Reticuloendothelial System Barrier to Drug Delivery with a "Don't-Eat-Us" Strategy. *ACS Nano*. 2019 Nov 26;13(11):13015-13026. doi: 10.1021/acsnano.9b05679.

Tao C, Zhu Y, Zhang C, et al. Association between tirofiban monotherapy and efficacy and safety in acute ischemic stroke. *BMC Neurol*. 2021 Jun 24;21(1):237. doi: 10.1186/s12883-021-02268-8.

Tao L, Nie Y, Wang G, et al. All-trans retinoic acid reduces endothelin-1 expression and increases endothelial nitric oxide synthase phosphorylation in rabbits with atherosclerosis. *Mol Med Rep*. 2018 Feb;17(2):2619-2625. doi: 10.3892/mmr.2017.8156.

- Taubert H, Greither T, Kaushal D, et al. Expression of the stem cell self-renewal gene Hiwi and risk of tumour-related death in patients with soft-tissue sarcoma. *Oncogene*. 2007 Feb 15;26(7):1098-100. doi: 10.1038/sj.onc.1209880.
- Tawil SE, Muir KW. Thrombolysis and thrombectomy for acute ischaemic stroke. *Clin Med (Lond)*. 2017 Apr;17(2):161-165. doi: 10.7861/clinmedicine.17-2-161.
- Taylor ZV, Khand B, Porgador A, et al. An optimized intracerebroventricular injection of CD4+ T cells into mice. *STAR Protoc*. 2021 Aug 6;2(3):100725. doi: 10.1016/j.xpro.2021.100725.
- Tenreiro MM, Ferreira R, Bernardino L, et al. Cellular response of the blood-brain barrier to injury: Potential biomarkers and therapeutic targets for brain regeneration. *Neurobiol Dis*. 2016 Jul;91:262-73. doi: 10.1016/j.nbd.2016.03.014.
- Thatcher JE, Isoherranen N. The role of CYP26 enzymes in retinoic acid clearance. *Expert Opin Drug Metab Toxicol*. 2009 Aug;5(8):875-86. doi: 10.1517/17425250903032681.
- Thibeault S, Rautureau Y, Oubaha M, et al. S-nitrosylation of beta-catenin by eNOS-derived NO promotes VEGF-induced endothelial cell permeability. *Mol Cell*. 2010 Aug 13;39(3):468-76. doi: 10.1016/j.molcel.2010.07.013.
- Tiebosch IA, Crielaard BJ, Bouts MJ, et al. Combined treatment with recombinant tissue plasminogen activator and dexamethasone phosphate-containing liposomes improves neurological outcome and restricts lesion progression after embolic stroke in rats. *J Neurochem*. 2012 Nov;123 Suppl 2:65-74. doi: 10.1111/j.1471-4159.2012.07945.x.
- Tiedt S, Buchan AM, Dichgans M, et al. The neurovascular unit and systemic biology in stroke - implications for translation and treatment. *Nat Rev Neurol*. 2022 Sep 9. doi: 10.1038/s41582-022-00703-z.
- Tolia NH, Joshua-Tor L. Slicer and the argonautes. *Nat Chem Biol*. 2007 Jan;3(1):36-43. doi: 10.1038/nchembio848.
- Trevelin SC, Shah AM, Lombardi G. Beyond bacterial killing: NADPH oxidase 2 is an immunomodulator. *Immunol Lett*. 2020 May;221:39-48. doi: 10.1016/j.imlet.2020.02.009.
- Unnithan AKA, M Das J, Mehta P. Hemorrhagic Stroke. 2022 May 16. In: *StatPearls* [Internet]. Treasure Island (FL): StatPearls Publishing; 2022 Jan-.
- Vaksman O, Hetland TE, Trope' CG, et al. Argonaute, Dicer, and Drosha are up-regulated along tumor progression in serous ovarian carcinoma. *Hum Pathol*. 2012 Nov;43(11):2062-9. doi: 10.1016/j.humpath.2012.02.016.

Valdmanis PN, Gu S, Schüermann N, et al. Expression determinants of mammalian argonaute proteins in mediating gene silencing. *Nucleic Acids Res.* 2012 Apr;40(8):3704-13. doi: 10.1093/nar/gkr1274.

van der Steen W, van de Graaf RA, Chalos V, et al. MR CLEAN-MED investigators. Safety and efficacy of aspirin, unfractionated heparin, both, or neither during endovascular stroke treatment (MR CLEAN-MED): an open-label, multicentre, randomised controlled trial. *Lancet.* 2022 Mar 12;399(10329):1059-1069. doi: 10.1016/S0140-6736(22)00014-9.

Van Stry M, Oguin TH 3rd, Cheloufi S, et al. Enhanced susceptibility of Ago1/3 double-null mice to influenza A virus infection. *J Virol.* 2012 Apr;86(8):4151-7. doi: 10.1128/JVI.05303-11.

Vanacker P, Lambrou D, Eskandari A, et al. Eligibility and Predictors for Acute Revascularization Procedures in a Stroke Center. *Stroke.* 2016 Jul;47(7):1844-9. doi: 10.1161/STROKEAHA.115.012577.

Vanhoutte PM, Zhao Y, Xu A, et al. Thirty Years of Saying NO: Sources, Fate, Actions, and Misfortunes of the Endothelium-Derived Vasodilator Mediator. *Circ Res.* 2016 Jul 8;119(2):375-96. doi: 10.1161/CIRCRESAHA.116.306531.

Varatharaj A, Galea I. The blood-brain barrier in systemic inflammation. *Brain Behav Immun.* 2017 Feb;60:1-12. doi: 10.1016/j.bbi.2016.03.010.

Veltkamp R, Rajapakse N, Robins G, et al. Transient focal ischemia increases endothelial nitric oxide synthase in cerebral blood vessels. *Stroke.* 2002 Nov;33(11):2704-10. doi: 10.1161/01.str.0000033132.85123.6a.

Vestweber D. VE-cadherin: the major endothelial adhesion molecule controlling cellular junctions and blood vessel formation. *Arterioscler Thromb Vasc Biol.* 2008 Feb;28(2):223-32. doi: 10.1161/ATVBAHA.107.158014.

Veys K, Fan Z, Ghobrial M, et al. Role of the GLUT1 Glucose Transporter in Postnatal CNS Angiogenesis and Blood-Brain Barrier Integrity. *Circ Res.* 2020 Jul 31;127(4):466-482. doi: 10.1161/CIRCRESAHA.119.316463.

Vilhais-Neto GC, Pourquié O. Retinoic acid. *Curr Biol.* 2008 Mar 11;18(5):R191-2. doi: 10.1016/j.cub.2007.12.042. Erratum in: *Curr Biol.* 2008 Apr 8;18(7):550-2.

Virani SS, Alonso A, Benjamin EJ, et al. American Heart Association Council on Epidemiology and Prevention Statistics Committee and Stroke Statistics Subcommittee. Heart Disease and Stroke Statistics-2020 Update: A Report From the American Heart Association. *Circulation.* 2020 Mar 3;141(9):e139-e596. doi: 10.1161/CIR.0000000000000757.

- Vittet D, Buchou T, Schweitzer A, et al. Targeted null-mutation in the vascular endothelial-cadherin gene impairs the organization of vascular-like structures in embryoid bodies. *Proc Natl Acad Sci U S A*. 1997 Jun 10;94(12):6273-8. doi: 10.1073/pnas.94.12.6273.
- Völler D, Linck L, Bruckmann A, et al. Argonaute Family Protein Expression in Normal Tissue and Cancer Entities. *PLoS One*. 2016 Aug 12;11(8):e0161165. doi: 10.1371/journal.pone.0161165.
- Von Bohlen Und Halbach O. Immunohistological markers for staging neurogenesis in adult hippocampus. *Cell Tissue Res*. 2007 Sep;329(3):409-20. doi: 10.1007/s00441-007-0432-4.
- Von Hanwehr R, Smith ML, Siesjö BK. Extra- and intracellular pH during near-complete forebrain ischemia in the rat. *J Neurochem*. 1986 Feb;46(2):331-9. doi: 10.1111/j.1471-4159.1986.tb12973.x.
- Vos EM, Geraedts VJ, van der Lugt A, et al. Systematic Review - Combining Neuroprotection With Reperfusion in Acute Ischemic Stroke. *Front Neurol*. 2022 Mar 17;13:840892. doi: 10.3389/fneur.2022.840892.
- Wald G. The molecular basis of visual excitation. *Nature*. 1968 Aug 24;219(5156):800-7. doi: 10.1038/219800a0.
- Walsh MC, Lee J, Choi Y. Tumor necrosis factor receptor- associated factor 6 (TRAF6) regulation of development, function, and homeostasis of the immune system. *Immunol Rev*. 2015 Jul;266(1):72-92. doi: 10.1111/imr.12302.
- Walton MR, Dragunow I. Is CREB a key to neuronal survival? *Trends Neurosci*. 2000 Feb;23(2):48-53. doi: 10.1016/s0166-2236(99)01500-3.
- Wang D, Zhang Z, O'Loughlin E, et al. Quantitative functions of Argonaute proteins in mammalian development. *Genes Dev*. 2012 Apr 1;26(7):693-704. doi: 10.1101/gad.182758.111.
- Wang F, Cao Y, Ma L, et al. Dysfunction of Cerebrovascular Endothelial Cells: Prelude to Vascular Dementia. *Front Aging Neurosci*. 2018 Nov 16;10:376. doi: 10.3389/fnagi.2018.00376.
- Wang F, Nojima M, Inoue Y, et al. Assessment of MRI Contrast Agent Kinetics via Retro-Orbital Injection in Mice: Comparison with Tail Vein Injection. *PLoS One*. 2015 Jun 10;10(6):e0129326. doi: 10.1371/journal.pone.0129326.
- Wang L, Cheng CK, Yi M, et al. Targeting endothelial dysfunction and inflammation. *J Mol Cell Cardiol*. 2022 Jul;168:58-67. doi: 10.1016/j.yjmcc.2022.04.011.
- Wang L, Dudek SM. Regulation of vascular permeability by sphingosine 1-phosphate. *Microvasc Res*. 2009 Jan;77(1):39-45. doi: 10.1016/j.mvr.2008.09.005.

- Wang L, Rohatgi AP, Wan YY. Retinoic acid and microRNA. *Methods Enzymol.* 2020;637:283-308. doi: 10.1016/bs.mie.2020.02.009.
- Wang L, Xiong X, Zhang L, et al. Neurovascular Unit: A critical role in ischemic stroke. *CNS Neurosci Ther.* 2021 Jan;27(1):7-16. doi: 10.1111/cns.13561.
- Wang Q, Tang XN, Yenari MA. The inflammatory response in stroke. *J Neuroimmunol.* 2007 Mar;184(1-2):53-68. doi: 10.1016/j.jneuroim.2006.11.014.
- Wang T, Liu YP, Wang T, et al. ROS feedback regulates the microRNA-19-targeted inhibition of the p47phox-mediated LPS-induced inflammatory response. *Biochem Biophys Res Commun.* 2017 Aug 5;489(4):361-368. doi: 10.1016/j.bbrc.2017.05.022.
- Wang X, Mulas F, Yi W, et al. OTUB1 inhibits CNS autoimmunity by preventing IFN- γ -induced hyperactivation of astrocytes. *EMBO J.* 2019 May 15;38(10):e100947. doi: 10.15252/embj.2018100947.
- Waninger JJ, Beyett TS, Gadkari VV, et al. Biochemical characterization of the interaction between KRAS and Argonaute 2. *Biochem Biophys Rep.* 2021 Dec 20;29:101191. doi:10.1016/j.bbrep.2021.101191.
- Watanabe T, Okuda Y, Nonoguchi N, et al. Postischemic intraventricular administration of FGF-2 expressing adenoviral vectors improves neurologic outcome and reduces infarct volume after transient focal cerebral ischemia in rats. *J Cereb Blood Flow Metab.* 2004 Nov;24(11):1205-13. doi: 10.1097/01.WCB.0000136525.75839.41.
- Weaver AM, Patton JG. Argonautes in Extracellular Vesicles: Artifact or Selected Cargo? *Cancer Res.* 2020 Feb 1;80(3):379-381. doi: 10.1158/0008-5472.CAN-19-2782.
- Wei W, Ba Z, Gao M, et al. A role for small RNAs in DNA double-strand break repair. *Cell.* 2012 Mar 30;149(1):101-12. doi: 10.1016/j.cell.2012.03.002.
- Welch C, Chen Y, Stallings RL. MicroRNA-34a functions as a potential tumor suppressor by inducing apoptosis in neuroblastoma cells. *Oncogene.* 2007 Jul 26;26(34):5017-22. doi: 10.1038/sj.onc.1210293.
- Wild JR, Staton CA, Chapple K, et al. Neuropilins: expression and roles in the epithelium. *Int J Exp Pathol.* 2012 Apr;93(2):81-103. doi: 10.1111/j.1365-2613.2012.00810.x.
- Williams RM, Shah J, Ng BD, et al. Mesoscale nanoparticles selectively target the renal proximal tubule epithelium. *Nano Lett.* 2015 Apr 8;15(4):2358-64. doi: 10.1021/nl504610d.

- Winter J, Diederichs S. Argonaute proteins regulate microRNA stability: Increased microRNA abundance by Argonaute proteins is due to microRNA stabilization. *RNA Biol.* 2011 Nov-Dec;8(6):1149-57. doi: 10.4161/rna.8.6.17665.
- Woo YS, Lee KH, Lee KT, et al. Postoperative changes of liver enzymes can distinguish between biliary stricture and graft rejection after living donor liver transplantation: A longitudinal study. *Medicine (Baltimore).* 2017 Oct;96(40):e6892. doi: 10.1097/MD.0000000000006892.
- World Stroke Organization Annual Report 2021. Accessed on 12 August 2022. https://www.world-stroke.org/assets/downloads/Annual_Report_2021_online_latest.pdf.
- Worzfeld T, Schwaninger M. Apicobasal polarity of brain endothelial cells. *J Cereb Blood Flow Metab.* 2016 Feb;36(2):340-62. doi: 10.1177/0271678X15608644.
- Wu C, So J, Davis-Dusenbery BN, et al. Hypoxia potentiates microRNA-mediated gene silencing through posttranslational modification of Argonaute2. *Mol Cell Biol.* 2011 Dec;31(23):4760-74. doi: 10.1128/MCB.05776-11.
- Wu F, Liu Z, Zhou L, et al. Systemic immune responses after ischemic stroke: From the center to the periphery. *Front Immunol.* 2022 Sep 20;13:911661. doi: 10.3389/fimmu.2022.911661.
- Wu J, Yang J, Cho WC, et al. Argonaute proteins: Structural features, functions and emerging roles. *J Adv Res.* 2020 Apr 29;24:317-324. doi: 10.1016/j.jare.2020.04.017.
- Wu S, Yu W, Qu X, et al. Argonaute 2 promotes myeloma angiogenesis via microRNA dysregulation. *J Hematol Oncol.* 2014 May 7;7:40. doi: 10.1186/1756-8722-7-40.
- Wu Z, Hofman FM, Zlokovic BV. A simple method for isolation and characterization of mouse brain microvascular endothelial cells. *J Neurosci Methods.* 2003 Nov 30;130(1):53-63. doi: 10.1016/s0165-0270(03)00206-1.
- Xing C, Li W, Deng W, et al. A potential gliovascular mechanism for microglial activation: differential phenotypic switching of microglia by endothelium versus astrocytes. *J Neuroinflammation.* 2018 May 15;15(1):143. doi: 10.1186/s12974-018-1189-2.
- Xu J, Chavis JA, Racke MK, et al. Peroxisome proliferator-activated receptor-alpha and retinoid X receptor agonists inhibit inflammatory responses of astrocytes. *J Neuroimmunol.* 2006 Jul;176(1-2):95-105. doi: 10.1016/j.jneuroim.2006.04.019.
- Xu L, Nirwane A, Yao Y. Basement membrane and blood-brain barrier. *Stroke Vasc Neurol.* 2018 Dec 5;4(2):78-82. doi: 10.1136/svn-2018-000198.

- Xu SY, Pan SY. The failure of animal models of neuroprotection in acute ischemic stroke to translate to clinical efficacy. *Med Sci Monit Basic Res.* 2013 Jan 28;19:37-45. doi: 10.12659/msmbr.883750.
- Yang C, Hwang HH, Jeong S, et al. Inducing angiogenesis with the controlled release of nitric oxide from biodegradable and biocompatible copolymeric nanoparticles. *Int J Nanomedicine.* 2018 Oct 16;13:6517-6530. doi: 10.2147/IJN.S174989.
- Yang FM, Zuo Y, Zhou W, et al. sNASP inhibits TLR signaling to regulate immune response in sepsis. *J Clin Invest.* 2018 Jun 1;128(6):2459-2472. doi: 10.1172/JCI95720.
- Yang GY, Gong C, Qin Z, et al. Tumor necrosis factor alpha expression produces increased blood-brain barrier permeability following temporary focal cerebral ischemia in mice. *Brain Res Mol Brain Res.* 1999 May 21;69(1):135-43. doi: 10.1016/s0169-328x(99)00007-8.
- Yang M, Chen Y, Chen L, et al. miR-15b-AGO2 play a critical role in HTR8/SVneo invasion and in a model of angiogenesis defects related to inflammation. *Placenta.* 2016 May;41:62-73. doi: 10.1016/j.placenta.2016.03.007.
- Yang M, Haase AD, Huang FK, et al. Dephosphorylation of tyrosine 393 in argonaute 2 by protein tyrosine phosphatase 1B regulates gene silencing in oncogenic RAS-induced senescence. *Mol Cell.* 2014 Sep 4;55(5):782-90. doi: 10.1016/j.molcel.2014.07.018.
- Yao Y, Zhang Y, Liao X, et al. Potential Therapies for Cerebral Edema After Ischemic Stroke: A Mini Review. *Front Aging Neurosci.* 2021 Feb 4;12:618819. doi: 10.3389/fnagi.2020.618819.
- Yardeni T, Eckhaus M, Morris HD, et al. Retro-orbital injections in mice. *Lab Anim (NY).* 2011 May;40(5):155-60. doi: 10.1038/labano511-155.
- Ye Z, Jin H, Qian Q. Argonaute 2: A Novel Rising Star in Cancer Research. *J Cancer.* 2015 Jul 16;6(9):877-82. doi: 10.7150/jca.11735.
- Ye ZL, Huang Y, Li LF, et al. Argonaute 2 promotes angiogenesis via the PTEN/VEGF signaling pathway in human hepatocellular carcinoma. *Acta Pharmacol Sin.* 2015 Oct;36(10):1237-45. doi: 10.1038/aps.2015.18. Erratum in: *Acta Pharmacol Sin.* 2018 Feb;39(2):329.
- Ye ZY, Xing HY, Wang B, et al. DL-3-n-butylphthalide protects the blood-brain barrier against ischemia/hypoxia injury via upregulation of tight junction proteins. *Chin Med J (Engl).* 2019 Jun 5;132(11):1344-1353. doi: 10.1097/CM9.0000000000000232.
- Yemisci M, Caban S, GURSOY-OZDEMIR Y, et al. Systemically administered brain-targeted nanoparticles transport peptides across the blood-brain barrier and provide neuroprotection. *J Cereb Blood Flow Metab.* 2015 Mar;35(3):469-75. doi: 10.1038/jcbfm.2014.220.

- Yew KS, Cheng E. Acute stroke diagnosis. *Am Fam Physician*. 2009 Jul 1;80(1):33-40.
- Yoshii SR, Mizushima N. Monitoring and Measuring Autophagy. *Int J Mol Sci*. 2017 Aug 28;18(9):1865. doi: 10.3390/ijms18091865.
- Yoshimura A, Ito M. Resolution of inflammation and repair after ischemic brain injury. *Neuroimmunol and Neuroinflammation*. 2020 Jul;7(3):264-276. doi: 10.20517/2347-8659.2020.22.
- Zeng LL, He XS, Liu JR, et al. Lentivirus-Mediated Overexpression of MicroRNA-210 Improves Long-Term Outcomes after Focal Cerebral Ischemia in Mice. *CNS Neurosci Ther*. 2016 Dec;22(12):961-969. doi: 10.1111/cns.12589.
- Zeng Y, Sankala H, Zhang X, et al. Phosphorylation of Argonaute 2 at serine-387 facilitates its localization to processing bodies. *Biochem J*. 2008 Aug 1;413(3):429-36. doi: 10.1042/BJ20080599.
- Zeng Z, Gong X, Hu Z. L-3-n-butylphthalide attenuates inflammation response and brain edema in rat intracerebral hemorrhage model. *Aging (Albany NY)*. 2020 Jun 21;12(12):11768-11780. doi: 10.18632/aging.103342.
- Zhang H, Lu M, Zhang X, et al. Isosteviol Sodium Protects against Ischemic Stroke by Modulating Microglia/Macrophage Polarization via Disruption of GAS5/miR-146a-5p sponge. *Sci Rep*. 2019 Aug 21;9(1):12221. doi: 10.1038/s41598-019-48759-0.
- Zhang H, Qiao L, Liu X, et al. Differential expression of Ago2-mediated microRNA signaling in adipose tissue is associated with food-induced obesity. *FEBS Open Bio*. 2022 Oct;12(10):1828-1838. doi: 10.1002/2211-5463.13471.
- Zhang J, Fan XS, Wang CX, et al. Up-regulation of Ago2 expression in gastric carcinoma. *Med Oncol*. 2013;30(3):628. doi: 10.1007/s12032-013-0628-2.
- Zhang J, Jin H, Liu H, et al. MiRNA-99a directly regulates AGO2 through translational repression in hepatocellular carcinoma. *Oncogenesis*. 2014 Apr 14;3(4):e97. doi: 10.1038/oncsis.2014.11.
- Zhang L, Li Y, Zhang C, et al. Delayed administration of human umbilical tissue-derived cells improved neurological functional recovery in a rodent model of focal ischemia. *Stroke*. 2011 May;42(5):1437-44. doi: 10.1161/STROKEAHA.110.593129.
- Zhang R, Li Y, Hu B, et al. Traceable Nanoparticle Delivery of Small Interfering RNA and Retinoic Acid with Temporally Release Ability to Control Neural Stem Cell Differentiation for Alzheimer's Disease Therapy. *Adv Mater*. 2016 Aug;28(30):6345-52. doi: 10.1002/adma.201600554.

- Zhang S, An Q, Wang T, et al. Autophagy- and MMP-2/9-mediated Reduction and Redistribution of ZO-1 Contribute to Hyperglycemia-increased Blood-Brain Barrier Permeability During Early Reperfusion in Stroke. *Neuroscience*. 2018 May 1;377:126-137. doi: 10.1016/j.neuroscience.2018.02.035. Erratum in: *Neuroscience*. 2018 Aug 21;386:351.
- Zhang X, Graves P, Zeng Y. Overexpression of human Argonaute2 inhibits cell and tumor growth. *Biochim Biophys Acta*. 2013 Mar;1830(3):2553-61. doi: 10.1016/j.bbagen.2012.11.013.
- Zhang ZG, Chopp M, Zaloga C, et al. Cerebral endothelial nitric oxide synthase expression after focal cerebral ischemia in rats. *Stroke*. 1993 Dec;24(12):2016-21; discussion 2021-2. doi: 10.1161/01.str.24.12.2016.
- Zhang ZG, Zhang L, Jiang Q, et al. VEGF enhances angiogenesis and promotes blood-brain barrier leakage in the ischemic brain. *J Clin Invest*. 2000 Oct;106(7):829-38. doi: 10.1172/JCI9369.
- Zhao T, Houg A, Reed GL. Termination of bleeding by a specific, anticatalytic antibody against plasmin. *J Thromb Haemost*. 2019 Sep;17(9):1461-1469. doi: 10.1111/jth.14522.
- Zhao Y, Vanhoutte PM, Leung SW. Vascular nitric oxide: Beyond eNOS. *J Pharmacol Sci*. 2015 Oct;129(2):83-94. doi: 10.1016/j.jphs.2015.09.002.
- Zhou J, Sinha RA, Lesmana R, et al. Pharmacological Inhibition of Lysosomal Activity as a Method For Monitoring Thyroid Hormone-induced Autophagic Flux in Mammalian Cells *In vitro*. *Methods Mol Biol*. 2018;1801:111-122. doi: 10.1007/978-1-4939-7902-8_11.